New Magnetic Nanoparticles for Catalysis and Bioapplication

Dissertation

zur Erlangung des akademischen Grades
doctor rerum naturalium
(Dr. rer. nat.)
im Fach Chemie
eingereicht an der

Mathematisch-Naturwissenschaftlichen Fakultät I
der Humboldt-Universität zu Berlin
von

M.Sc.Radosław Grzegorz Mrówczyński

Präsident der Humboldt-Universität zu Berlin
Prof. Dr. Jan-Hendrik Olbertz

Dekan der Mathematisch-Naturwissenschaftlichen Fakultät I
Prof. Stefan Hecht, PhD

Gutachter: 1.Prof. Dr. habil. Jürgen Liebscher

2.Prof. Dr. habil. Hans Börner

3.Prof. Dr. Oliver Reise

Tag der mündlichen Prüfung: 31st of January 2014

I dedicate this thesis to my wife Marta

Acknowledgements

I want to express my sincere gratefulness to Prof. Jürgen Liebscher for giving me opportunity to extend my scientific skills during this PhD work. I am gratefully for a pointing an interesting research topic to me and spending time during fruitful discussions while guiding me through this demanding period. I thank for all advices and the possibility to work under his supervision what allowed me to finalize this work.

I want to thank all people, who supported me during my stay in Germany and Romania. I thank to my colleagues, dr. Sebastian Karsten, dr. Alexander Bunge, dr. Alexandrina Nan, dr. Rodica Turcu, dr. Zekarias Yacob, dr. Lidia Magerusan, dr. Crina Socaci, dr. Izabell Craciunescu and dr. Anca Petran for a great atmosphere in the team and inestimable help during the laboratory work. I appreciate having gained experiences from their advices and hints. Special thanks go to Ildiko Macavei for laboratory assistance and permanent smile. I am also indebted to dr. Joachim Leistner for conducting thermogravimetry measurement and HR-MS analysis. My research could not be conducted without help from the NMR group of I.N.C.D.T.I.M and Babes-Bolyai University in Cluj Napoca. I wish to acknowledge help of dr. Ioan Bratu and his team for performing FTIR analysis. I am indebted to dr. Lucian Barbu for TEM investigation, dr. Cristian Leostean and dr. Lidia Magerusan for VSM and XPS assistance. I am grateful to prof. H. Börner, Humboldt-Universität zu Berlin, for providing silica coated magnetic nanoparticles and prof. I. Morjan, National Institute for Laser, Plasma and Radiation Physics in Bucharest, for delivering carbon coated iron magnetic nanoparticles. I want to thank to dr. A.Nan for providing NP stabilized with phosphate derivative and acrylic acid.

I want to express my eternal gratefulness to my wife Marta for being at my side all the time. She is the source of my power and happiness. I could not do anything without her devotion, encouragement and unbreakable love.

I am gratefully to my parents Urszula and Grzegorz for support and unremitting faith in me and love.

I thank to my sister Ela, brother Maciej and their spouses for being close to me when I needed it.

I strongly believed that all my efforts, work and success would not have been possible without their involvement in my life.

Only as a warrior can one withstand the path of knowledge. A warrior cannot complain or regret anything. His life is an endless challenge, and challenges cannot possibly be good or bad. Challenges are simply challenges.

Carlos Castenada

Abstract

Magnetische Nanopartikel (MNP) wurden mit neuen Fettsäurederivaten modifiziert. Auf diese Art und Weise wurden wichtige biologische und organokatalytische Funktionen auf die Oberfläche von magnetischen Nanopartikeln aufgebracht. Das folgende Kapitel präsentiert eine Veränderung von mit Polydopamin (PDA) bedeckten magnetischen Nanopartikeln via CuAAC-Reaktion. Zum Beweis der Wirksamkeit dieser Methode wurden biologische Funktionen wie Biotin, Galaktose oder Dansyl an die magnetischen Nanopartikel über einen 1,2,3-Triazolring gebunden, ebenso Prolin als organokatalytische Einheit. Weiterhin wurde das unerwartete Verhalten von Polydopamin als Organokatalysator in Aldol- und Knoevenagel-Reaktionen gezeigt und untersucht. Für diese Reaktionen wurde ebenfalls das Recycling der mit PDA bedeckten Nanopartikel getestet. Desweiteren wurde gezeigt, daß PDA als reaktives Beschichtungsmaterial für oberflächeninitiierte Ringöffnungs-polymerisation von Lactid dienen kann. Somit kann Polymilchsäure (PLA) auf verschiedene Materialien, welche mit PDA beschichtet sind, aufgebracht werden – MNP, Kohlenstoff-beschichtete Eisennanopartikel, oder Aluminiumoxid. Das letzte Kapitel beschäftigt sich mit dem Einsatz von Polyacrylaten zur Funktionalisierung von MNP. Mit dieser Methode wurden Prolin-, Lysin- und Threoninderivate an die MNP gebunden. Die katalytische Aktivität dieser neuen Materialien wurde untersucht.

Schlüsselworte: magnetische Nanopartikel, Polydopamin, CuAAC-reaktion, Polyacrylate, geträgerte Organokatalysatoren

Magnetic nanoparticles (MNP) were modified with new fatty acid derivatives. In this way important biological and organocatalytic functions were introduced on the surface of magnetic nanoparticles. The following chapter is presenting a modification of polydopamine (PDA) coated magnetic

nanoparticles via CuAAC reaction. As a proof of principle biological moieties like biotin, galactose, dansyl were bound to magnetic nanoparticles through a 1,2,3-triazole ring, as well as proline – an organocatalytic unit. Further unexpected behaviour of polydopamine as organocatalyst for aldol and Knoevenagel reaction was demonstrated. Recycling of MNP covered with PDA was tested for the aforementioned reactions. Furthermore, it has been proved that PDA may serve as reactive coating agent for surface initiated ring opening polymerization of lactide. As a result polylactic acid (PLA) can be introduced on different materials covered with PDA - MNP, carbon covered iron magnetic nanoparticles or aluminium oxide. The last chapter is describing the employment of polyacrylates for functionalization of MNP. Using this method proline, lysine and threonine derivatives are fixed to MNP. The catalytic activity of the newly prepared materials was investigated.

Keywords: magnetic nanoparticles, polydopamine, CuAAC reaction, polyacrylates, supported organocatalysis

Table of Content

Abbreviation List

arom.	aromatic
Ac	Acetyl
AIBN	Azobisisobutyronitrile
AOT	Dioctyl sodium sulfosuccinate
APS	Ammonium persulfate
ATRP	Atom Trasfer Radical Polymerization
BA	Benzoic acid
Bn	Benzyl
Boc	*tert*-Butyloxycarbonyl
CTBA	Cetyltrimethylammonium bromide
CuAAC	Copper(I)-catalyzed alkyne-azide cycloaddition
DCC	*N*,*N*'-Dicycylohexylcarbodiimid
DCM	Dichloromethane
DIPEA	*N,N*-Diisopropylethylamine
DMAP	4-Dimethylaminopyridine
DMF	N,N-Dimetylformamid
DMSO	Dimethyl sulfoxide
dr	Diastereomeric ratio
EA	Elemental analysis
EDC	1-Ethyl-3-(3-dimethylaminopropyl)carbodiimide
ee	Enantiomeric excess
ESI	Electrospray ionization
Et	Ethyl
EtOAc	Ethyl acetate
EtOH	Ethanol
FA	Folic acid
FTIR	Fourier transform infrared spectroscopy
HMBPyne	1-hydroxy-1-phosphonopent-4-ynyl)phosphonic acid
HOBt	Hydroxybenzotriazole
MAS	Magic angle spinning
Me	Methyl
MeOH	Methanol
MNP	Magnetic nanoparticles
MRI	Magnetic resonance imaging
MW	Microwave
Na-Asc	Sodium ascorbate
NBS	*N*-Bromosuccinimide
NHS	*N*-Hydroxysuccinimide
NMR	Nuclear magnetic resonance
NP.	Nanoparticles
OA	Oleic acid

PDA	Polydopamine
Ph	Phenyl
PVP	Polyvinylpyrrolidone
quant.	quantitativly
RAFT	Reversible Addition-Fragmentation Chain Transfer
ROP	Ring opening polymerization
rt	Room temperature
SDS	Sodium dodecyl sulfate
ssNMR	Solid-state nuclear magnetic resonance
TBTA	Tris[(1-benzyl-1*H*-1,2,3-triazol-4-yl)methyl]amine
t-Bu	*tert*-butyl
t-BuOH	*tert*-Butanol
TEM	Transmission electron microscop
TFA	Trifluoroacetic acid
TGA	Thermogravimetric analysis
THF	Tetrahydrofuran
THPTA	3 [tris(3-hydroxypropyltriazolylmethyl)amine)
Ts	*para*-Toluenesulfonyl (tosyl)
VSM	Vibrating sample magnetometer
XPS	X-ray Photoelectron Spectroscopy

List of Figures

List of Tables

1 Introduction

Recent years have brought big impact in nanosciences.[1-11] New synthesis techniques and development in material science has brought tremendous achievements and progress in the nanoparticles field. Variety of sizes and shapes of nanoparticles (NP) are easily accessible via routine synthesis techniques. This caused wide application of nanoparticles in many fields e.g. drug delivering, MRI contrast agent[12-13] or proteins purification.[14] They have been applied in hyperthermia for cancer therapy or as support for catalysts.[15] Application in biotechnology and molecular biology or bioscience is still growing. More and more important has become the employment of NP in metal extraction. Application of magnetic nanoparticles (MNP) is not limited to the aforementioned, since they were successfully used in a broad range of disciplines including magnetic fluids, data storage,[16] catalysis,[17] magnetic cell and macromolecules separation.[18] Biomedical application comprises also labelling and tracking agents. MNP has been utilized in analytical chemistry too.[19-20]

NP can be composed of a variety of materials including noble metals (Au, [21] Ag[22], Pt[23], Pd[24]), semiconductors (CdSe, CdS, ZnS[25], TiO_2[26], PbS[27]) and magnetic compounds based on iron. The criterion, which allows defining objects as nanoparticles, is a size below 100 nm. However, there are structures with diameter above 100 nm still considered as nanoparticles. That is why this criterion is not rigid. NP are unique and attractive due to the exhibited features. Decreasing the size of a particle results in a larger share of atoms being located on the surface, which can increase the influence of surface effects on material properties. The large surface is an important issue especially in catalyst immobilization where high catalyst loading and catalyst availability are crucial parameters. It has been shown theoretically and experimentally that decreasing the size of a metal particle will confine electron motion. Consequently, the electron bands of the crystal get gradually quantized, thereby, resulting in an increase in the band-gap energy. New properties which are not found neither in the bulk nor in molecules or atoms in solid state can be found in nanostructures.

One type of nanoparticles, which has been extensively investigated are magnetic nanoparticles. To this group belong structures derived from Co, Fe (e.g. Fe_2O_3, Fe_3O_4, Co[28], $CoFe_2O_4$[29], FePt[30], CoPt[31]) and Ni[32]. Particularly iron oxides take up a dominant position. Iron oxide can occur in several types. Fe_3O_4 (magnetite), $Fe^{II}Fe^{III}{}_2O_4$, α-Fe_2O_3

(hematite, weakly ferromagnetic or antiferromagnetic), γ-Fe_2O_3 (maghemite, ferromagnetic), FeO (wüsite, antiferromagnetic), α-Fe_2O_3 and β-Fe_2O_3.[33] Among these types magnetite and maghemite are often used due to the proven biocompatibility and established routine synthesis methods. It is important to stress that hematite is the oldest known iron oxide widespread in soil and rocks. But this is not the only natural source of magnetic materials.

Recently, magnetosomes have attracted scientist's huge attention.[34] Magnetosome chains are membranous prokaryotic organelles present in magnetotactic bacteria. They contain 15 to 20 magnetite crystals that together act like a compass needle to orient magnetotactic bacteria in geomagnetic fields, thereby simplifying their search for their preferred microaerophilic environments. Each magnetite crystal within a magnetosome is surrounded by a lipid bilayer, and specific soluble and transmembrane proteins are sorted to the membrane. Recent research has shown that magnetosomes are invaginations of the inner membrane and not freestanding vesicles.[35] Magnetite-bearing magnetosomes have also been found in eukaryotic magnetotactic algae, with each cell containing several thousand crystals. More detailed information can be found in the literature.[36]

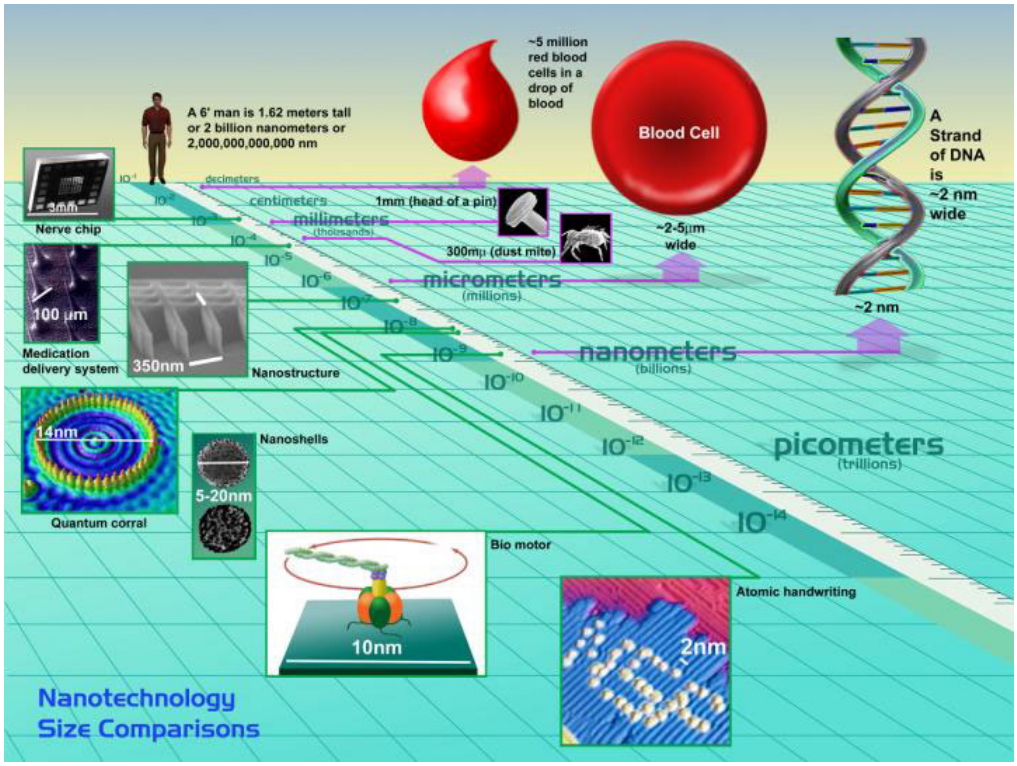

Figure 1. Nanoscale bar.[37]

MNP show unique magnetic attributes such as superparamagnetic behaviour, high coercivity, low Curie temperatures and high magnetic susceptibility. The characteristic features of magnetic materials are magnetic dipoles which are generated by spinning of their electrons. Each electron spin might take a position parallel or anitparallel with respect to the neighbour in the same crystal lattice. Depending on the magnetic respond we can classify magnetic materials as paramagnets, ferromagnets, ferrimagnets or antiferromagnets. An essential fact is that magnetic behaviour can be altered by tuning material size.

Paramagnetism occurs in materials which have unpaired electrons. The electron spins are randomly orientate and essentially have their own magnetic moment due to weak coupling being overcome by thermal energy. When there is an external magnetic field some of the spins align with the field, depending on the moment of the material and the external field. Removal of the field enables thermal agitation to dominate which randomises the spins so no net magnetisation is seen.

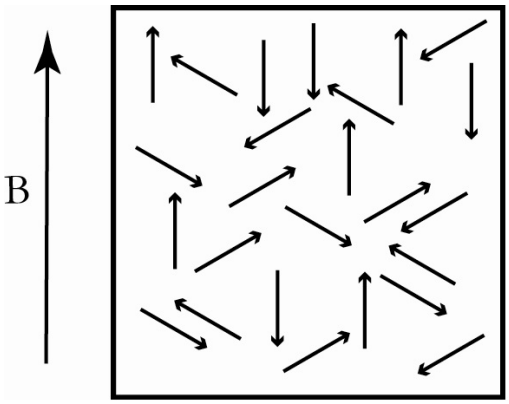

Figure 2. Spin orientation in paramagnetic materials.

Ferromagnetism appears when magnetic dipoles align parallel to each other. This alignment is very strong (albeit not strong enough to form a covalent bond), and produces a large net magnetic moment. This phenomenon occurs even without an external magnetic field.

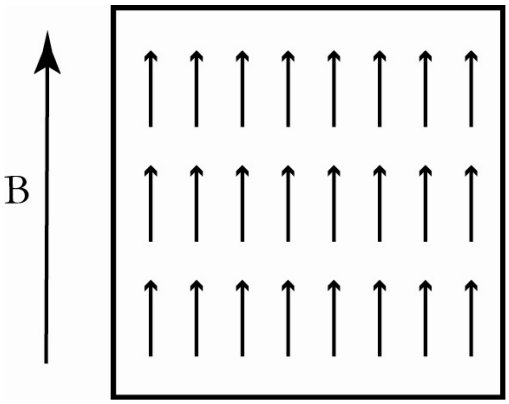

Figure 3. Spin orientation in ferromagnetic materials.

An interesting feature of ferromagnetic materials is an event called hysteresis. Hysteresis loop[38] shows the relationship between the induced magnetic flux density and the magnetizing force. The loop is generated by measuring the magnetic flux of a material while the magnetizing force is changed. We can point three major parameters describing strength and magnetization of material (see Figure 4). The first parameter is the coercive field H_C (C). It describes the external magnetic field directed opposite to magnetic dipoles in material, which is necessary to reduce magnetization to zero. This parameter is related to the minimal energy required for the reversal of the magnetization. The second parameter is saturation magnetization M_S (A). It exhibits the maximum value of magnetization, which can be achieved under sufficient magnetic field. The third parameter is the residual magnetization M_R (B), which shows remaining magnetization at zero applied field.

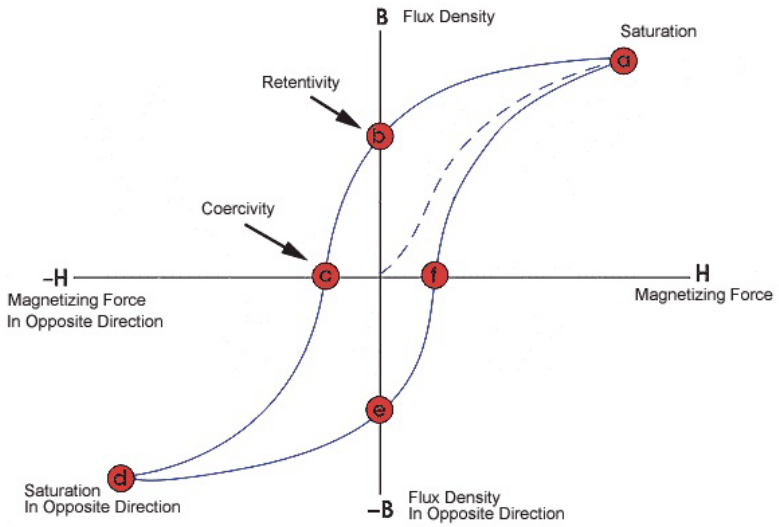

Figure 4. Hysteresis loop of magnetic materials.

As stated before, magnetic properties depend on the size of the material. Size reduction below a certain value of the radius, the so called superparamagnetic radius leads to changes in both ferri- and ferromagnetic nanoparticles in such a way that they become superparamagnetic. However, still high magnetic moments are observed while there is not remanent magnetization after the external magnetic field is removed. In other words, they lack hysteresis loop. The phenomenon of superparamagnetism is strictly connected with magnetic nano sized materials composed of magnetic single domains and appears when thermal energy is big enough to overcome the energy barrier for changing the magnetic moments orientation.

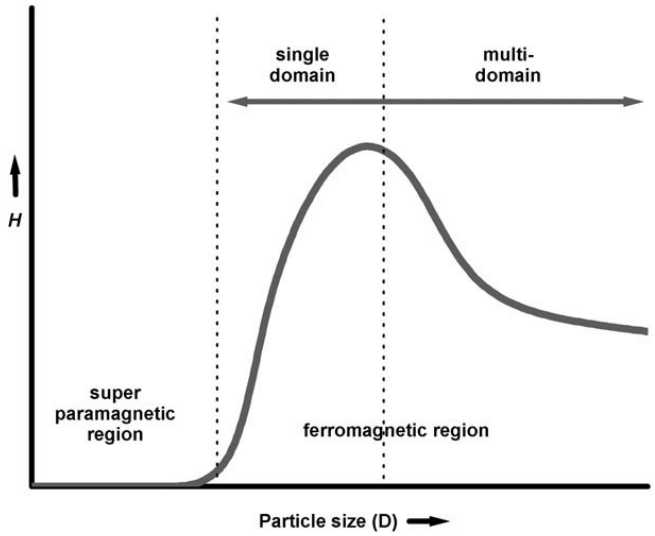

Figure 5. Magnetic coercivity versus particle size.[1]

Characteristic is a high surface to volume ratio resulting in high surface charge and activity of naked nanoparticles. Thus, they tend to aggregate to minimize energy. Moreover high chemical reactivity causes oxidation of nanoparticles. Consequently, they may lose magnetism and dispersibilty.

In the last years enormous work was done to develop efficient methods to synthesize shaped-controlled, stable and monodispersed MNP. Thereby, prevention of aggregation is crucial for the stability of the synthesized MNP. This has been achieved by addition of stabilizers during the synthesis or replacement of primary stabilizer with another one by ligand exchange reaction. For these strategies organic molecules have been applied, for instance, polymers[39] or long-chain surfactants.[40] It has been demonstrated that small

molecules like amino acids[41-42], dopamine[43], thiols[44], phosphates[45], diols[46] might have positive influence on MNP stability and even more complex structures e.g. proteins[47] have been bound to MNP successfully. As coating agents, also inorganic species including silica[48] and carbon[49] have been utilized. It is noteworthy that in many cases the protecting shells not only stabilize the nanoparticles, but can also contain functional groups useful for several applications. Stable MNP can form diverse structures, albeit the core-shell form and clusters are the most common. In an ideal case of core-shell structures each single nanobject is covered with a continuous layer of a polymer. Clusters are formed when several nanoparticles are enclosed in a polymer matrix.

1.1 Synthesis of magnetic nanoparticles

The great interest in MNP has furnished many ways of preparation. Several popular methods, including co-precipitation, thermal decomposition and/or reduction, hydrothermal synthesis, laser pyrolysis techniques, microemulsion approach and sonochemical synthesis, have been directed towards the synthesis of high-quality magnetic nanoparticles. Previously mentioned magnetosome crystals of natural origin are also a source of magnetic material showing high chemical purity, narrow size ranges, specific crystal morphologies.[1,4,11,50-51]

Among these methods co-precipitation method is the most popular due to simplicity, convenience and readily available metal precursors. It usually involves treatment of a solution of a mixture of iron salts (Fe^{2+} and Fe^{3+}) with a base under an inert atmosphere at room temperature or elevated temperature (see Scheme 1). The type of the salt (such as chlorides, sulfates, nitrates, perchlorates etc.) is known to influence the size and shape of the synthesized MNP. It has been proved that pH value, ionic strength, temperature, and ferric / ferrous ions ratio affect the size and the attributes of nanoparticles. Even stirring rate can influence these properties.[9] Because of the high chemical reactivity of naked MNP being subject to oxidation (see Scheme 2), the co-precipitation method has to be done in anaerobic conditions. Main advantage of this method is, when all parameters are set, that it gives reproducible results even in multi kilogram scale.[11] Thus, it is attractive for industrial application. The major drawback of the co-precipitation method is the generation of polydispersed particles with a wide size distribution. This affects magnetization and blocking temperatures of the MNP as strongly size dependent factors. That problem of polydisperity has been overcome by the addition of stabilizers like surfactants i.e. oleic acid, oleyamine, some diols or polymeric agents such as dextran or polyvinyl alcohol.

$$Fe^{2+} + 2Fe^{3+} + 8OH^- \longrightarrow Fe_3O_4 + 4H_2O \quad (1)$$

$$Fe_3O_4 + 0.25O_2 + 4.5H_2O \longrightarrow 3Fe(OH)_3 \quad (2)$$

Monodispersed magnetic nanocrystals with smaller size (often below 10 nm) can be synthesized through the thermal decomposition of organometallic compounds in high-boiling organic solvents containing stabilizing surfactants. Organometallic precursors including metal acetylacetonates, [M(acac)$_n$], (M=Fe, Mn, Co, Ni, Cr; n=2 or 3), metal cupferronates [M^{x}Cup$_x$][52] or carbonyls[53] are utilized. As a surfactant mostly oleic acid, hexadecylamine and others fatty acids are applied. Sun and Zhang have reported the synthesis of monodispersed magnetite NP derived from Fe(acac)$_3$ through thermal decomposition at 265 ^{o}C in diphenyl ether in presence of oleic acid and oleylamine (see Scheme 3).[54] As a result of the reaction highly monodispersed magnetite NP with diameter up to 20 nm were obtained by seed-mediated growth method. Prepared magnetite NP were easily dispersed in nonpolar solvents e.g. hexane.

$Fe(acac)_3$ +1,2-$RCH(OH)CH_2OH$+$RCOOH$+RNH_2

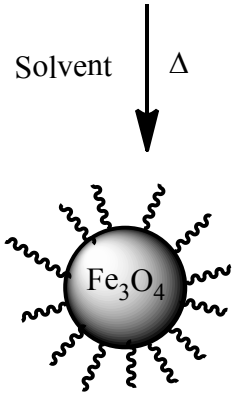

(3)

Heyon et. al. presented the synthesis of magnetite NP via thermal decomposition of Fe(CO)$_5$ at 100 ^{o}C in the presence of oleic acid as an coating agent.[55] These NP were converted to γ-Fe$_2$O$_3$ by using controlled oxidation process employing trimethylamine oxide as an oxidant. Resulting NP size was in range of 4-16 nm dependent on the experimental parameters. The same group showed a similar thermal decomposition approach to preparation of magnetite NP from simple sodium oleate and iron (III) chloride

to generate an iron oleate complex *in situ* which was then decomposed at temperatures between 240 and 320 ^{o}C in different solvents, such as 1-hexadecene, dioctyl ether, 1-octadecene, 1-eicosene, or trioctylamine.[56] Particles were in the range of 5–22 nm, depending on the decomposition temperature and aging period. Thermal decomposition is not only limited to iron oxide MNP. This route was effectively applied in manufacturing cobalt nanostructures by Alivisatos and Chaudret.[57-58] Magnetic alloys ($CoPt_3$[59] and FePt[60]) and phosphate (FeP[61], MnP[62]) have also been obtained with this method. Altogether, the thermal decomposition method gives nicely monodispersed magnetic nanoparticles with narrow size distribution, but they are stable only in nonpolar organic solvents.

Ultrasound has been used in preparation of various magnetic nanocomposites. It was shown by Vijayakamura that simple sonication of iron(II)acetate in water under argon gave pure Fe_3O_4 powder with particle size around 10 nm.[63] However, the magnetic values for this material were low <1.25 emu/g. Pinkas et al. conducted sonolysis of Fe(acac) in presence of a controlled amount of water under Ar leading to amorphous Fe_2O_3.[64] Organic coating and surface area were water dependent.

The microemulsion technique is another important method applied in the synthesis of MNP. Microemulsion is a thermodynamically stable dispersion of two immiscible phases (water/oil) in the present of a surfactant. Surfactant molecules may form a monolayer at the interface between the two phases.[65] Synthesis of MNP in this system gives access to different forms of NP. Size of MNP may be changed by the surfactant type and concentration. Water-in-oil microemulsion has been utilized to synthesize iron nanoparticles, polymer coated magnetite nanoparticles and other nanoparticles derived from gold, platinum or copper.[66-68] A variety of surfactants have been utilized during in this preparation including AOT (dioctyl sodium sulfosuccinate),[69] SDS (sodium dodecyl sulphate),[70] CTBA (cetyltrimethylammonium bromide) or PVP (polyvinylpyrrolidone). Disadvantages of this method are difficulties in scale-up and influence of residual surfactant on NP.

The hydrothermal method is an alternative technique applied for the preparation of MNP. This route uses wet chemical technologies of crystallizing substances in sealed containers from high temperature water solutions (130-250 ^{o}C) at high vapour pressures (0.3 – 4 Mpa). The synthesis may be conducted with or without surfactants. Wang[71] reported the preparation of MNP in the absence of surfactant. Fe_3O_4 nanopowder (ca. 40 nm) was afforded at 140 ^{o}C over 6 hours with high magnetic saturation value 88 emu/g.

The application of surfactants was reported by Zhang et al.[71] MNP were obtained with diameters around 27 nm in the presence of AOT. The hydrothermal method has been used to furnished sophisticated structures like nanocubes[72] or hollow spheres.[73]

Laser pyrolysis of $Fe(CO)_5$ and ethylene mixtures was applied to synthesize MNP with 14 nm diameter and covered with 4 nm of an oxide shell. Studies on laser pyrolysis concluded that the MNP size can be tuned by the oxygen amount used in the oxidizing step and does not depend on laser power. Nonetheless, preparation of pure materials require precise control of many factors such as oxygen content, gas phase impurities and heating time. Furthermore, this method involves expensive equipment. Morjan et al.[74] reported preparation of nano-iron cores embedded in carbon layers and their preliminary application to the growth of carbon nanotubes. CO laser pyrolysis of volatile iron and carbon precursors in a gas flow reactor was used in order to obtain the Fe–C nanocomposites in a range of 3 to 7 nm.

1.2 Coating of magnetic nanoparticles

Aggregation of MNP is a result of Brownian motion of bare nanoparticles enhanced by Van der Waals and magnetic dipole-dipole interaction.[10] Consequently, magnetic properties and nanoscale attributes might be lost. In case of catalysis, aggregation leads to a decreasing number of accessible reactive groups and less specific surface areas. As a result, the whole catalytic process can be blocked.[75] In order to prevent this unwanted phenomenon a great deal of work has been done to produce colloidally stable MNP. Colloidal suspensions can be gained by utilizing repulsive force strong enough to overcome the attractive ones. This is achieved either by electrostatic stabilization or by steric stabilization or combination of both. Especially steric stabilization plays an important role in nanoparticles surface engineering. However, colloidal stability is not the only reason which should be taken under considerations. Lack of efficient covering can result in fast oxidation of MNP (e.g. Ni, Co, Fe) as a consequence of their sensitivity to air. This can be crucial in applications in biomedicine were an exact stable coating should limit the risk that MNP affect the patients in an unwanted way. Steric stabilization is provided by organic molecules, such as surfactants, polymers, and designed ligand or by inorganic coating like silica, gold, silver and carbon. It is essential to underline that the stabilizing agents are directly involved in MNP surface modification. In most cases they are not only capping agents but they can also bear functional groups which allows tailoring surface properties and might render them compatible with another phase. Stabilizer introduction

can be implemented by several ways presented on Figure 6. In case of using organic molecules the structure of introduced ligand is an important issue. Generally, one can distinguish non polymeric capping agents or polymers. When the ligand is involved in surface functionalization it bears functional groups in most cases. They can already be the desired function, or provide a reactive group able for further reaction in order to attach the desired functionality. Ligand exchange is another way leading to MNP stabilization and surface engineering. This concept is based on exchanging originally introduced ligands, in most cases surfactants, with excess of new ligands without changing the intrinsic properties of the iron core. This methodology is often used, when it is essential, to change solubility of magnetic nanoparticles from organic medium into water phase. This has significance in preparation of MNP for bioapplication. The introduction of ligands might also be conducted during the preparation step. For stabilizing MNP by polymers additionally surface initiated polymerization seems to be a useful approach.

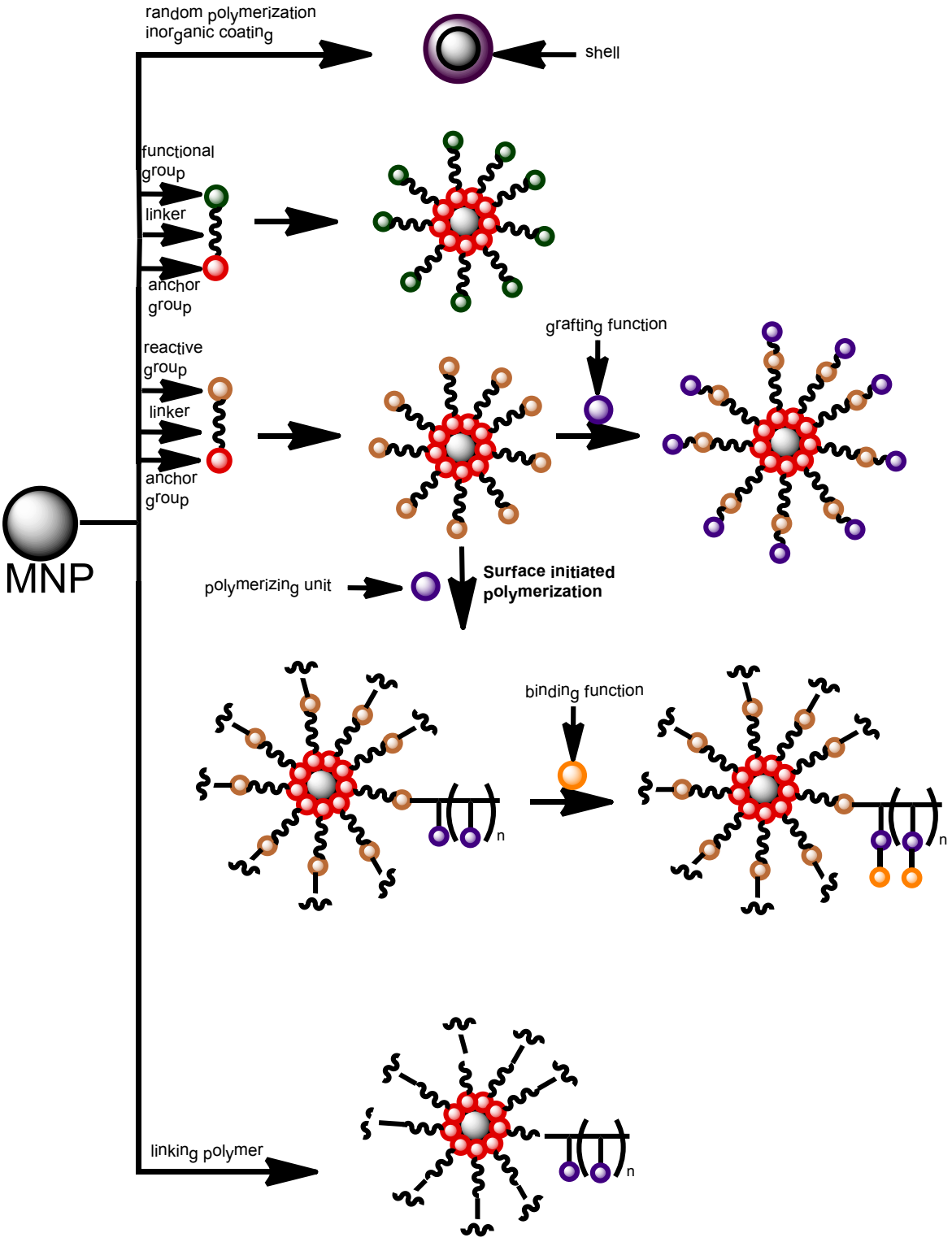

Figure 6. Routes to MNP functionalization with different stabilizer types.

1.2.1 Non-polymeric coating agents

The structure of non polymer coating agent is crucial for the properties of MNP. First of all it should contain a group which allows anchoring at the surface of the MNP. Various anchoring groups such as carboxylic acids, diols, amines, catechols, phosphate and bisphosphonates but also phosphine and ammonium salts serve this purpose.

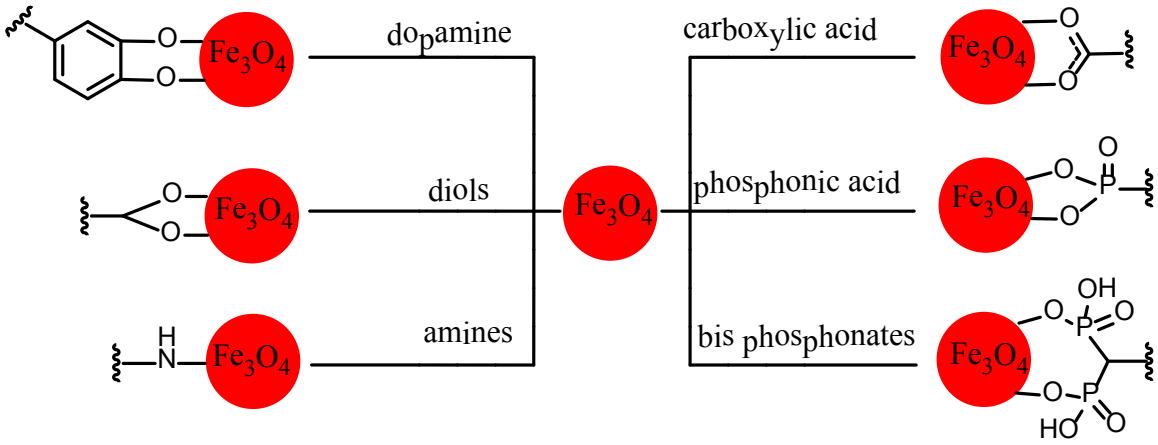

Figure 7. Selected anchoring groups for MNP functionalization.

Oleic acid is the most common surfactant applied to stabilize MNP. It is built of 18 carbon atoms and contains a *cis* C-C double bond in the middle forming a kink. Such a kink is considered as a factor for more effective stabilization. Indeed, stearic acid without double bond does not provide such a good stabilization like oleic acid.[76] Additionally, oleic acid creates dense protective layer, thus producing uniform and monodispersed nanoparticles with high colloidal stability. The surfactants are added directly during the preparation step. A carboxylic group is chemisorbed on magnetite NP surfaces composing a carboxylate anion. Changing the media from hydrophobic to hydrophilic is possible with magnetite NP stabilized with OA (oleic acid) by coating with a second layer of OA.[77] Carboxylic groups of the second layer are exposed outside and create hydrophilicity. Such a system allows preparation of magnetic ferrofluids stable in water. Magnetite NP covered with one layer of OA are often used in ligand exchange reaction because they are easily obtained, but they lack functionality. Therefore, they serve as starting point for further functionalization of magnetite NP. Stable suspension of magnetite NP in water are observed when hydroxy carboxylic acids are used, for example ricinoleic acid, citric and galactaric acid.[78] Recently, it has been shown that amino acids behave as well as coating agents.[79] It has been reported that acrylic acid might be attached to magnetite NP as well.[80]

Mercapto acids might serve as a stabilizer for magnetic nanoparticles too.[81] It has been presented recently by Gao that PEG modified cysteine (Cys) stabilizes magnetite NP. The thiol and the carboxylate groups of Cys can form bi-dentate binding to the Fe ions on the NP surface. Furthermore, oxidation of thiol groups can lead to cross linked disulfide between Cys residues on the NP surface, which can further increase the stability of ligand functionalization. It is worth mentioning that ligand introduction was achieved via ligand exchange reaction while cysteine-derived ligand replaced an original layer of oleic acid.

Diols are another class of compounds applied in MNP stabilization. It was demonstrated that 1,2–hexanedecanodiol and oleylamine are co-stabilizers added during magnetite NP synthesis through the thermal decomposition method. Binder presented a series of manifold diols bound to MNP employing ligand exchange.[46] Rotello conducted ligand exchange reaction of amine stabilized Fe_2O_3 NP with monoalcohols and diols comprised of long alkyl chain.[82]

Catechols have been recently addressed in MNP stabilization in hydrophilic media.[83] Among them, dopamine, a derivative of the amino acid DOPA (*L*-3,4-dihydroxyphenylalanine), which is abundantly present in the adhesive protein of the mussel *Mytilus edulis* is the most considered high affinity binding group to stabilize iron oxide nanoparticles. Nevertheless, the suitability of dopamine for iron oxide nanoparticles stabilization is still under debate. It has been demonstrated that degradation of MNP occurs upon adsorption of dopamine on iron oxide nanoparticles.[84] Moreover, dopamine has attracted much attention because of its unique features. It can polymerize in basic solution in presence of air giving rise to polydopamine.[85] This type of material is extensively investigated in many groups, including ours.

Amine surfactant-type molecules are also used for covering MNP. Trioctyl amine, octylamine and oleylamine are common representatives. They are added as main capping agents or they give synergic effect with others surfactants, such an oleic acid.

Phosphonates or phosphonic acids are organic compounds containing C-$PO(OR)_2$ or C-$PO(OH)_2$ groups, respectively. A major feature of this class of compounds is the fact that the anchorage can be mono-, bi-, or trident.[86] A strong interaction between the inorganic core and the phosphonic moiety is reported and the more interesting fixation moiety seems to be bisphosphonates. Xu described Fe_3O_4 MNP modified with bisphosphonates bearing dopamine moiety for efficient fishing uranyl ions from blood and water.[87] Lalatonne reported the synthesis of maghemite nanoparticles where the surface was passivated using a bifunctional passivating agent such as 5-hydroxy-5,5-

bis(phosphono)pentanoic acid (called HMBP–COOH).[88] The resulting ferrofluid was stable in large concentrations and pH ranges. The same group showed the application of bisphosphonates covered maghemite NP in click chemistry.[89] This type of anchoring was also used by the Sukenik team to coat Fe_2O_3 MNP for further applications in binding antibodies.[90]

1.2.2 Polymeric coating agents

Polymeric materials are ideal candidates to synthesize and encapsulate inorganic colloids, as a wide range of functionality can be installed on the polymer backbone and fixed onto the nanoparticles shell. Furthermore, polymeric surfactants may enable the tuning of the nanoparticles size and morphology in a manner not accessible when using small molecule or surfactants. By variation of the molecular weight, the composition, and the architecture of the polymer, a wide range of hybrid nanocomposites have been prepared. Polymers are used often to stabilize MNP in terms of steric stabilization. However, they can also enhance stability via ionic interactions. The most common polymeric coating agents are dextran[91], chitosan[92], poly(vinylpyrrolidone)[93], poly(ethylene oxide)[94], poly(vinyl alcohol)[95], poly(*N,N*-dimethylethylamino acrylate)[96], poly(imine)[97] poly(acrylic acid)[98], poly(*N*-isopropylacrylamide), poly(styrene)[70]. Heterocyclic compound like pyrrole, gives easy access to polypyrrole covered magnetite NP, which form core-shell structures.[99-100]

Introduction of a polymer may be achieved by several ways. First manner comprises of *in situ* particle synthesis in presence of the polymer. This direct polymer introduction was exploited to synthesize magnetite NP covered with dextrane.[101] Obtained iron oxide nanoparticles were in 10–20 nm size range. In a similar way magnetite NP covered with poly(vinyl alcohol) were obtained.[102] The preparation of crystalline, superparamagnetic Fe_3O_4 colloids of 4–10 nm diameter was confirmed using XRD, VSM, and TEM. The second most common method for synthesizing polymer coated MNP is based on conducting the free radical polymerization in presence of MNP. In this way random polymerization occurs. This leads to different nanostructures which can be controlled by reaction parameters such as time, temperature or monomer concentration. It is possible to polymerize either monomer itself or use copolymerization between unfunctionalized monomer and functionalized one. This manner has been applied to prepare magnetite NP covered with pyrrole copolymer bearing functional groups like biotin or galactose.[100] The free radical polymerization was also used to modify surface of magnetic nanoparticles with

polyacrylates suitable for click chemistry[103] or to introduce polymers based on poly(ethylene glycol) monomethacrylate and *N*-isopropylacrylamid.[104] This method has also disadvantages. A big part of the polymer synthesized during reaction is not fixed to the surface of nanoparticles, thus, has to be removed and discarded.

The latest studies conducted on covering MNP with polymer are focused on surface initiated polymerization. The advantage of this approach is the potential to apply controlled, or living polymerizations to precisely modify the molar mass and the composition of polymer chains grown from colloidal surfaces. Important issue in this approach is binding of appropriate initiating group while suppressing undesirable flocculation of colloids. The most common methods exploit surface initiated polymerization are RAFT[105] (Reversible Addition-Fragmentation chain Transfer**)** and ATRP[106] (Atom transfer radical polymerization**)**. Organic halides, especially bromides, have been shown to be the most useful initiator for ATRP while RAFT uses dithioesters, thiocarbamates, and xanthates. The introduction of surface bound initiators can be achieved by either *in situ* particle formation using a functional surfactant, or via a ligand exchange onto preformed nanoparticles.[106-107]

Silanization reactions with functionalized alkoxysilanes have often been used in the synthesis of functionalized MNP. It can either be performed on uncovered MNP or at MNP stabilized with one layer of oleic acid.

The silica-containing shell is formed by reaction between hydroxyl groups which attack and displace the alkoxy groups on the silane thus forming a covalent -Si-O-Si- bond. In this way de Palma et al. synthesized water dispersible ferrite $CoFe_2O_4$ NP from hydrophobic ferrite NP covered with oleic acid.[108] Silanization can also be done in two steps. First, the decomposition of tetraethyl orthosilicate via the Stö ber method gives MNP covered with silane and subsequently a functional alkoxysilane reacts with the first silica shell according to the aforementioned mechanism. It was shown that the thickness of the silica shell can be controlled. It depends on many factors including monomer concentration, pH, time and temperature.[109-110]

Chemists took lessons from nature by exploiting the strong adhesive power exhibited by mussels by means of catechol moieties in proteins. In this way dopamine and polydopamine have entered the field of material science.[85,111] Recently, Messersmith et al.[85] showed that dopamine can be easily polymerized by oxidation on a variety of materials like noble metals (Au, Ag, Pt, Pd), SiO_2, Al_2O_3 and polymers (polystyrene, polyethylene polycarbonate, polyethylene terephthalate) in basic solution resulting in

strongly adherent layers. The mechanism of this oxidative polymerization is not known exactly but is believed to be similar to melamine formation running via intermediate *o*-quinone systems resulting in 5,6-dihydroxylindoles.[112] This methodology has also been applied to cover magnetite nanoparticles (Fe_3O_4).[113-114] It has been presented that gold NP covered with polydopamine are biocompatible.[115]

Amazingly, the structure of polydopamine has not been fully proved yet.[116] In the literature there are *o*-quinoid and catechol containing indole structures such as **1** and **2** discussed, where the monomer units are connected by C-C bonds (Figure 8. 1, 2). As a recent alternative, structure **3** was proposed wherein quinoid and catechol containing indoles were connected just by hydrogen bonding between oxygen atoms.[116] Polydopamine coated materials show reactivity towards amines or thiols thus counting for quinoid functions as found in each of the proposed polymer structure. This feature allows covalent binding of proteins, enzymes or lipophilic amines to the polymer film.[117-118] Important contribution towards better understanding of polydopamine structure was also given by our group (see chapter 2.2.2).

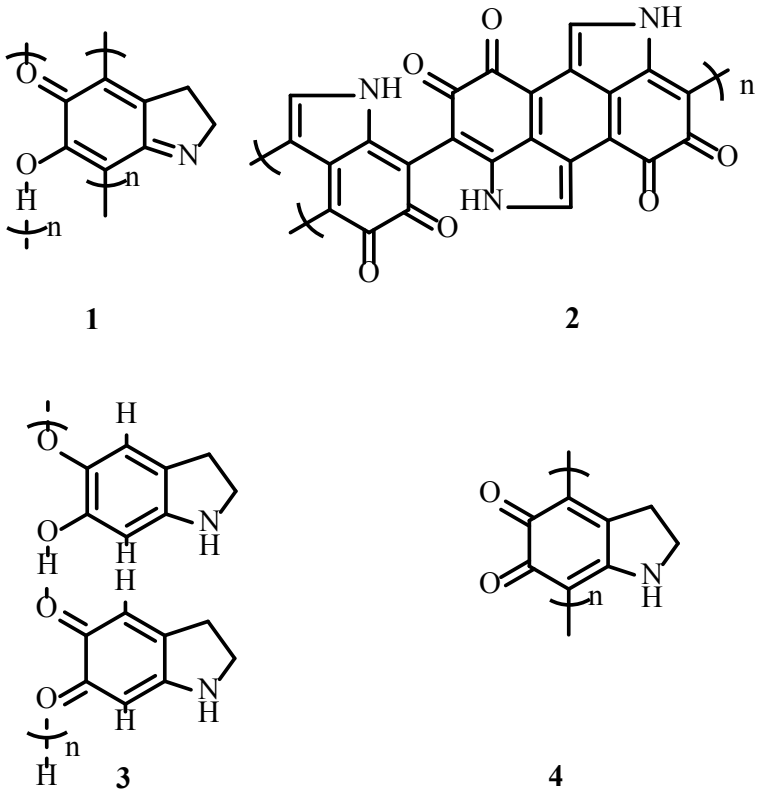

Figure 8. Examples of proposed polydopamine structures.

Ring opening polymerization (ROP) is a type of surface initiated polymerization which leads to surface derivatization. This method requires nucleophilic groups attached to

the surface initiating the polymerization reaction. Thus the resulting polymer is attached covalently to the surface of the material. For polylactic acid and polycaprolactone usually alcohols serve as nucleophilic starters. This methodology has been successfully used to bind biodegradable polylactic acid and polycaprolactone on the surface of magnetite NP.[119] These materials show attractive properties like excellent mechanical strength and nontoxicity. In this approach hydroxyl groups were used as initiator, which react with lactide (3,6-dimethyl-1,4-dioxane-2,5-dione) as the cyclic ‘‘dimer’’ of LA[120] or with ε-caprolactone.[119] Initiating hydroxyl groups were introduced to the surface of magnetite NP by anchoring glycolic acid or racemic serine. In general, reaction with LA “dimer” can be catalyzed either by metal compounds of tin[121], aluminium,[122] lead[123], zinc[124], bismuth[123], iron[125], and yttrium[126] or small organic molecules, for example, DMAP, PPh_3, N-heterocyclic carbenes or enzymes.[127-128] The ROP on magnetite NP might be improved by microwave irradiation.[120] Lately, norepinephrine was polymerized in presence of various materials including ceramics, noble metals or semiconductors affording a polymer layer with hydroxyl groups which was used as a initiator for ROP of ε-caprolacton.[129] It was believed that simple polydopamine, which in fact is much cheaper than norepinephrine, cannot be used in this reaction due to the lack of hydroxyl groups. Our results revealed that on the contrary polydopamine is able to performed ROP polymerization of cyclic ‘‘dimer’’ of LA on various materials (see chapter 2.2.4).

1.3 Functionalization and application of magnetic nanoparticles

The stability of MNP is an important issue when it comes to their further application. Ways to stabilize MNP were discussed in previous sections. However, in order to obtain functionalized MNP respective functional groups have to be introduced after stabilization. To modify MNP a variety of chemical reactions are available. Grafting of molecules can be achieved either by direct coupling or stepwise by first utilizing linkers which next react with active groups. It is more common to prepare the aimed ligand in full and to immobilize it in the last step.

Amino groups attached to the shell of MNP are very versatile in order to fix functionality. A variety of reactions can be used for this purpose (see Figure 9).

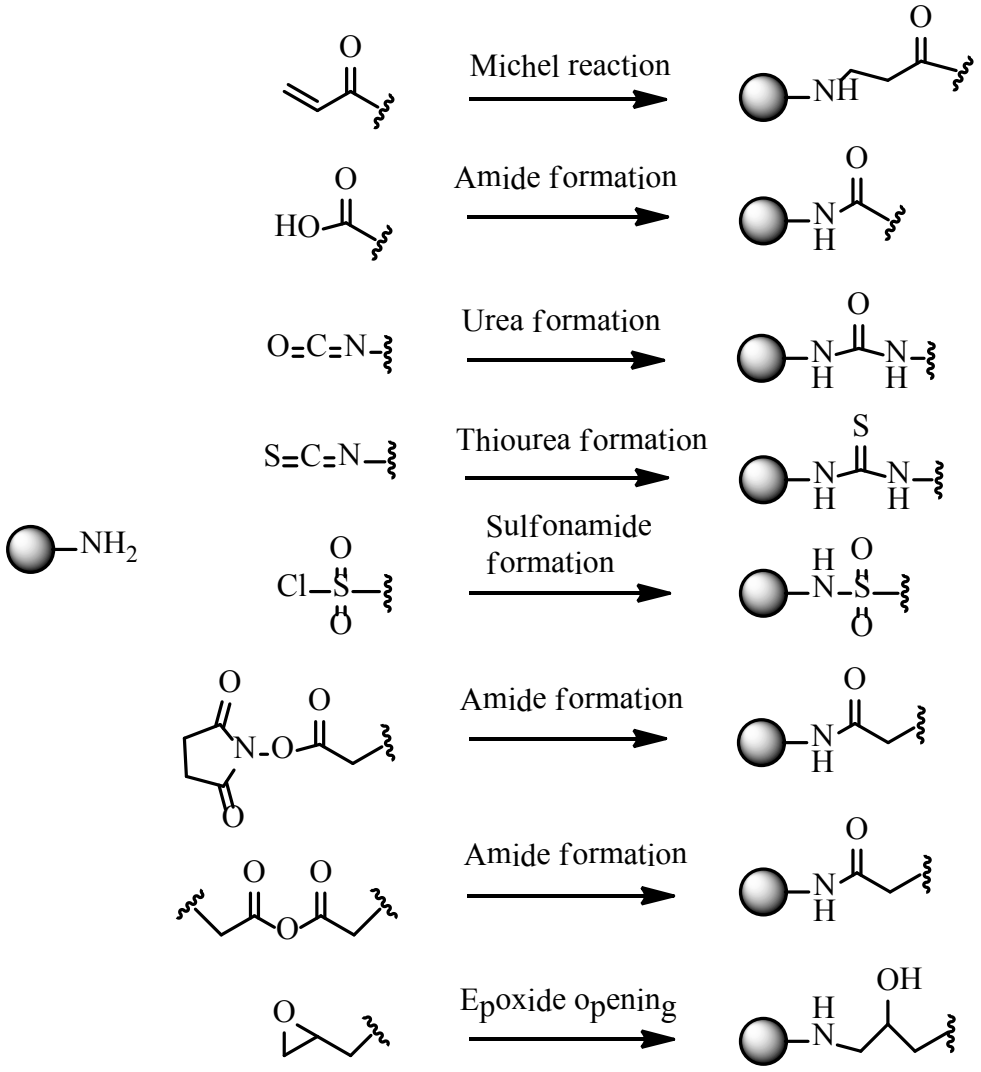

Figure 9. Possible reactions of amino functionalized MNP.

Amongst them, amide formation with carboxylic acid is the most common. Moreover, this way is not only limited to relatively small molecules but can be applied to bind proteins too.[130] Amide bond can be formed also in reaction between amino groups of the particles and activated carboxylic moieties, e. g. anhydrides, *N*-hydroxysuccinates or acyl chorides.[131] The reaction with isothiocyanates or isocyanates forming thioureas or ureas, respectively runs under very mild conditions and thus has been used often e. g. in bio-related cases.

If further functionality is to be introduced to MNP containing amino by a linker in a two step-procedure, glutaraldehyde has been used in particular for fixing proteins. It forms imines with the amino groups of the MNP in a first step while the second aldehyde moiety is used later on in the reaction with a protein. Besides glutaraldehyde iodoacetyl and a maleimide group were frequently used as linkers.[132]

Literature data about functionalization of MNP with various molecules or biomolecules is enormous. Therefore, only few examples are cited to exemplify aforementioned ways.

Xu[87] et al. used a double amide formation protocol to combine protected dopamine with bisphosphonates derivative via succinate linker. After cleaving the protecting groups the obtained dopamine derivative was submitted to ligand exchange reaction with magnetite NP and used for removing uranyl ionons from blood and water. Since the dopamine molecule contained two units with affinity to magnetite NP surface it was important to know which moiety interacts with Fe_3O_4 surface. Conducted test showed that the catechol unit was bounded to maghemite NP surface while the bisphosphonate part acted as chelating agent for uranyl ions. In an analogous way a succinate linker was used to fix *N*α,*N*α-bis(caboxymethyl)lysine as metal chelating agent.[83] Modification of maghemite NP bearing chelating group with Ni, Co and $SMCo_{5.2}$ allowed to bind protein from cell lysate through histidine tagging. Such systems were stable in high salt concentrations and at elevated temperature. Similar methodology was also utilized by Lin and co-workers in order to graft bis nitrilotriacetic acid (NTA) moiety.[133] Sun synthesized an amide, from dopamine and a tetraethylene glycol diacid, which was introduced to magnetite NP via ligand exchange reaction.[134] In the next step, they attached a fluorescent Eu (III) complex of tris(dibenzoylmethane)-5-amino-1,10-phenantriline by EDC/NHS coupling protocol. Modified MNP were often used as a probe for magnetic resonance and fluorescent imaging. Choi reported the reaction between magnetite NP covered with polyacrylic acid and 2-aminoethyltrimethyammonium chloride hydrochloride via EDC.[135] The resulting

magnetite NP were used as labelling agent for human mesyncham stem cells. Gu[136] et al. performed amide formation as key reaction to prepare peptide dendrimers based on lysine. Dendrimers were built from dopamine by applying amide formation. The dendrimers were grafted on magnetite NP replacing an original layer of oleic acid. The resulting magnetite NP exhibited very high magnetization values and could be used as nano platform for bioapplication. Börner et al. utilized amino modified magnetite NP for peptide synthesis in "quasi solution".[137] Amide formation was used to attach Rink-Linker which serves as a starting point for further reactions. The group of Kang used the Michael reaction to prepare dendrimers.[138] At first a layer of silica was deposited on magnetite followed by grafting of 3-aminopropyltrietoxysilane (APS) to obtain amino functionalized MNP. The resulting magnetite NP were submitted to Michael reaction with propargyl acrylate and successive click reaction with azidopolyesteramine, which underwent again Michael reaction with propargyl acrylate. Dendrimers modified magnetite NP were used in CuACC reaction with azido floureseine. Resulting floureseine functionalized magnetite nanoparticles were nontoxic towards certain fibroblasts. Sulfonamide linking was used to bind dansyl chloride to amino modified magnetite NP covered with amino silane shell.[139] Magnetic NP were applied as a probe for MRI imaging coupled with confocal microscopy. Bae et al. reported a reaction between triethoxy(3-isocyanatopropyl)silane and modified terpyride to form an urea.[140] This was bound on MNP and modified with Cu^{2+}. The resulting nano-complex was applied in protein purification through histidine tagging. Horak et al. used thiourea linking to attach FTIC on silica coated and carboxymethyl chitosan coated magnetite NP.[141] Rat brain imaging was performed with these two types of magnetite NP. The Chen group presented a reaction between glutaraldehyde and amino silane covered magnetite NP to yield imine formation.[142] In the next step aminophenylboronic acid was added followed by reduction with $NaBH_3CN$. The achieved magnetite NP were used in selective capture of glycoproteins.

If MNP are covered with groups bearing carboxylic acids again amide formation is a good strategy to fix desired functional molecules. In addition, esterification protocol can be taken under consideration. Santamaria et al. performed amide formation on magnetite NP containing carboxylic groups and model antibodies.[143] Immunoreactivity was checked by the ELISA test.

Magnetite NP possessing thiols on the surface can undergo reaction with maleimide and pyridyl disulfide from activated molecules or proteins.[144] It has been shown that molecules containing thiols may react with magnetite NP bearing disulfide on the surface

as well. Recently thiol groups have often been used in the so called thiol-ene click reaction. Here, thiol is added to double or triple bond in presence of radical initiator like AIBN or light irradiation. This methodology was applied to bind cysteine to allyl modified MNP.[145] The obtained MNP were tested as probes for MRI. Warner et al.[146] utilized the thiol-ene click concept to attach allyl modified diphosphonic acid, to magnetite NP covered with 3-mercaptopropionic, acid by UV irradiation. The resulting MNP were checked as sorbent for metals. Garrel et al.[147] applied thiol-ene click chemistry for the synthesis of various ligands including proline and quinine. All these ligands were based on triethoxysilanes and were applied to coat magnetite NP.

The concept of click chemistry was first described by Sharpless in 2001.[148] It involves reactions which connect small units in a fast and reliable way. Ideally, a click reaction should exhibit the following features:

- be modular;
- be wide in scope;
- give very high chemical yields;
- generate only inoffensive by-products;
- be stereospecific;
- be physiologically stable;
- exhibit a large thermodynamic driving force to favour a reaction with a single reaction product;
- have high atom economy.

There are several types of reactions, which fulfil the aforementioned requirements. The Cu(I)-catalyzed azide-alkyne cycloaddition (CuAAC), other cycloaddition reactions, addition of nucleophilies (-SH, NH) to α,β-unsaturated carbonyl/sulfonyl compound are the most important. For functionalization of MNP the CuAAC reaction has been most often used.

Originally, the mechanism was proposed by Sharpless and seems to be still the most up- to-date.[149-150]

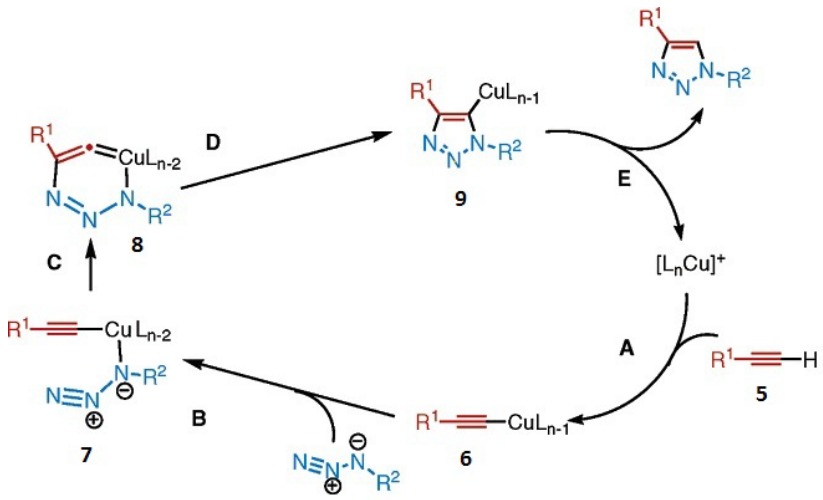

Figure 10. CuAAC mechanism proposed by Sharpless.

In the first step (A) copper coordinates to alkyne and looses one ligand (either acetonitrile or water). In the next step (step B) the azide replaces other ligand and binds to the copper atom via the nitrogen proximal to carbon, forming intermediate **7**. Attack of the distal nitrogen on C-2 acetylide carbon atom yields six-membered copper(III) metallacycle **8** in step C, which undergoes ring contraction (step D) forming the triazole-Cu-compound **9**. In the last step (E) the intermediate **9** is hydrolyzed and releases the triazole by regenerating the Cu-catalyst.

Starting materials for CuAAC click reaction are either commercial or often accessible in a straightforward way. The functionality to be introduced by CuAAC can be found either in the azide or in the alkyne partner. Here, only a few examples are given to present the versatility of CuAAC in functionalization of MNP.

Turro et al. bound either phosphonic acid derivatives bearing azide or carboxylic acids with alkyne moiety via ligand exchange reaction on maghemite NP. [151] The resulting nanomaterials were submitted to reaction with an appropriate partner either alkyne or azide yielding the 1,2,3-triazol ring. Müller et al. fixed pentynoic acid on dopamine by amide formation and attached the material to magnetite NP by ligand exchange reaction.[152] Thereafter, magnetite NP were submitted to reaction with azido modified rhodamine resulting in fluorescent and water stable magnetite NP. In order to prepare nano-object equipped with azide or alkyne on the surface. Wu[153] et al. used magnetite NP covered with poly(acrylic acid). Amide formation with 3-azidopropane-1-amine or ester synthesis with propargyl alcohol gave magnetite NP ready for “click” reaction. As a proof of principle some molecule, like polyglycol or rhodamine were grafted on the surface of these

magnetite NP by CuAAC. An interesting way for the introduction of alkynes on MNP was presented by Hayashi et al.[154] Allyl-functionalized magnetite NP were submitted to reaction with NBS. As a result bromo hydrine was obtained. Nucleophilic substitution of bromide with NaN_3 yielded azido magnetite NP, which underwent reaction with an alkyne derivative of folic acid (FA). Immobilization of FA without affecting the α-carboxylic acid group resulted in the formation MNP useful for biomedical application. Motte et al. [89] applied (1-hydroxy-1-phosphonopent-4-ynyl)phosphonic acid (HMBPyne) as a scaffold for click reaction with variety of functional molecules. The reaction was enhanced by microwave (MW). The typical reaction time of 24 h was reduced to 2 minutes. Silane covered magnetite NP are often modified through "click chemistry". One of the earliest report comes from Jiang et al.[155] Magnetite NP equipped with amino groups were condensed with propiolic acid through an amide bond. The alkyne modified magnetite NP were then submitted to reaction with the azido partner like functionalized 3'-azido-3'-deoxythymidine (AZT), biotin, propanoic acid and 11-mercaptoundecanoic acid. Lin used sequences of reactions to synthesize magnetite NP bearing azido moieties.[156] Initially, amino functionalized magnetite NP were reacted with suberic acid diester. Remaining unreacted ester groups were next used in reaction either with 3-azidopropylamine or propargyl amine to furnish azide and alkyne modified magnetite NP. In this way, various useful compounds including flag peptide and biotin were joined to the surface of the magnetite NP. Moreover, alkyne green fluorescent protein was bound to azido magnetite NP. Other non specific binding was excluded by carrying out experiments with amino, alkynated or aminated magnetite NP where fluorescent was not observed. A straightforward method for the introduction of azide into MNP was shown by Prosperi et al[157] by diazotransfer reaction applied to amino group modified magnetite NP. This method has the advantage that subsequent "click" reaction could be conducted in one pot. In this way HAS protein was bound without losing activity. Xian et al. applied "click" chemistry to bind rhodamine B on magnetite NP.[158] Magnetite NP were first covered with silica via Stöber method. Later reaction with an aminoalkyltrialkoxy silane yielded aminated magnetite NP, which reacted with glutaric anhydride by ring opening. The resulting carboxylic magnetite NP were converted into propargylamides. Lastly, an azido rhodamine was attached to alkyne magnetite NP through CuAAC reaction. Kang used Michael and CuAAC reaction to built dendrimer from magnetite NP surface.[138] They did not show a significant cytotoxicity toward 3T3 fibroblasts and RAW macrophages after 24 h. Thus they might be used as suitable supports for multifunctional application. CuAAC allowed to

bind oligonuclotides to magnetite NP.[159] The tris(3-hydroxypropyltriazolylmethyl)amine (THPTA) ligand was necessary to catalyze the reaction in addition to cupper ions. Prepared particles exhibited sharp melting transitions and high cellular uptake, indicative of their dense functionalization. Das et al.[160] showed that magnetite NP can be functionalized chemoselectively by applying CuAAC. At first magnetite NP were covered with 2-aminoethyl phosphonic acid. The resulting magnetite NP were the basis for further chemoselective functionalization. Reaction with glutaric anhydride gave carboxylic modified magnetite NP. Unreacted amino groups were submitted to reaction with triflic azide to yield azido groups. The surface of the final MNP consisted of three types of reactive groups, carboxylic acids, azides and amines. Their different reactivity was exploited to bind three distinct functions. Amino groups underwent reaction with rhodamine isothiocyanate, azides reacted with propargyl folate and carboxylic groups were submitted to reaction with an anticancer drug via a carbodiimide protocol. This nanoplatform was deeply investigated and considered as "smart" multifunctional material. Indeed, in *vitro* cell uptake, MRI imaging, and apoptosis studies showed that the nanoparticles could simultaneously target, image and kill folate receptor overexpressing cancer cell.

1.4 Introduction to magnetic nanoparticles as a support for organocatalysts

Catalysis is one of the most important issues in chemistry. There is a still growing interest in synthesis of pharmaceutical and fine chemicals.[161] For a long time a major role has been played by metallic and organometallic catalysts and in part also by enzyme catalysis. However, recent years has brought big impact in so-called organocatalysis. The term organocatalysis refers to a form of catalysis, whereby the rate of a chemical reaction is increased by an organic catalyst, devoid of any metal, consisting (mainly) of carbon, hydrogen, sulphur, nitrogen, oxygen and phosphorus.[162-164] Organocatalysts are chiral or achiral small organic molecules, which accelerate a reaction in substoichiometric amounts. In addition, organocatalysts can often be applied under aerobic conditions in contrary to many metal based catalysts. They are often cheaper and meanwhile some of them are commercially available. Most of the chiral organocatalysts are derived from the chiral pool of nature. Higher catalyst loading in comparison to metal catalysis is one of the major disadvantages often faced in organocatalysis. To overcome this drawback much work has

been done to develop low loading organocatalysts, which can work with 2 mol% loading or lower.[165] This research is crucial for future development in organocatalysis. To privileged chiral catalysts belong proline, some primary amino acids, cinchona alkaloids, TADDOL and binaphtol derivatives.

Catalyzing organic reaction by small molecules is known for many years. Indeed, the discovery of the first organocatalytic reaction is attributed to J. von Liebig, who found that dicyan is transformed into oxamide in the presence of an aqueous solution of acetaldehyde (see Scheme 4).[166]

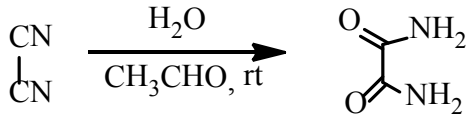

(4)

10 **11**

In mid 1950s activities of Prelog at al.[167] led to progress in asymmetric synthesis. Development in this field was also achieved by Pracejus[168] who reported that methyl phenyl ketene could be converted to (-) α phenyl methylpropionate in 74% ee by using *O*-acetyl quinine as catalyst. Next key event in the history of organocatalytic reaction was the discovery of L-proline-mediated asymmetric Robinson annulation reported during the beginning of 1970s.[169] This so-called Hajos-Wiechert-Eder reaction yielded products with 93 % ee if 30 mol % catalyst was applied (see Scheme 5).

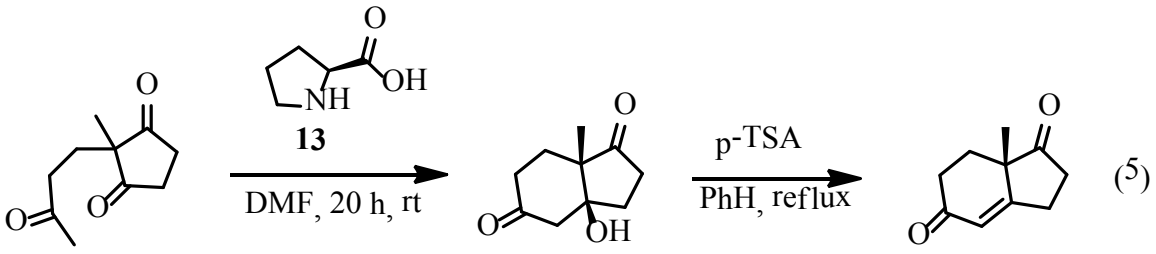

(5)

12 **14** **15**

The latest flourishing time for organocatalysis has started with pioneering results from List[170], MacMillan[171] and Dalko.[163-164] Since then, organocatalysis has found application in many reaction types, such as aldol and Michael reaction[172], asymmetric version of Diels-Alder cycloaddition,[173-174] domino reactions[175] and natural product synthesis[176-177] It has been shown that it is possible, using organocatalysts, to perform asymmetric synthesis of such a complex systems like indolines[178] (domino reaction), six-

membered carbocycles[179] or important motif in natural product synthesis the Wieland–Miescher ketone.[180] Among the privileged catalysts, proline and its derivatives seems to be one of the most common.[181] What favours proline among others is that is cheap and easy available in two enantiomeric forms. It is bifunctional with a carboxylic acid and an amine moiety. These two functional groups can both act as an acid or base and can facilitate chemical transformation. All these criteria might be applied for other amino acids but proline is secondary, cyclic and thus more rigid. These structural factors led to increased pKa values than in others amino acids. Originally, List proposed an enamine activated pathway for proline catalyzed reaction between acetone and isobutyraldehyde. MacMillan postulated iminium intermediates for his reaction. Both intermediates in addition to others are accepted now. Recently, original enamin[182] and iminium[183] catalysis has been extended to dienamine[184-185] and trienamine[186-187] and SOMO[188] (singly occupied molecular orbital) catalysis characterized by the formation of enamine radical cations.

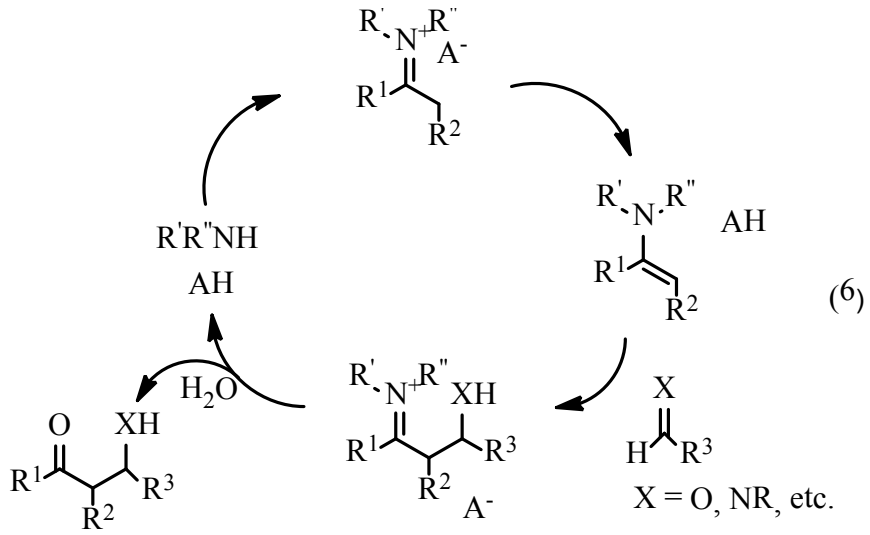

(6)

Immobilization of either metal- or organocatalysts is a branch of catalysis of great interest to industries. This field is intensively explored and many solid supports have been introduced. Fixing catalysts on solid supports allows to reuse it without contamination of final product what is often a problem in homogenous catalysis. Finally the so-called greenness of a process can also be addressed when considering the immobilization. For immobilization of proline often expensive 4-hydroxyproline is used as starting material. Its immobilization gives the chance for reuse and for a more economic and "green" application. Fixed catalysts sometimes give close results to their homogeneous equivalents. Nevertheless, in some cases selectivity and reactivity are reduced as a result of steric and

mass transport effects, since the large portion of the catalyst actives sites is buried in the supporting matrix[189]. Thus reactants have limited access to active sites, a phenomenon not occurring in homogenous catalysis. Such a situation may even lead to total blocking of the catalyst or limits in repetitive recycling of the catalyst.

Organocatalysts immobilization can be achieved in three ways:[190]

- Covalently supported catalysis

Here two types of supports are possible, such as soluble supports: PEG (polyethylene glycol), dendrimers, soluble polymers, or insoluble supports: porous materials (i.e. MCM-41), polystyrene (Merrifield resin) and other polymers (i.e. Wang resin, TenataGel^{TM}), magnetic nanoparticles and silica gel.

- None covalently supported catalysis[191]

In this group the catalyst is adsorbed (i.e. on IL (ionic liquid)-modified silica gel) or dissolved (polyelectrolytes), included (β-CD) or attached by electrostatic interactions (PS/SO_3H and layer double hydroxide (LDH)).

- Biphasic catalysis

In this case, catalyst is dissolved in ionic liquid and product is extracted using immiscible solvent. Development in this type of supported catalysis has led to ionic liquid tagged catalysts. Such catalysts are mostly based on imidazol[192] or triazole ionic liquids.[193-194]

In order to solve problems in heterogeneous catalysis a lot of efforts have focused on the preparation of new catalytic systems, which allow easy separation and provide selectivity of chemical transformations with excellent yield. Magnetic nanoparticles have an attractive high surface area, which is comparable with those of porous materials but without the inherent problems of mass transport and accessibility of active sites. MNP can be employed in a quasi homogeneous phase and are considered as an intermediate between homogenous and heterogeneous catalysis.[1,195] MNP have been successfully used as a supports for metal-containing catalysts. This field seems to be more exploited than

organocatalysts immobilized on MNP. Magnetic tagging of organocatalysts is a rapidly growing field in contemporary research. One of the first reviews summarizing immobilization of organocatalysts on MNP was published by us. Similar classification like for homogenous organocatalysis can be applied to magnetically supported organocatalysts.[196] In this thesis only chiral amines and amino acid derivatives fixed on MNP will be mentioned.

1.4.1 Immobilization of chiral amines on magnetic nanoparticles and application in catalysis

Surprisingly, in the literature there are only a few reports about linking of magnetic nanoparticles to chiral amines and their application in asymmetric synthesis. (S)-Diphenylprolinol trimethylsilyl ether (so-called Jørgensen-Hayashi-type catalyst) is known to be one of the most powerful organocatalyst and was applied in numerous types of reactions. This catalyst was fixed on magnetic nanoparticles either via the phenyl or the pyrrolidine moiety.

In the first case (Scheme 7, compound **20**) the vinyl derivative **16** was converted into a trimethoxysilane **18** by thiol ene-click reaction and then connected to silica covered magnetite NP **19**.[197] The resulting MNP **20** (diameter 200 nm) performed very well in Michael addition of several aldehydes to nitrostyrenes but not as good as the homogenous version of the catalyst. Recycling via magnetic separation was performed for 4 times without a significant loss of catalytic efficiency. In another approach (Scheme 7, catalyst **24**),[198] linkage of the catalytic unit was implemented by CuAAC click reaction of its propargyl ether **23** with azidopropylsilyloxy coated magnetite NP **22** (5 nm size). The nano-catalyst was also applied to Michael reaction of propanal to *trans*-β-nitrostyrenes and performed better in comparable cases than **20** linked via the phenyl unit, although the catalyst **24** was even applied in less amounts (10 mol% versus 20 mol%, respectively). Recycling was demonstrated for 4 subsequent runs while a drop of yield from 81 to 57 % occurred after the 3rd recycling. It was assumed that the drop was caused by hydrolytic loss of the silyl group attached to the catalytic moiety and to some extent by ligand leaching. An astonishing fact was observed when **24** was used in Michael addition of acetaldehyde to *trans*-β- nitrostyrene because this gave rise to a racemic mixture of products.

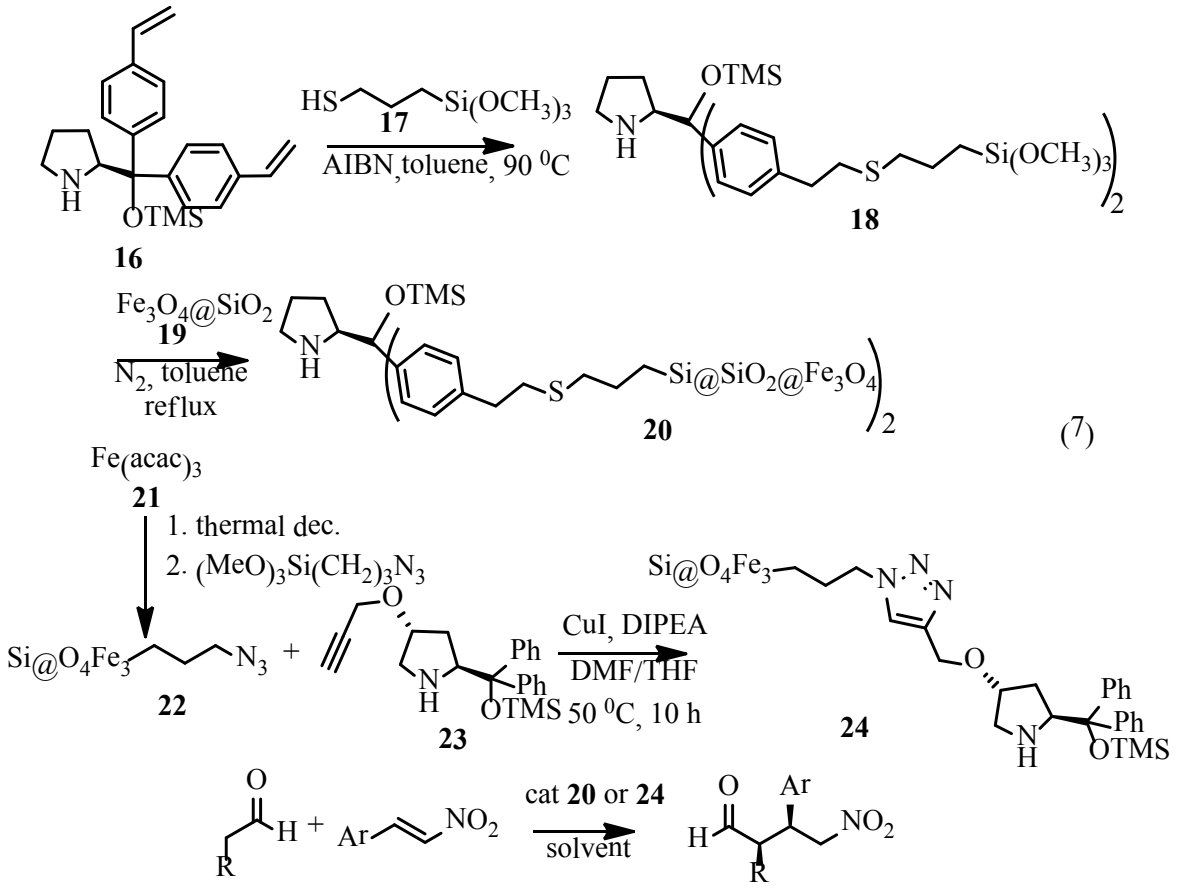

Results for **20** (20 mol%): yield 53 - 96%, ee 75 - 90%, dr 75:25 - >99:1
24 (10 mol%): yield 70 - 89%, ee 75 - 97%, dr 75:25 - 89:11

Alternatively to magnetite NP **20** and **24**, carbon-coated cobalt NP **25** were used as supports for a Jørgensen-Hayashi-type catalyst. They were transformed into Merrifield resin-like core shell structures and further modified by click methodology (Scheme 8).

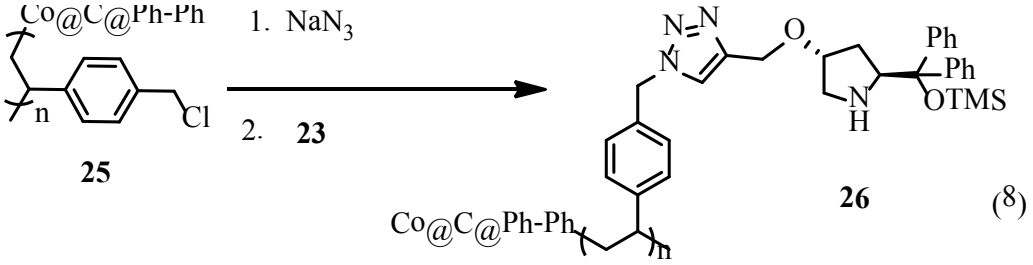

(8)

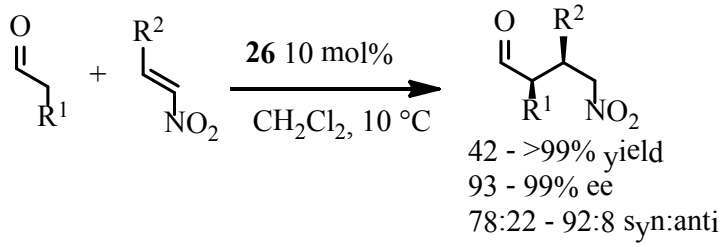

42 - >99% yield
93 - 99% ee
78:22 - 92:8 syn:anti

Material **26** was applied to nitro-Michael reaction giving very good results in terms of yields, enantioselectivity and diastereoselectivity. However, recycling of this catalyst was not so efficient as compared to the aforementioned catalysts **24** and **20**. A noticeable drop of yield from 99 % to 34 % occurred in the fourth run.[199]

Silanization was employed to fix the chiral diaminocyclohexane derivative **28** (see Scheme 9).[200] The resulting catalyst **29** was successfully applied in direct asymmetric aldol reactions of aromatic aldehydes with acetone or cyclohexanone in the presence of TFA as co-catalyst in water at room temperature. The catalyst could be recycled 10 times in a model reaction wherein it did not show a significant drop in yields and stereoselectivity during the first seven runs.

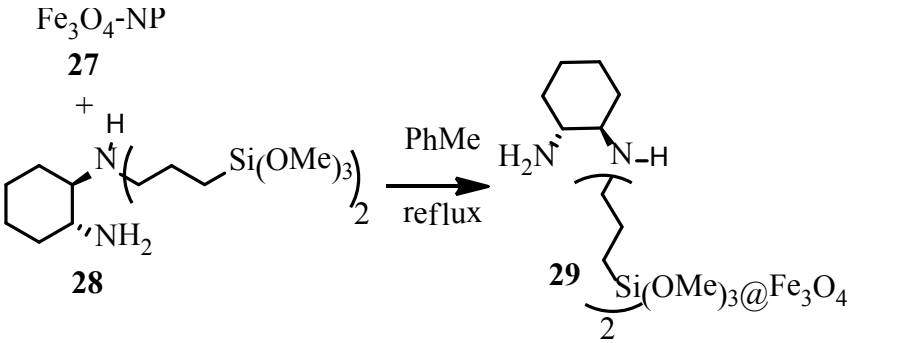

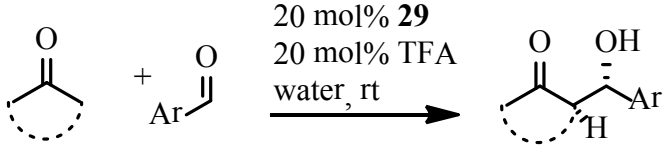

(9)

60-98% yield, 84-98% ee. 2:1-13:1 dr

A chiral Steglich base type catalyst consisting of pyridine and a chiral pyrrolidine **32** was synthesized on magnetite NP by covering them first with N-methyldopamine **30** followed by nucleophilic substitution at the 4-chloropyridine **31** (Scheme 10).[201] The resulting catalyst was used in kinetic resolution of cycloalkanols or 1,2-dihydroxycycloalkanes with very good enantioselectivity even at conversions higher than 50%. Recycling tests showed high recyclability and indicated complete absence of degradation. It is noteworthy to mention that application seems to be limited to cycloalkanols with a large group close to the OH group.

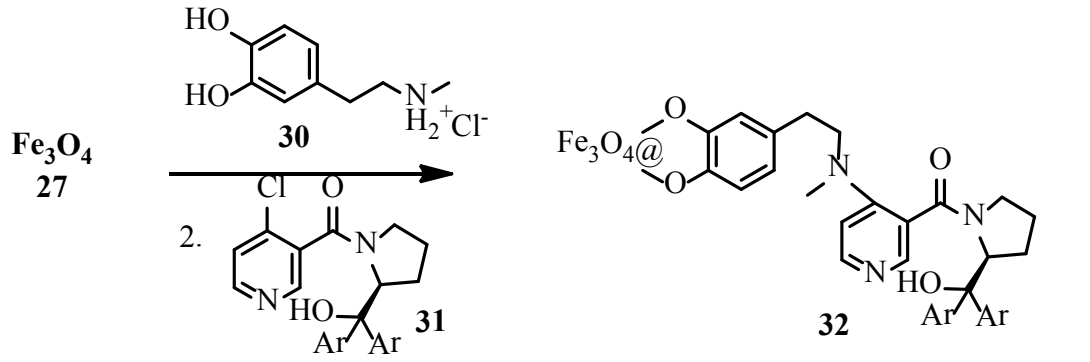

(10)

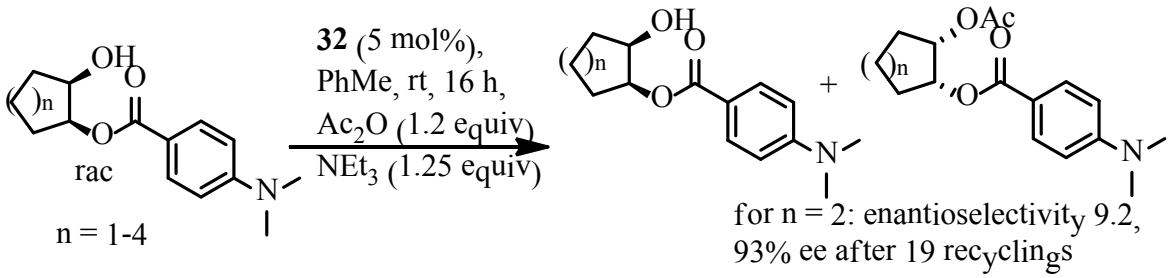

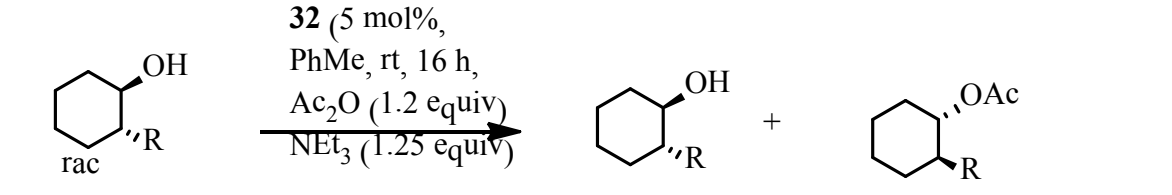

Cinchonine-derived ureas **33** and or sulfonamides **33a** were linked to **34** via silanization and thiol ene click reaction (Scheme 11).[202] Resulting catalyst **35** was successfully applied in Michael addition of dimethyl malonate to ß-nitrostyrene but the

enantioselectivity was modest (up to 71% ee) and the catalytic activity dropped in the fourth recycling to 46% conversion (Figure 19). The performance of the sulfonamide **36** in desymmetrization of meso esters with methanol or allylic alcohol was better. Excellent yields up to 97% and ee up to 82% were achived. The catalytic systems could be reused 28 times without showing any diminished performance. In addition, **36** was applied to different reactants in different subsequent runs.

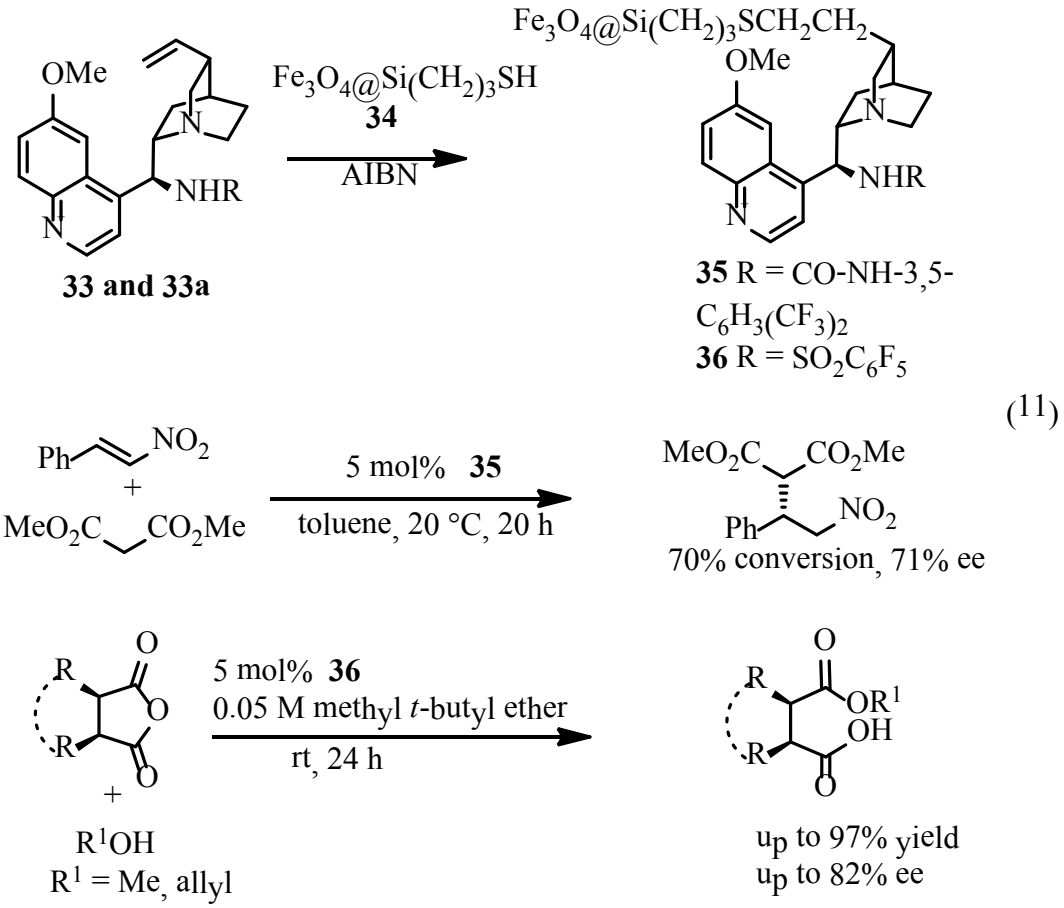

Cinchonine-derived thiourea was fixed to mercaptoalkylsilyl-functionalized magnetite NP by thiol-ene reaction. NP **37** were applied in Diels-Alder-reactions of inversed electron demand. A variety of diene components was used giving either cyclohexene cycloadducts or azlactones with excellent yields impressive enantioselectivities (Scheme 12). Recycling experiments did not show a significant drop in yield and enantioselectivity up to 10 runs.[203]

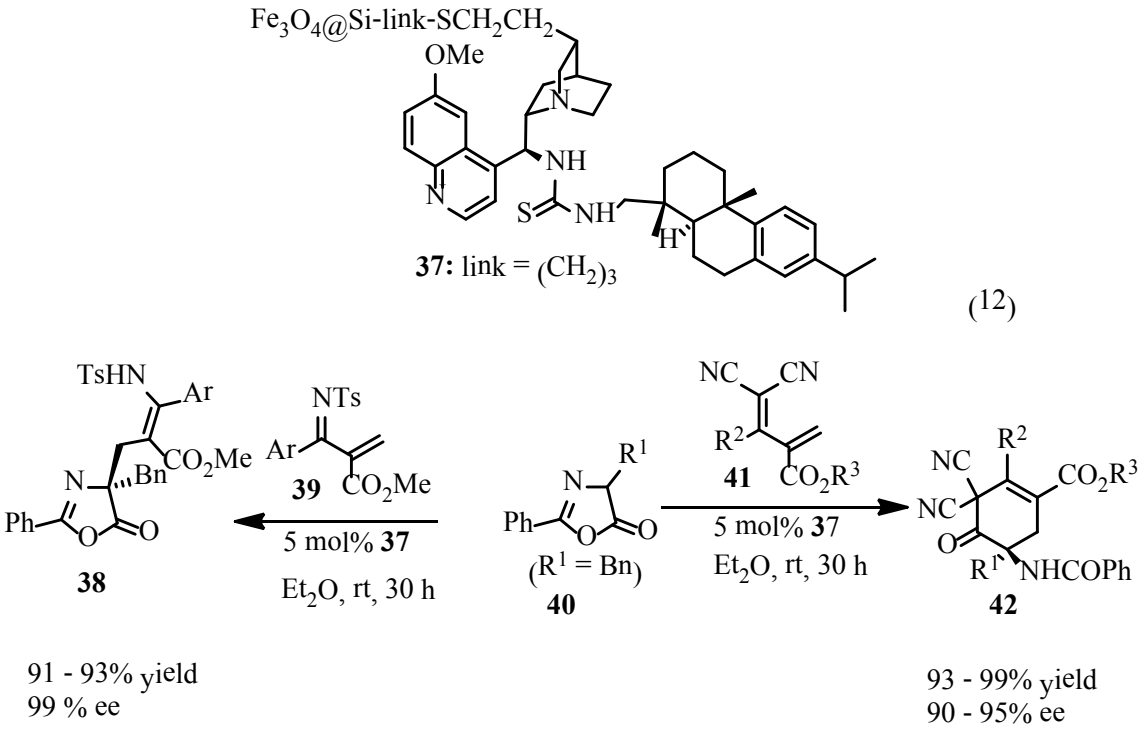

1.4.2 Immobilization of amino acids on magnetic nanoparticles and application in catalysis

One of the first few examples of applications of amino acids and derivatives in asymmetric synthesis was elaborated in our group by Zekarias Yacob.[17] Various types of acrylate and methacrylate monomers bearing the (*S*)-proline moiety differing in length of linkers were submitted to polymerization reactions in the presence of magnetite NP covered with acrylic acid or a methacryloyl-containing phosphate (Scheme 13). The resulting magnetite NP **46**, **47, 48** and **50** were successfully applied in 10 mol% to direct asymmetric aldol reactions of arylaldehydes with ketones (see Scheme 15). The application of benzoic acid as co-catalyst was a key factor in order to obtain high yields and excellent enantioselectivities, in particular when **48** was used. The catalyst **48** could be used with variety of substrates and easily be separated by magnetic decantation. Recycling tests revealed that the catalyst **48** maintained its excellent catalytic performance till 10 recyclings while the type of reactants could be changed in the different steps.

4-Hydroxyproline was converted into triethoxysilylpropanecarbamate derivative and latter on attached to magnetite NP via silanization reaction. (Scheme 14).[204] Catalyst preformed in aldol reaction of cyclohexanone with several benzaldehydes yielding moderate to good yields, diastereoselectivities and enantioselectivities. Nevertheless, the results were not as good as in cases of the polymer coated magnetite NP **48** mentioned

above even when 20 mol% catalyst was used instead of 10 mol% (see Scheme 15). Furthermore, only 5 recycling could be carried out without significant loss of performance.

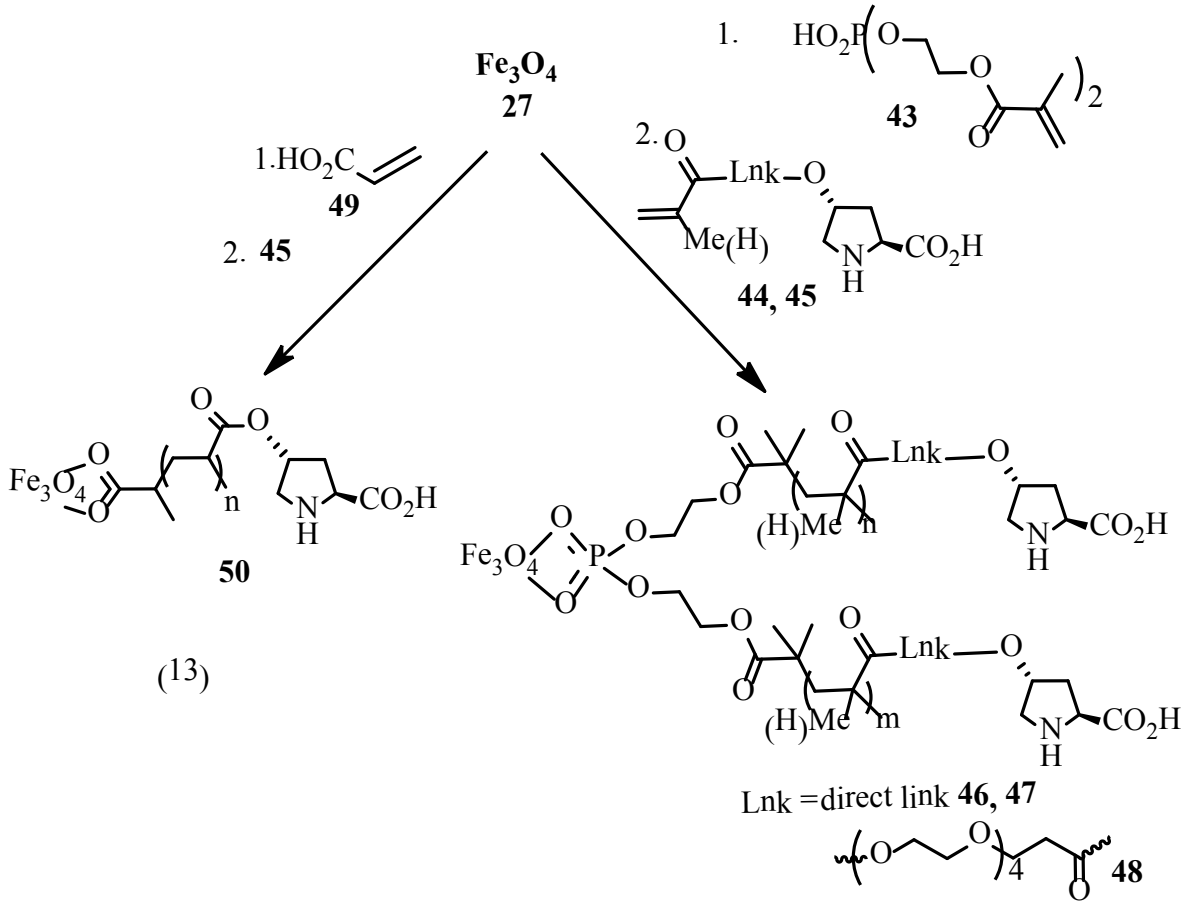

(13)

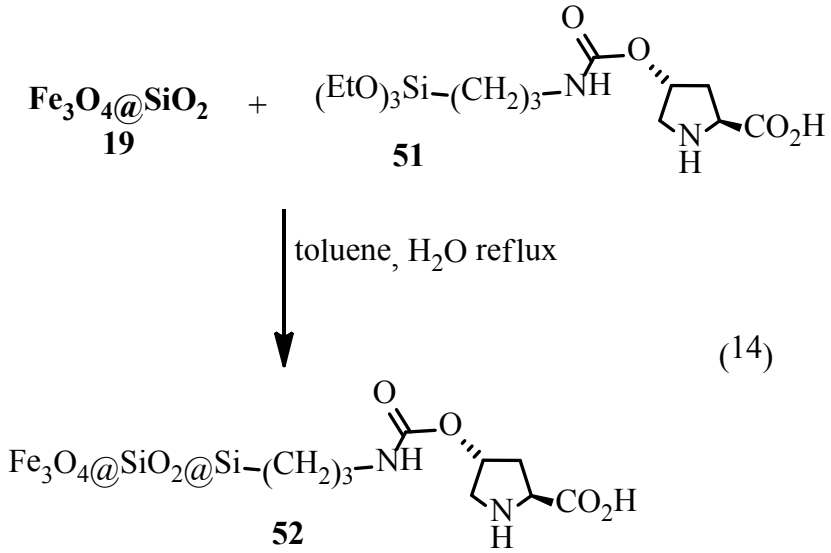

(14)

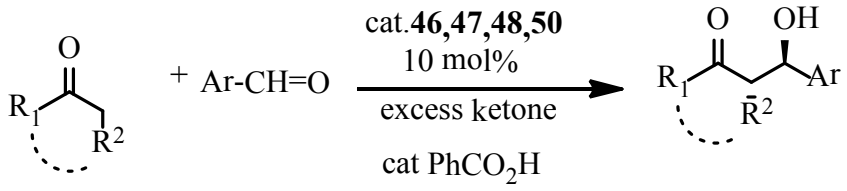

Results for catalysts **46,47,48,50** 76 - 94% yield
88 -> 99% ee
dr 55:45 - 83:17

(15)

20 mol% **52**, EtOH

Results for catalysts **52** 24 - 96% yield
6 - 99% ee
dr 45:55 - 98:2

(*S*)-Proline was also linked to MNP by transforming their carboxyl groups into amides starting with silica coated magnetite NP **27** (Scheme 16). Either they were first covered with imidazolylalkylsilane **53** and then alkylated with the proline derivative **54** affording magnetite NP **55.** Alternatively, treatment of magnetite NP **27** with **56** followed by acylation reaction with the *N*-protected proline **57** gave functionalized MNP **58**. Catalyst **55** performed better when applied in asymmetric direct aldol reaction than catalyst **58** giving high yields and enantioselectivities in selected cases. Recycling experiments revealed that the yield slightly diminished from initially 92% to 89% while the ee remained constant at 85% after the fifth run.[205]

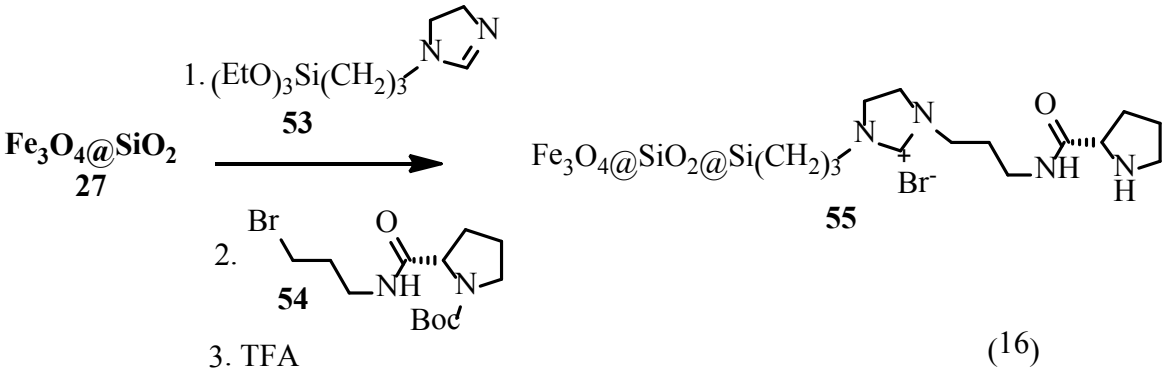

(16)

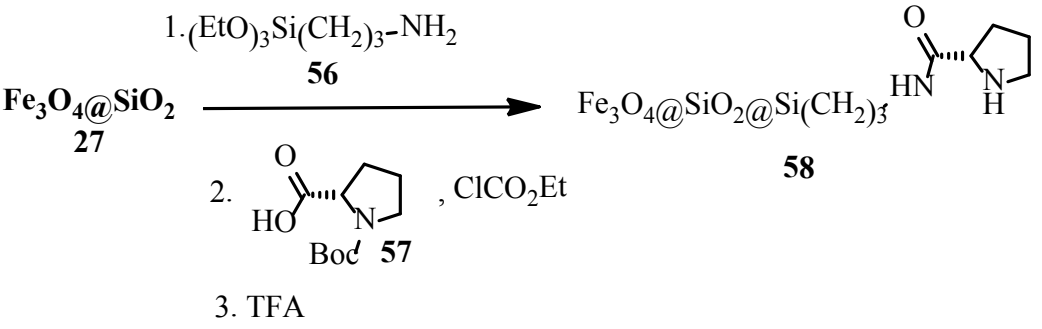

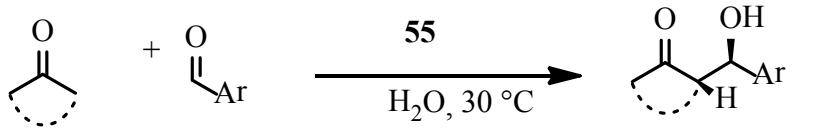

30 - 96% yield
45 - 86% ee
33:67 - 99:1 d.r.

The immobilization of a MacMillan type catalysts, based on (*S*)-phenylalanine, on magnetite NP was demonstrated by CuAAC click chemistry (Scheme 17).[206] The initial magnetite NP were obtained by thermal decomposition followed by covering with an azidopropylsilyloxy-shell. In the next step they were submitted to copper catalyzed cycloaddition reaction with the appropriate phenylalanine propargyl ether derivative. The resulting nano-catalyst **59** was used in asymmetric Friedel-Crafts alkylation (Michael type reaction) of N-substituted pyrroles with α,β-unsaturated aldehydes. In a similar way the MacMillan type catalyst was also immobilized on polystyrene. Its application applied in the same reaction led to higher yields and enantioselectivities in shorter times. However, the activity of the catalyst attached on magnetite NP retained until the fifth recycling while

the polystyrene based catalyst led to a decrease in yields after the third cycle. In both cases the ee´s were unchanged until the sixth cycle. That is why modified magnetite NP were better, from the practical point of view, than polystyrene bearing the same catalyst because they could be easier separated and revealed more stability in the recycling test.

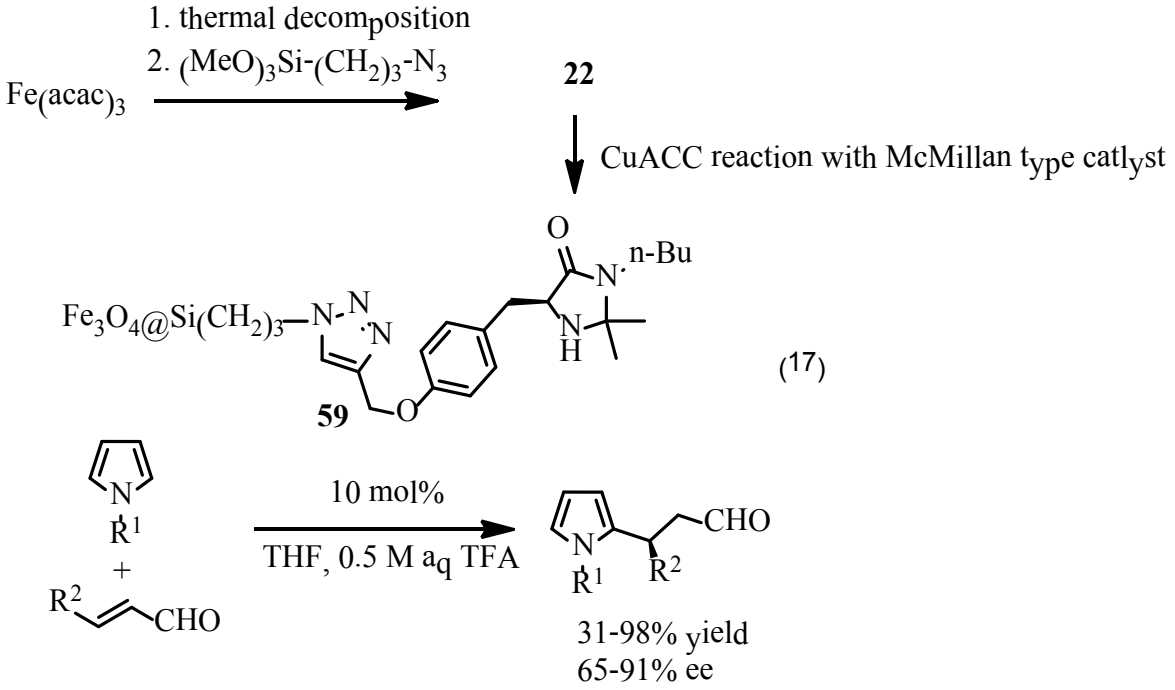

(17)

The Mannich reaction between cyclohexanone, anilines and benzaldehydes was catalyzed by magnetite NP **60** functionalized with cysteine (Scheme 18).[207] Products were obtained under neat conditions with 5 mol% catalyst in moderate to excellent yields. Nevertheless unsatisfactory diastereoselectivities were obtained. It is important to stress that information about enantioselectivities are missing. The catalyst could be used in nine consecutive cycles. The same nano-catalyst was applied in 3-component synthesis of hydrogenated quinoline carboxylates.

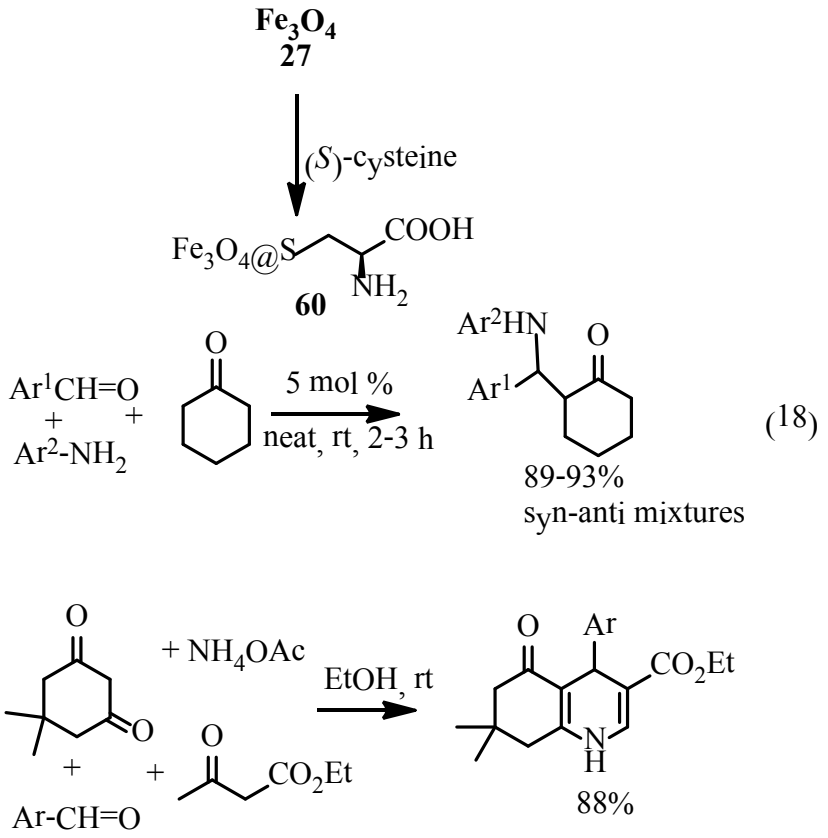

Cysteine was attached to vinyl modified SBA-15 via thiol-ene click chemistry. These mesoporous materials were mixed with magnetic nanoparticles what afforded incorporation of magnetite NP into the pores. The Fe_3O_4@mesoporous nanocatalyst **62** was applied in Biginelli condensation of aldehydes, acetoacetate and urea to obtain dihydropyrimidones in good yields (Scheme 19). Recycling test presented that this catalysts could be used 7 times without a significant loss of activity. Again, the issue of enantioselectivity, which can be expected with this chiral catalyst, was not addressed.[208]

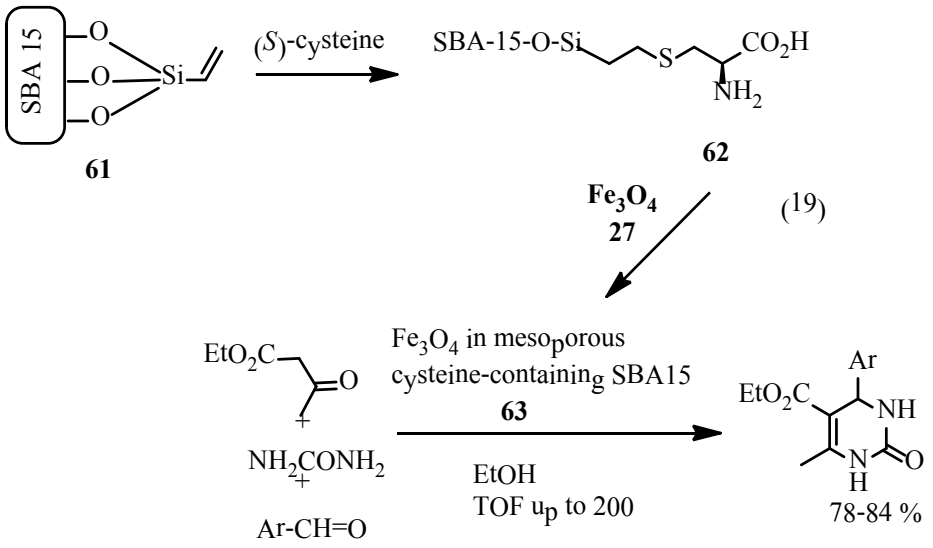

1.5 Aim of the Work

Taking into consideration the huge importance gained by the magnetic nanoparticles so far, the present thesis aims to new contributions to this field by the development of new magnetic nanoparticles useful as organocatalysts and with interest for bioapplications. For reasons of availability, price and biocompatibility magnetite is used as magnetic core in most cases while organic materials serve as shells for the new core shell nanoparticles. The target nanoparticles have to be designed in such a way that they are superparamagnetic with high saturation magnetisation values in order to manipulate them by external magnetic fields. Four types of organic shells are to be addressed:

1. New fatty acids with applicatory functions connected to the terminus;
2. Dopamine derivatives with reactive, catalytic or biorecognition functions attached to the amino group;
3. Polydopamine with reactive, catalytic or biorecognition functions;
4. Polyacrylic or polymethacrylic acid derivatives with reactive, catalytic or biorecognition functions.

In order to fix the applicatory functions to the magnetic nanoparticles two strategies have to be taken into consideration: First, a “grafting to” like fashion where precursor molecules already containing the applicatory function are used to cover the magnetite core. Second, in a “grafting-to” like manner the applicatory function is fixed to the core-shell nanoparticles by proper reactions tolerating the functionality. The new magnetic core-shell nanoparticles are to be characterized by several methods such as FTIR (Fourier transform infrared spectroscopy), elemental analysis, XPS (X-Ray Photoelectron Spectroscopy), magnetic measurements, TEM (Transmission electron microscopy), TGA (Thermogravimetric analysis) and DLS (Dynamic light scattering). Monomer precursor compounds have to be characterized by NMR, MS and FTIR spectroscopy. The new magnetic core-shell nanoparticles furnished with a catalytic function are to be tested as organocatalysts in appropriate reactions, while the important feature of recycling of the catalyst by magnetic decantation has to be investigated.

2 Results and Discussion

2.1 Synthesis of magnetic nanoparticles stabilized with new non-polymeric coating agents

2.1.1 Synthesis of magnetic nanoparticles stabilized with novel derivatives of fatty acids

Fatty acids have been used as stabilizers for magnetic NP for a long time. It was stated before that the carboxylic group has affinity to the surface of magnetic NP and one of the most common applied fatty acid is oleic acid. Unfortunately, this compound can be utilized only as a stabilizer without giving the possibility to link functionality. Click chemistry has been successfully applied in magnetic NP surface engineering.[209] We tried to apply the CuAAC methodology to introduce functionality onto magnetite NP covered with modified fatty acids.[210]

The following synthetic route was chosen to prepare novel derivatives of fatty acids (Scheme 20). Commercially available bromododecanoic acid **64** was converted into the known azide derivative **65** by reaction (20) with sodium azide in DMSO.[211]

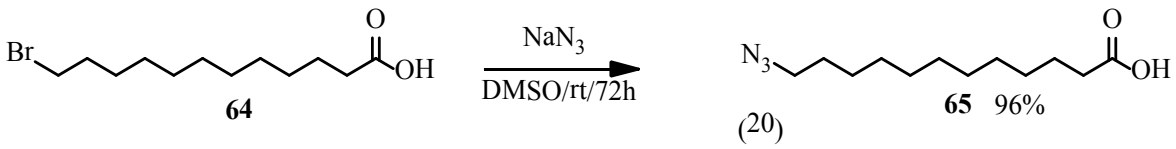

As partners for CuAAC four alkynes derivatives of proline[212] (organocatalyst), quinine[213] (organocatalyst), biotin[214] (recognition function) and galactose[215] (cancer therapy) were synthesized according to literature procedures.

The alkyne derivative **68** was obtained by reaction of quinine **66** with Br_2 in DCM followed by a dehydrobromination step performed with 10 eq. of dry NaOH in THF at rt. In this way, the desired compound **68** was obtained in moderate yield 40 %, which was lower than reported in the literature 66 %.

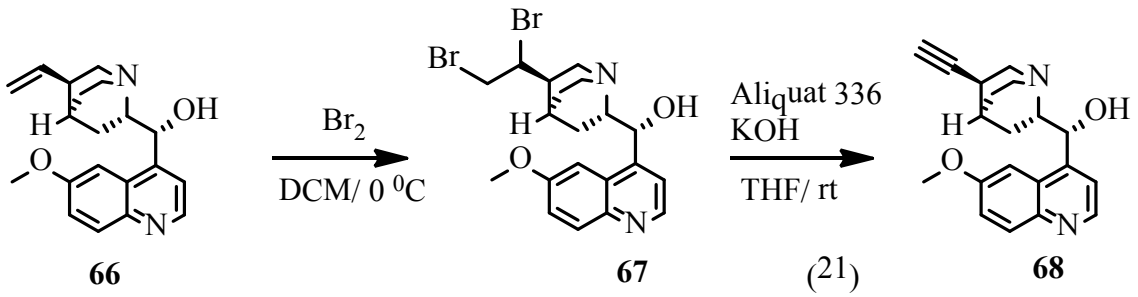

66 **67** (21) **68**

The propargylated 4-hydroxyprolinate **72** was obtained from *trans*-4-hydroxy-L-proline **69** in a three steps procedure by *N*-Boc protection (formation of **70**) using $(Boc)_2O$ and 10% NaOH, transformation into the *t*-butylate **71** (excess of *t*-BuBr (22 eq) in presence of K_2CO_3 and catalytic amount of benzyltriethylammonium chloride and finally propargylation with propargyl bromide in presence of NaH in dry DMF gave target molecule **72** in yield of 75 %.

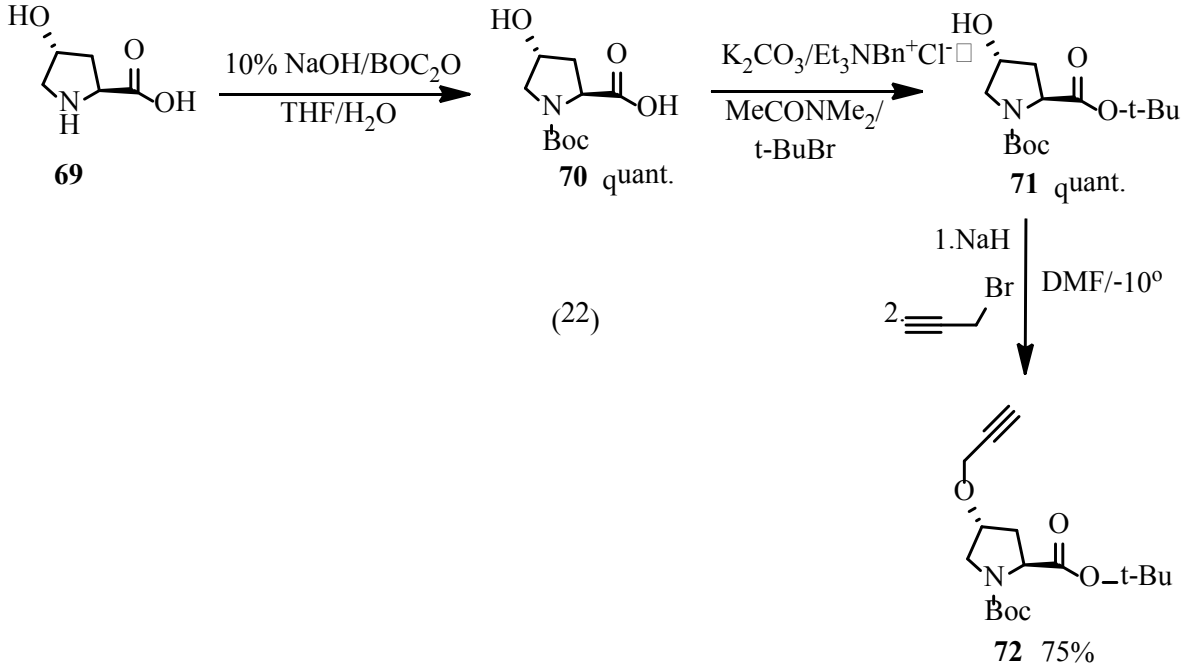

69 **70** quant. **71** quant.

(22)

72 75%

Commercially available propargyl amine **74** was used to introduce alkyne moiety into biotin via amide bond formation using a standard EDC coupling protocol with HOBt and DIPEA as tertiary amine. The biotin derivative **75** was obtained in very good yield 90 %.

73 **74** **75** 90% (23)

The galactose alkyne derivative **78** was prepared in 80% yield, in cooperation with dr. Alexandrina Nan from I.N.C.D.T.I.M, in reaction of commercial galactose **76** with propargyl alcohol **77** using BF_3*Et_2O as a Lewis acid.

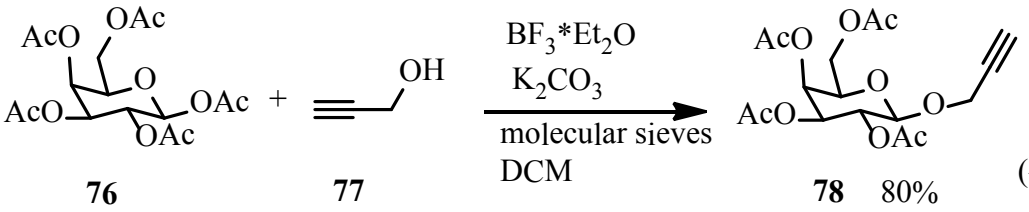

76 **77** **78** 80% (24)

CuAAC reaction between azide **65** and alkynes **68**, **72**, **75** and **78** in *t*-BuOH/H_2O and catalytic amount of TBTA provided new fatty acids **79 a-d** in 70-75% where interesting molecules quinine, proline, biotin, and galactose are linked with the anchoring part via 1,2,3 triazole (see Scheme 25). Pleasingly, in case of **79c** bearing biotin column chromatography was not necessary. The product was precipitated after washing the organic phase with water and could be easily collect by filtration.

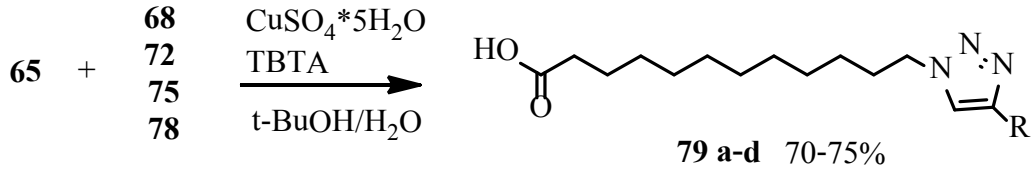

79 a-d 70-75%

(25)

The functionalized fatty acids **79a-d** were submitted to ligand exchange reaction at Fe_3O_4 stabilized with one layer of oleic acid **80**. The starting ferrofluid was provided by prof. L. Vekas from Academy of Science, Branch Timisoara. Reactions were performed in 1,2-dichlorobenzene at 80 ^oC with 4-fold excess of ligand for 24 h. In case of the quinine

composite **79a** small amounts of DMF were added (5mL). Due to poor solubility of **79c**, DMSO was used as a solvent instead of 1,2-dichlobenzene.

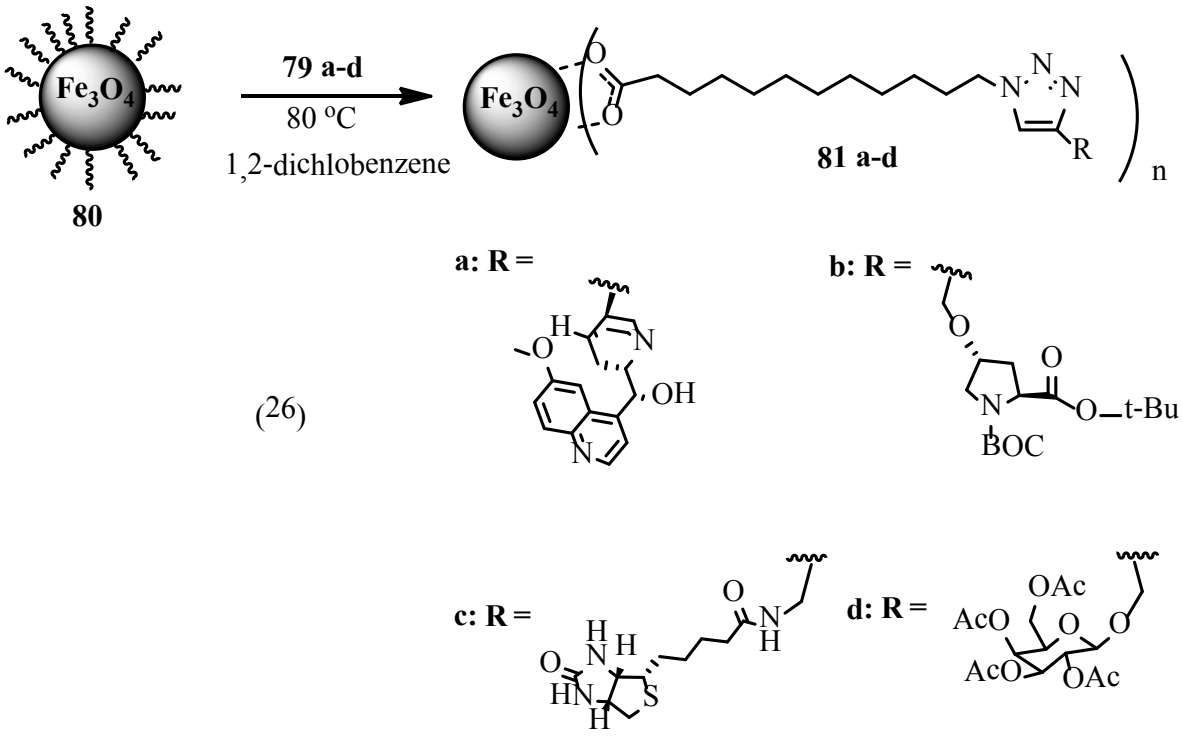

(26)

Full replacement of oleic acid of the starting MNP was confirmed by FTIR spectroscopy of the achieved magnetite NP **81**. In all cases typical peaks of the HC=CH moiety of oleic acid [108] at 3062cm^{-1} (ν_a, CH=), 3004cm^{-1}, (ν_x, CH=) 1543 cm^{-1} (ν, C=C) were missing while characteristic bands were present from modified fatty acid **81**. For all new prepared NP **81** bands at 580 cm^{-1} and 637cm^{-1} confirmed the presence of Fe_3O_4. CH_2 group signals were observed at 2855 cm^{-1} and 2920 cm^{-1} due to the stretching C-H vibration. Bands of carboxylic acids observed in FTIR spectra of functionalized fatty acids **81** were not presented in spectra of magnetite NP **81** due to complex formation of the carboxylate with the surface of the Fe_3O_4 NP by the ligand exchange. The resulting carboxylate bands are superimposed with other bands. Magnetite NP **81a** have bands at 1600 cm^{-1} and 1430 cm^{-1}, which were assigned to the C=C stretch vibration of the aromatic ring of quinine. The characteristic peak at 1250 cm^{-1} was assigned to C-N stretch vibration in the quinoline ring of quinine. Functionalization of MNP **81b** was confirmed by exhibiting IR bands at 1700 cm^{-1} and 1737 cm^{-1} which correspond to C=O stretching bands of amide and ester respectively. Bands at 2850 cm^{-1}, 2930 cm^{-1} and 2890 cm^{-1} belonged to CH_2 groups of the carbon chain, the proline moiety and methyl group of *t*-Bu ester.

Formation of MNP **81c** was demonstrated by the presence of bands at 1580 cm^{-1} and 1610 cm^{-1}, which were caused by N-H bend vibration and C=O stretching vibration of carbonyl group from amide. Relatively strong C-O stretching bands at 1068 cm^{-1} were observed for magnetite NP **81d** where also an intensive band was present for C-C(O)-C stretch vibration at 1215 cm^{-1} of the acetate groups in the protected galactose. Furthermore, the stretching band of C=O of esters was visible at 1750 cm^{-1}. It is important to emphasise that all functionalized magnetic NP **81a-d** formed stable colloidal suspensions in DCM.

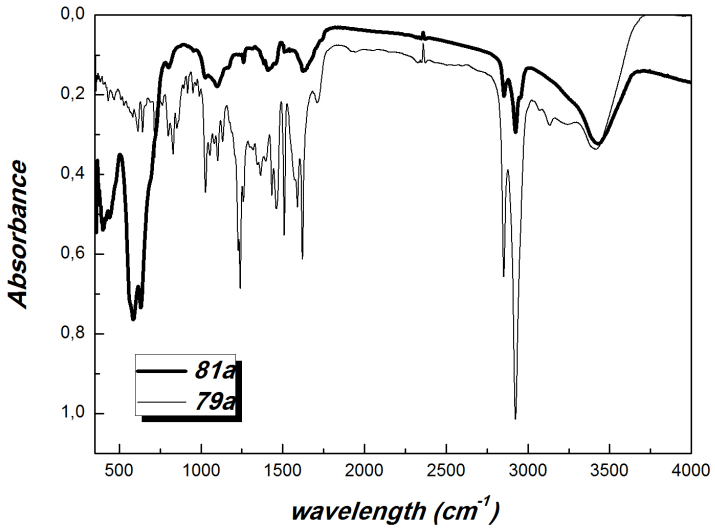

Figure 11. FTIR spectra of ligand **79a** and modified magnetite NP **81a**.

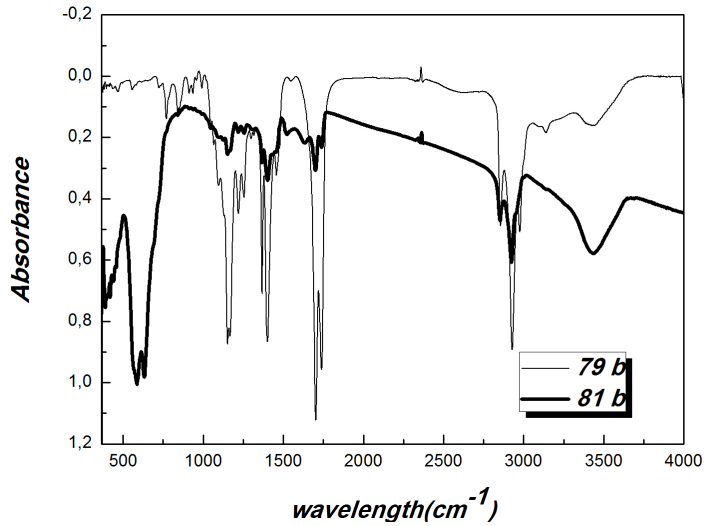

Figure 12. FTIR spectra of ligand **79b** and modified magnetite NP **81b**.

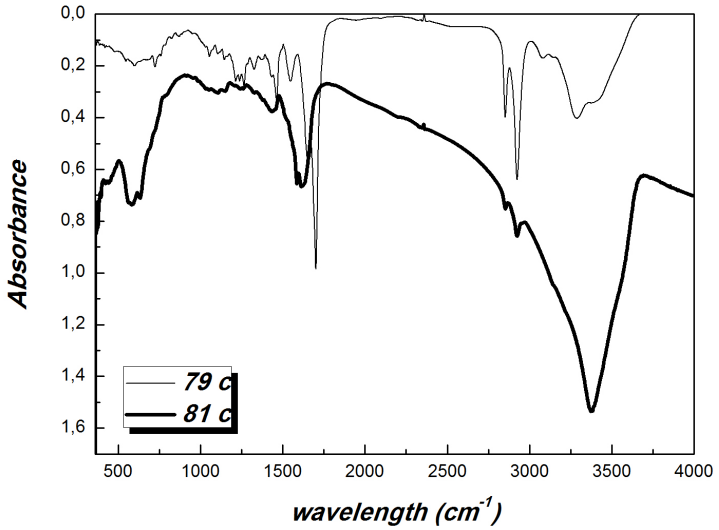

Figure 13. FTIR spectra of ligand **79c** and modified magnetite NP **81c**.

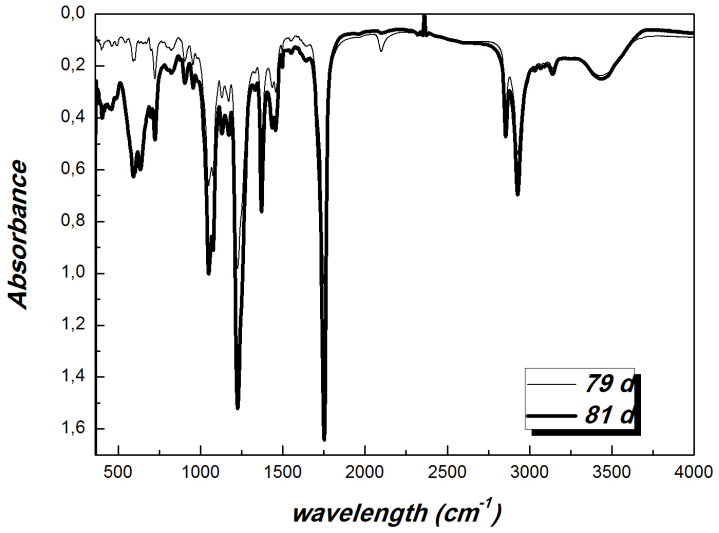

Figure 14. FTIR spectra of ligand **79d** and modified magnetite NP **81d**.

The superparamagnetic behaviour of magnetite nanoparticles **81a-d** was evidenced by the missing hysteresis loop in the magnetization vs. applied magnetic field dependences, at room temperature (Figure 15). The values of saturation magnetization varied from one type of magnetite NP to the other (Ms=61.2 emu/g (**80**), Ms=9.85 emu/g **(81a**), Ms=32.1 emu/g (**81b**), Ms=45.42 emu/g (**81c**) and Ms=12.85 emu/g (**81d**). These differences were caused by the different coating layers and their thicknesses on the surface of NP. Relatively high values of saturation magnetization recommend all products for further application, in the research where they can be controlled by external magnetic field.

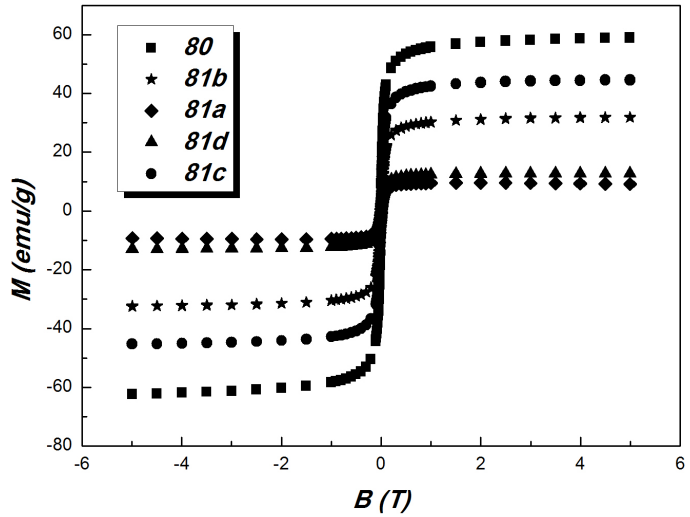

Figure 15. Magnetization *vs*. applied magnetic field at room temperature of magnetic nanoparticles **80** and hybrid magnetic nanostructures **81a-d**.

We decided to extend the application of fatty acids in functionalization and tailoring of magnetite NP by another strategy employing 11-azidoundecanoc acid **83** as a ligand with versatile azido group. The target molecule was obtained in the reaction of commercial bromo derivative **82** with 6 eq. of sodium azide in CH_3CN under reflux. The product was obtained in excellent yield (98%). This ligand was introduced on magnetite NP according to the above mentioned ligand exchange method furnishing the universal nanoplatform **84**. It has to be mentioned that this method was used by Samanta[216] in the formation of colloidosomes by aggregating magnetite NP covered with **82** with alkyne-functionalized MNP by CuAAC. Here, we applied this methodology in order not to cause later aggregation, but to link functionalities and to obtain magnetite NP, which are stable and can be used for interesting practical application.

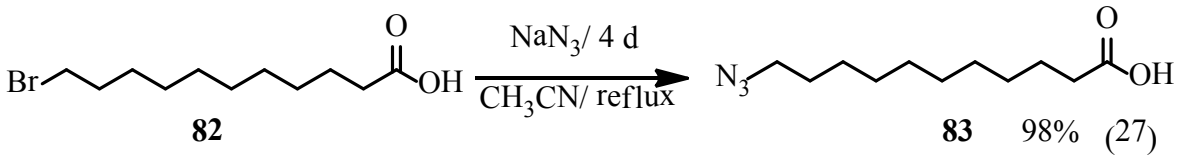

82 **83** 98% (27)

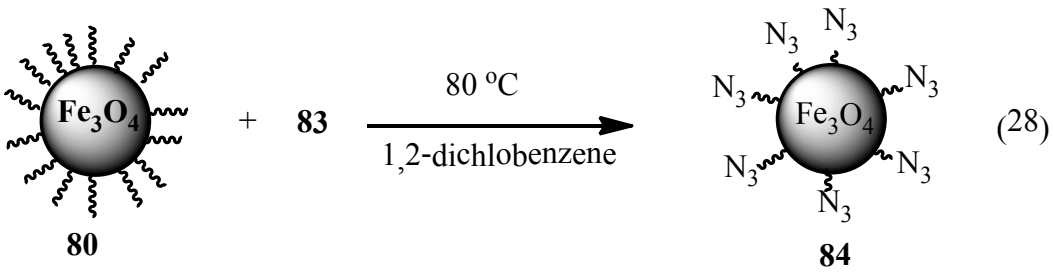

= oleic acid

N_3 = 11-azidoundecanoic acid

Surface modification of **80** with **83** was confirmed by FTIR analysis. Characteristic band at 2088 cm^{-1} was observed and was assigned to the N_3 group.

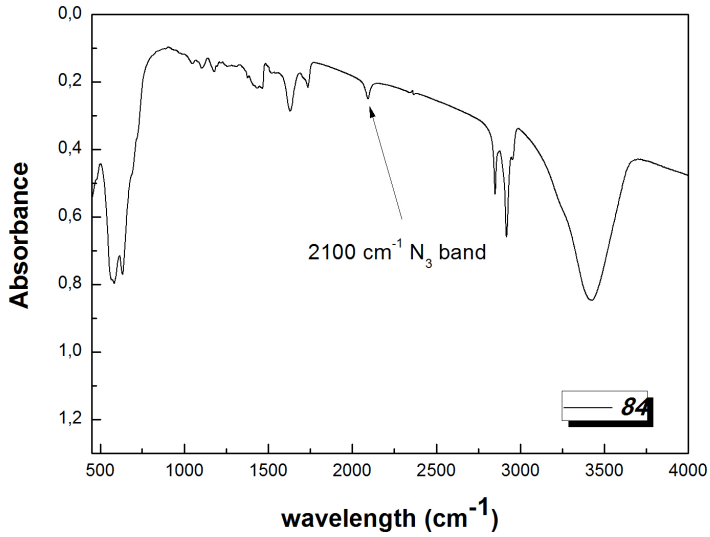

Figure 16. FTIR spectrum of the azido functionalized magnetic nanoparticles **84**.

To demonstrate the high potential of this magnetic support we decided to fix interesting catalytic functions like the Hayashi type catalyst and the proline derivative **72** by CuAAC. Propargyl derivative of Hayashi prolinol was prepared according to literature protocol.[217]

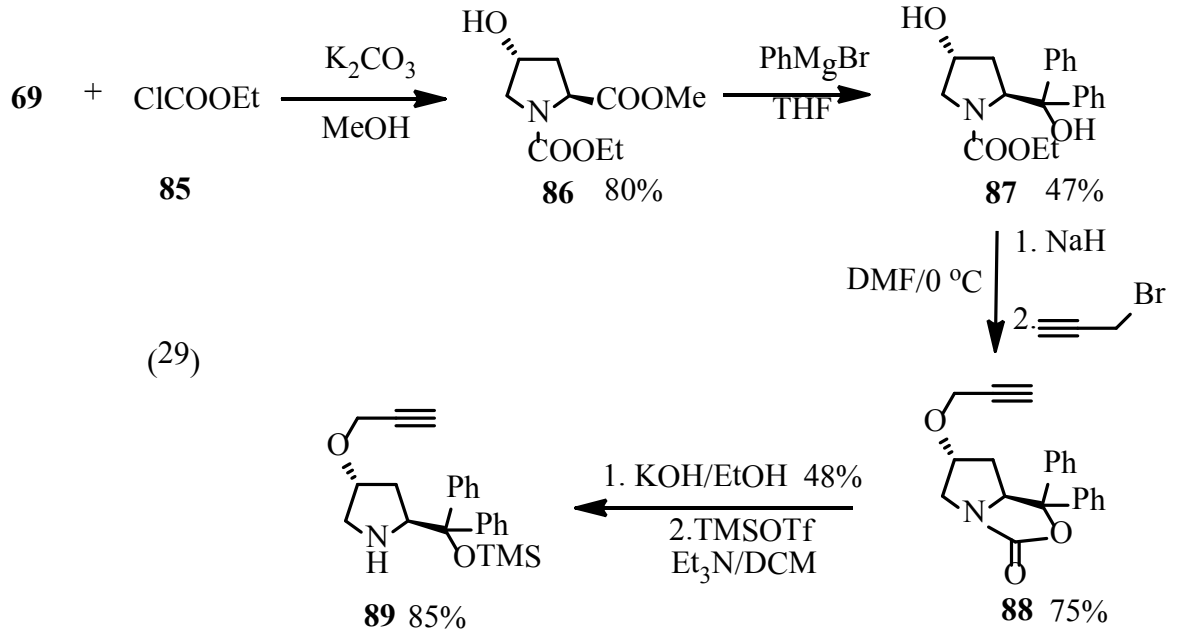

Reaction of 4-hydroxyproline **69** with ethyl chloroformate **85** yielded the N and C protected proline derivative **86**. Reaction with excess of Grignard reagent led to diphenylprolinol **87** with a good yield. An alkyne moiety was introduced in **88** with propargyl bromide using NaH in dry DMF. Under the same conditions occurred the reaction between hydroxyl group from prolinol and carbamate what afforded new, internal cyclic carbamate. Basic hydrolysis of **88** followed by reaction with triflic anhydride yielded desired **89**.

Afterwards, compounds **89** and **72** were submitted to the CuAAC reaction with magnetite NP **84** in MeOH in presence of catalytic amount of copper (0.2 eq) and TBTA (0.2 eq). According to standard protocol Na-Asc was used as a reducing agent. Proline derivatives were attached to magnetite NP via 1,2,3 triazole rings (see Scheme 30).

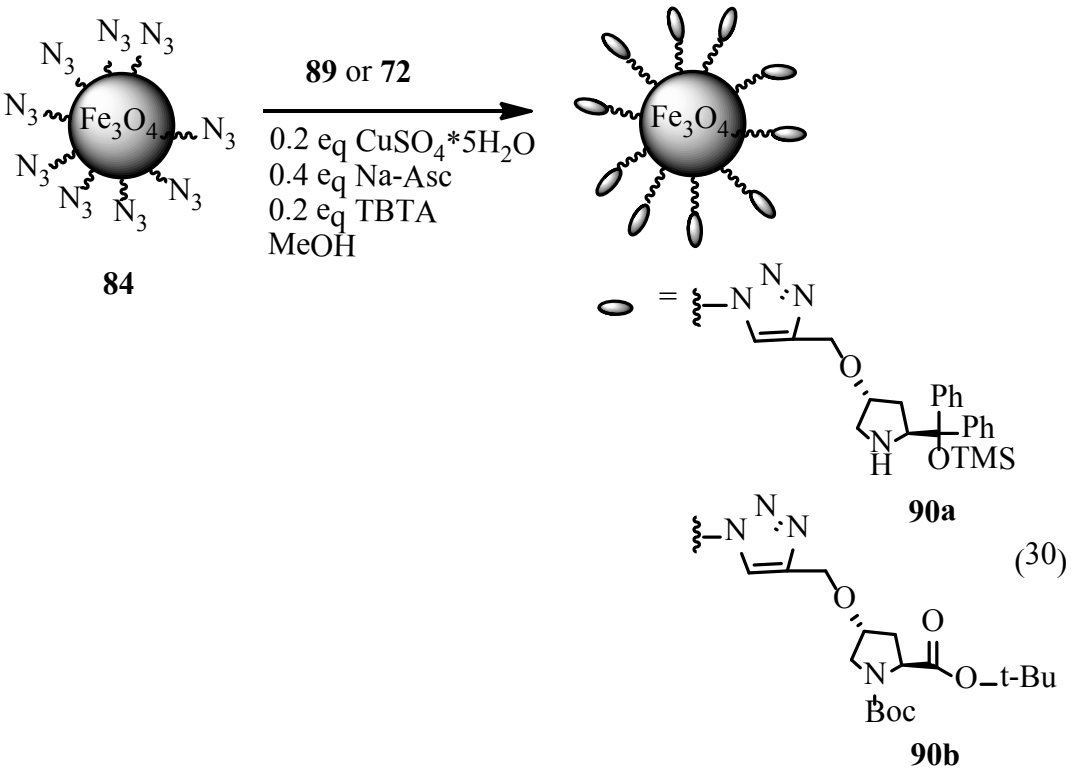

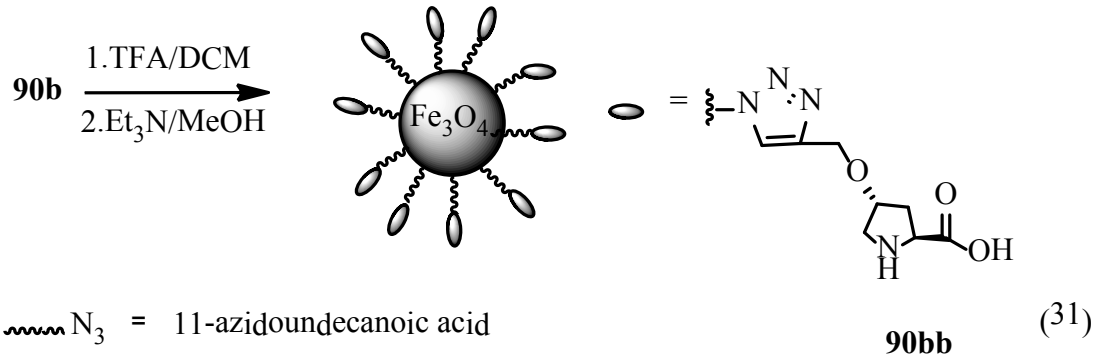

N3 = 11-azidoundecanoic acid

= 11-azidoundecanoic acid-1,2,3 triazole

Both transformations of **84** into **90a** and **90b** could be monitored by FTIR measurements, where azido bands at 2088 cm^{-1} from starting compound **84** were not found in the final MNP **90**. In case of **90a** bands in the region between 890 cm^{-1} to 1260 cm^{-1} typical for the Hayashi catalyst moiety appeared. In case of **90b** a new signal at 1740 cm^{-1} appeared, which was assigned to the C=O moiety of ester and carbamate. In case of **90b** deprotection of *t*-Bu and Boc was necessary and performed with TFA. The free base of the catalyst **90bb** was obtained by washing with 2% Et_3N/MeOH solution.

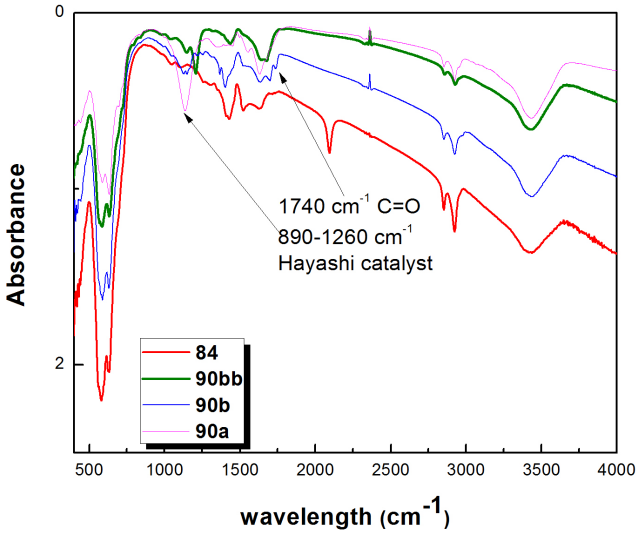

Figure 17. FTIR spectrum of azido magnetite NP **84** and new magnetite NP **90a**, **90b**, **90bb**.

Magnetic investigation of **84** and **90a** using VSM proved the superparamagnetic behaviour with saturation magnetization values Ms=40.7 emu/g and Ms=19.1 emu/g respectively. The magnetic materials could be easy handled by an external magnet.

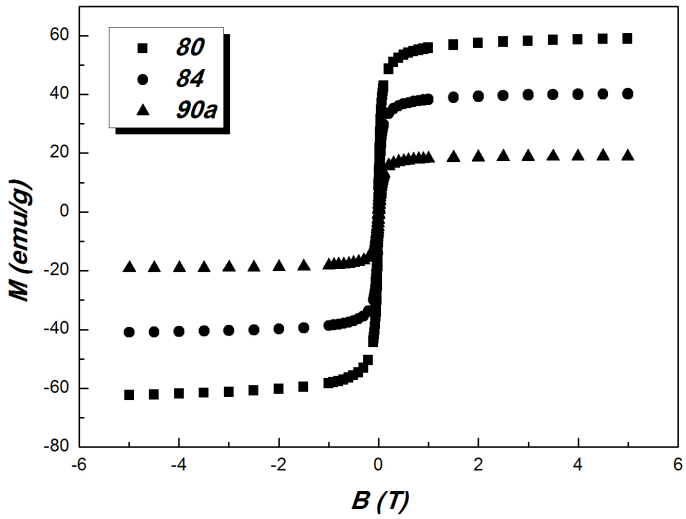

Figure 18. Magnetization *vs*. applied magnetic field at room temperature of magnetic nanoparticles **80** and hybrid magnetic nanostructures **84**, **90b**.

An important issue in heterogeneous catalysis is catalyst loading on a solid support. Elemental analysis is one of the most convenient methods for loading determination. The amounts of catalytic units attached to NP were evaluated by the N content since the only source of N was the catalyst molecules **90a**, revealed 2.46% of N what corresponded to the

loading of 0.41 mM/g, while **90bb** contained 0.94% nitrogen corresponding to 0.168 mM/g. The lower value of **90bb** could be the consequence of TFA treatment of the protected catalyst **90b**. It has been shown in the literature that TFA may deteriorate iron magnetite NP[218]. In addition, leaching of the catalyst could also take place.

The morphology of the MNP **81a-d**, **90a**, **90b** and **90bb** was investigated by TEM. Only one image is presented here (Figure. 19, **81a**) to exemplify the shape of the prepared magnetic The others NP are presented in the appendix to this thesis (see Appendix, A 1).The images show nearly spherical shapes, their size being influenced by the type of fatty acid derivative **79a-d** used. Partial agglomeration of the magnetic nanoparticles occurred during the TEM samples preparation process. The corresponding histograms of log-normal particle size distribution function revealed different values of the mean diameters D_0 and σ depending on the coating layers used: NP **80** – D_0= 18.7 nm and σ = 0.017, **81a** - D_0 = 29.1 nm and σ = 0.038, **81b** - D_0 = 26.3 nm and σ = 0.011, **81c** - D_0 = 26.5 nm and σ = 0.013, **81d** - D_0 = 20.9 nm and σ = 0.036.

In case of NP **90a** the TEM images showed the formation of some aggregates and thus determination of the particle size distribution was not possible.

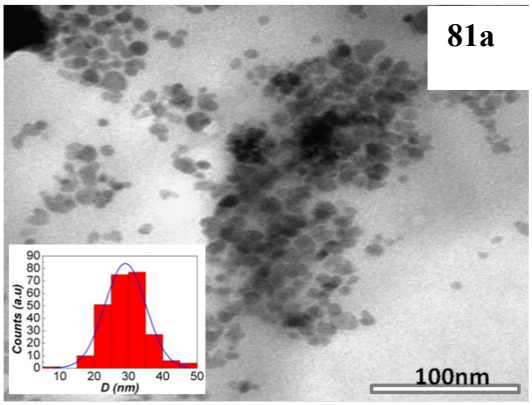

Figure 19. TEM picture of magnetite NP **81a**.

DLS investigation of some of the magnetite NP was done. Magnetite NP **80**, **81b** and **81b** formed stable suspension in DCM. Thus it was possible to determine the particle size distribution. The results indicated log-normal size distributions for all investigated samples with the following average hydrodynamic diameters (Dh): 55 nm for MNP **80** (obviously some aggregation), 25 nm for **81b**, and 34 nm for **81d**. In these two cases the ligand exchange procedure leads to a better dispersion of magnetite NPs since the hydrodynamic diameters of NP **81b** and **81d** are smaller as compared to the ferrofluid **80**. In case of

magnetic NP **81b**, **81c**, and **90a**, DLS measurements showed that the hydrodynamic size increases over time once dispersed in DCM, indicating particle agglomeration. This effect may be attributable to the hydrogen bonding between different particles since the fatty acids derivatives **79a** and **79c** used in the functionalization contain –NH and –OH units.

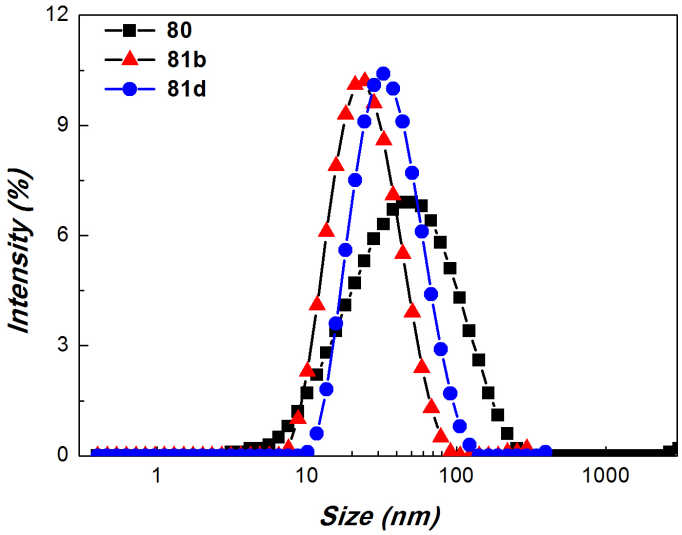

Figure 20. DLS of magnetite NP **80**, **81b** and **81d**.

In conclusion, novel magnetic nanoparticles were prepared via one step ligand exchange reaction with novel fatty acids. Both fatty acid derivatives and functionalized magnetite NP were obtained in straightforward way. Click reaction was used as powerful tool either in the synthesis of the fatty acids and in tailoring the surface of magnetic NP. This attitude gave access to magnetite NP equipped with quinine, proline, biotin and galactose which are important molecules either in catalysis (quinine and proline) or biology (biotin and galactose). This method could also be used to prepare an azido functionalized magnetic nanoplatform, which was used to attach a Hayshi type organocatalyst or propargyl ether of proline. Thus the method turned out to be versatile with great potential in further applications. The new fatty acids functionalized magnetite NP were characterized by FTIR, VSM and TEM. Particles possessed good magnetic properties and, confirmed superparamagnetic behaviour, with relatively small sizes bellow 30 nm. They formed stable colloidal suspension in organic solvent. Additionally it was found that ligand **79b** and **79d** were better coating agent than the original oleic acid.

2.1.2 Synthesis and characterization of new dopamine based nanoparticles

Recently, a high content of 3,4-dihydroxy-L-phenylalanine (DOPA) and lysine (Lys) has been found in the mussel adhesive protein Mefp-5 (*Mytilusedulis* foot protein-5) located at the top of the adhesive pad, which is in direct contact with substrates. The connection between adhesive the pad and the surface is strong and robust. Thus dopamine or the dopamine-lysine motif has been utilized in material chemistry as strong anchors mimicking the natural adhesive feature. This nature-inspired attitude has been already used to cover MNP with different dopamine derived molecules like dopamine modified with PEG giving water stable magnetic suspension. This chapter will show attempts in functionalization of magnetite NP with simple dopamine or dopamine derivatives in combination with CuAAC or amide formation towards proline immobilization and application in organocatalysis.

To prepare the azide partner **92** for CuAAC reaction dopamine hydrochloride **91** was reacted with azidoundodecanoic acid **83** according to an EDC amide formation protocol. Reaction performed in dry DMF at rt in presence of a slight excess of EDC and HOBt with 99% yield. The product **99** consisted of an anchoring catechol moiety and an unpolar linker with the azido group in the end

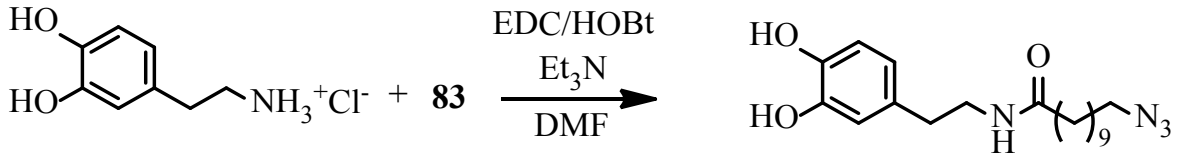

91 **92** 99% (32)

Ligand exchange reaction between oleic acid stabilized magnetite NP **80** and the new ligand **92** (5.2 mM) in a MeOH/$CHCl_3$ mixture gave access to magnetite NP nanoplatform **93** equipped with azido group ready for submission to CuAAC reaction. The magnetic nanoparticles **93** were investigated by FTIR showing a characteristic peak for the azide moiety at 2090 cm^{-1}. New important bands were observed at 1423 cm^{-1} and 1630 cm^{-1}. They were assigned to C=C stretching vibration of the benzene ring and C=O stretching vibration of the amide moiety respectively.

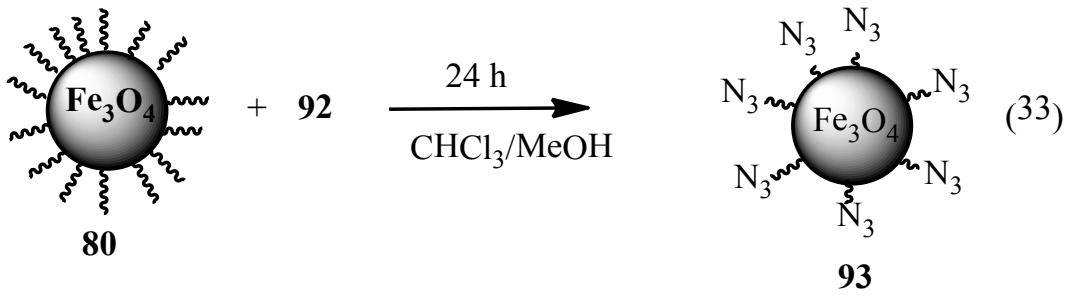

(33)

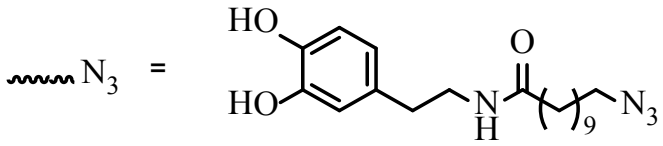

= oleic acid

The azido modified magnetite NP **93** were submitted to CuAAC reaction with proline **94** obtained from the protected proline derivative **72** after deprotection with TFA. Here the deprotection step was performed directly on proline not linked to magnetic NP in order to avoid interaction of magnetite NP with TFA and exclude leaching of the catalyst. After "click" reaction the **95** magnetite NP were washed with 5% Et_3N/MeOH solution to convert the proline salt into the free amine.

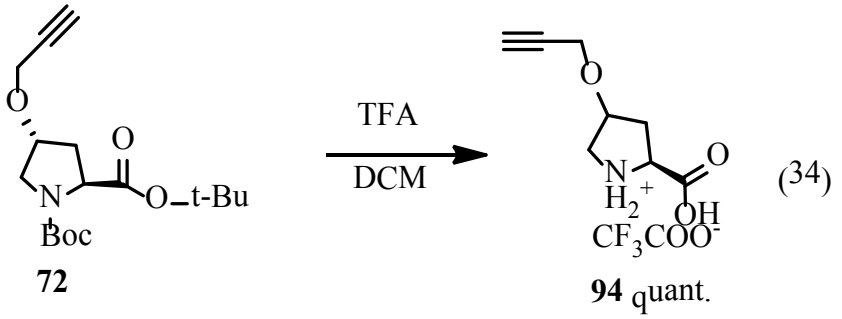

(34)

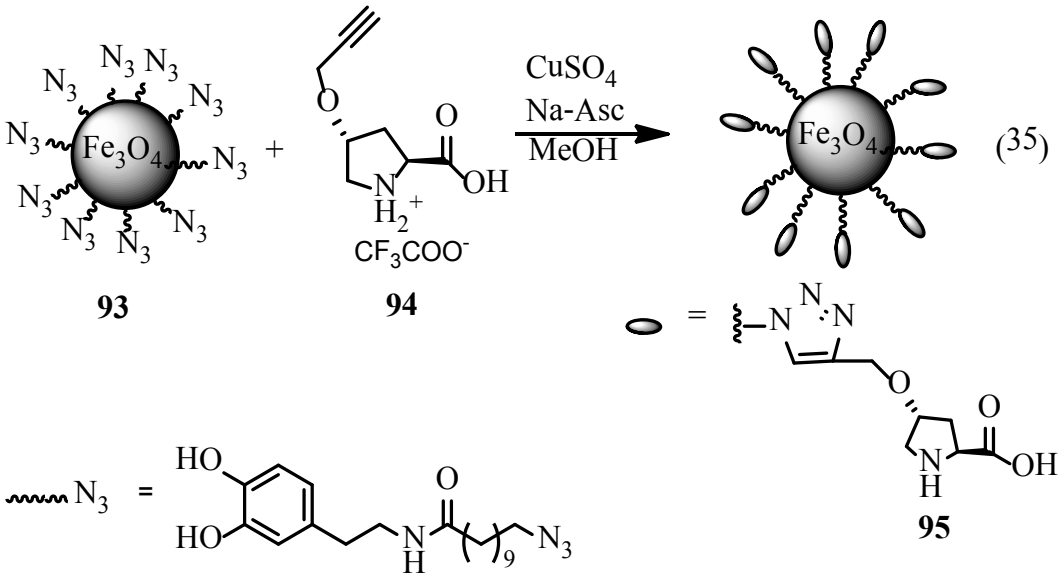

(35)

The FTIR spectrum showed disappearance of the azide band, hence reaction of **94** was found to be successful. Bands at 2850 cm^{-1} and 2920 cm^{-1} were visible and were ascribed to CH_2 groups. However, FTIR did not show a signal of a C=O group found in the proline carboxylic moiety. This effect may be caused by low proline loading on magnetite NP.

In fact, this assumption was proved by a spectrophotometric test with picric acid to estimate the amount of bound proline. Picric acid test is widely used in evaluation of amine quantities fixed to resins.[219] This method is based on interaction of picric acid with primary or secondary amines, including proline. The salt formed from picric acid and the amine fixed on solid support is washed repeatedly to remove excess of unbound picric acid. The bound picric acid is removed from the solid support by washing with base solution. The concentration of picrate in this solution is determined spectrophotometrically at 358 nm using an extinction coefficient of 14,500 mL $mmol^{-1}$ cm^{-1} and reflects the amine loading on the support. Tests performed with the magnetite NP **95** according to the given procedure

showed that proline loading was only 0.062 mmol/g. Elemental analysis could not be carried out owing to the limited access to this service on this stage of work.

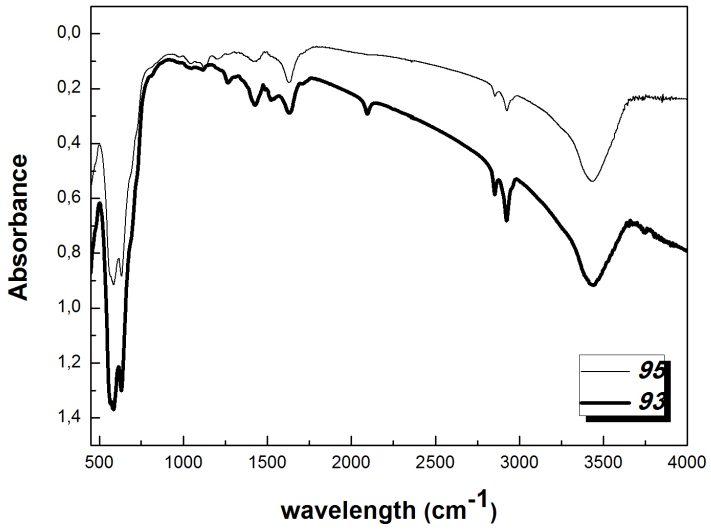

Figure 21. FTIR spectra of magnetite NP **93** and functionalized magnetite NP **95** modified with proline via CuAAC.

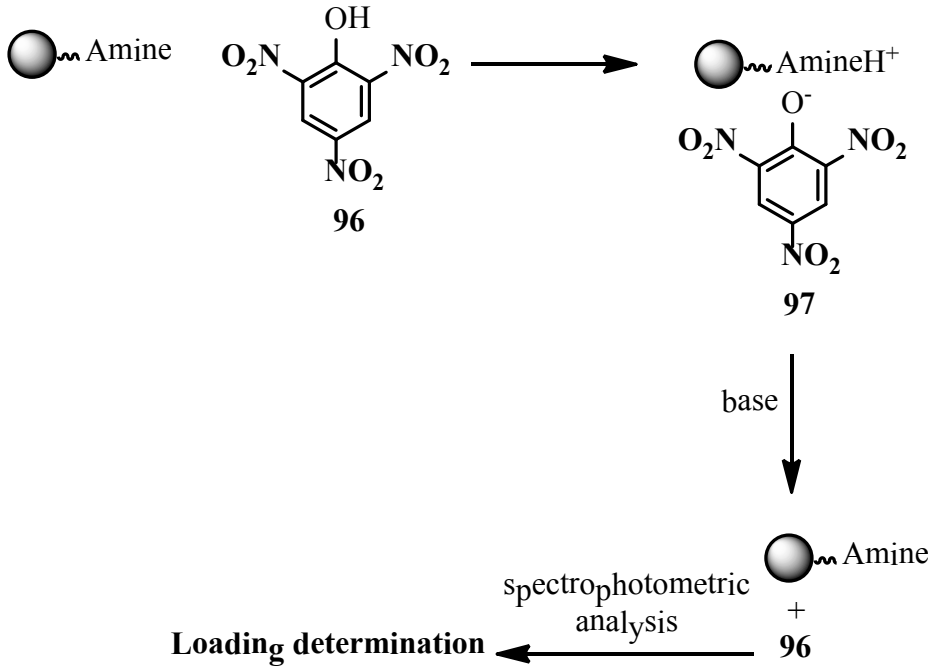

Figure 22. General route for quantitative determination of amine fixed to solid support via picrate formation.

TEM measurement of magnetite NP **95** revealed almost spherical shape. Some small aggregation was observed because of sample preparation process (see Appendix, A 2). Magnetic measurements confirmed superparamagnetic behaviour and a high saturation magnetization of Ms=68.7 emu/g so magnetic nanoparticles were easily attracted by external magnetic field (see Appendix, A 3).

Following another approach, two new nanomaterials were synthesized using amide formation reaction between dopamine stabilized magnetite NP and proline derivatives equipped with linkers of different lengths. To assure appropriate long distance of proline from the magnetic core compound **79b** with a 12 carbon chain was employed in the coupling reaction (see Scheme 38). In the second case bis-protected proline **71** was reacted with glutaric anhydride yielding **98** with a five carbons chain spacer. The product was obtained in good yield according to a known procedure.[220]

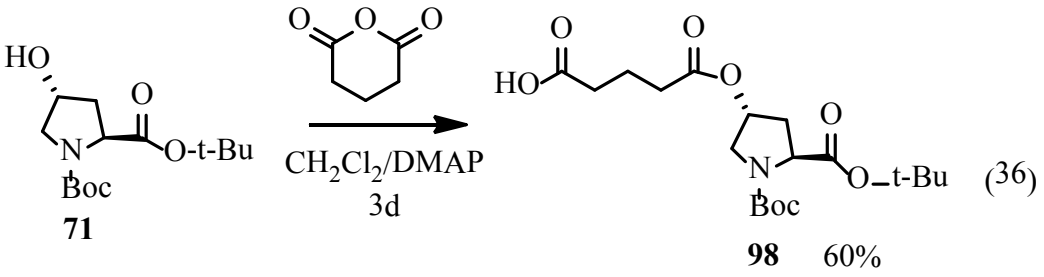

(36)

Magnetite NP **80** stabilized with one layer of oleic acid were submitted to reaction with dopamine hydrochloride **91** in a $CHCl_3$/MeOH mixture yielding magnetite NP **99** with amino groups on the surface, which were later on used in amide formation with two synthesized carboxylic acids **79b** and **98**. Amine loading for **99** was determined by spectrophotometric method employing picric acid. It was found that loading was only 0.086 mM/g. The value was similar to previous for compound **95** 0.062 mM/g.

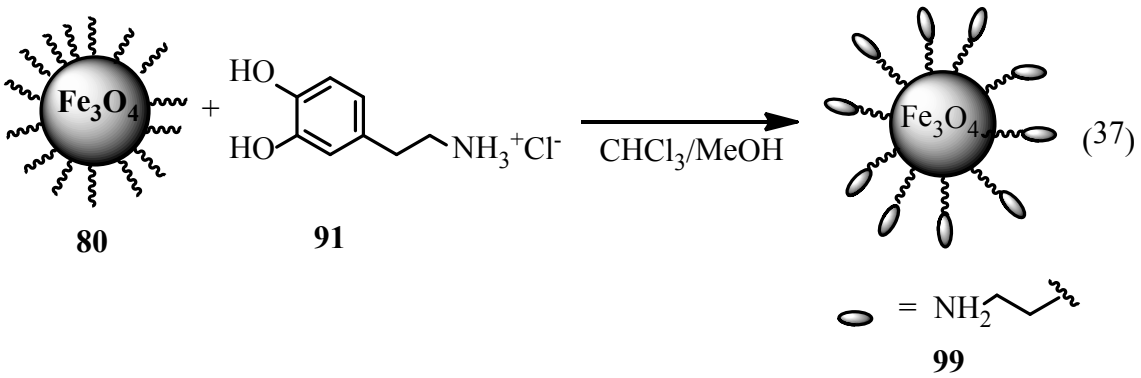

80 **91** **99**

Coupling reactions were performed with EDC, HOBt in presence of tertiary amine in dry DMF and excess of the triazolyldodecanoic acid **79b** and prolinoxyglutarate **98**. Gained magnetite NP **100a** and **100b (**see Scheme 38) were reacted with acetic anhydride in CH_3CN at rt for 2.5 h (similar to the protocol for non supported dopamine[221]) to block eventually remaining unreacted free amino groups. After this capping step magnetite NP were treated with TFA to remove *t*-Bu and Boc protecting groups. In order to obtain the respective free proline bases the resulting magnetic NP were washed with 5% Et_3N solution in MeOH affording magnetite NP **101a** and **101b**. The loading of magnetite NP **101a 101b** with proline was not determined but was concluded from the assumption that the coupling was quantitative.

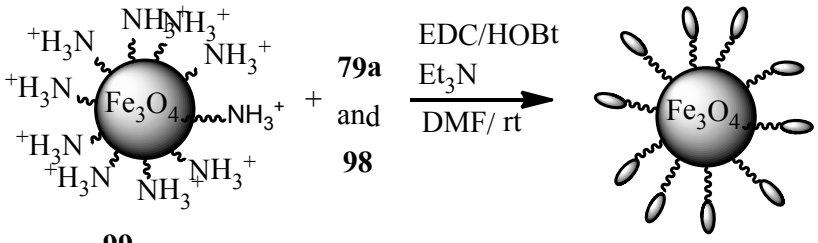
EDC/HOBt
Et3N
DMF/ rt
79a
and
98
99
100a
100b

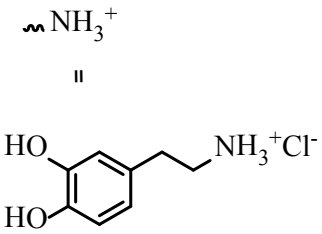

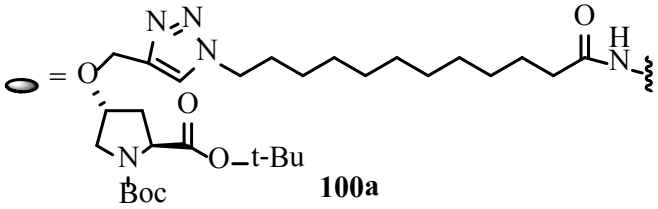
100a

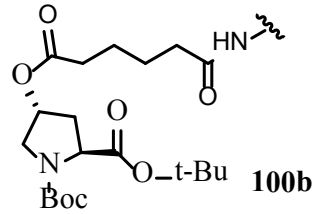
100b

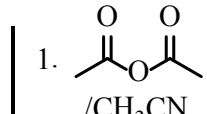
1.
/CH3CN
2. TFA/DCM

(38)

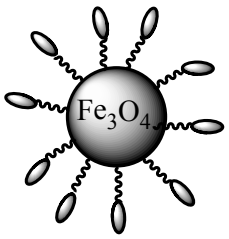

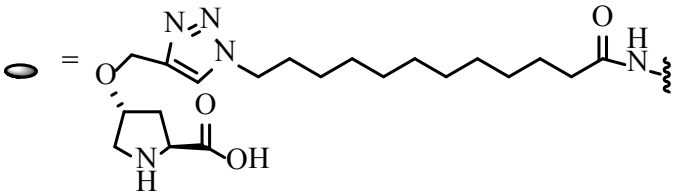
101a

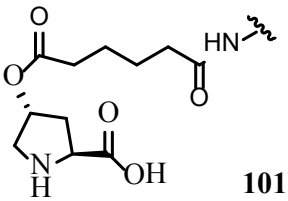
101b

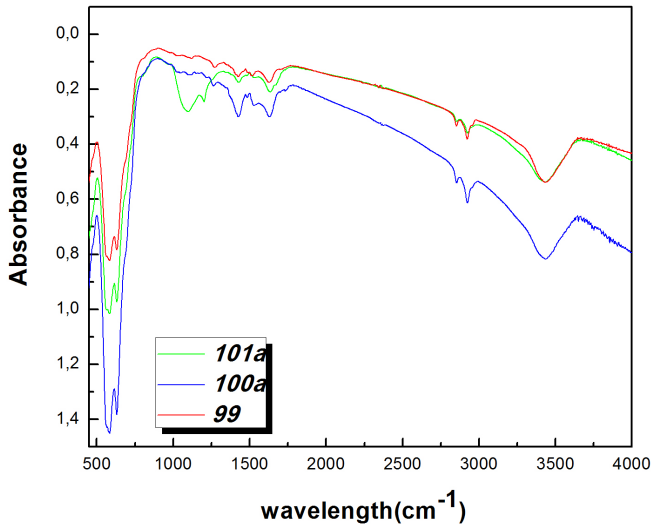

Figure 23. FTIR spectra of magnetite NP with linker **79b**, after coupling reaction (**100a**) and after deprotection (**101a**).

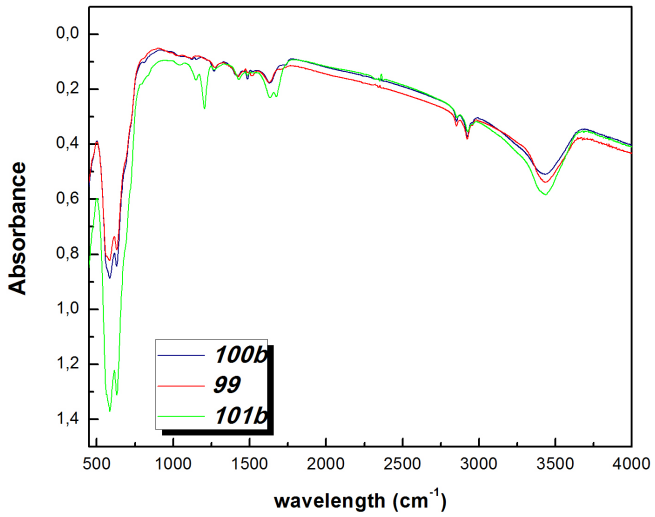

Figure 24. FTIR spectra of magnetite NP with linker **98**, after coupling reaction (**100b**) and after deprotection (**101b**).

FTIR spectroscopy did not reveal any significant changes in both NP **101a** and **101b**. In both spectra peaks of C=O were not observed and the only noticeable changes were presented after TFA treatment. FTIR spectra were not informative enough to draw any conclusion. Indirect proof for functionalization was given by the performed catalytic tests (see chapter 2.1.3).

To summarize, new magnetic nanoparticles **95**, **101a**, **101b** with interesting surface functionalization were prepared by CuAAC or amide formation. They were characterized by several available analytical methods such as FTIR, TEM, or VSM. While all of them

were equipped with proline, which is known to be excellent organocatalysts, they underwent catalytic tests (see chapter 2.1.3).

2.1.3 Application of fatty acids derivatives and dopamine based magnetic nanoparticles in catalysis

In previous chapters the synthesis and characterization of magnetite NP functionalized with different proline derivatives were described (see chapter 2.1.1 and 2.1.2.). In this section results in application of these magnetite NP as supported organocatalysts for Michael and aldol reactions are disclosed.

It has been shown that Hayashi type catalysts fixed to different solid supports including magnetic NP (see chapter 1.4.1) can catalyze Michael reaction between propionaldehyde and trans-β-nitrostyrene.[222] Thus this reaction was chosen as a model reaction for catalytic tests to check the activity of prolinyl fatty acid based catalyst **90a**.

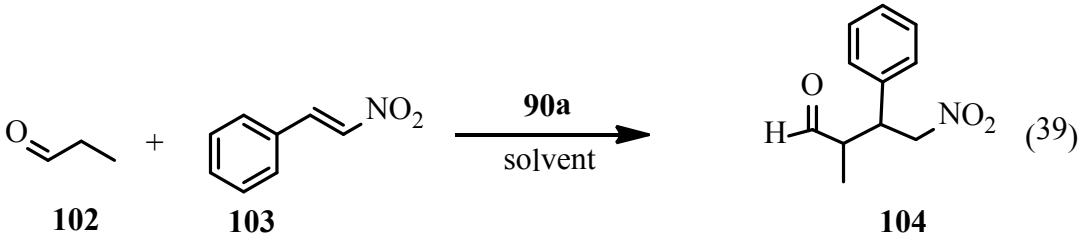

Table 1. Summary of catalytic test with magnetite NP **90a** as nanocatalyst.

Entry	102 [mM]	103 [mM]	Catalyst amount [mg]	Loading mol %	Solvent	T [h]	Yield [%]	ee %	dr syn/anti
1	0,7	0,4	150	15	DCM	18	---	n.d.	n.d.
2	0,7	0,4	300	30	DCM	48	---	n.d.	n.d.
3	0,35	0,2	300	60	DCM	48	---	n.d.	n.d.
4	2	0,2	300	60	DCM/ H_2O	72	---	n.d.	n.d.
5	2	0,2	300	60	H_2O	120	---	n.d.	n.d.
6	0,35	0,2	45	10	DCM	24	---	n.d.	n.d.

First attempt was performed with 15 mol % of catalyst in DCM (see Table 1, entry 1). Applied conditions were alike as reported before by Riente.et al.[198] Unfortunately product **104** was not observed under this condition. Increasing of the quantity of the catalyst up to 30 mol % or 60 mol % with extended reaction time (see Table 1, entry 2 and 3) did not lead to desired product either. Conditions were changed to those applied by Wang et al.[197] where 10 fold excess of **102** was used and reaction was conducted in a 1:1 mixture of DCM/H_2O over 72 h. Also in this case product was not formed and also any other side products. To see if change of solvent polarity can improve the reaction DCM was replaced with pure water (see Table 1, entry 5) but reaction did not occur either. It is known that acids can improve the Michael reaction. Therefore, 10 mol % of benzoic acid was added to a mixture of a fresh portion of the catalyst (10 mol %) with slight excess of **102** in DCM 10 mol % (see Table 1, entry 6). However, also this attempt was unsuccessful.

Magnetite NP functionalized with proline-containing dopamine were tried in a model aldol reaction between cyclohexanone and 4-nitrobenzaldehyde. Catalyst **95** obtained by CuAAC reaction of TFA proline salt with azido modified magnetite NP equipped with long linker was first checked under solvent free conditions. In order to work with a suspension rather than an inhomogeneous mixture only 100 mg of nanoparticles were used at the beginning. As a consequence, only small amount of catalyst was available in reaction. After 24 h the expected product **108**, was obtained in moderate yield (53%) but in almost racemic form. To improve the reaction the amount of magnetite NP was increased, the reaction time was prolonged and a solvent was applied (see Table 2, entry 2 and 3). Under neat condition the yield and ee were slightly improved but when DMSO was used the product was not observed. Further addition of catalysts **95** into already used portion of magnetite nanocatlyst to 300 mg corresponding to 4 mol % of catalytic units did not give better results. The product was obtained in moderate yield as a racemate even with addition of benzoic acid and water (see Table 2, entry 4 and 5). It is important to mention that stirring of the reaction mixture was hard and thus it was obvious that not all NP had contact with the reagents. To check if further addition of catalyst can lead to better catalytic activity 110 mg was added to previous portion of nanoparticles what gave 410 mg in total of the catalyst were used (see Table 2, entry 6 and 7). Also the amount of the aldehyde was diminished to have higher catalyst loading. In this way 10 mol % of **95** were achieved. Indeed, the product was obtained with excellent yield 99 % but moderate ee was observed (Table 2, entry 6). Addition of benzoic acid led to lower chemical yield, however, a better ee was obtained (see Table 2, entry 6 and 7). To confirm that there was not a

background reaction catalyzed by Et_3N, which could be adsorbed on magnetite NP during washing in the final preparation step. A fresh portion of the catalyst **95** was resynthesized. Here this portion is numbered as a **105**. In contrast to the first batch catalyst was not washed with methanolic solution of Et_3N to avoid Et_3N interaction with magnetite NP. Loading determination by the picric acid test revealed 0.054 mM/g, which was closed to this one obtained for **95**.

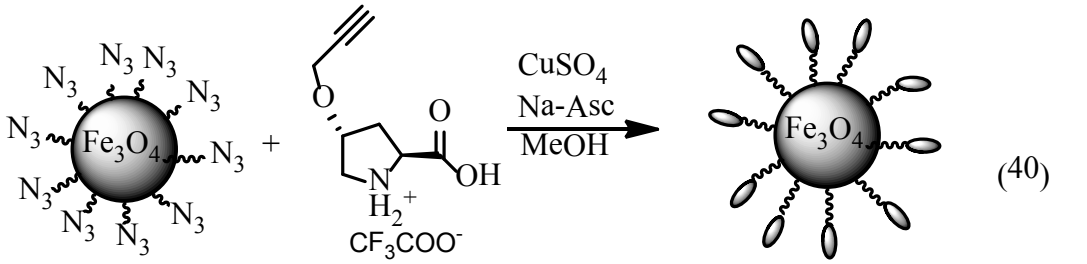

93 **94** (40)

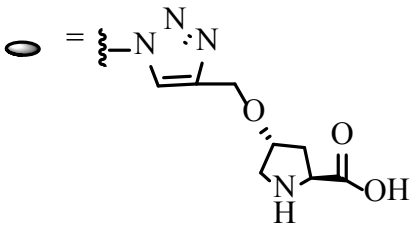

105

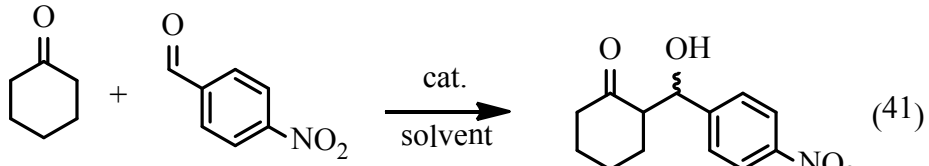

106 **107** **108** (41)

Table 2. Summary of catalytic results with nanocatalysts **95**, **105**, **101a**, **101b** based on dopamine coating.

Entry	106 [ml]	107 [mM]	Catalyst	Catalyst amount [mg]	Loading mol %	Solvent	T [h]	Yield [%]	Ee[c] % anti	dr[d] syn/anti
1	1	0.5	**95**	100	1.2	Neat	24	53	6	n.d
2	1	0.5	**95**	150	2	Neat	48	68	14	n.d.
3	0.5	0.5	**95**	150	2	DMSO	48	----	n.d.	n.d
4	1	0.5	**95**	300	4	Neat	24	56	rac	n.d.
5[a]	1	0.5	**95**	300	4	Neat	72	48	rac	n.d
6	0.5	0.25	**95**	410	10	Neat	48	**99**	36	n.d
7[b]	0.5	0.25	**95**	410	10	Neat	72	**73**	**48**	n.d.
8	0.5	0.25	**105**	250	5	Neat	72	50	48	50:50
9[a]	0.5	0.25	**105**	250	5	Neat	72	traces	n.d.	n.d.
10	0.5	0.2	**105**	380	8	Neat	72	50	36	60:40.
11	0.5	0.25	**101a**	308	7	Neat	24	**68**	**52**	70:30
12[a]	0.5	0.25	**101a**	308	7	Neat	24	35	rac	95:5
13[b]	0.5	0.25	**101a**	308	7	Neat	48	46	48	73:27
14	0.5	0.25	**101b**	420	10	Neat	48	**80**	**52**	55:45
15[b]	0.5	0.25	**101b**	420	10	Neat	48	55	55	60:40

a) Addition of water 0.1 ml and 10 mol % BA
b) 10 mol % of BA was added
c) Determined by chiral HPLC
d) Determined by NMR

The catalyst **105** gave moderate results in terms of yields (50%) when around 5 mol % was applied (see Table 2, 8). However, the aldol product was obtained with 48 % ee. Higher amounts of catalyst (380 mg gained by the addition of fresh portion of the catalysts to previously used one) **105** gave lower yields and ee´s (see Table 2, entry 10). Product was observed in trace amount when water and benzoic acid were added (see Table 2, entry 9). The magnetite NP obtained via amide formation were also evaluated in aldol reaction. Catalyst **101a** gave fair result in terms of ee and acceptable yield (see Table 2, entry 11). The effect of additional water and the application of benzoic acid as co-catalyst were also checked. Combination of these two additives gave the product in 35 % yield but in racemic form (see Table 2, entry 12). On the other hand, when BA was applied without the addition of water a non-racemic product was obtained in higher yield and with 48 % ee (see Table 2, entry 13). Therefore the conclusion can be drawn that this large amount of water inhibited the reaction. Catalyst **101b** with shorter linker afforded the desired aldol product in good yield 80% and 52 % ee (see Table 2, entry 14). Addition of benzoic acid slightly improved the ee to 55 %, however the yield dropped to 55 % (see Table 2, entry 15). Diastereoselectivity is another important issue. Unfortunately, this parameter could not be

determined for all samples due to the lack of access to the services in the time when the tests were performed. Nevertheless, important information can be deduced from the values obtained for some samples (Table 2). Thus the *syn*-isomer is predominantly formed while usually the *anti* aldol is dominating in proline catalyzed reactions. This phenomenon can lead to the conclusion that there could be background catalysis in addition to the catalysis by proline.

The proline-containing azido fatty acid derived catalyst **90bb** was investigated in aldol reaction as well. After 72 h the product was obtained in 40 % yield in racemic form. Diasteroselectivity determined by NMR revealed again the *syn* aldol as major diasteromer.

Table 3. Application of nanocatalyst **90bb** in aldol reaction and influence of bare magnetite NP on aldol reaction.

Entry	106 [ml]	107 [mM]	Catalyst	Catalyst amount [mg]	Loading mol %	Solvent	T [h]	Yield [%]	Ee % anti	dr syn/anti
1	0.5	0.25	**90bb**	146	10	Neat	72	40	rac	65:35
2	0.5	0.25	**27**, **13**	**27**/300	**13**/10	Neat	72	48	48	70:30
3	0.5	0.25	**27**	**300**	**---**	Neat	72	23	rac	n.d.

This observation together with the above mentioned result obtained with dopamine modified magnetite NP allowed to suppose that low loading of the catalyst resulting in incomplete covering of magnetite NP surface could give background reaction where bare magnetic nanoparticles were involved in the catalytic cycle. To check this assumption, reaction was performed in presence of naked magnetite NP **27** and proline **13**. Indeed, aldol product was formed in yields similar to those when catalyst **90bb**, **95**, **105** were used and the dr´s were in the same range with excess of the *syn* diasteroisomer (see Table 3, entry 2). Test performed with bare magnetite nanoparticles gave rise to product formation with 23 % yield. (see Table 3, entry 3). However, the condensation product between cyclohexanone and 4-nitrobenzaldehyded was dominant in this reaction (75 % yield).

To recapitulate, novel MNP based on fatty acid linker modified with diphenylprolinol trimethylsilyl ether (Jorgensen-Hayashi type catalyst) were checked in Michael reaction between propionaldehyde **102** and nitrostyrene **103**. These attempts were unsuccessful even when several reaction parameters including catalyst loading, time and solvent were varied. It is hard to explain why magnetite NP **90a** could not catalyze the reaction at all. It can be assumed that cleavage of the silyl ether moiety occurred giving

rise to an inefficient moiety, what is a known phenomenon of this catalytic unit. As another reason it can presumed that there is not enough freedom at the catalytic moiety in the fatty acid modified magnetite NP. Also a combination of these two factors could lead to catalyst deactivation. Furthermore, a variety of magnetite NP equipped with dopamine anchors and functionalized with proline were checked in aldol reaction between ketone **106** and aldehyde **107**. The results indicate that those materials can be used as a magnetic support for organocatalyst. However, it was obvious that the limiting factor of our catalyst was the low loading of catalytic units at the magnetite NP. In consequence, moderate yields and enatioselectivities were afforded. Since the amount of catalytic units at the magnetite NP was low, huge quantities of the magnetite NP were necessary. Thus, the inhomogeneous reactions were hard to handle. In addition to the low catalyst loading in the reaction mixtures there could be competing catalysis by bare magnetite NP. This may also explain the fact that the *syn* diastereomer was dominant and the products were obtained as racemates. In order to improve the catalytic activity of nanomaterials it seems that tighter and stronger coating of the magnetite cores is necessary. At the same time loading of magnetite NP with the catalyst should be increased allowing to apply lower quantities of catalytic NP und thus to avoid problems with overloading the reaction mixture with solid material. One way to increase the quantity of catalytic units fixed to a magnetite NP is to include the catalytic moiety in a monomer, which later on forms a polymer at the surface of the NP.

2.2 Synthesis of new magnetic nanoparticles with different polymeric coating agents

2.2.1 Preparation of magnetite NP covered with polydopamine and functionalization by CuAAC or ROP reaction

Coating of magnetic NP plays an important role in preparation of magnetic NP. The covering agent has to assure not only stabilization of the magnetic NP but also should allow later modification of the nanomaterials. A lot of different polymeric agents have been introduced in the field of magnetic NP so far (see chapter 1.2). One of them, which recently have attracted much attention of material chemists, is the biomimetic polymer polydopamine. This polymer is obtained by oxidative polymerization of dopamine and has the ability to create strong adhesive layers on almost all kind of surfaces including magnetite NP. Different structures **1**, **2**, **3**, **4** were proposed in the literature so far. The

common structural elements are quinoid functions present in all proposed structures. Thus polydopamine exhibits reactivity towards nucleophilies bearing amine or thiols. This feature allows covalent binding of proteins, enzymes or lipophilic amines to the polymer film. Since this functionalization has its limitations as far as the reacting functional groups are concerned the extension to other types of linking reactions would enlarge the versatility of polydopamine coating considerably. In this chapter a novel strategy is demonstrated for extension of the surface reactivity of polydopamine coated magnetite NP by introduction of azide groups ready for CuAAC reaction.[223] This attitude is exemplified by fixing interesting molecules such as biotin, galactose, proline and dansyl (fluorescence marker).

As suitable bifunctional compound comprised of an amine and an azide moiety 4-azidobutylamine **111** was synthesized according to a reported protocol.[224] 1,4-dibromobutane **109** was reacted with NaN_3 in CH_3CN affording the pure diazide **110** which later on was submitted to selective Staudinger reduction with PPh_3. It is worth to mention that the reaction was performed by utilizing a syringe pump in biphasic system Et_2O/5 % HCl. Immediately after one azide group was reduced the amine was extracted from the organic phase by aqueous acid. This suppressed double reduction and allowed to obtain the pure product **111** in a satisfactory yield (57 %).

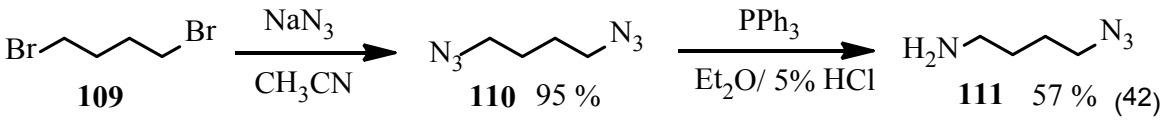

109 **110** 95 % **111** 57 % (42)

Reaction of one layer oleic acid stabilized magnetite nanoparticles **80** with dopamine hydrochloride **91** in Tris buffer under basic pH resulted in replacement of the original layer of oleic acid and coating magnetite NP with final polydopamine shell.

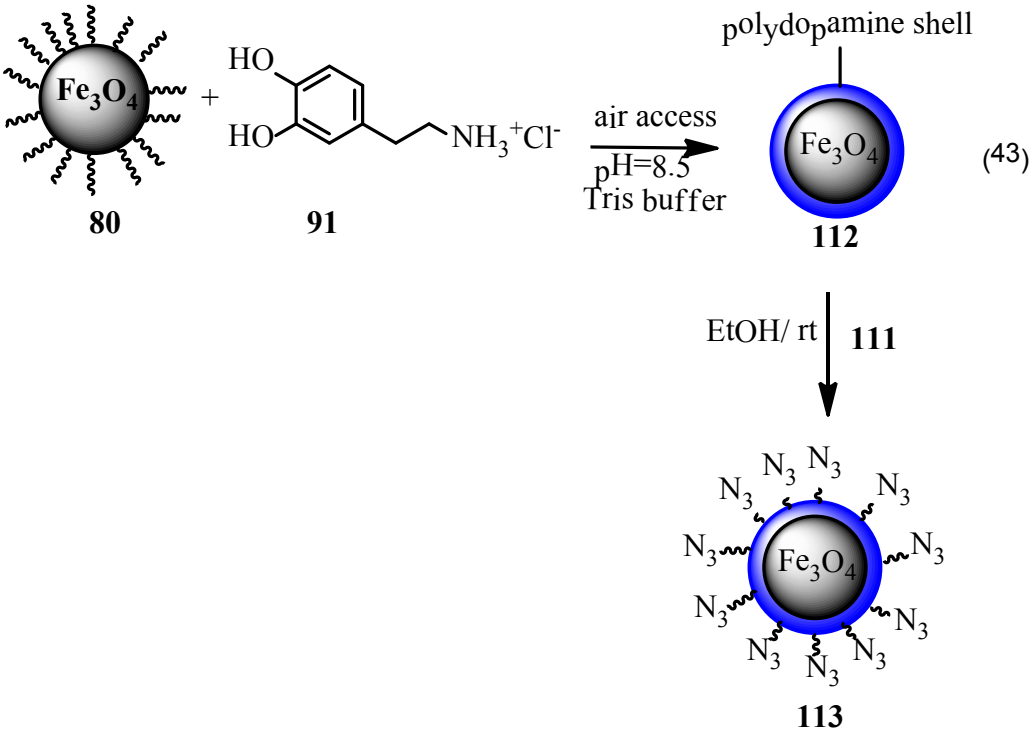

80 **91** **112** (43) **113**

This transformation could be monitored by FTIR (see Figure 28). Typical peaks of the HC=CH moiety of oleic acid at 3062 cm^{-1}, 3004 cm^{-1}, 1543 cm^{-1} were missing while new bands of polydopamine at 1440-1620 cm^{-1} were found.[225] An additionally peak at 586 cm^{-1} was attributed to a Fe-O vibration proving the presence of magnetite in the sample. It has been shown that anchoring of dopamine to the surface of magnetite NP can be reversible.[43] In our case, linking of polydopamine seems to render irreversible attachment of the polymer to the magnetite NP surface. The NP **112** exhibited superparamagnetic behaviour with Ms= 53.8 emu/g (see Figure 30).

In next step Michael reaction between quinoid function of polydopamine and excess of the azidoamine **111** was performed in EtOH at rt. As a consequence electrophilic groups (Michael system or carbonyl group) of polydopamine reacted with the amino group of the linker **111** either via Michael addition or imine formation yielding magnetite NP **113** with exposed azido groups. Successful modification was confirmed by FTIR analysis. The new NP **113** showed a characteristic peak at 2100 cm^{-1} typical for azides. Magnetite NP **113** showed superparamagnetic behaviour and could be easily manipulated by external magnetic field. However, magnetization measurements allowed to deduce that a small amount of **111** was fixed to the magnetite NP **112** surface because there is not a significant difference between the values of saturation magnetization, for the samples **113** (Ms =54.8 emu/g) and MNP **112** (Ms = 53.8 emu/g), which indirectly depends on the mass of the shell linked to the surface of magnetic nanoparticles.

To have a better look into the structure of the magnetite NP **112** and **113** XPS analysis was performed. The C 1s spectrum of **112** can be deconvoluted into two components: the most intensive component located at 284.6 eV corresponds to carbon atoms of C-C/C-H and the component at 288 eV is ascribed to C=O groups found in the polydopamine shell. The O 1s spectrum exhibits also two components assigned to C=O and to metal oxides (magnetite and the oxidized indium support). The fact that only one type of oxygen was found for the organic shell is interesting in terms of the structures proposed for polydopamine in the literature. The N 1s spectrum shows the contribution of nitrogen atoms of N-H groups in the polydopamine structure. The Fe 2p core level spectrum contains the doublet of Fe 2p3/2 and Fe 2p1/2 and their satellites. Each peak of the Fe 2p spectrum can be deconvoluted into two components corresponding to Fe^{3+} and Fe^{2+} ions found in magnetite. High resolution XPS spectra also allowed to prove the functionalization of **113** with azido groups. Comparison of the N 1s XPS spectra of **112** (Figure 25) and **113** (Figure 26) shows significant differences. The N 1s core-level spectrum of magnetite NP **113** shows three components: (i) the intense component at 399 eV corresponds to N-H/C-N; (ii) the component located at 402 eV is ascribed to the negatively charged terminal nitrogen atom =N- of the azido group (R-N=N+= N-); (iii) the high binding energy component located at 403.7 eV corresponds to a positively charged nitrogen =N+= of the central nitrogen atom of the azido group. The deconvolution of the C1s spectrum of **113** shows three contributions corresponding to C-C/C-H (284.6 eV), C-N (285.9 eV) and C=O (287.8 eV).

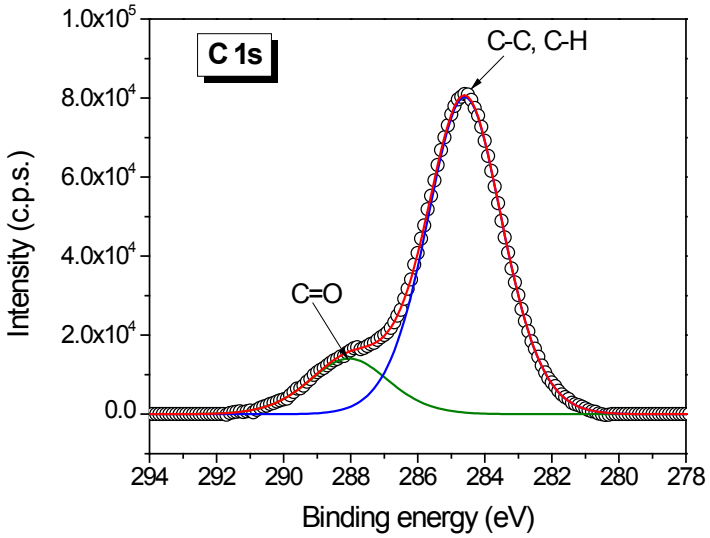

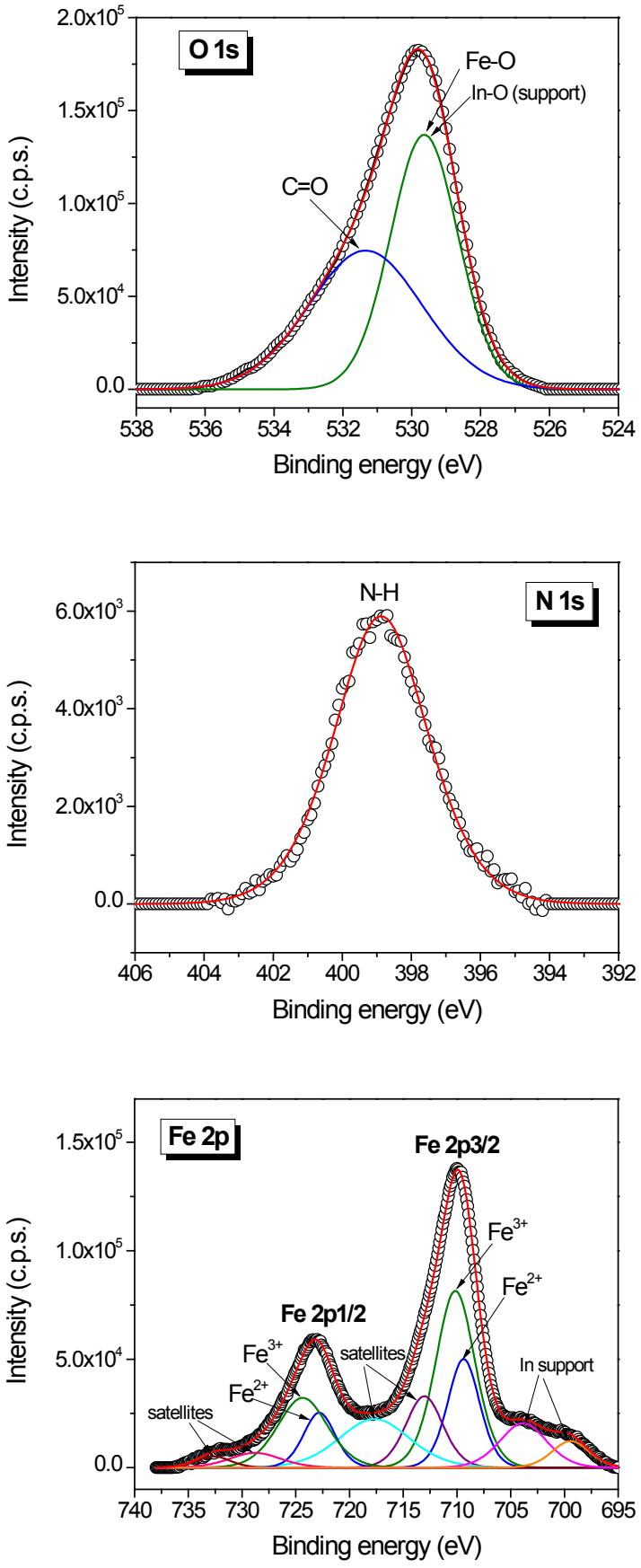

Figure 25. High resolution XPS spectra of magnetite NP **112**.

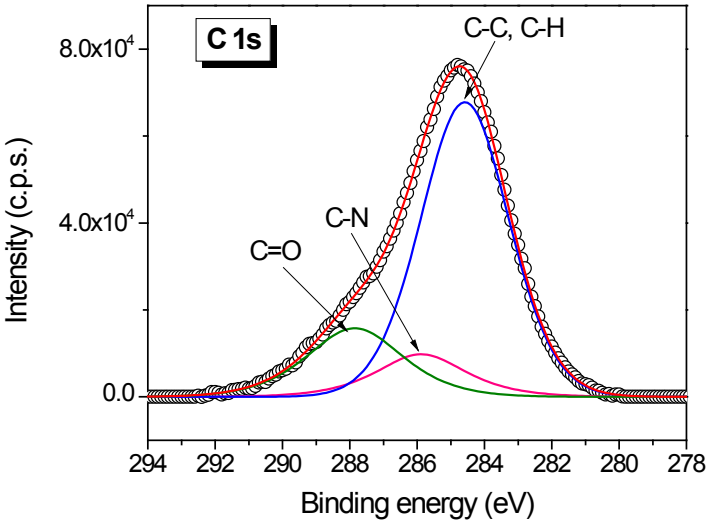
C 1s
C-C, C-H
C-N
C=O
Intensity (c.p.s.)
8.0x10^4
4.0x10^4
0.0
294 292 290 288 286 284 282 280 278
Binding energy (eV)

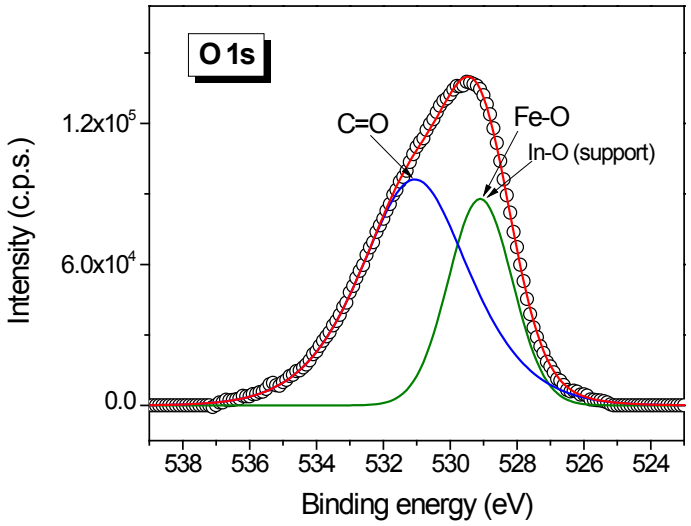
O 1s
C=O
Fe-O
In-O (support)
Intensity (c.p.s.)
1.2x10^5
6.0x10^4
0.0
538 536 534 532 530 528 526 524
Binding energy (eV)

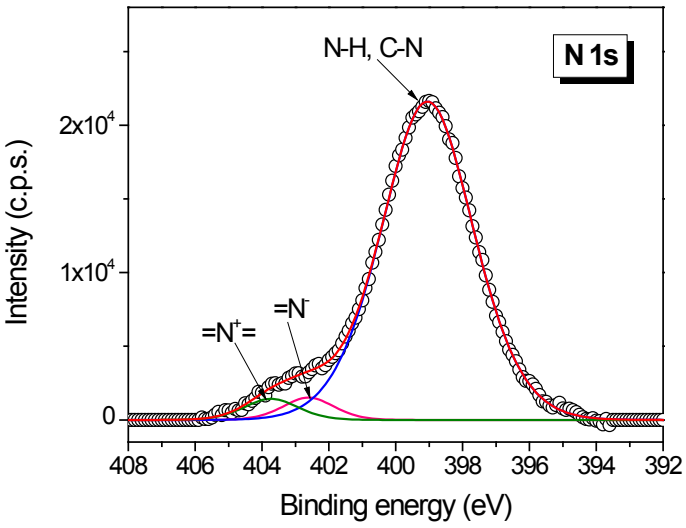
N-H, C-N
N 1s
=N-
=N+=
Intensity (c.p.s.)
2x10^4
1x10^4
0
408 406 404 402 400 398 396 394 392
Binding energy (eV)

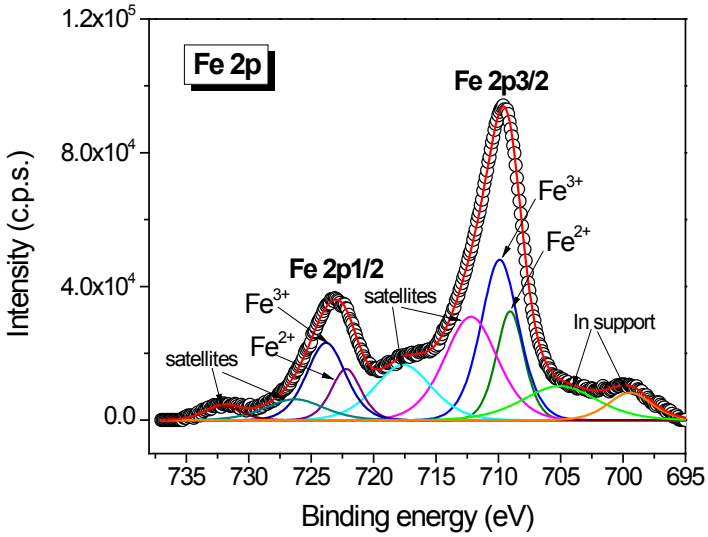

Figure 26. High resolution XPS spectra of C 1s, O 1s, N 1s and Fe 2p core levels of magnetite NP **113**.

To obtain a more comprehensive look into the structure of the functionalized polydopamine shells of the core-shell nanoparticles ^{1}H-NMR spectra were recorded first time. Normally, it is difficult to obtain NMR spectra of magnetic materials because of the magnetism of magnetic NP. MAS-NMR can help to overcome the problem caused by magnetic cores. In fact, acceptable ^{1}H NMR spectra were obtained for **112** and **113** (see Figure 27) by applying this technique in collaboration with H. A. Scheidt, University Leipzig. Surprisingly, aromatic CH-signals in the region of 6–7.5 ppm are very week in both spectra what allows to conclude that comparatively few CH-signals of a benzene ring were found in the material. Reliable assignment of all signals in the spectra of **113** and **112** was impossible. It was assumed that the signals at 2.80 and 8.01 correspond to CH_2N of 2,3-dihydroindole and the CH in 2-position of an indol-5.6-dione moiety, respectively. The reaction of azidoamine **111** with the polydopamine shell of MNP **112** gave rise to new signals at 3.25 and 7.97 which were explained by the change of some of the carbonyl groups of an indole-5.6-dione into an azomethine. These preliminary conclusions support a structure of polydopamine similar to **2** or **4** (see chapter 1.2.2). This phenomenon is described in more detail in chapter 2.2.2 where also polydopamine, which is not fixed to magnetite nanoparticles, was investigated.

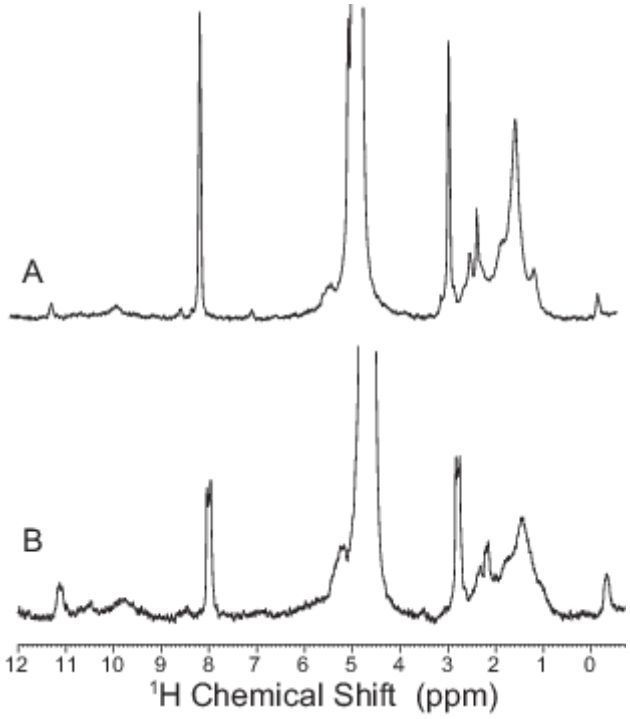

Figure 27. ssNMR spectra of MNP **112** (A) and **113** (B**)** in D_2O/DMSO- d6 solution at a temperature of 30 °C and a MAS-frequency of 5000 Hz.

As a proof of principle the azido modified magnetite NP **113** were submitted to CuAAC reaction with propargyl derivatives of biotin **75**, proline **72**, galactose **79** and the fluorescence marker dansyl. The propargyl dansylamide **116** is easily available by reaction of dansyl chloride **114** with propargyl amine **115**.[226]

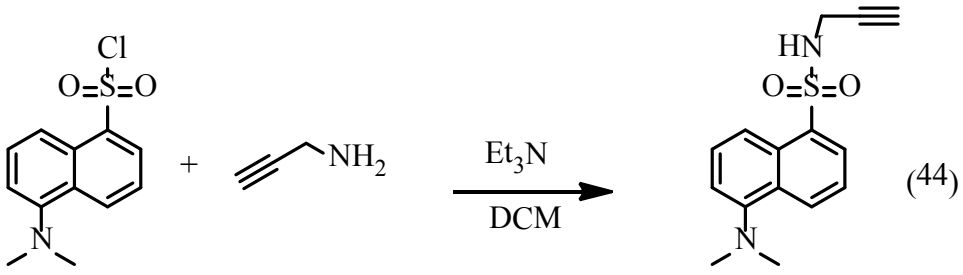

114 **115** **116** 88%

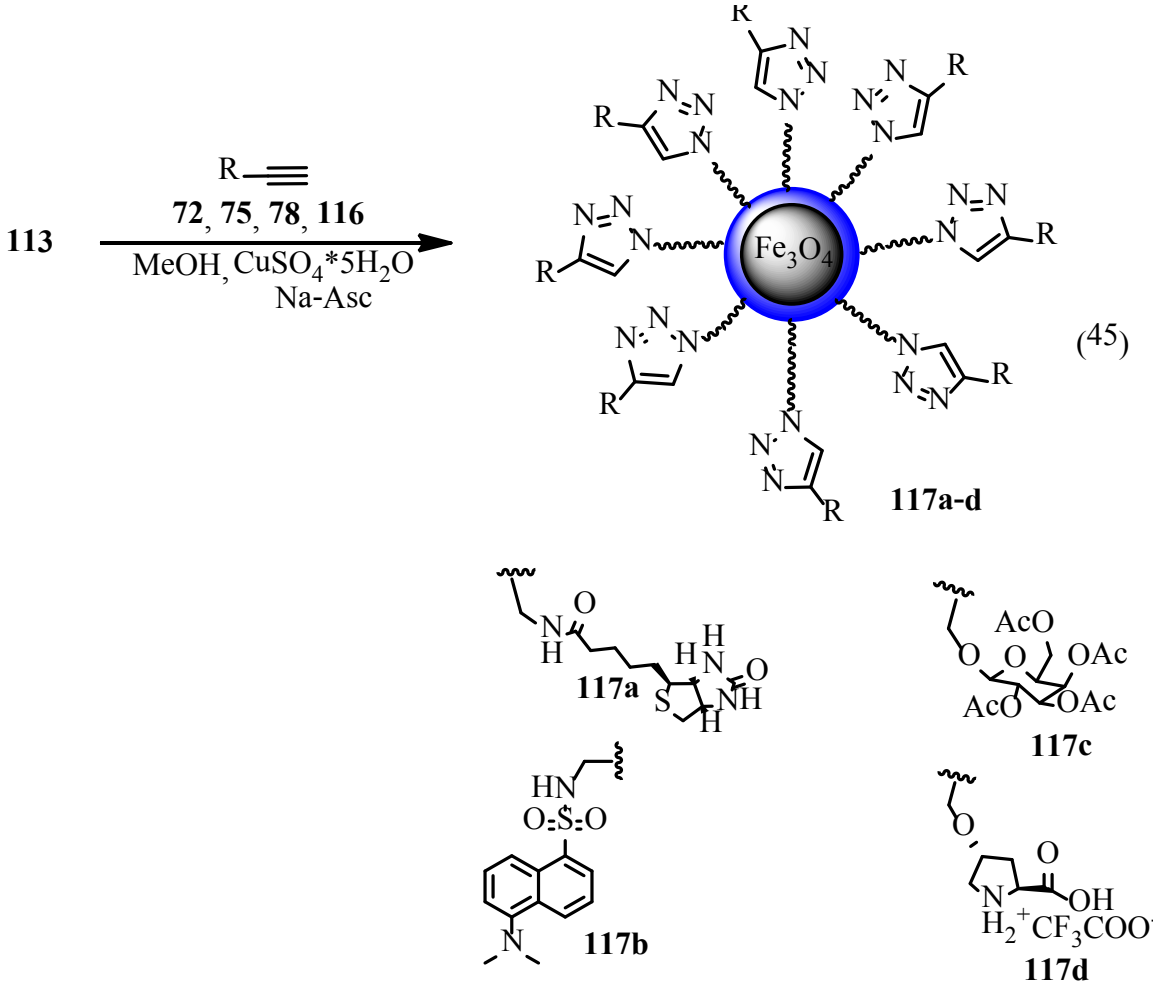

All click reactions of azido functionalized polydopamine coated magnetite NP were performed in MeOH using $CuSO_4$/Na-ascorbate as catalytic system. In all cases the expected functionalized magnetite NP **117** were obtained. Each type of NP **117** showed bands of CH_2 groups at 2825 cm^{-1} and 2925 cm^{-1} in the FTIR spectra (see Figure 28 and Appendix A 4). Furthermore, characteristic signals of the specific functions were observed such as at 1757 cm^{-1} and 1225 cm^{-1} due to the C=O stretching vibration of carbonyl groups and C-C(O)-C of acetate groups, respectively, in the galactose-tetraacetate containing magnetite NP **117c**. As a matter of fact, FTIR spectra also revealed (very weak remaining azido bands at 2090 cm^{-1}) that not all azido functions found in the MNP **113** were accessible to transformation into 1,2,3- triazoles by CuAAC. Such week azido bands were still found when the click reaction ran for extended times (72 h) and when ultrasound was applied. A similar effect was observed by Panella et al.[227] at magnetite NP covered with amino-functionalized silane shells, where attenuated total reflection spectroscopic investigations revealed that even less than 40% of the existing amino groups were able to

react. In our case, however, this fact does not create problems because the remaining azido groups do not interfere in further applications and anyway they seem to be hidden in the interior of the magnetite NP **117** rather than at the surface.

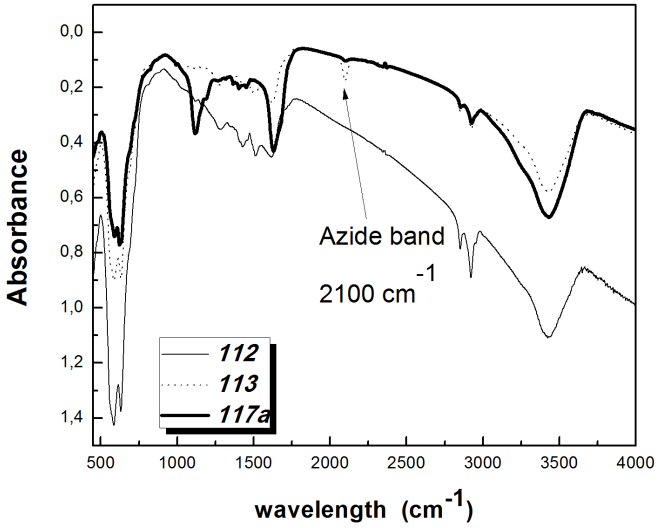

Figure 28. FTIR spectra of starting magnetite NP **112**, after functionalization with azide (**113**) and after CuAAC reaction (**117a**).

XPS spectra of functionalized MNP **117a** confirm the attachment of biotin to only a part of the azido groups of MNP **113** as the N 1s spectrum of **117a** contains the contributions of the nitrogen atoms of the azido group (R-N=N+= N-) similar to the N 1s spectrum of magnetite NP **113**. The C 1s spectrum of MNP **117a** shows an increased contribution of the component corresponding to C-N groups of biotin as compared with C 1s of MNP **113** (see Figure 29). The O1s spectrum of MNP **117a** consists of four components. The oxygen with high binding energy (534.9 eV) was not observed in magnetite NP **113** and is ascribed to water adsorbed at the functionalized MNP **117a**. An interesting feature can be seen at the S 2p spectrum (see Figure 29), which contains two peaks corresponding to sulphur atoms from –C-S-C- groups in biotin and to a sulfone group –C-SO_2-C- respectively.[228] Each peak contains the 2p3/2 and 2p1/2 doublet with an area ratio 2:1 and the position at the following binding energies: (i) for –C-S-C- , S 2p3/2 162.7 eV, S 2p1/2 164.1 eV; (ii) –C-SO_2-C- , S 2p3/2 168.5 eV, S 2p1/2 169.8 eV. Obviously the sulfone moiety belongs to biotin sulfone formed by oxidation of the biotin which occurs easily with different oxidizing reagents such as peroxides under mild conditions and is also observed in the biological metabolism of biotin.[229]

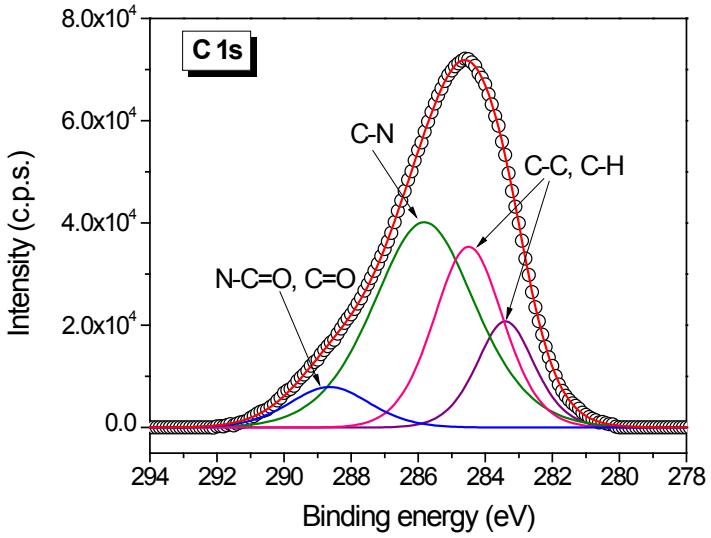
C 1s
C-N
C-C, C-H
N-C=O, C=O
Intensity (c.p.s.)
Binding energy (eV)

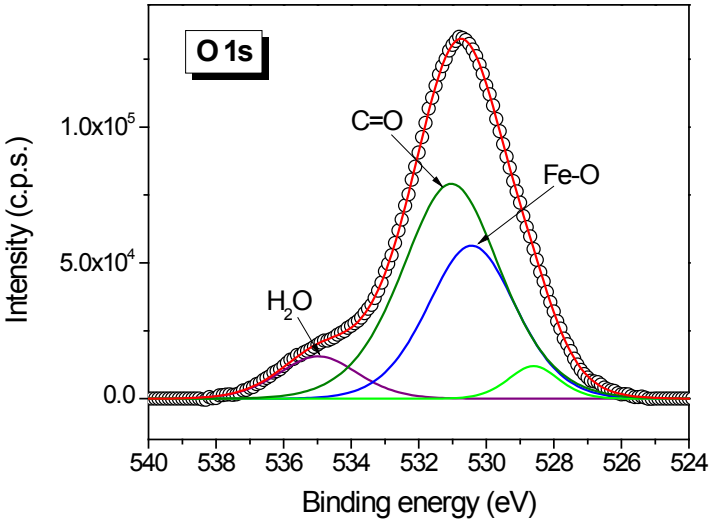
O 1s
C=O
Fe-O
H2O
Intensity (c.p.s.)
Binding energy (eV)

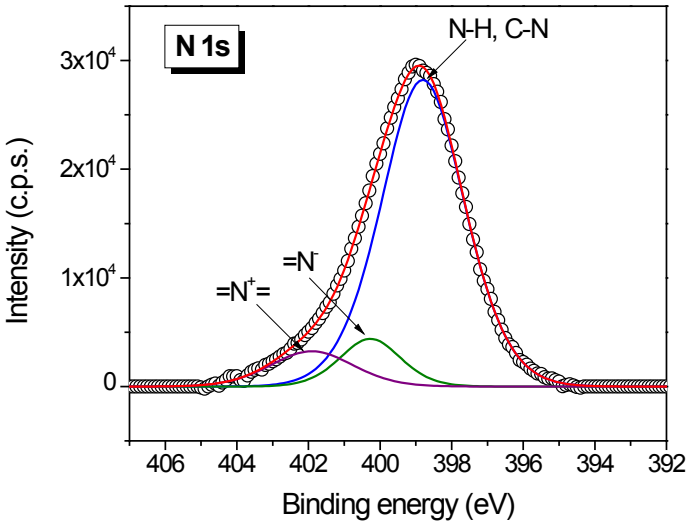
N 1s
N-H, C-N
=N-
=N+=
Intensity (c.p.s.)
Binding energy (eV)

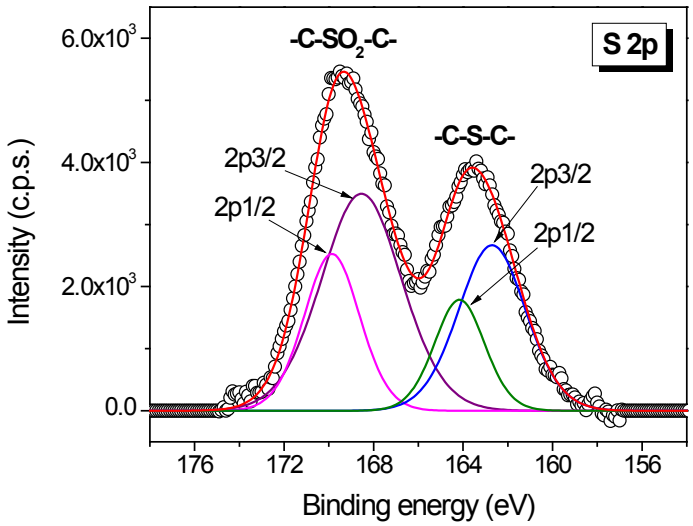

Figure 29. High resolution XPS spectra of C 1s, O 1s, S2p core levels of NP **117a**.

The functionalized magnetite NP **117** showed superparamagnetic behaviour as can be seen by missing of a hysteresis loop in the curve of magnetization vs. applied magnetic field at room temperature (Figure 30 and Appendix A 5). Despite of the increased mass of the shells of the magnetite NP **117** in comparison with the precursor **113** the values of saturation magnetization were still high and slightly differ with the type of functionality tethered to the NP (**117a**: 40.3 emu/g, **117b**: 36.3 emu/g, **124c**: 36.2 emu/g, **117d**: 42.8 emu/g, see also Appendix).

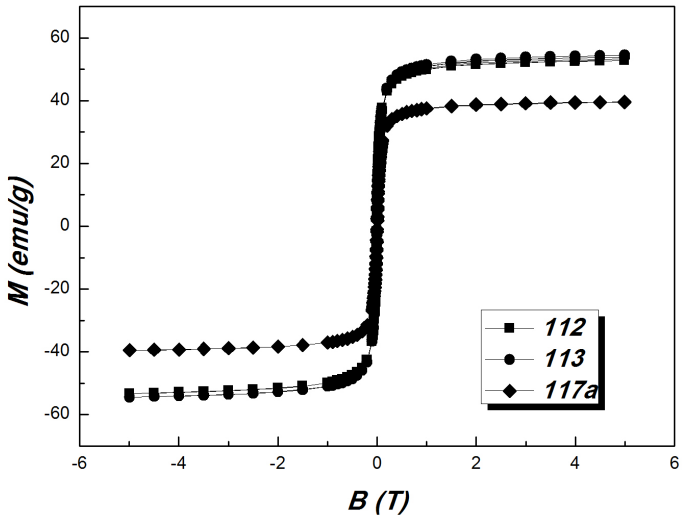

Figure 30. Magnetization vs. applied magnetic field at room temperature of magnetic nanoparticles **112**, **113** and **117a**.

Information about loading of magnetite NP with organic shells was obtained by thermogravimetric analysis (TGA). The results revealed that the polydopamine-covered MNP **112** contain about 20 % of organic material (volatile components disappearing until a temperature of about 100 °C were neglected) (see Figure 31). Mass increase of organic material during the conversion of **112** into the azido-functionalized NP **113** is only 6.3 % (Figure 32). If all reactive units of the shell would have reacted with the azidoamine **111** an increase of organic material of 75.1 % was expected from the stoichiometry of the reaction. Thus only about 8.4 % of the dopamine reactive units had reacted with **111**. Taking this azido-loading into consideration, the next step, i. e. click-reaction to **117a**, should have resulted in a mass increase by 17.4 % (assumption based on reaction stoichiometry). But the increase determined by TGA is only 9.4 % (Figure 32 and 33). Therefore it could be concluded that 54 % of the azido groups of **113** had undergone reaction with alkyne partner to form the triazole while the rest remained unchanged. This conclusion was in agreement with the observations that azido groups were still present in **117a** as confirmed by FTIR and XPS (vide supra).

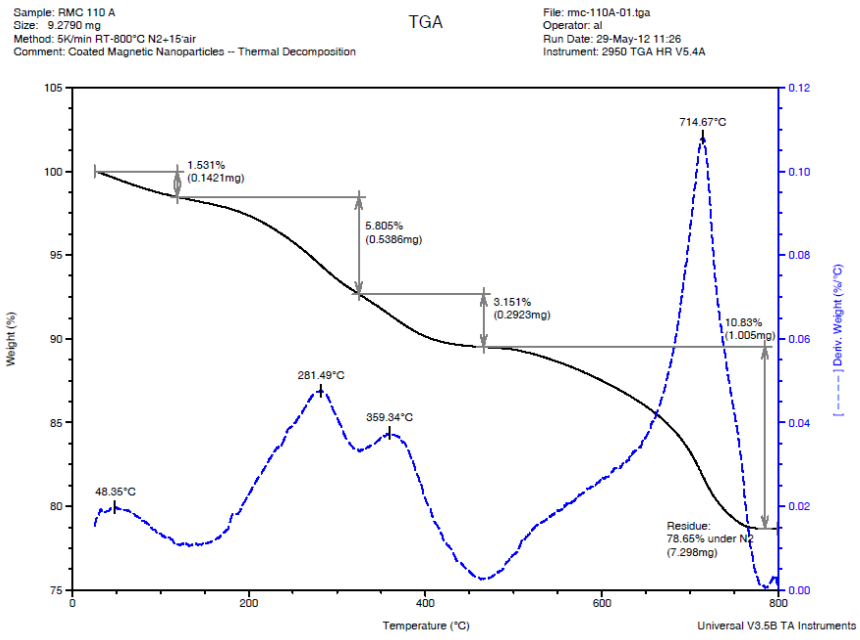

Figure 31. TGA of polydopamine coated magnetite NP **112**.

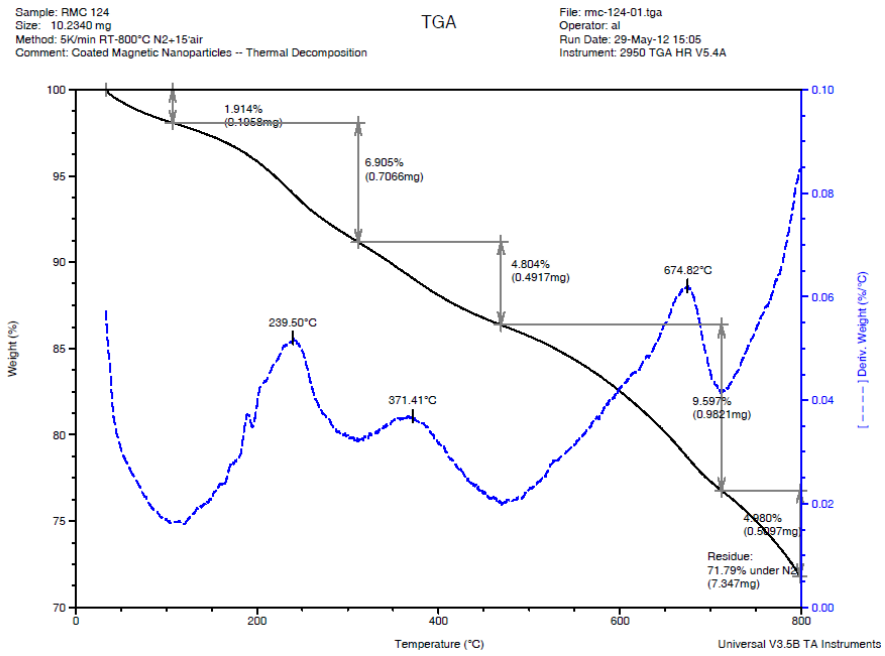

Figure 32. TGA of azide modified magnetite NP **113**.

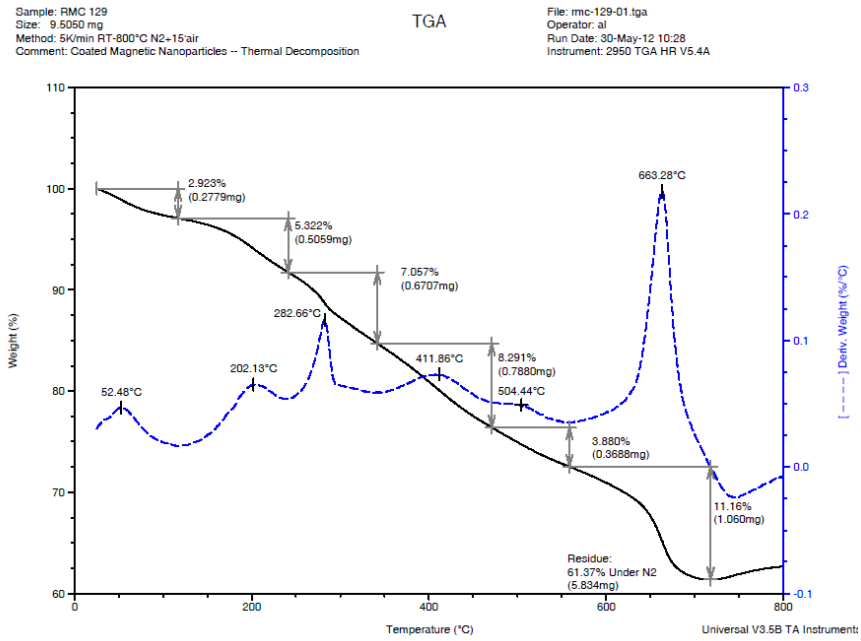

Figure 33. TGA of biotin modified NP **117a**.

In the further course of the research a similar strategy wherein a functionalized amine was added to the shell of PDA-coated magnetite NP was applied. Magnetite NP **112** were submitted to reaction with commercially available 5-amino-1-pentanol in EtOH. Reaction afforded magnetite NP **118** with hydroxyl groups on the surface of MNP. The magnetite NP **118** were isolated by simple magnetic separation. FTIR did not give clear evidence for

the expected functionalization because of overlapping bands (see Figure 34). NP **118** were used to run ROP of "lactic dimer" starting from the alcohol groups found at the organic shell. Reaction was performed in boiling PhMe and almost stoichiometric amount of DMAP as an organocatalyst. In this way biodegradable polylactic acid (PLA) was fixed on magnetite NP yielding magnetite NP **119.** FTIR spectra exhibited new band at 1746 cm^{-1}, 1635 cm^{-1} and two bands in the range 1215-1120 cm^{-1}. The first band was assigned to C=O stretching bond of the carboxylic moiety of polylactic acid. The latter two bands were ascribed to C-O-C symmetric stretching vibration bands that are typically observed in the 1050–1250 cm^{-1} range. These signals clearly indicated that the polymerization was successfully conducted and thus a new type of biocompatible polylactic acid coated nanoparticles was obtained, which is interesting for biomedical application, e. g. for magnetic imaging.

The material can further be used to attach additional applicatory function to the PLA of magnetite NP **119**. As an example biotin **75** was fixed to the PLA shells by Steglich esterification with DCC and DMAP as a catalyst. The FTIR spectrum was ambiguous because of overlapping bands. To get a proof of fixing **75** (biotin) to magnetite NP **120** XPS measurements were performed which clearly indicated the presence of sulphur. It is important to notice that also oxidation of a part of the sulphur atoms to sulfones occurred in this case (see Appendix, A 6).

The polymerization of "lactic dimer" and functionalization with biotin was done in cooperation with dr. Alexandrina Nan.

Magnetic measurement of the new nanomaterials confirmed superparamagnetic behaviour. NP **118**, **119**, **120** exhibited high magnetization values **118**:60.6 emu/g, **119**: 59.0 emu/g, **120**: 46.2 emu/g and hence could be easily attracted and controlled by an external magnet (see Figure 35).

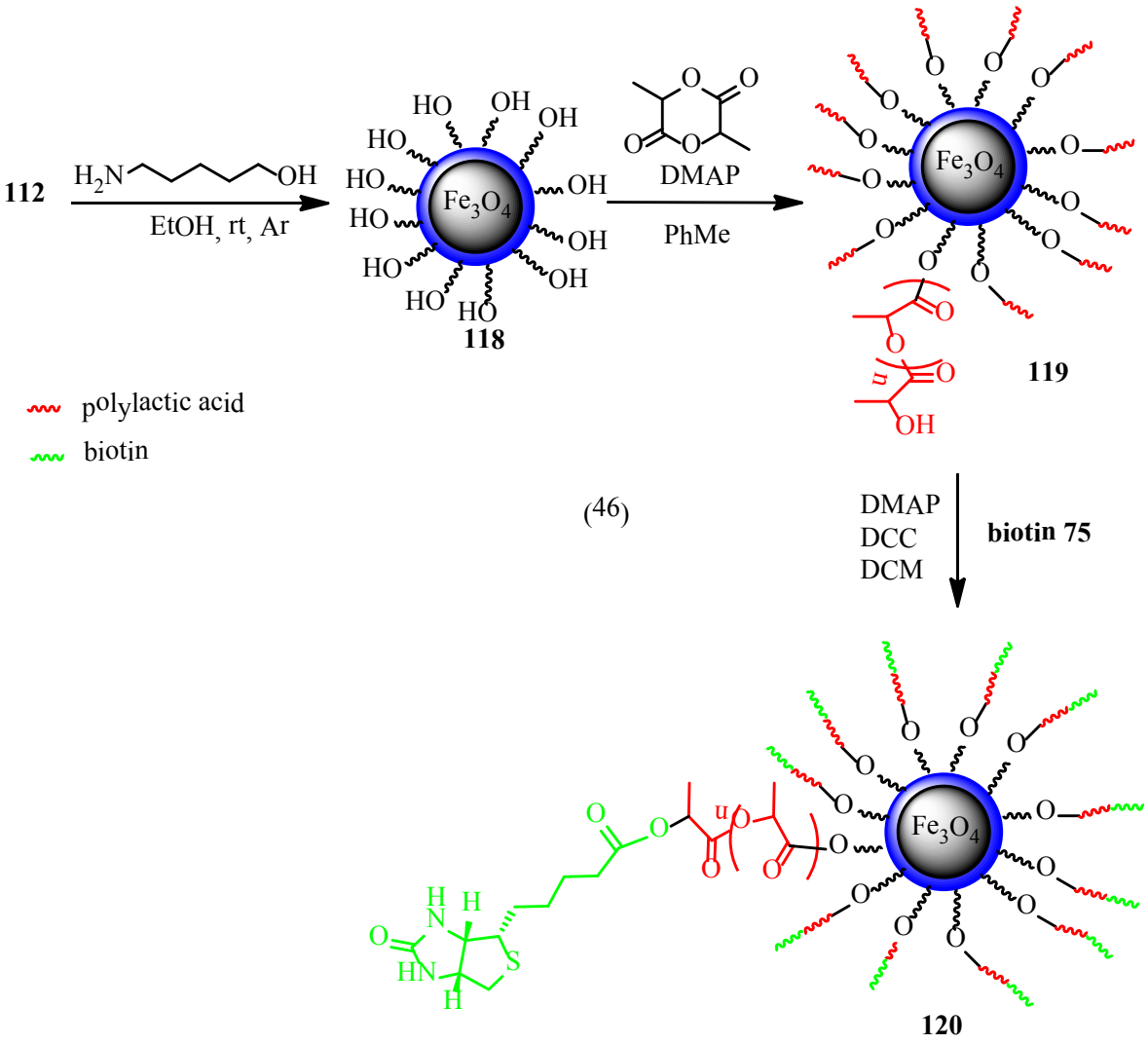

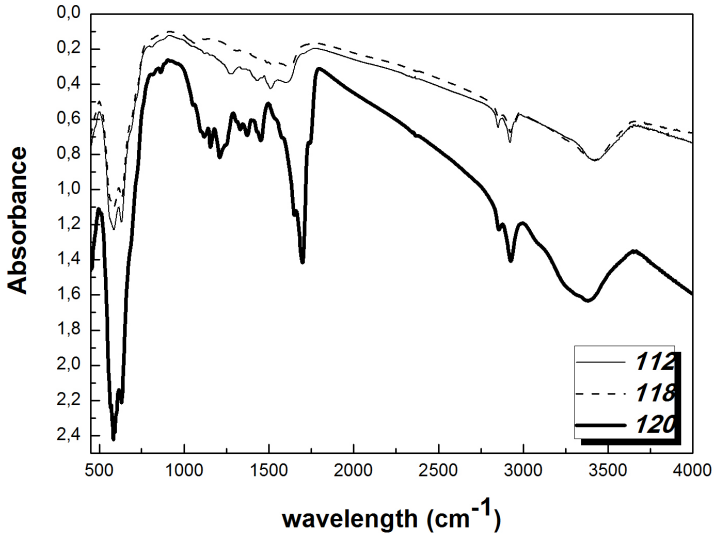

Figure 34. FTIR spectra of NP **112,** functionalization with hydroxyl groups (**119**) and with biotin (**120**).

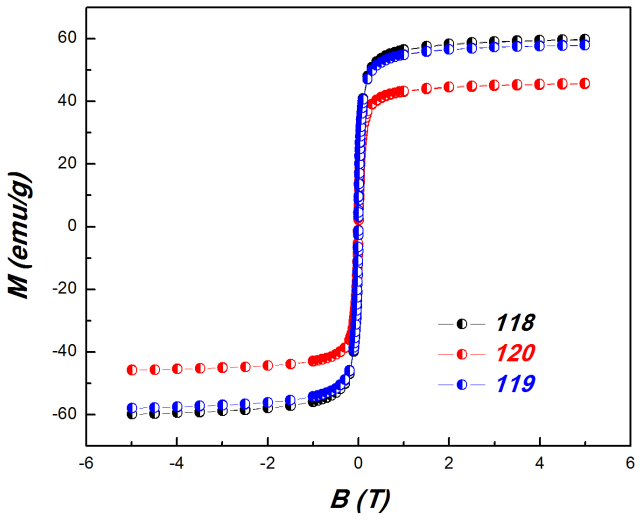

Figure 35. Magnetization curves of magnetite NP **118**, **119**, and **120**.

TEM investigation of NP **120** showed an almost spherical shape. They dispersed well in water and their aqueous suspension was stable, nevertheless slight agglomeration took place (see Appendix, A 7 for TEM images for **112**, **118** and **120**).

In conclusion, a versatile method for surface functionalization of magnetite NP coated with polydopamine with biocompatible and biorelevant entities was developed utilizing a bifunctional linker strategy. In this manner, azido modified magnetite NP were obtained which served as novel nanoplatform for CuAAC reaction. Important biological and catalytic units i.e. biotin, galactose, dansyl, and proline were attached to the NP in this way. The magnetite NP were characterized by different analytic techniques like FTIR, XPS and VSM. The morphology of the sample was checked by TEM. All analysis confirmed modification of the NP surface and thereafter evidenced tethering of the above mentioned compounds. In addition, changing the linker to 5-aminopentanol gave access to magnetite NP bearing hydroxyl groups exposed to the surrounding. This magnetite NP could be applied to surface modification by ROP of “lactic dimer” giving rise to polylactic acid covered magnetite NP. The potential to fix interesting biochemical entities at the terminal hydroxy groups of the PLA was demonstrated by the introduction of biotin by Steglich esterification.

2.2.2 New aspects of the polydopamine structure

Strange phenomena observed in the ssNMR spectra of polydopamine coated magnetite NP **112** encourage us to reconsider the structures of polydopamine postulated in the literature. This was done in a detailed manner in collaboration with other groups and the results were published.[230] Here, only a part of these results is included, which is necessary to explain the observed phenomena and to draw conclusions to further syntheses.

Polydopamine was prepared by oxidative polymerization of dopamine hydrochloride **91** under basic conditions and air access either in Tris buffer or phosphate buffer following reported procedures.[85] The solid black materials obtained by these two methods showed identical properties but the yield was much lower in the latter case. More insoluble, black polymer was collected when reaction was conducted in Tris buffer. The following results refer to PDA obtained in Tris buffer.

(47)

In addition to the structures of polydopamine **1**-**4** in the introduction part also other alternatives were proposed. Some of them were postulated on the basis of known eumelanin structures as naturally occurring pigments (see **122**-**131**). Based on proposed structures and ^{1}H ssNMR data obtained of magnetite NP **112** and **113** (see Figure 27) we assumed that open chain amioethyl groups with saturated and unsaturated rings, as shown in formula **132** could be involved in the structure of polydopamine. Thus aliphatic protons at about 1.4 ppm (CH_2−C), 2.9 (CH_2−C or CH_2−N), and 4 ppm (CH_2−N) and aromatic CH signals at about 7 and 8.1 ppm (indole positions 3 and 2, respectively) were observed in the ^{1}H ssNMR spectrum of **112**. The aliphatic signals appeared to be slightly downfield shifted as a result of the anisotropy effects exerted by the aromatic moieties. It has to be stressed that peaks at around 6.6 ppm, typical for monomer 2,3-dihydroindoles with H atoms in positions 4 and 7, as would display structure **3** proposed by Dreyer,[116] were not observed.

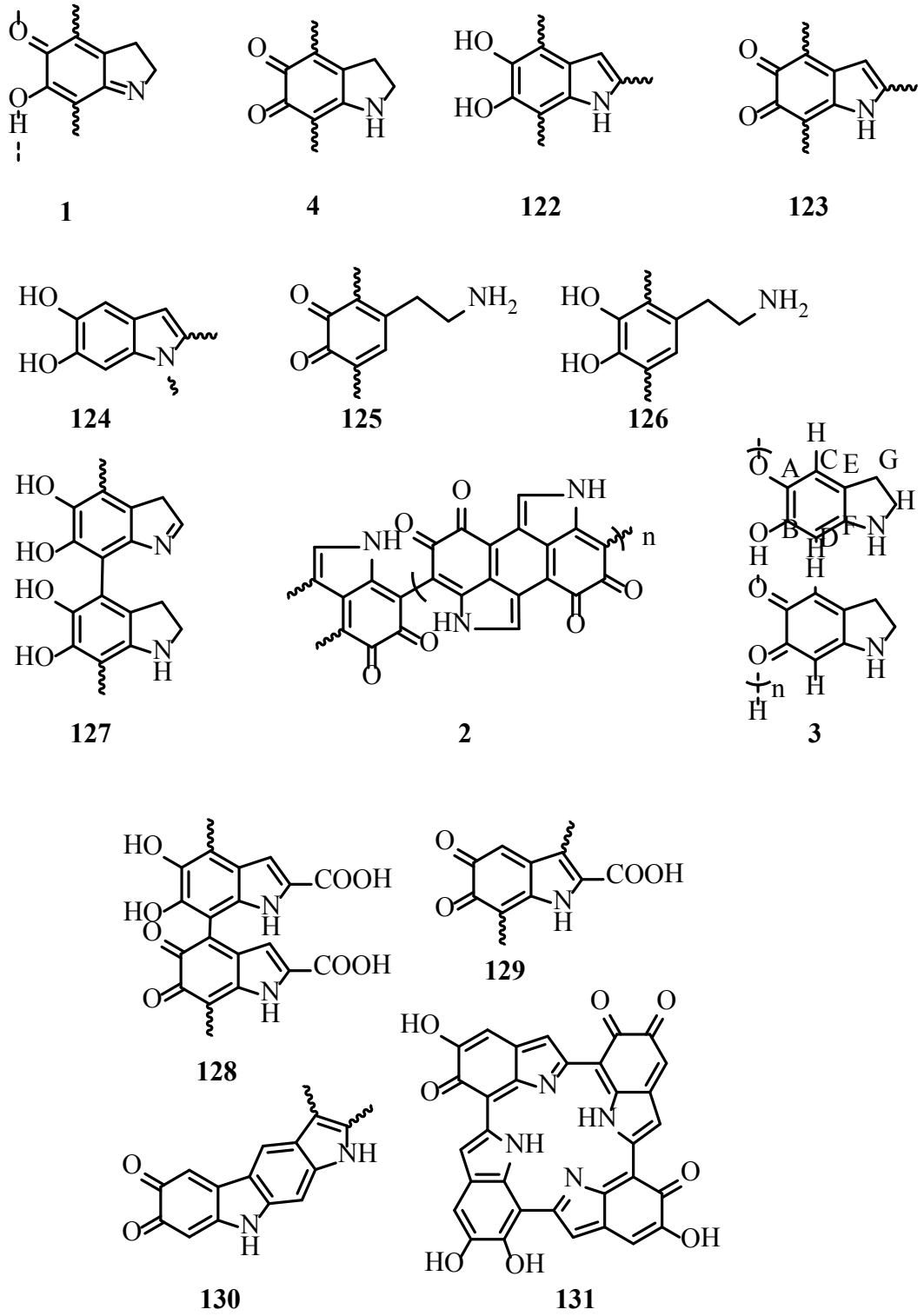

Figure 36 Different proposed structures of polydopamine **1**,**2**,**3**,**4** and **122-131**.

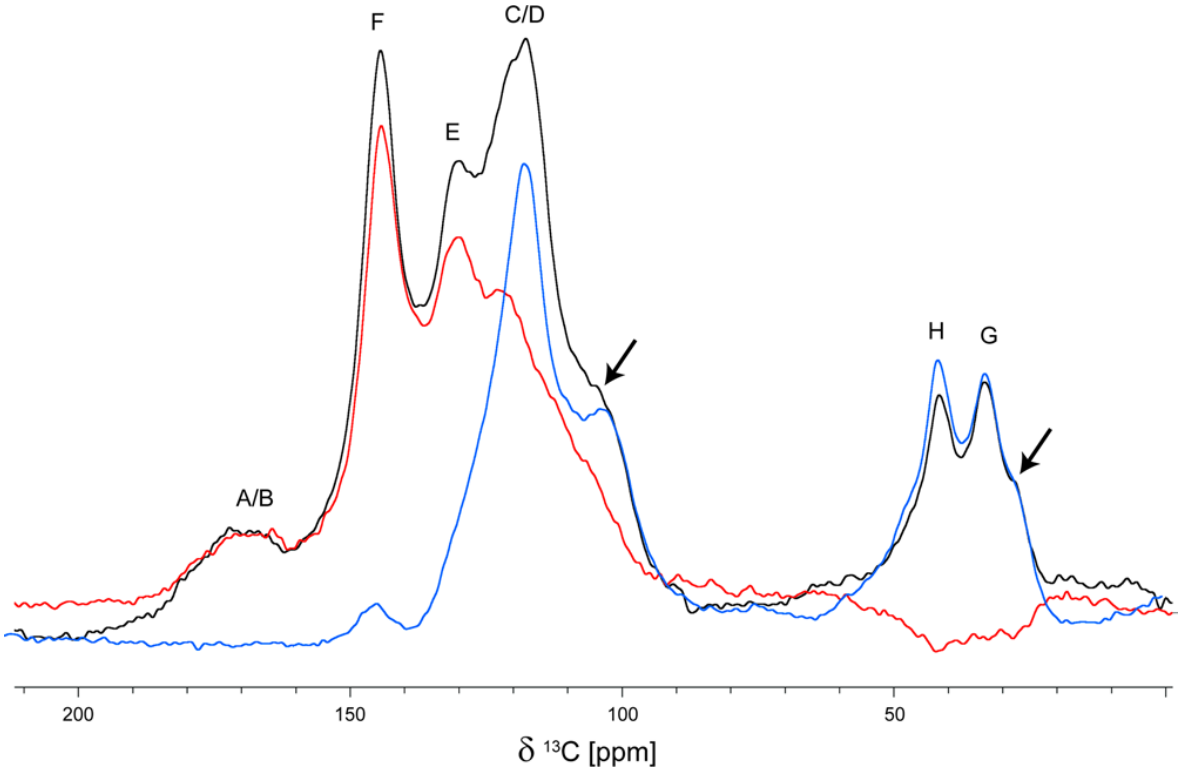

Figure 37. ^{13}C ss-NMR spectra of PDA (Tris sample) recorded at 14 kHz MAS frequency by using the standard CP-MAS sequence at long (2 ms, black line) and short (80 μs, blue line) contact times and CPPI sequences (red line).

More advanced ^{13}C ssNMR and ^{13}C CPPI MAS NMR (cross-polarization polarization−inversion magic angle spinning) spectra of polydopamine were recorded (see Figure 37). Parameters for recording ^{13}C CPPI MAS NMR spectrum were established after conducting tests on Lisinopril (a relatively rigid phenyl containing organic solid). For this model system, it was established that the CH carbons in the phenyl ring fully depolarize at τ_0 values ranging from 48 to 53 μs so that an average value of τ_{inv} = 50 μs was chosen to record the CPPI spectrum of PDA. At this polarization inversion time, the ^{13}C lines at 104 and 118 ppm disappeared (Figure 37, in red), whereas all of the others had reduced intensities, which correlated with partial depolarization or repolarization in the opposite direction of the corresponding ^{13}C nuclear spins. This is an important result indicating that the two carbon lines labeled C/D in the publication of Dreyer et al. cannot both be protonated. If this were the case, then the line at 120 ppm would also disappear in our CPPI spectrum.

With all this results in hand (and others described more in detail in our publication[230]) following structure of polydopamine **132** was postulated**.** The signals at 118

ppm was assigned to aromatic tertiary carbon atoms (CH) in position F of openchain dopamine units in cyclotetramers (Figure 57) and in terminal monomer units of oligomer chains (positions T in structure **132**, see also the oligomer structures verified by HR MS in Figure 38). Quaternary carbon atoms at 120 ppm were assigned to benzo positions D at bridging points (positions 4 and 7 for indole units) between monomer units. This conclusion is in accordance with the ^{13}C CPPI spectrum (Figure 37) where nonprotonated C atoms (C, D) are found for the benzo ring at postion 4 or 7 of indole structures that are adjacent to aromatic C−O or C=O moieties of the dopamine units. Out of all the nonprotonated carbon atoms, C/D has the strongest coupling with other protons in the vicinity, which is the only explanation for the fact that the intensity of the line at 120 ppm is reduced to a larger extent as compared to the extent of reduction of the E/F (130/144 ppm) and A/B (172 ppm) ^{13}C signals.

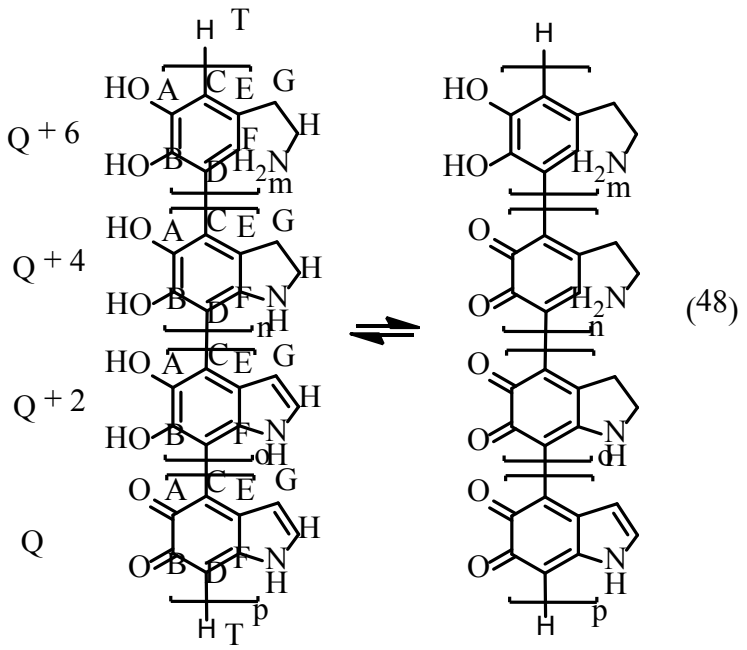

(48)

132 **132´**

Further proof of the proposed structure **132** for PDA was provided by ES (+)-MS. Interesting sets of peaks were detected for several oligomers differing by 2 m/z caused by different degrees of saturation (see Figure 38, 39, Table 1 in Appendix for PDA tetramers (4Q+6 to 4Q+18) and a PDA octamer (4Q +36)). The same pattern of signals was observed for PDA trimers (peaks corresponding to oligomers 3Q to 3Q+16) and pentamers (peaks assigned to oligomer species 5Q+8 to 5Q +22) The hydrogen atoms found at sites of saturation can be distributed in several ways in the oligomer chain, and additional

tautomers can also exist (e.g. **132** and **132´**). However, the appearance of the peak at m/z 602.2316 (Figure 38 a) proves the existence of open-chain dopamine units, because otherwise it is impossible to host 18 additional H atoms starting from the fully unsaturated tetramer 4Q. No difference in the ES(+) spectra of PDA samples obtained in Tris or phosphate buffer was observed (see Appendix, Table 1 and A 8-10). However, it has to be mentioned that the HRMS signal at m/ z 595.1841 (4 Q + 12H) not only matches with an openchain tetramer **132** but also with a cyclotetramer, similar to structure **131** postulated as a protomolecule for natural eumelanin.[231]

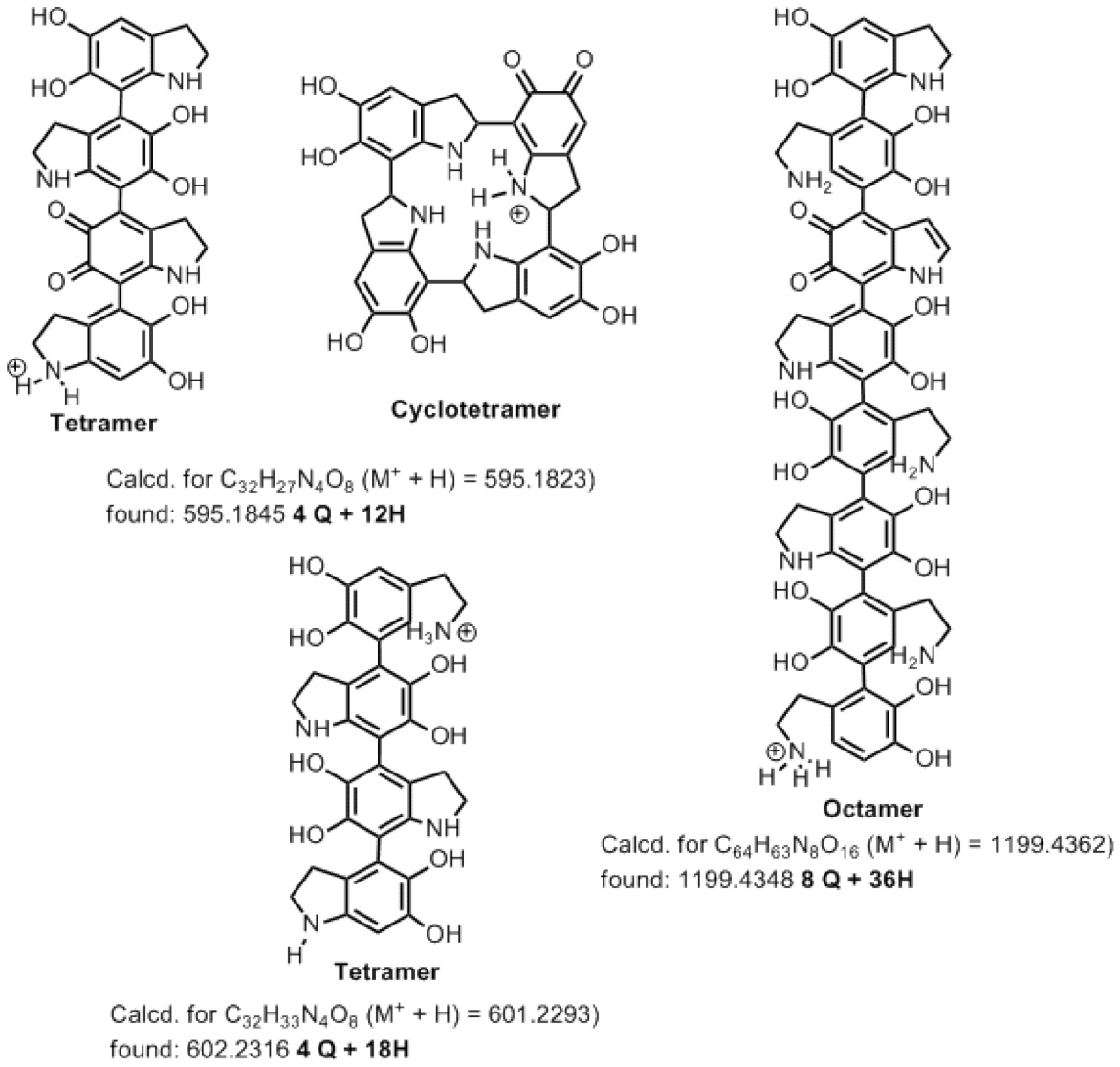

Figure 38. HR-MS peaks for tetramers and an octamer of PDA found by high-resolution ES(+)-MS.

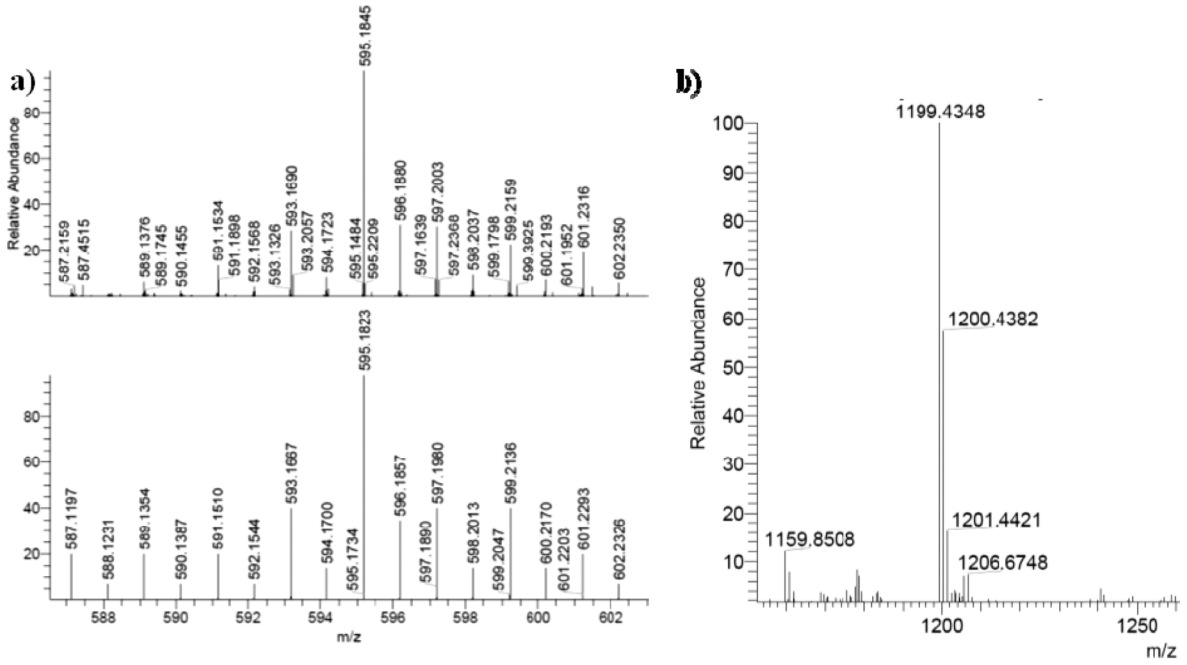

Figure 39. ES(+)-HRMS spectrum of PDA (0.1 mg/mL) in 97/2/1 methanol/DMSO/TFA. (a) Comparison of the experimental spectrum (top) and simulated isotopic patterns (bottom) for PDA tetramers with different degrees of saturation (4Q+6 to 4Q+18). (b) HR-MS peak of a PDA octamer (8Q+36).

The XPS spectra of polydopamine provided additional proof for the proposed structure **132** of polydopamine. The O 1s spectrum (see Appendix, Figure A 11) shows two main contributions. One was ascribed to C=O (530.4 eV) and the other to OH (532.1 eV), while another component of very low intensity located at 536.1 eV was assigned to COOH. This signal is caused by a contamination by environment which is a known phenomenon in XPS. The fit for the C 1s spectrum (see Appendix, A 11) was obtained with three components corresponding to the carbon atoms: C−C/CHx (284.1 eV), C−N/C−OH (285.2 eV), and C=O (287.9 eV). The N 1s spectrum (Figure 40) contains only one contribution found at 399.4 eV, which is typical for amine NH. It has to be stressed that that imine nitrogen atoms as shown in the structure proposed by Shalev [232] were not found in the XPS spectrum.

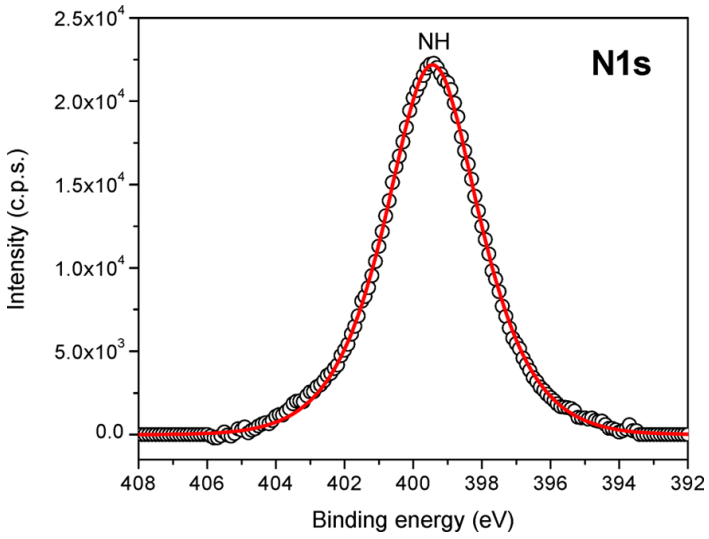

Figure 40. High-resolution XPS spectra of N 1s core levels of PDA.

In summary, it has been proved that PDA consists of units covalently bound by C-C. The results indicate that single indoline units linked by hydrogen bonding as recently proposed by Dreyer[116] are not possible. In addition, the presence of various oligomers, most of them, in different states of saturation, was shown by HR-MS. These experiments also evidenced that aminoethyl chains (open form) occur in the oligomer chain of PDA. Based on these results a new structural model of PDA was proposed based on mixtures of different oligomers wherein indole units with different degrees of (un)saturation and open-chain dopamine units are connected by C-C-bonds.

2.2.3 Novel catalytic properties of Polydopamine

It was mentioned before (see chapter 2.2.1) that polydopamine is reactive towards nucleophilic amino or thiol groups. To exploit the possibility of functionalization of PDA by thio Michael reaction in order to get magnetically supported organocatalysts *N*-Boc protected cysteine[233] **134** was submitted to the reaction with magnetite NP **112** coated by PDA. After acid treatment cysteine modified magnetite NP **135** were obtained.

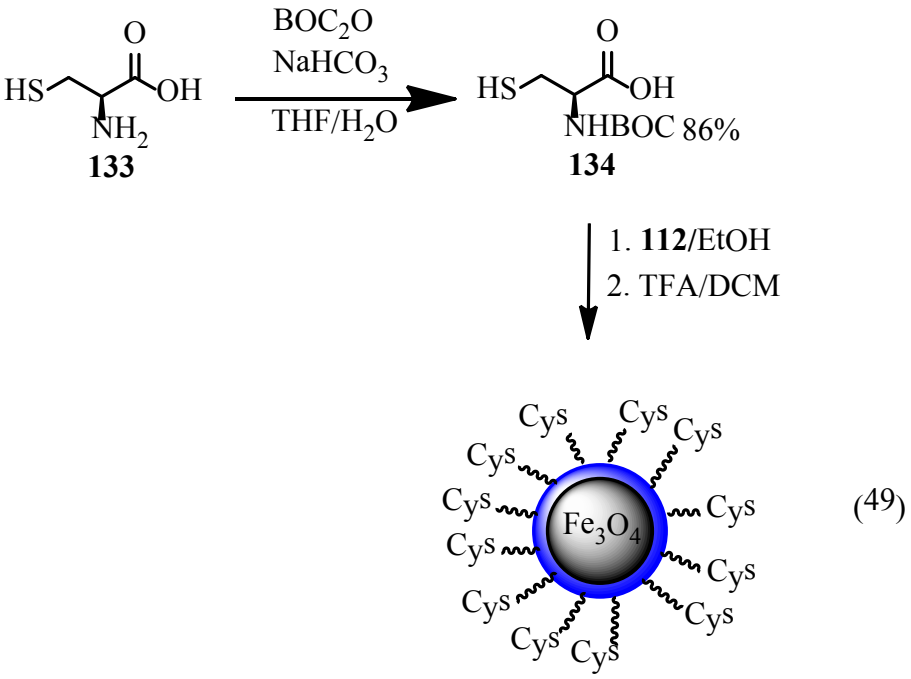

(49)

A new weak peak was observed at 1715 cm^{-1} in the FTIR spectrum of **135**, which was ascribed to the stretching vibration of C=O group. Magnetic investigation revealed Ms = 58 emu/g. (see Appendix, Figure A 12).

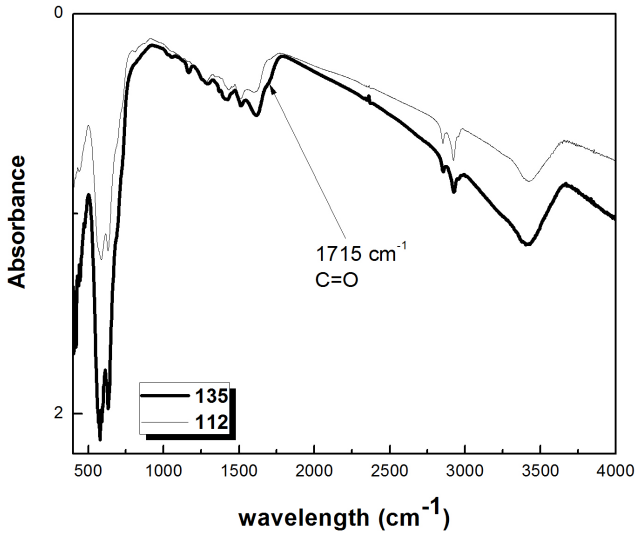

Figure 41. FTIR spectrum of magnetite NP **135**.

In order to get clear evidence for the attachment of cysteine in magnetite NP **135** XPS was performed (Figure 42). It proved that the sample contained sulphur. As already observed in cases of biotin derivatives part of the sulphide sulphur atoms were oxidized to the corresponding sulfone.

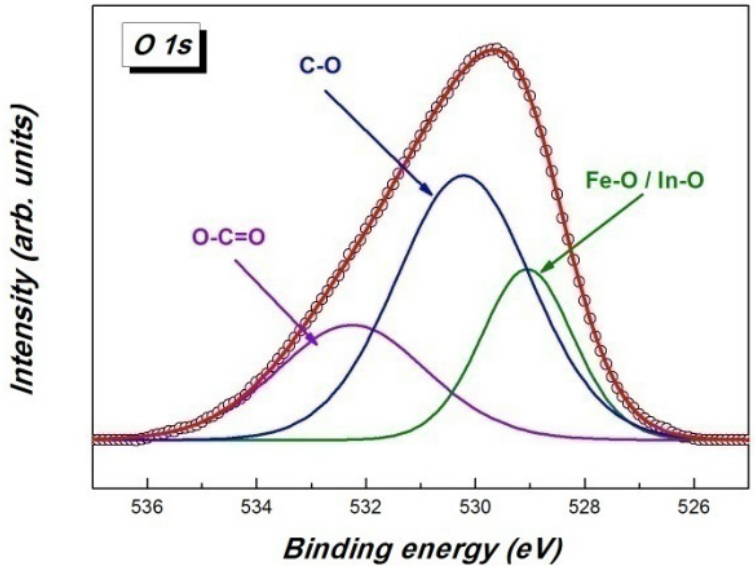
O 1s
C-O
Fe-O / In-O
O-C=O
Intensity (arb. units)
536
534
532
530
528
526
Binding energy (eV)

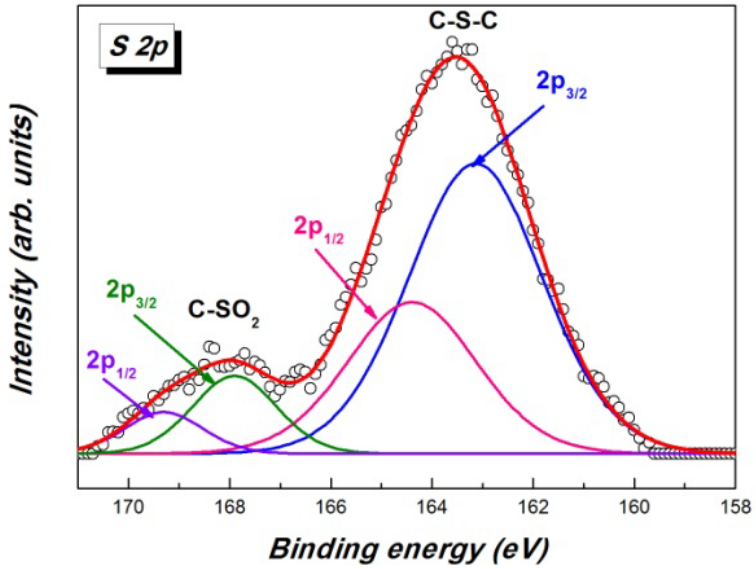
S 2p
C-S-C
2p3/2
2p1/2
2p3/2
C-SO2
2p1/2
Intensity (arb. units)
170
168
166
164
162
160
158
Binding energy (eV)

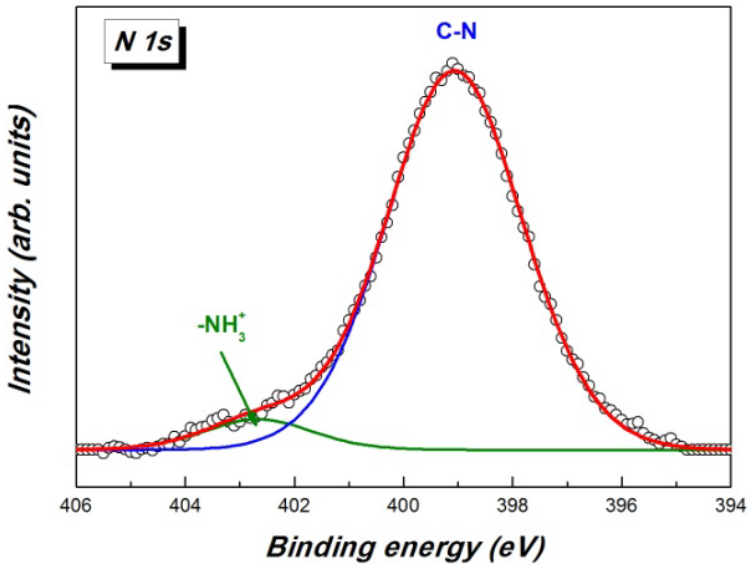
N 1s
C-N
-NH3+
Intensity (arb. units)
406
404
402
400
398
396
394
Binding energy (eV)

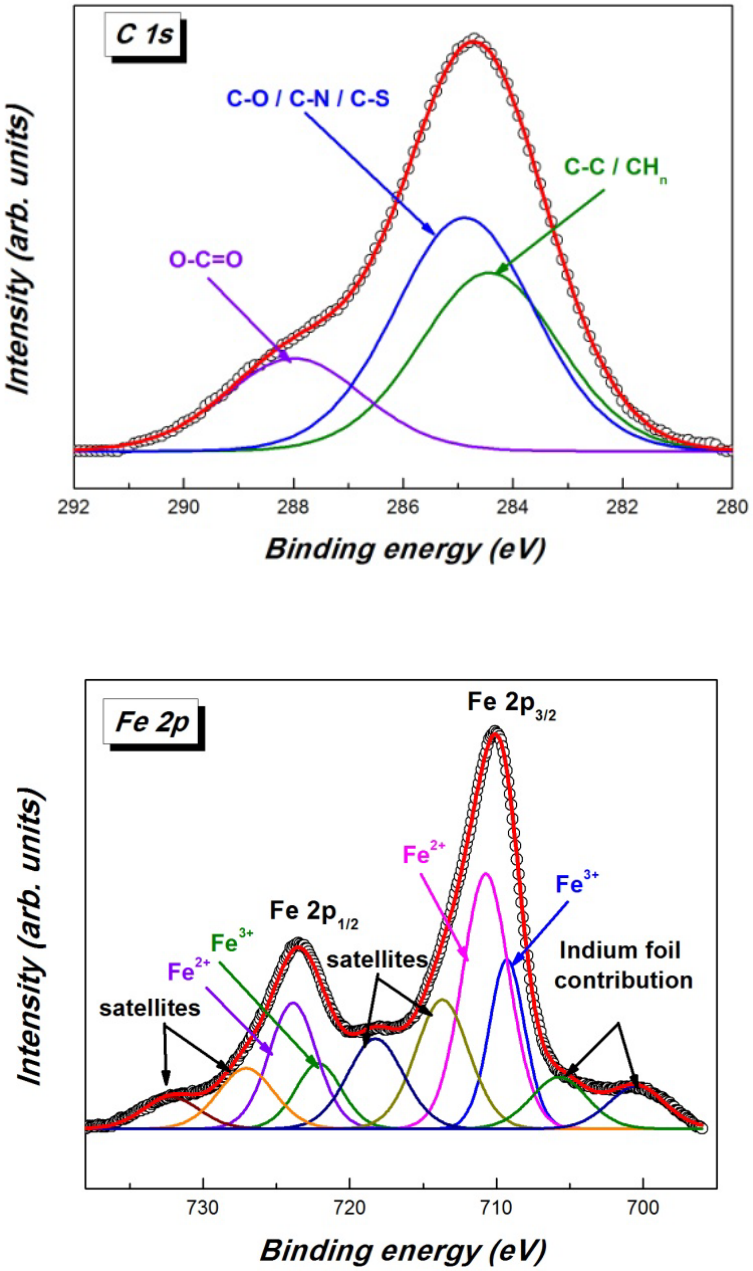

Figure 42. High resolution XPS spectra of magnetite NP **135** with cysteine.

The high resolution XPS confirmed that the magnetite core was not affected by the reaction with cysteine. The NP **135** possess an almost spherical shape and are well covered the with a PDA layer as can be seen by TEM (see Appendix, Figure A 13).

Magnetic composites **117d** and **135** (functionalized with proline and cysteine, respectively) bear catalytic units. Thus activity of these magnetite NP as magnetic organocatalysts can also be expected. Again, the aldol reaction of cyclohexanone **106** and 4-nitrobenzaldehyde **107** served as model reaction. Unexpectedly, magnetite NP **135** failed

to imply enantioselectivity but gave the aldol product as racemic mixture in 48 % yield. A lack of enantioselectivity was also observed when magnetite NP **117d** were applied under the same conditions. These phenomenon together with structural studies of PDA (see chapter 2.2.2) which revealed the presence of ethylamino chains as well as 2,3-dihydroindole rings in PDA, led us to the conclusion that a non-stereoselective background reaction takes place catalysed by these structural elements of PDA .

Thereafter, we checked non-supported PDA (see Figure 43) and PDA fixed to magnetite NP (**137**, **138**) in this respect. To be sure that there was no side reaction catalyzed by the magnetic core industrially produced magnetite NP **136** covered with silane where used and coated with PDA

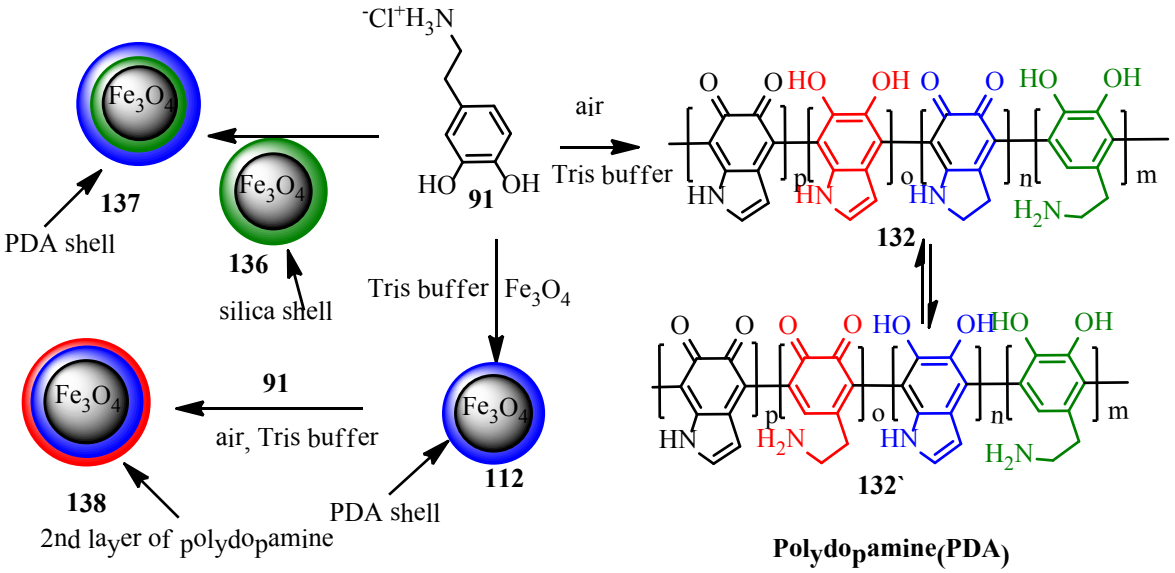

Figure 43. Synthesis of supported and non-supported PDA polymer for catalytic test in aldol reaction.

All materials were prepared by oxidative polymerization of dopamine hydrochloride in Tris buffer solution under air access and in the presence of the respective magnetite NP. Attachment of PDA to the NP was proved by FTIR (see Figure 44 and 45). Superparamagnetic behaviour was checked by VSM measurements (see Figure 46 and 47, missing hysteresis loop) where Ms Values 47.66 and 32.34 emu/g for **112** and **138**, respectively, were determined. The Ms value dropped from 48.43 emu/g to 36.56 emu/g when magnetite NP **136** were transformed into the PDA-coated magnetite NP. **137**. The magnetic character of all these magnetite NP allowed their manipulation by an external

magnetic field. TEM analysis showed that the NP were almost spherical in shape and small aggregation took place (see Appendix, A 14).

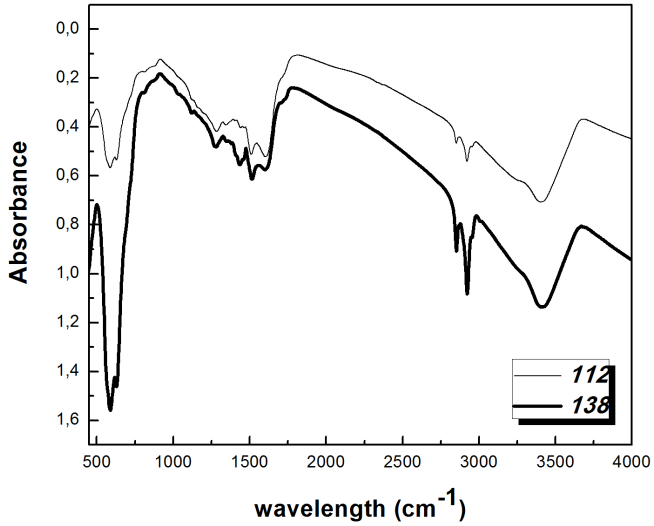

Figure 44. FTIR spectra of magnetite NP **112** and **138**.

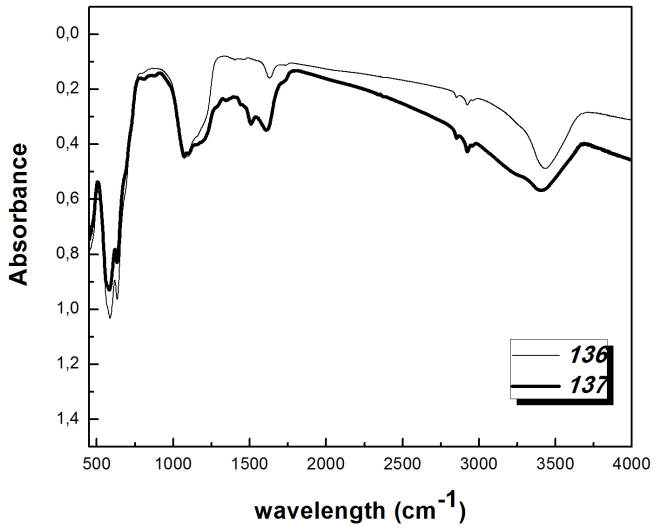

Figure 45. FTIR spectra of magnetite NP **136** and **137**.

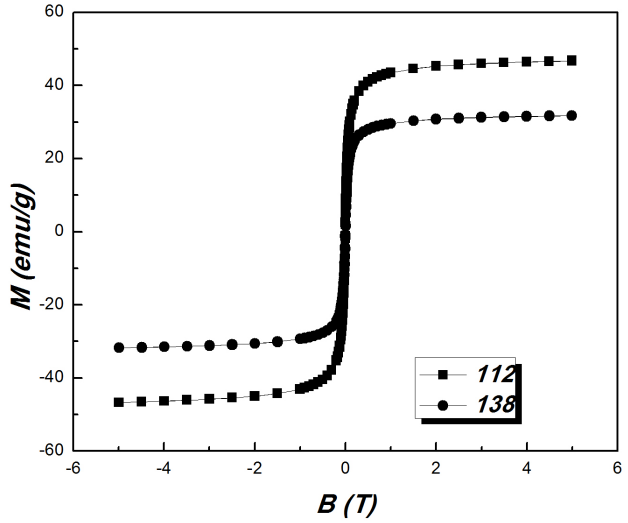

Figure 46. Magnetization *vs*. applied magnetic field at room temperature of NP **112** and **138**.

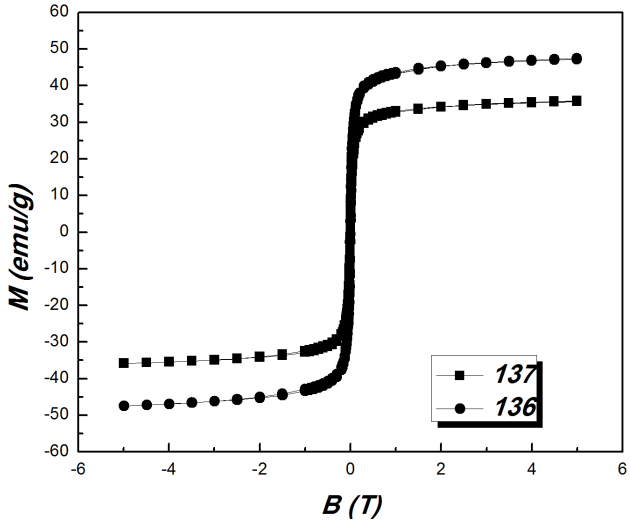

Figure 47. Magnetization *vs*. applied magnetic field at room temperature of magnetite NP **137** and **136**.

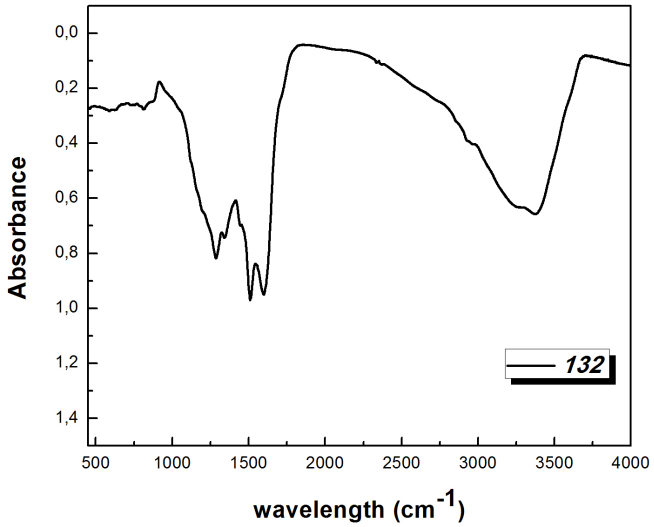

Figure 48. FTIR spectrum of PDA as non supported polymer

The PDA-coated MNP **112**, **137** and **138** as well as non-supported PDA **132** were applied in the aldol reaction of cyclohexanone and 4-nitrobenzaldehyde under solvent free conditions at 50 ^{o}C in order to find out if they exhibit catalytic activity (see Table 4).

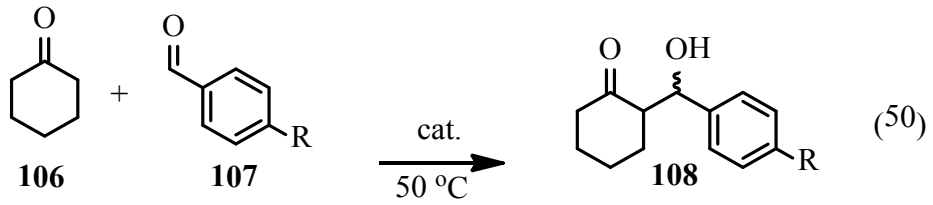

106 **107** **108** (50)

108 R

a NO_2

b Br

c H

d OMe

Table 4. Catalytic tests with PDA **132**, NP **112**, **137** and **138** as well as substructures **139-142** for elucidation of the catalytic motif.

Entry	Product 108	Catalyst[a]	Amount [mg]	Time [h]	Yield [%]	dr syn/anti
1	**a**	**132** [b]	100	24	Traces	n.d.
2	**a**	**132**	50	8.5	65	56:44
3	**a**	**132**	100	5.5	90	57:43
4	**a**	**132** 1st run	100	24	93	56:44
5	**a**	**132** 2nd run	115	24	75	48:52
6	**a**	**132** 3rd run	125	24	66	49:51
7	**a**	**132** 4th run	123	24	70	51:49
8	**a**	**132** 5th run	~120	24	75	53:47
9	**a**	**112**	200	12	50	65:35
10	**a**	**112**	340	24	86	65:35
11	**a**	**112** 2nd		24	70	63:37
12	**a**	**138** 1st run	100	24	97	55:45
13	**a**	**138** 2nd run		24	70	53:47
14	**a**	**138** 3rd [c]		24	13	70:30
15	**a**	**138** MeI[d]	85	24	35	57:43
16	**a**	**138** MeI[e]	100	24	43	60:40
17	**a**	**138** Ac_2O[f]	100	24	37	72:28
18	**a**	**137** 1st run	100	24	75	55:45
19	**a**	**137** 2nd run		24	40	54:46
20	**a**	**137** 3rd run	in water	24	traces	n.d.
21	**a**	**91**[g]	10 mol %	24	80	60:40
22	**a**	**139**[h]	10 mol %	24	traces	n.d.
23	**a**	**140**[h]	10 mol %	24	traces	n.d
24	**a**	**141**[g]	10 mol %	24	25	49:51
25	**a**	**142**[h]	10 mol %	24	75	53:47
26	**b**	**138**	100	24	48	56:44

27	**c**	**1385**	100	24	traces	n.d.
28	**d**	**138**	100	24	Traces	n.d.
29	**a**	**138**[i]	100	24	67	60:40
30	**a**	**138**[j]	100	24	52	67:33

[a]Reaction conditions: aldehyde (0.25 mM), cyclohexanone (0.5 ml), H_2O (140 μl), 50 °C, [b] Reaction without addition of water at rt, [c] Catalysts was washed with 5 ml of 1 M HCl for 5 min, [d] MeI in EtOH, rt were used to methylate nucleophilic sites of **3** before reaction, [e] K_2CO_3 and MeI at 50 °C were used to methylate nucleophilic sites of **3** before reaction. [f] Acetic anhydride, triethylamine, MeCN, rt, 24 h was used to acetylate nucleophilic sites of **3** before reaction. [g] Reaction performed with 10 mol % of catalyst, aldehyde (1mM), cyclohexanone (2 ml), H_2O (560 μl), 50 °C and 10 mol % Et_3N, [h] Reaction performed with 10 mol % of catalyst, aldehyde (1 mM), cyclohexanone (2 ml), H_2O (560 μl), 50 °C,[i] NP were left with 4-nitrobenzaldehyde in 140 μl of H_2O, at 50 °C for 4 days before using in aldol reaction, [j] NP were left with cyclohexanone (0.5 ml) and 140 μl of H_2O for 4 days at 50 °C before using in aldol reaction.

Unexpectedly, when mere PDA **132** was applied in 100 mg, the aldol product was obtain in 90 % yield (Table 4, entry 3). This reaction proved that PDA could catalyze the aldol reaction. It is worth mentioning that a catalytic amount of water was necessary to make the reaction effective (Table 4, entry 2-4). This is common also in other organocatalyzed reactions where water must hydrolyse intermediate iminium salts formed in the catalytic cycle to release the aminocatalyst (see also Scheme 6).[234] Centrifugation was used to collect PDA after the reaction in order to check the catalytic activity after recycling. The recycling tests showed a drop of yield from 90 % to 75 % after 1st recycling (Table 4, entry 5). However, the yields remained almost constant in the next 3 consecutive runs (Entry 6-8). Certainly some changes occurred on catalyzing groups when PDA was utilized in the first catalytic trail what diminished the number of catalytic moieties of PDA. Nevertheless, the reused polymer still possessed catalytically active moieties which remained active in the next runs. When PDA was fixed to magnetite NP (**112**) and applied in the aldol reaction (Table 4, entries 9-11) catalytic activity was observed giving rise to the aldol product in 86 % yield (Table 4, entry 10). The advantage of this system in comparison to non-supported PDA is found in the possibility of collecting the catalyst by an external magnet rather than using laborious and time consuming centrifugation. Also here, the yield of product dropped after recycling (Table 4, entry 10, 11) as in case of mere PDA (Table 4, entry 5). As compared with non-supported PDA higher amount of magnetite NP **112** was necessary to obtained similar result. In order to increase the number of catalytic units and to compensate eventual loss of PDA from the surface of magnetite NP **119** a second shell of PDA was added affording magnetite NP **138**. However, their application in aldol reaction gave similar results like for magnetite NP **112** bearing only one PDA shell. The yield dropped down from 97% (Table 4, entry 12), in first run, to 70% (Table 4, entry 13) in the second run. An even higher decrease was observed in the third

run where the product was formed only with 13% yield. This was surprising and hard to explain (see next paragraphs). The diastreoselectivity observed in the aldol reactions products is another interesting point. Non supported PDA **132** gave product with diasteroselectivity almost 1:1 while a little big higher values were observed in case of MNP **112** (Table 4, entries 9-11) with one layer of polydopamine. Similar values like for PDA were observed for magnetite NP **138** with a double layer of PDA. However, after two runs the dr increased from 55:45 (entry 12) to 70:30 (entry 14). Magnetite NP covered before with silica layer and then with PDA **137** exhibited similar behaviour in aldol reaction. A drastic drop of yield took place after the first run from 75% to 40% (Table 4, entry 18, 19). To be sure that there was enough water to hydrolytically cleave intermediates from the catalytic sites of the PDA and thus to prevent blockage of the catalytic cycle, the reaction was performed in water. But the product was formed only in traces (Table 4, entry 20). The same situation was observed when the doubly coated magnetite NP **138** where applied under the same conditions (result not included in the table). In addition, magnetite NP **138** were applied in aldol reaction between cyclohexanone and other subtitled arylaldehydes (Table 4, entry 26-28). The 4-bromophenyl substituted product **108b** was yielded with 48% while benzaldehyde and anisaldehyde failed (Entry 27 and 28). It has been shown in the literature that arylaldehydes without withdrawing groups are not so active in organocatalyzed aldol reactions.[235]

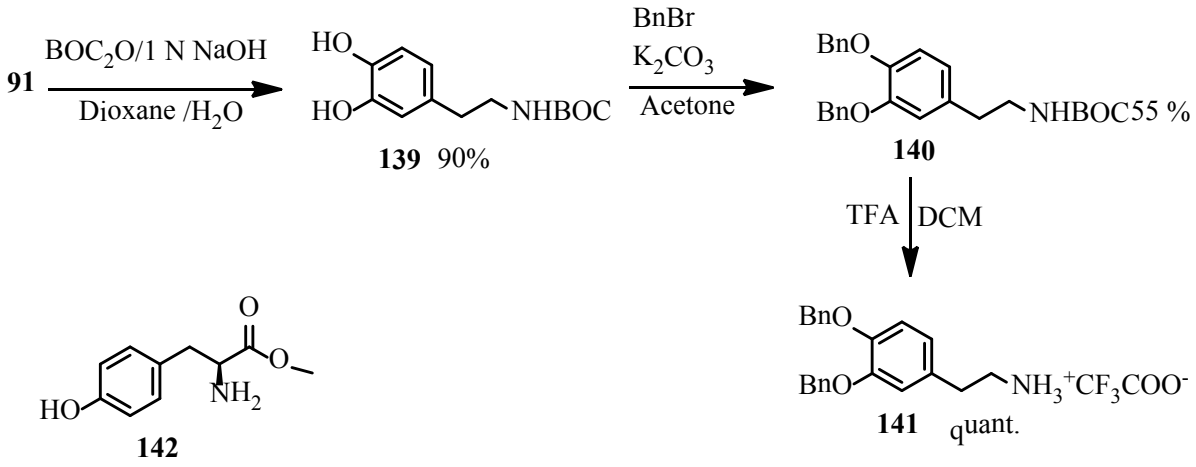

(51)

In order to obtain information about structural motifs being important for the catalytic activity of PDA motif also dopamine **91** as monomer and its derivatives **139**, **140**, **141**, **142** were tested. The necessary products where prepared in a few steps.[83] The *N*-Boc protected dopamine **139** was obtained in quantitative yield by reaction of dopamine **91** with Boc anhydride in presence of NaOH. The phenolic OH groups of the *N*-Boc dopamine were protected by reaction with BnBr under basic conditions affording product **142** in moderate yield. Removal of the Boc group with TFA gave the *O*,*O*-diprotected product **141** with a free amino group in quantitative yield.

When dopamine hydrochloride **91** was used as a catalyst in the aldol reaction the product was yielded in 80% (Table 4, entry 21). On the other hand, the reaction failed when the amino group was protected (**139**, see Table 4, entry 22) or both the amino and the phenolic functions (**140**, see Table 4, entry 23) were blocked. Modest catalytic activity was observed when only the phenolic groups were blocked (**141**, see Table 4, entry 24). All these results allowed assuming that dopamine and probably polydopamine reacted as dual catalyst where amino groups behave as an enamine forming organocatalyst while acidic phenolic OH groups assist catalysis. This is in agreement with observed enhancement of proline-catalyzed aldol reactions when catalytic amount of different catechols were added. [236] We found that tyrosine methyl ester **142** also catalyzed aldol reaction (75 % yield, see Table 4, entry 25) although it possesses only one phenol group in addition to an amino moiety.

All these data let us propose a transition state for dopamine/polydopamine catalyzed aldol reactions wherein the amino group forms an enamine and the phenolic OH group activate the carbonyl component as Brønsted acid by hydrogen bonding (see Figure 49).

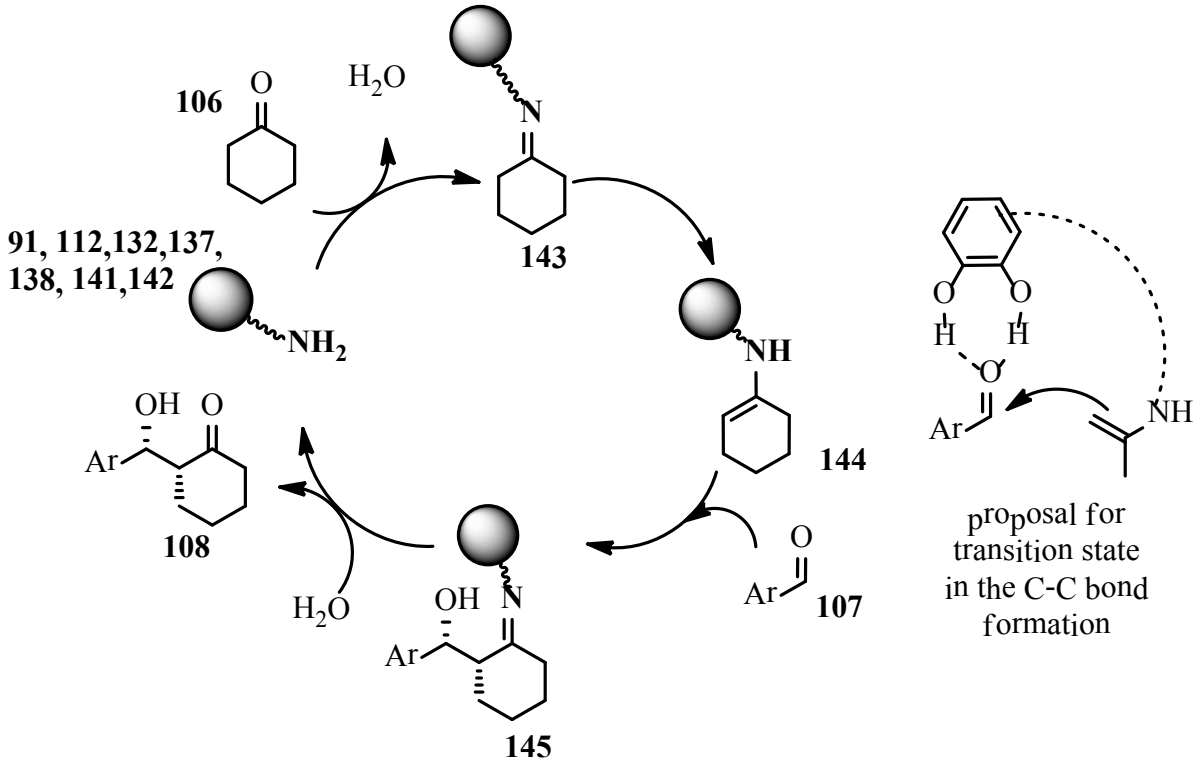

Figure 49. Proposed catalytic cycle and transition state of the C-C-bond forming step of aldol reaction catalyzed by dual dopamine or PDA.

To prove that amino groups of PDA behaved as catalytic moieties we tried to block them by methylation with MeI (Table 4, entries 15, 16) or acetylation with acetic anhydride (Table 4, entry 17). Conducted tests showed that PDA after reaction with methyl iodide gave a big drop in yield to 35% but still some catalytic groups remained.

The deactivation of PDA in repeated applications in aldol reactions could have two reasons. First, it may be due to irreversible blocking of the amino catalytic sites by formation of intermediates in the catalytic cycle. This assumption is supported by the fact that the mass of PDA used in aldol reaction increased after each run. Second, leaching of the catalyst from the bulk PDA or the PDA-coated nanoparticles has to be taken into consideration. Elemental analysis revealed a reduction of the nitrogen content when magnetite NP **138** (2.96% to 0.61% after the five runs) or **137** (0.83% before application to 0.42% after the three runs) were used in aldol reaction. The FTIR spectra of **144** and **145** after being used in catalytic tests showed two new bands in both cases (see Figure 50 and 51). These new peaks were assigned to N-O stretching vibration from nitro group. That indicated that reaction between free amino groups from polydopamine shell and 4-nitrobenzaldehyde occurred. Additional test was performed where fresh portion (not used

in catalysis) of magnetite NP **138** was left to react with 4-nitrobenzaldehyde for 4 days at 50 ^{o}C with small amount of water (140 μl). Peaks belonging to nitro group were observed in the FTIR spectrum (see Figure 52) hence, introduction of aldehyde into polymer structure was confirmed.

To have a further look in this interesting issue XPS analysis of magnetite NP **138** reacted with 4-nitrobenzaldehyde was conducted. It shows indeed an energy (404.8 eV) in the high resolution XPS *N*-spectrum, which can be assigned to nitro group (see Figure 53) Furthermore, an imine structure was found as well (398.5 eV).

Thus it can be concluded that deactivation of the catalyst is a combination of two factors: blocking of the amino groups by imine formation with the aromatic aldehyde and physical loss of catalytic sites (PDA) from the nanoparticles.

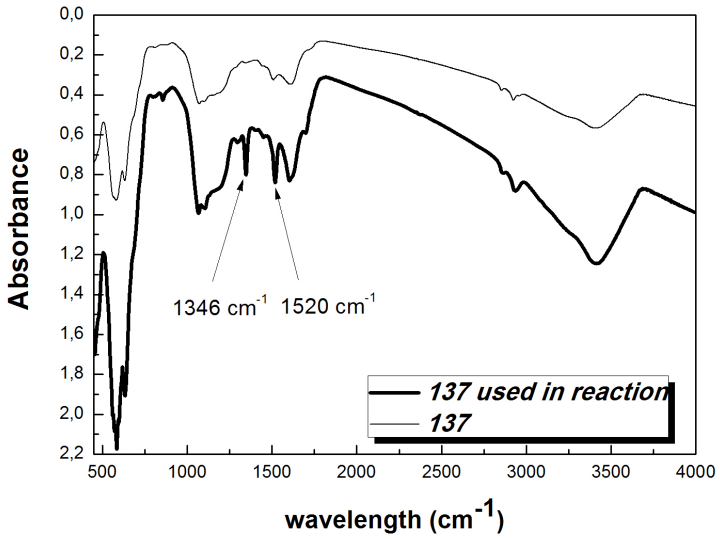

Figure 50. Comparison of FTIR spectra of fresh magnetite NP **137** and after application in catalysis.

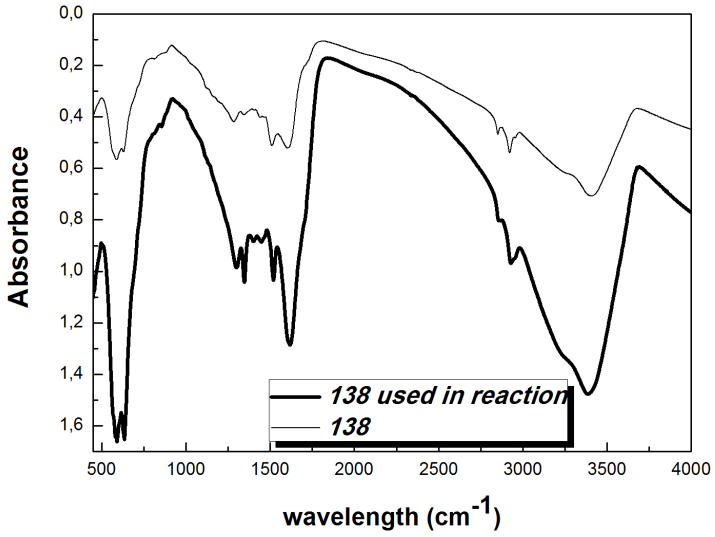

Figure 51. Comparison of FTIR spectra of fresh magnetite NP 138 and after application in catalysis.

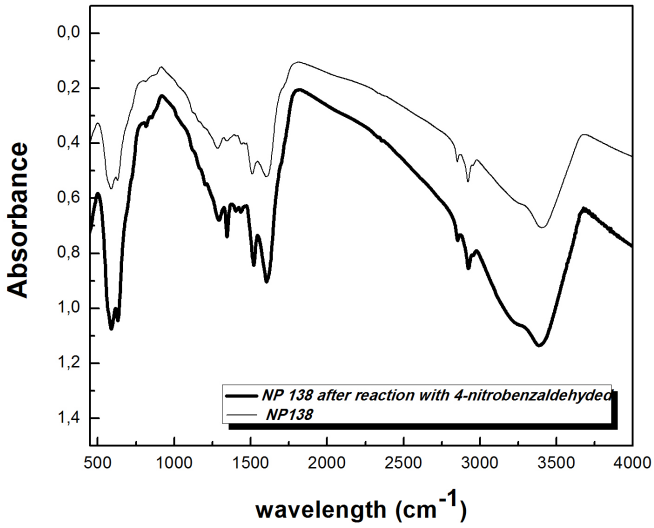

Figure 52. Comparison of FTIR spectra of magnetite NP **138** and after reaction with 4-nitrobenzaldehyde for 4 days at 50 ^{o}C.

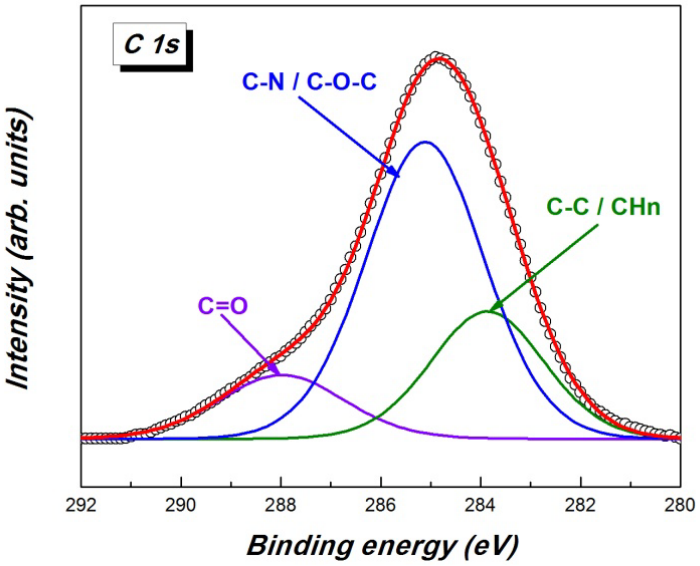
C 1s
C-N / C-O-C
C-C / CHn
C=O
Intensity (arb. units)
292
290
288
286
284
282
280
Binding energy (eV)

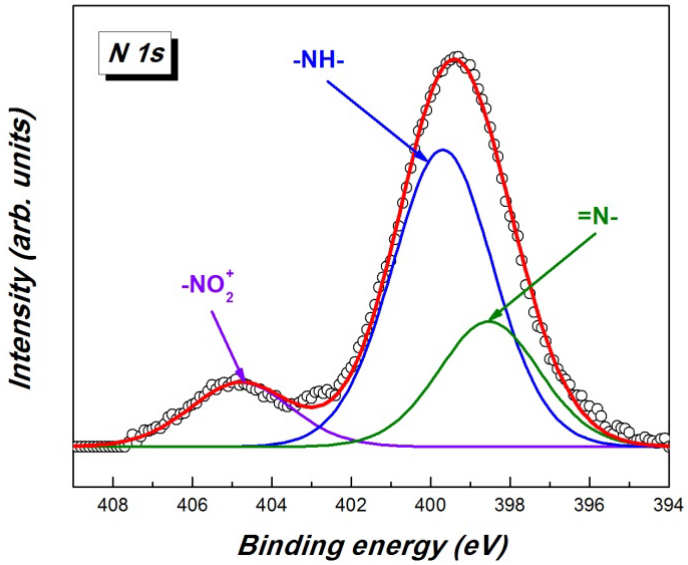
N 1s
-NH-
=N-
-NO2+
Intensity (arb. units)
408
406
404
402
400
398
396
394
Binding energy (eV)

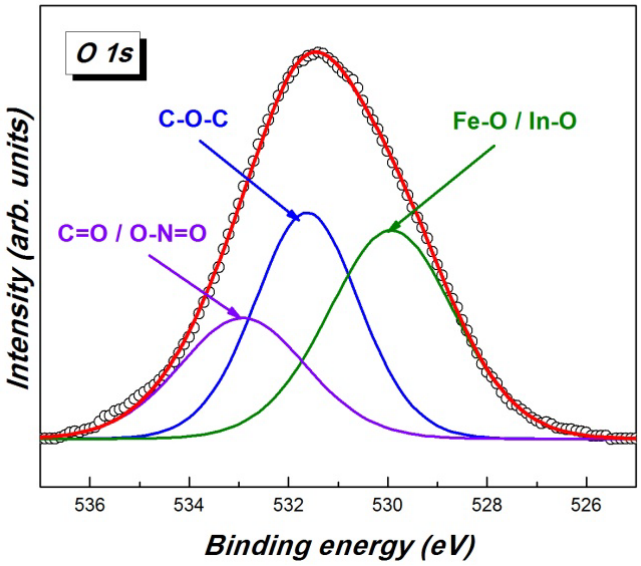
O 1s
C-O-C
Fe-O / In-O
C=O / O-N=O
Intensity (arb. units)
536
534
532
530
528
526
Binding energy (eV)

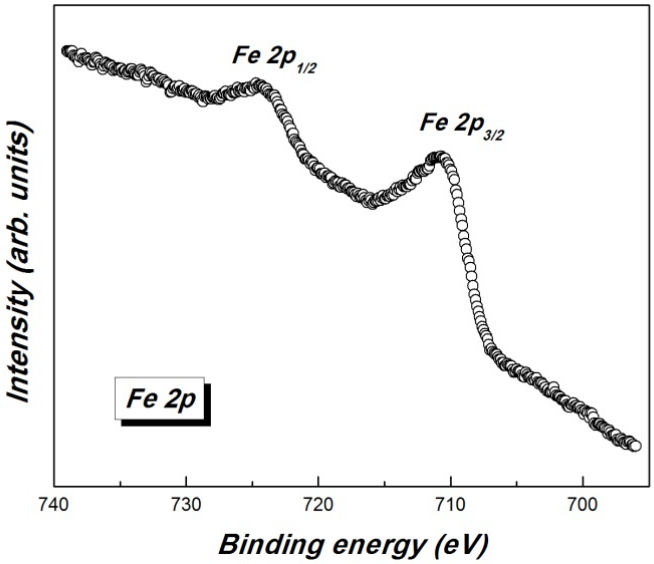

Figure 53. High resolution spectra for magnetite NP **138** after reaction with 4-nitrobenzaldehyde for 4 days at 50 ^{o}C.

In order to check whether the treatment with 4-nitrobenzaldehyde triggered some changes in the NP we used them in aldol reaction (Table 4, entries 29, 30). In case of magnetite NP blocked with 4-nitrobenzaldehyde lower catalytic activity was observed. Also when MNP **138** were reacted with cyclohexanone (for four days), before using in reaction, the aldol product was obtained in lower yield 52 %. These experiments confirm that a part of the catalytic units were either blocked by reaction with carbonyl compounds or they were disconnected from the magnetite NP by reacting with these carbonyl structures.

After finding out the interesting phenomenon that PDA can catalyze direct aldol reaction we were curious if it can also be applied as catalyst in other reactions. As a proof of principle PDA coated magnetite NP **138** were applied in the Knoevenagel reaction of arylaldehydes with malononitrile at 50 °C with only 50 mg whereas 1 mmol of malononitrile and cyclohexanone were used. Excellent yields were obtained, which remained virtually unchanged after four recyclings. The nature of substituents in the aromatic aldehyde did not play such a decisive role like in aldol reaction. This can be rationalized by the differences in the mechanisms of the aldol and the Knoevenagel reaction. In the aldol reaction catalyst has to go through enamine formation while in the Knoevenagel reaction deprotonation of malonitrile is the key step of the catalysis.

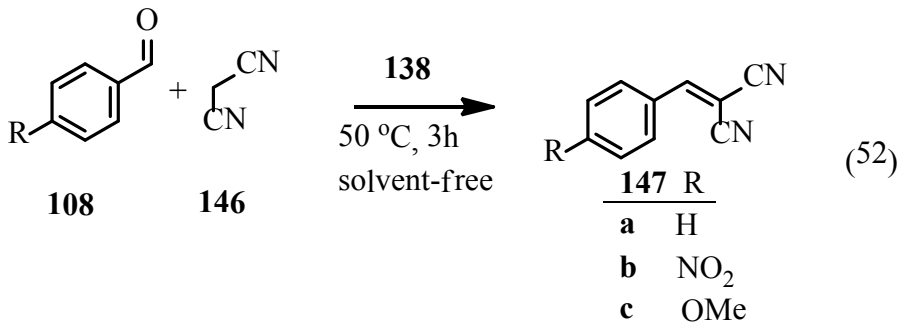

108 146 (52)

Table 5. Application of magnetite NP **138** in Knoevenagel reaction.

Entry	Product[a] 147	Catalyst	Amount [mg]	Time [h]	Yield [%]
1	a	**138**[a]	50	3	99
2	a	**138**[a] 2nd run	50	3	99
3	a	**138**[a] 3rd run	50	3	99
4	a	**138**[a] 4th run	50	3	99
5	a	**138**[a] 5th run	50	3	97
6	b	**138**[a]	50	3	90
7	c	**138**[a]	50	3	80

[a] Reaction conditions: aldehyde (1 mM), malononitrile (1 mM), 50 °C

To conclude, new unexpected catalytic behaviour of polydopamine was shown. This biomimetic polymer could catalyze the aldol reaction between 4-nitrobenzaldehyde and cyclohexanone with excellent yield in the first run. Also magnetite NP covered with this polymer exhibited catalytic properties in aldol and Knoevenagel reaction. Especially in case of the Knoevenagel reaction the MNP **138** were efficient and could be used at least 5 times without significant loss of activity. The magnetic properties of the PDA-coated MNP **138** allowed their manipulation by an external magnetic field and replaced the tedious centrifugation (mere PDA) by magnetic separation. All nanomaterials were characterized by FTIR, VSM and TEM. Also XPS and elemental analysis was utilized to characterize nanoparticles. In addition, a proposal of the catalytic cycle was elaborated. Experiments which indicated that polydopamine behaved as dual catalyst were conducted. It was found that both the amino and the phenolic OH groups are essential for catalytic activity of PDA. Reasons for the observed deactivation of the catalyst after firs run were found in the loss of polymer because of irreversible fixing of intermediates at the PDA shells.

2.2.4 Application of polydopamine for ROP of "lactide dimer"

Polydopamine has been considered as a robust shell which covered tightly different kind of materials but it is limited as a support for covalent linkage of interesting functions by reactions with amines and thiols. Results presented in this thesis evidence that functionality of polydopamine can be easily extended by utilizing a linker strategy (see chapter 2.2.1). Detailed structural investigation revealed that polydopamine contains aminoethyl motifs in the polymer chain and because of this fact exhibits hitherto unknown catalytic activity in aldol and Knoevenagel reactions (see chapter 2.2.3).

Norepinephrine was used instead of dopamine to cover various materials.[129] The authors claim that this is advantageous because the polymer formed by oxidation contains additional hydroxyl groups as compared with PDA. Such materials were submitted to reactions with ε-caprolactone what allowed to obtain polycaprolactone attached to the surface of these materials. The ROP reaction was catalyzed by addition of tin salts. In the light of the results described in previous sections it can be assumed that polydopamine itself can serve as an initiator for ROP. Because of the great importance of polylactic acid, ROP of lactide was chosen for covering PDA coated magnetite NP. In addition to the amino groups of PDA acting as nucleophiles in the ring opening of lactide also the participation of the acidic phenol groups of PDA can be expected to catalyse this reaction. There are reports in the literature wherein the involvement of the phenolic OH-group of PDA is claimed in the formation of esters with 2-(dodecylthiocarbonothioylthio)-2-methylpropionic acid[237] or 2-bromoisobutyryl bromide[238] which serve as initiators for RAFT and ATRP respectively. However, in the light of our results in the structure elucidation of PDA it seems to be more likely that these moieties are fixed by amide formation to the amino groups present in PDA.

Magnetite NP **112** covered with polydopamine were submitted to reaction with 3,6-dimethyl-1,4-dioxane-2,5-dione (lactide) in presence of DMAP (see Scheme 53).

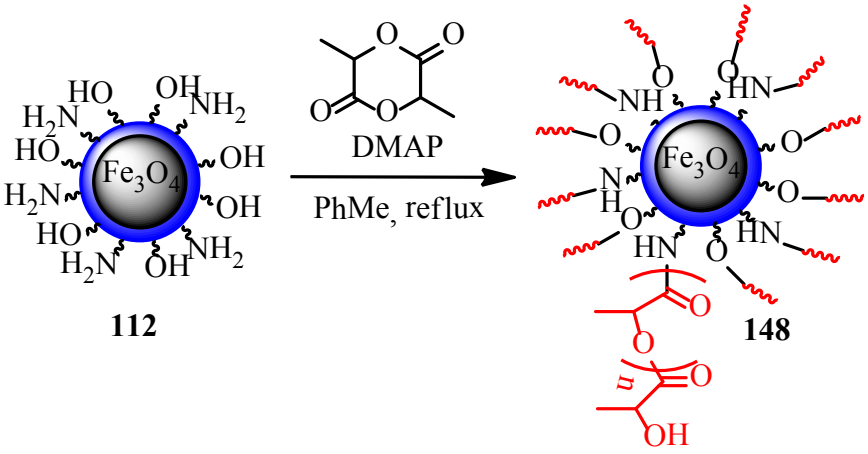

112 **148** (53)

FTIR spectra proved that PLA was fixed to the magnetite NP affording novel magnetite NP **148**. Peaks in the range 2993-2846 cm^{-1} were assigned to symmetric and asymmetric vibration from CH_2 and CH_3 groups. A new characteristic peak observed at 1750 cm^{-1} was ascribed to stretching vibrations of C=O. This is typical situation for a polyester because the C=O signal of the monomer is observed around ~1730 cm^{-1}. Signals in the region 1430-1650 cm^{-1} corresponded to bending vibrations of CH_3 (asymmetric and symmetric) and vibrations of polydopamine moieties. Another region in the FTIR spectrum indicative for successful polymerization exists at 1090-1270 $cm^{-1}$for the C-O-C symmetric stretching vibration.

Encouraged by this result we tried to extend this methodology to other types of magnetic NP: Magnetite NP **137** covered with silica and iron NP **149** covered with a carbon layer, which could be considered to mimic glass or various carbon materials, respectively. Applying the same protocol, i.e. first covering with PDA (formation of magnetite NP **137** and **149**) and second ROP of lactide, the magnetite NP **151** and **152** were obtained.

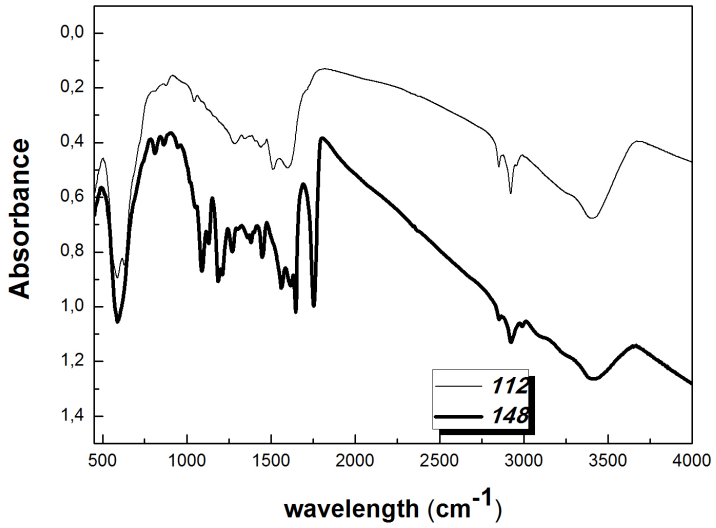

Figure 54. FTIR spectra of magnetite NP **112** and after performed ROP (**148**).

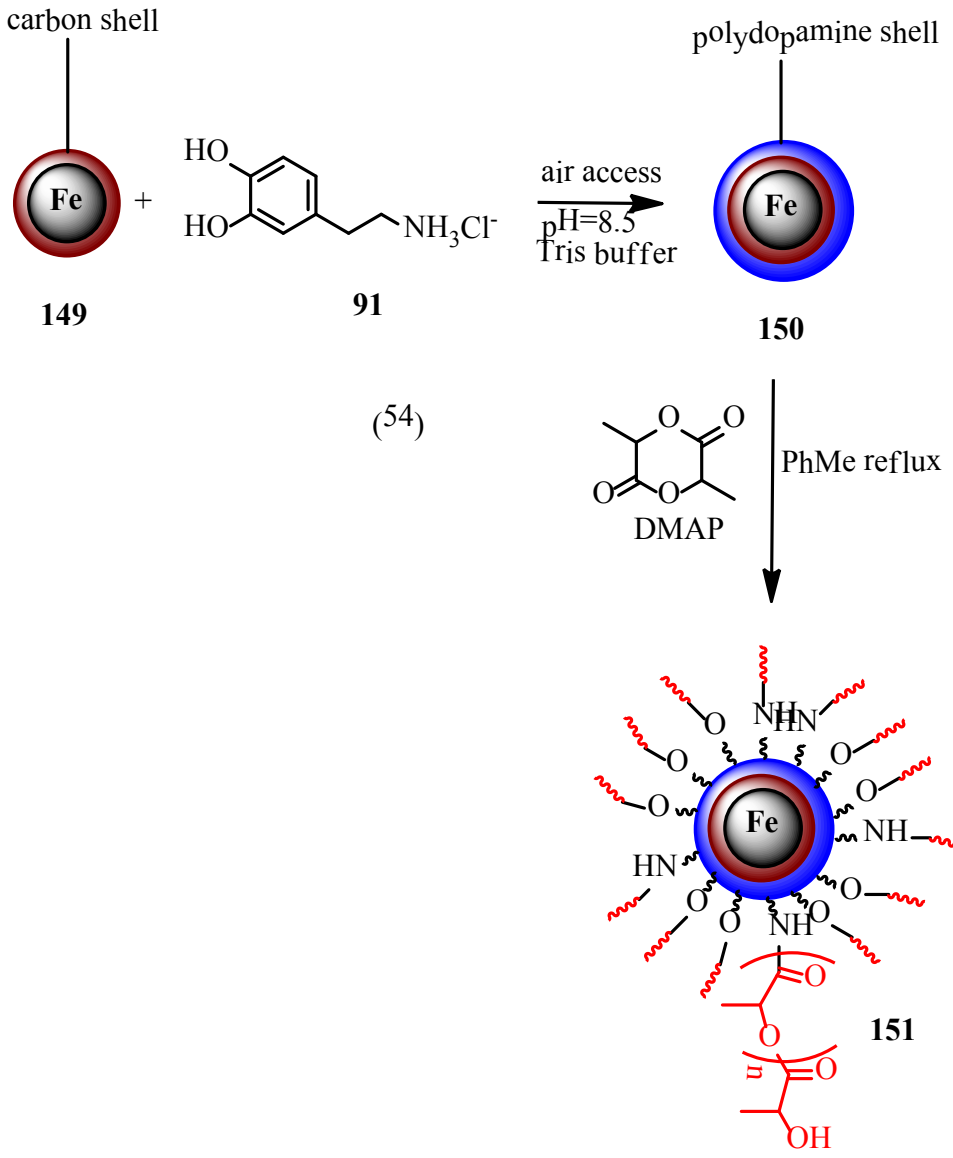

FTIR-spectroscopy confirmed the changes of the iron NP in each reaction step. Characteristic peak at 1440-1620 cm^{-1} for polydopamine were found. The spectrum after functionalization with polylactic acid can be divided into three main parts like for NP **148**. Peaks in the range 2916-2825 cm^{-1} were assigned to symmetric and asymmetric vibration from CH_2 and CH_3 groups. A new peak observed at 1745 cm^{-1} was ascribed to stretching vibrations of C=O. Signals in the region 1440-1660 cm^{-1} correspond to bending vibrations of CH_3 (asymmetric and symmetric) and to polydopamine. The region 1060-1270 cm^{-1} was assigned to C-O-C symmetric stretching vibration bands. NP exhibited strong magnetic properties and could be easy controlled by an external magnetic field.

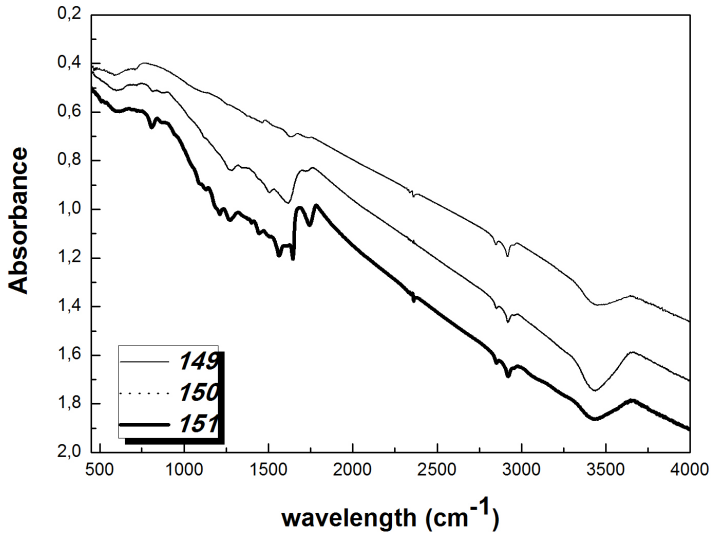

Figure 55. FTIR spectra of starting carbon coated Fe NP **149,** after modification with dopamine **150** and with polylactic acid **151**.

MNP **137** bearing silica and polydopamine layers were also used as nanoplatform for ROP affording MNP **152**. The FTIR spectrum was similar to previous once and thus evidenced successful polymerization reaction (see Figure 54, 55 and 56).

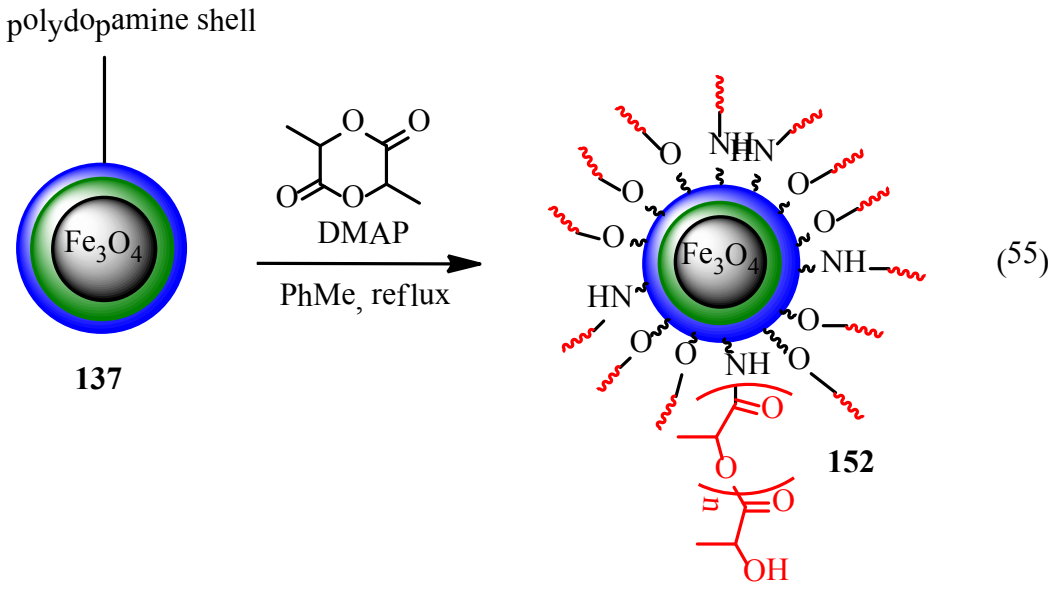

(55)

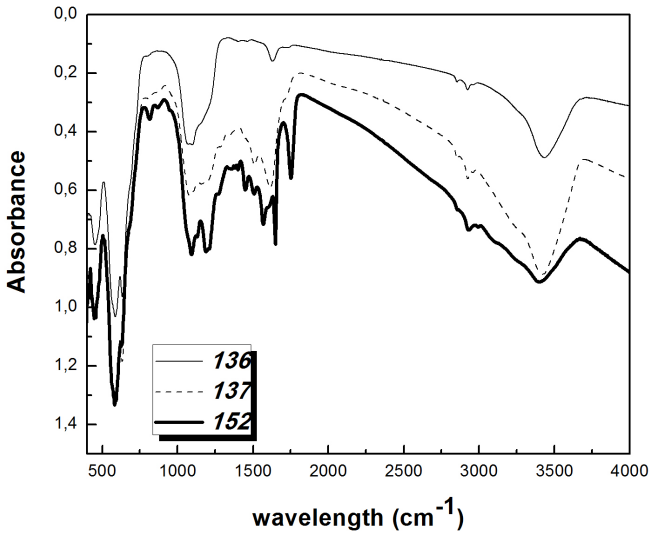

Figure 56. FTIR spectra of modified magnetic nanoparticles **136**, **137**, **152**.

Polylactic acid is known from its biocompatibility and biodegradability.[239] Also Al_2O_3 is biocompatible and found application as component of bioceramic materials for joint replacement.[240] Thus we performed ROP of lactide on neutral aluminium oxide for column chromatography (**153**). Al_2O_3 was covered with polydopamine in oxidative polymerization reaction of dopamine **91** in Tris buffer. This yielded **154** were used in ROP of lactide catalyzed by DMAP and afforded **155** with PLA as outer shell.

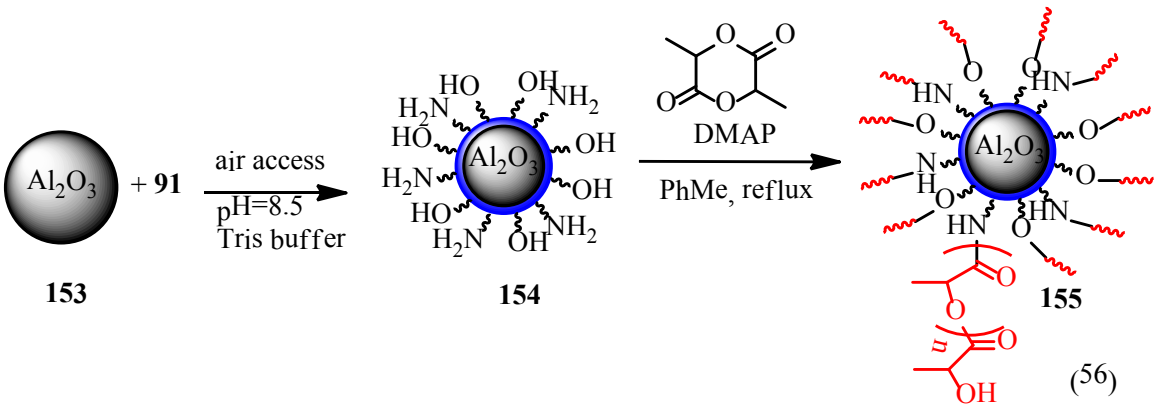

(56)

The FTIR spectra proved successful functionalization after both steps by showing similar bands for the PDA and the PLA functionality. Typical for Al-O vibration and thus for Al_2O_3 is a band at 599 (see Figure 57).

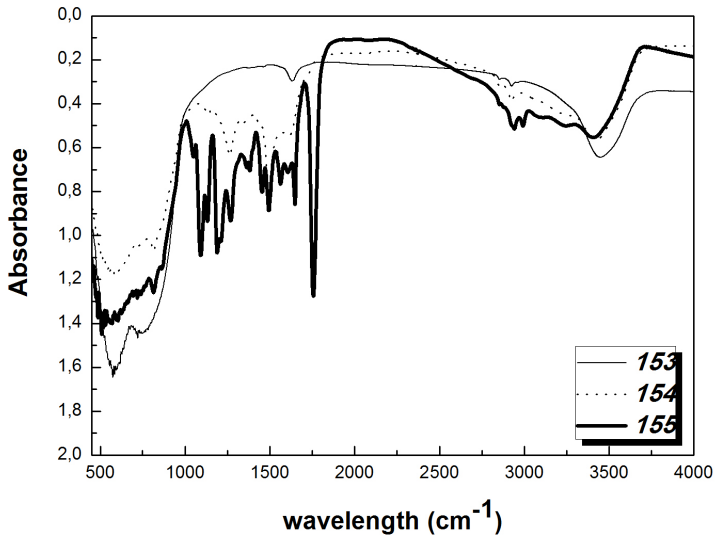

Figure 57. FTIR of mere Al_2O_3 (**153**) and Al_2O_3 modified with PDA (**154**) and polylactic acid (**155**).

Nanomaterials **148**, **150**, **151**, **152** were investigated by TEM to determine their morphology (see Appendix, A 15). Small aggregation was observed as a consequence of sample preparation. Nevertheless, larger clusters rather than single core-shell structures were observed for each type of these materials. TEM revealed that magnetite NP covered with polylactic acid were better dispersed in aqueous medium than those only covered with polydopamine.

Characterization in terms of magnetic properties evidenced superparamagnetic behaviour of magnetic nanoparticles which exhibited Ms values of 32.7 emu/g for NP **148**,

73.2 emu/g –NP **150**, 35.9 emu/g –NP **137,** 34.4 emu/g –NP **152** and 62.3 emu/g for NP **151** (see Figure 58).

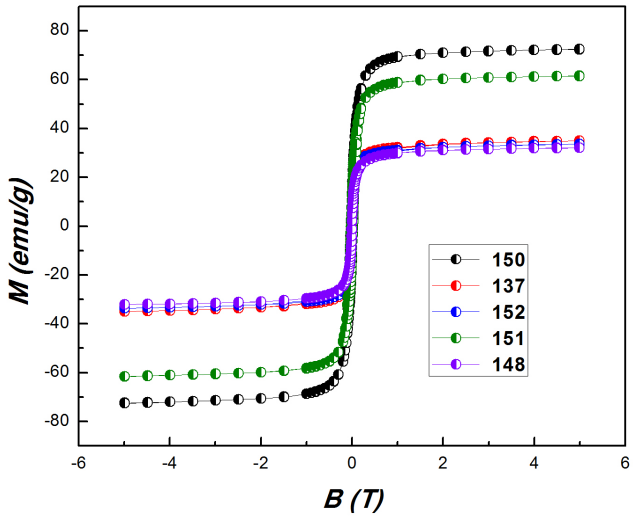

Figure 58. Magnetization vs. applied magnetic field for NP **137** and **150** covered with polydopamine and after ROP **148**, **151** and **152**.

Another proof for successful functionalization was provided by the XPS spectrum of magnetite NP **148** wherein all expected components were found (see Appendix, A 16).

To conclude, ROP of lactide was performed on various materials precoated with polydopamine. In this way a new characteristic of polydopamine, as surface initiator for ROP was demonstrated,. This method allowed to cover bare magnetite NP or magnetite NP precoated with silica (glass imitation) or a carbon shell with an important biodegradable and biocompatible polymer. Following the same methodology also non-magnetic Al_2O_3 was covered with PLA by this two step methodology. It is noteworthy that clusters were observed by TEM in the majority of cases rather than typical core-shell structures.

2.2.5 Magnetic tagging of amino acids via polyacrylates

The first report about fixing proline to magnetite NP through polymerization of acrylic proline derivatives came from our group. The resulting magnetite NP performed well in aldol reaction (see chapter 1.4.2). For this reason we decided to employ the same strategy to other amino acids exhibiting known organocatalytic activity and also to new proline derivatives. This chapter will present synthesis and catalytic application of new magnetite nanoparticles equipped with threonine, lysine and proline.

Reaction of threonine **156** with acryloil or methacryloil chloride in TFA, according to a reported protocol,[241] furnished derivatives **157** and **158**. To provide space between the polymer backbone and the amino acid units the acrylate **161** was synthesized. By following

a reported procedure[242] the succinate **159** was converted into the acyl chloride **160** by reaction with $SOCl_2$ and subsequently esterification with threonine **156**.

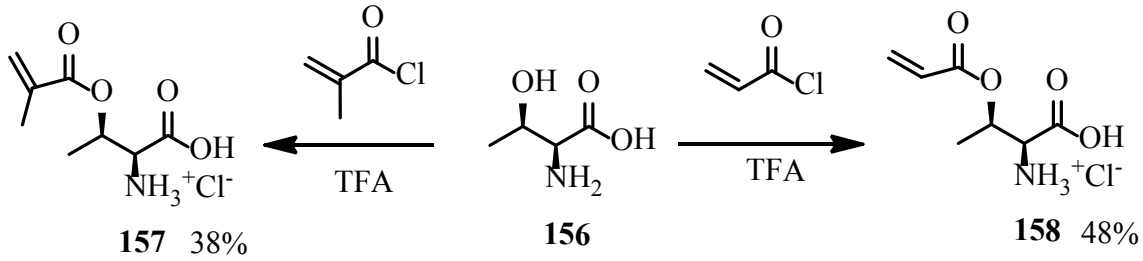

157 38% **156** **158** 48%

(57)

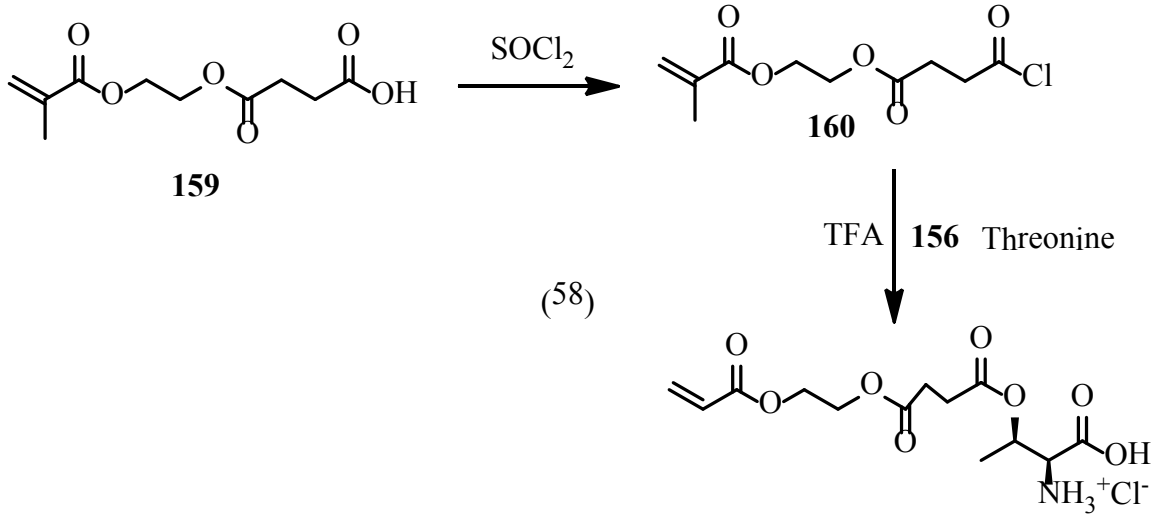

159 **160**

(58)

161 70%

The products were obtained by precipitation with diethyl ether in moderate yields for threonine derivatives **157**, **158** and in good yield for **169**. They did not require further purification.

Commercially available *N*-Boc-lysine **162** was changed into the acryl amide **164** by a known two-step procedure.[243] Reaction with acryloil chloride gave product **161** with very good yield. Deprotection in TFA afforded **164** quantitatively.

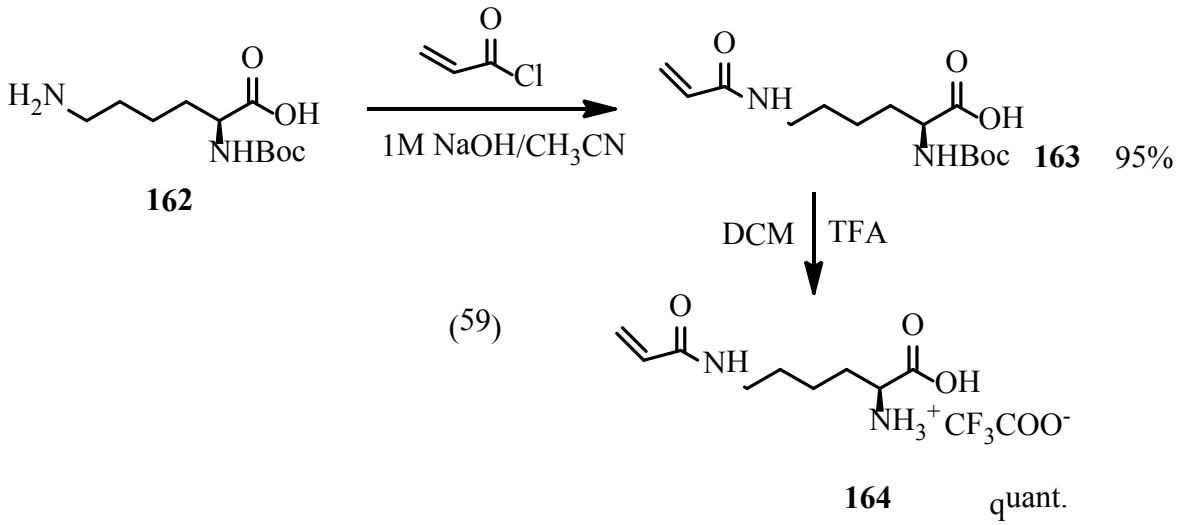

(59)

It has been shown in the literature that chiral triazole pyrrolidine derivatives[244] can catalyze Michael reaction between cyclohexanone and propionaldehyde. In order to prepare the desired triazole derivatives bearing acrylate we performed the following synthetic strategy.

Azido derivative[245] **168** was obtained in few synthetic steps starting from commercial *N*-Boc protected proline **165**. Reduction under mild conditions with BH_3*DMS afforded prolinol **166** with high yield. To replace OH with azide, the hydroxyl group was converted into tosylate **167** by treatment with tosyl chloride. Nucleophilic substitution of the tosylate with excess of NaN_3 in DMF gave *N*-Boc protected azide **168** with 80% yield.

.

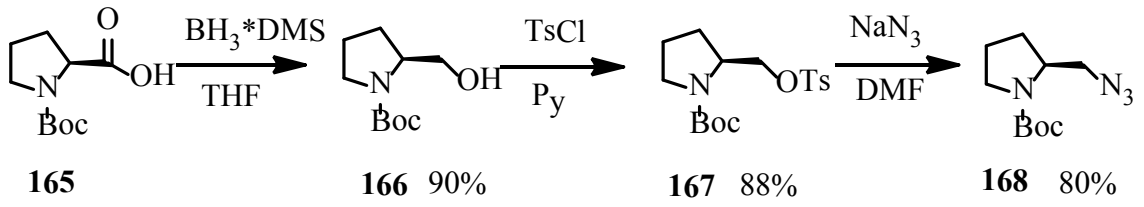

165 **166** 90% **167** 88% **168** 80%

(60)

Tetraethylene glycol **169** and 1,12–dodecanodiol **172** were chosen as starting materials for the synthesis of alkyne as partners **171** and **174** for CuAAC. They provide larger distance between the inorganic core and the polymer backbone. They posses different polarities that might play a role in the envisaged catalytic application. Reaction of a high excess of tetraethylene glycol **169** with NaH and propargyl bromide generated the mono substituted alkyne derivative **170** with 50% yield. Acylation with acryloyl chloride in DCM gave the known acrylate **179** with moderate yield 46 %.[246]

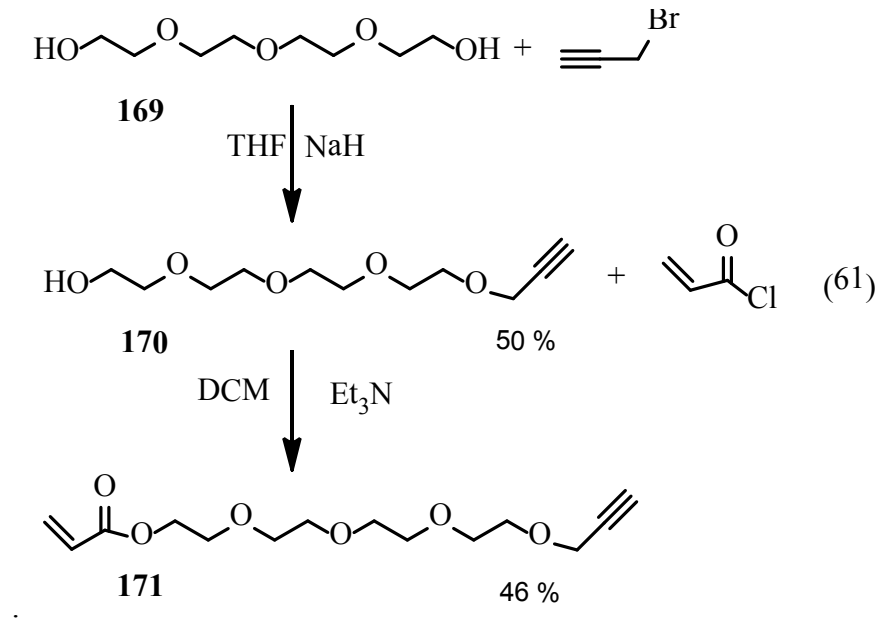

(61)

A similar synthetic route (cooperation with Dr. Crina Socaci) led to the bifunctional compound with unpolar chain[103] in moderate yield.

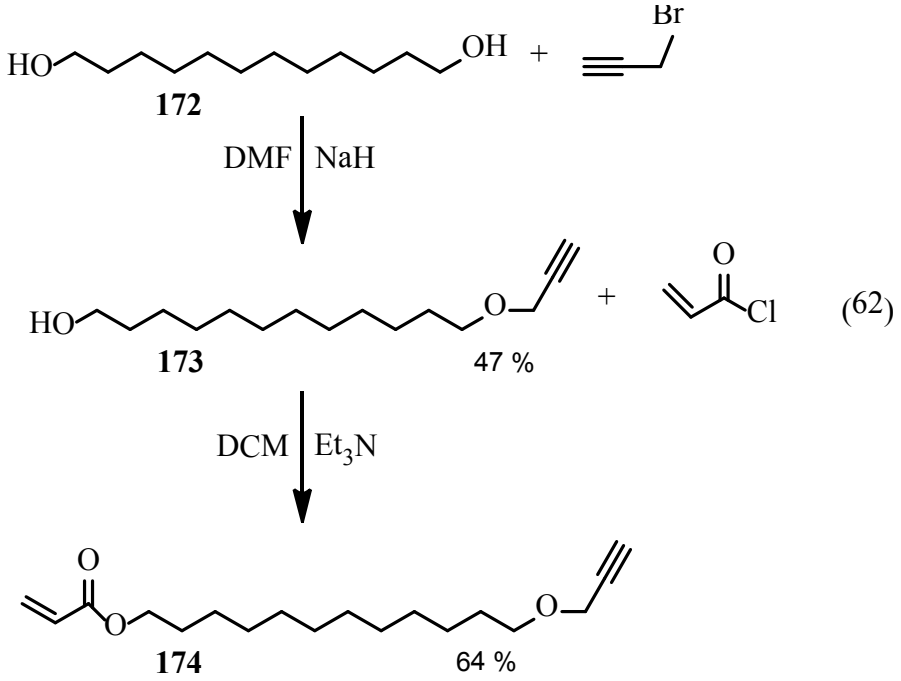

(62)

The CuAAC reaction between compound **168** and bifunctional linkers **171** and **174** afforded new triazole pyrrolidine derivative **175** and **176** with fair yields 63% and 55%, respectively.

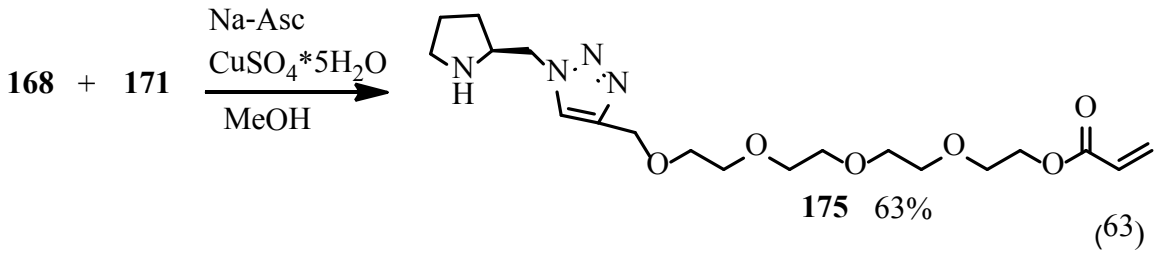

175 63%

(63)

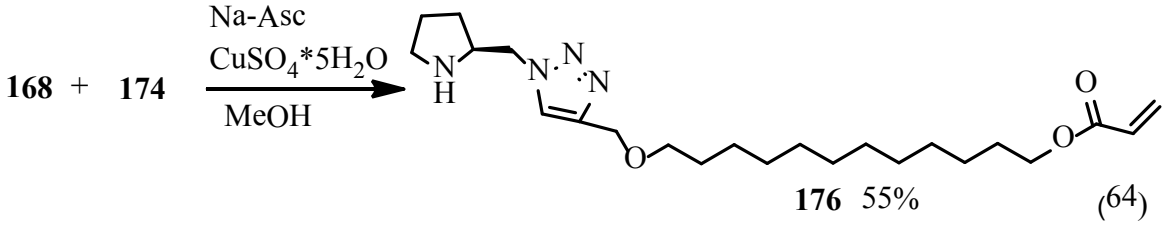

176 55%

(64)

In another manner CuAAC click reaction was used to connect the azide **168** with commercial propargyl acrylate. This reaction allowed to obtain the acrylic derivative **177 (**collaboration with Dr. Zekarias Yacob) with a relatively short linker with an overall 83 % yield.

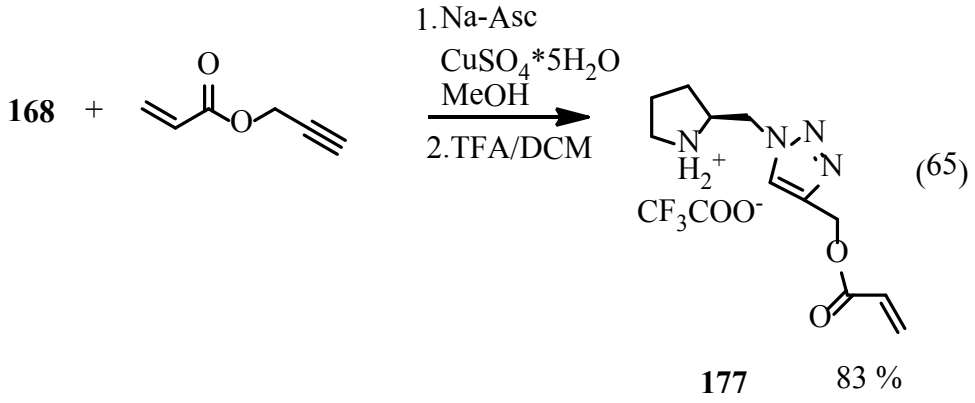

(65)

177 83 %

All these monomers were employed in polymerization reactions with magnetite NP containing methacryloil phosphate **178.** The way how monomers were fixed to magnetite NP can be considered as "grafting from" like-fashion. Polymerization reactions were performed in dry DMF under inert gas atmosphere with excess of monomers. A catalytic amount of AIBN was utilized to start reactions. After two days modified magnetite NP were collected by an external magnet and washed with mixtures of solvents. As a result, new NP were obtained equipped with threonine **179**, **180a** and **180b**, lysine **181** and new proline triazole derivatives **182a**, **182b**, and **183**. Following another approach, magnetite

NP **184** stabilized with acrylic acid were used for tethering polyacrylate derived from proline derivative **177**.

It has to be underlined that in all cases FTIR spectroscopy was not able to conclude on the functionalization of magnetite NP. Due to the high amount of phosphate acrylic derivative on magnetite NP and to the many overlapping bands, reliable analysis of FTIR spectra was not possible. As a matter of fact, spectra were the same before and after functionalization and no significant changes were observed (see Figure 59 and 60 and Appendix A 17). The intensive peak at 1070 cm^{-1} was assigned to P-O-C stretching vibration. The band at 1733 cm^{-1} was ascribed to C=O group. Two signal at 2860 and 2930 cm^{-1} confirmed the presence of CH_2 groups.

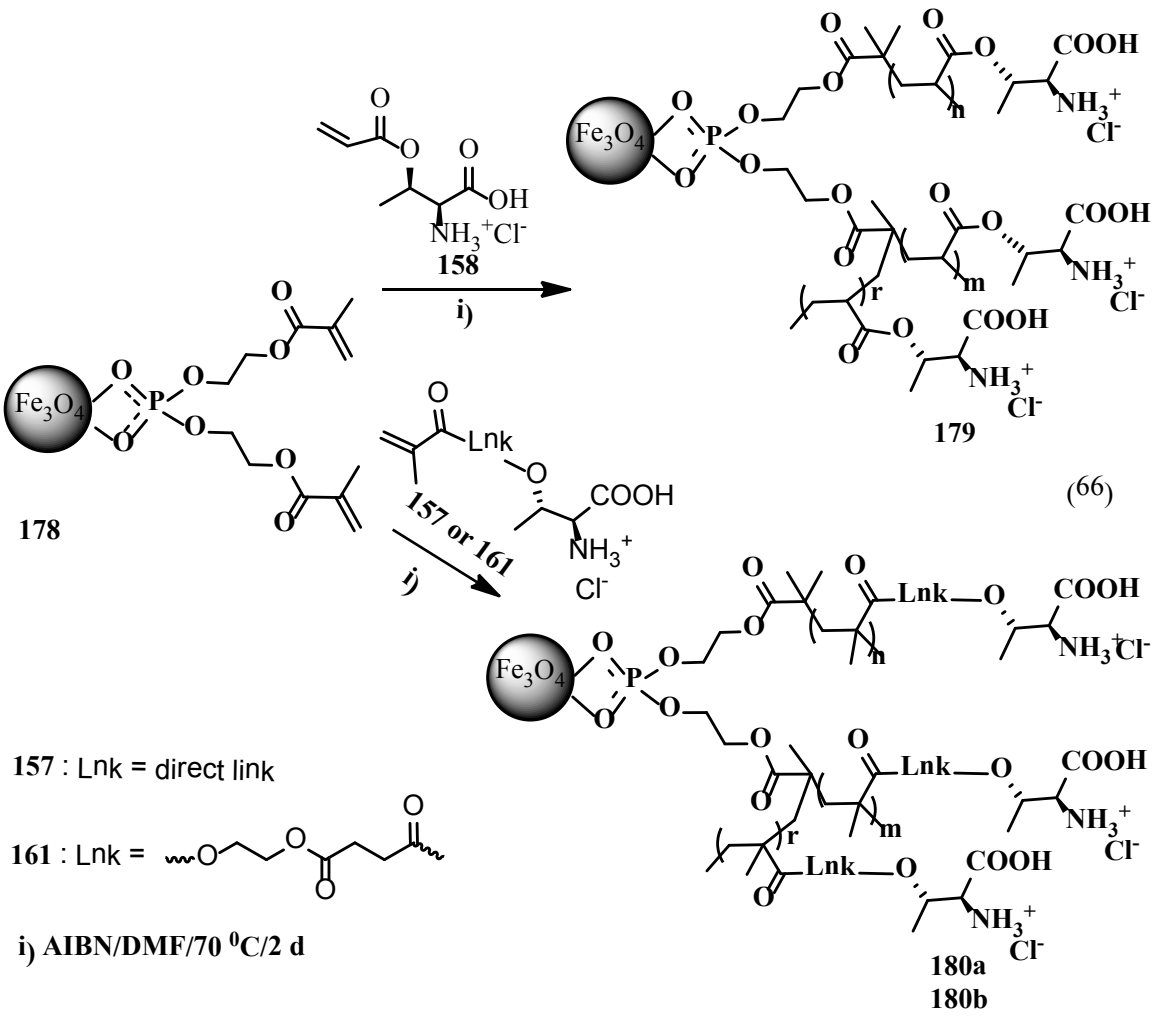

(66)

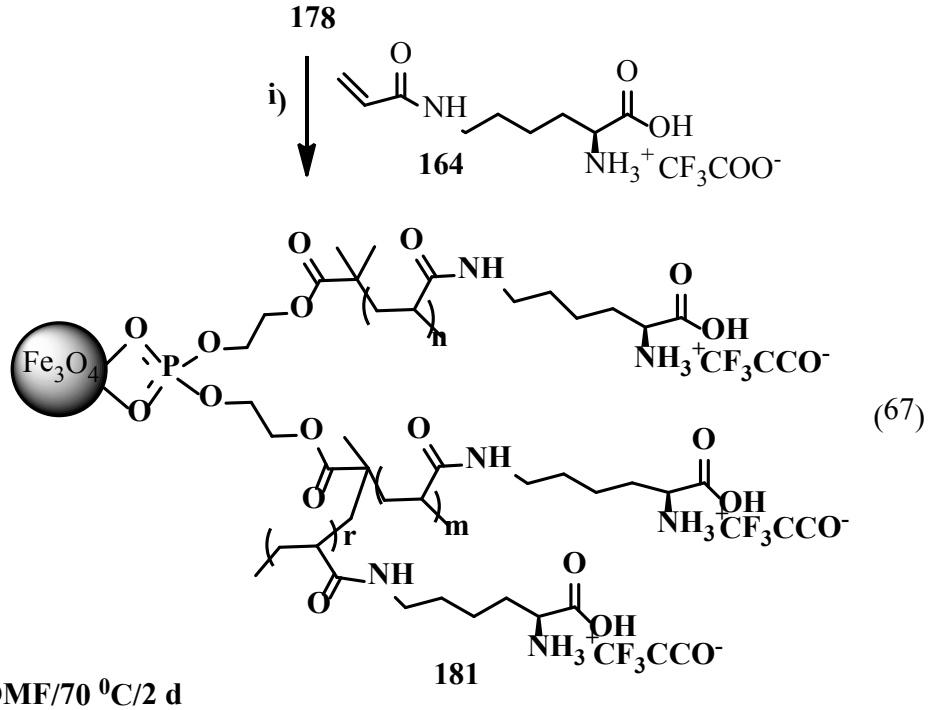

(67)

i) AIBN/DMF/70 ^{0}C/2 d

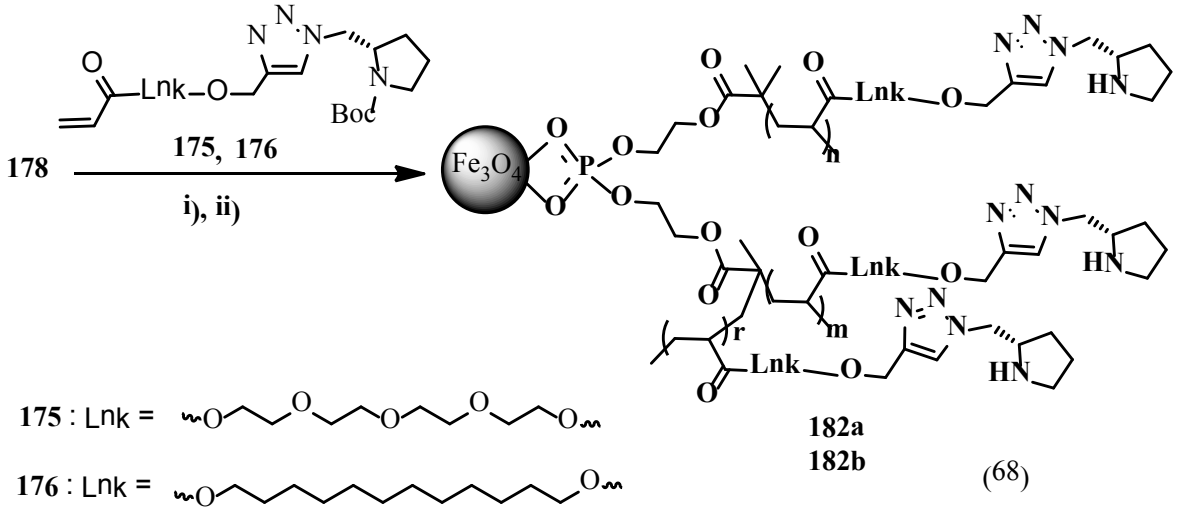

(68)

i) AIBN/DMF/70 ^{0}C/2 d

ii) TFA/DCM/ 20 h then 2 % Et_3N/MeOH

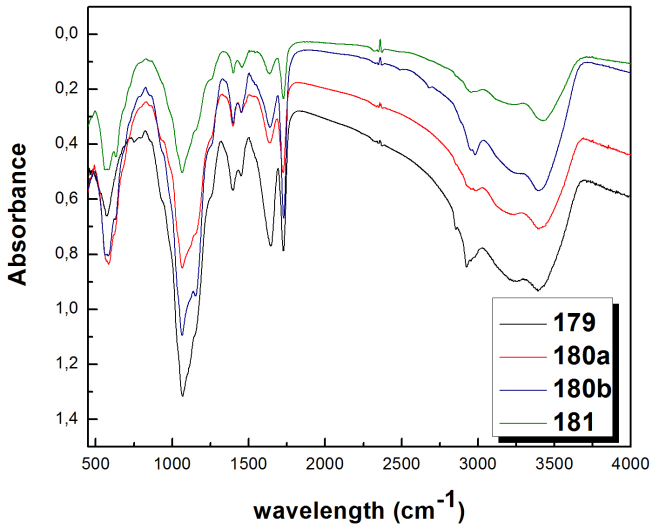

Figure 59. FTIR spectra of magnetite NP **179**, **180a**, **180b**, **181** coated with polyacrylates derived from threonine and lysine.

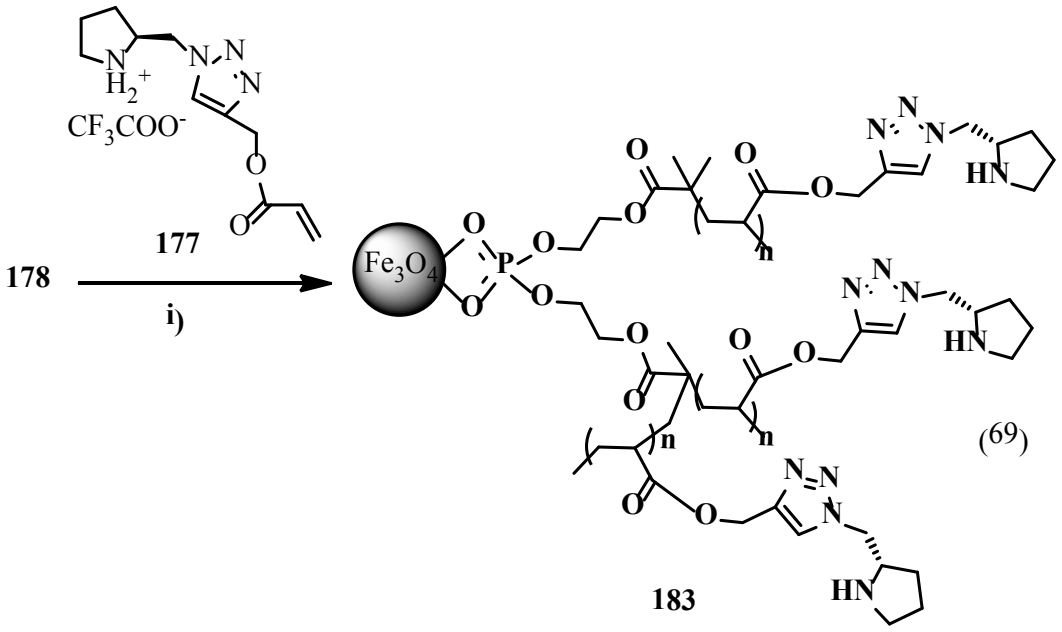

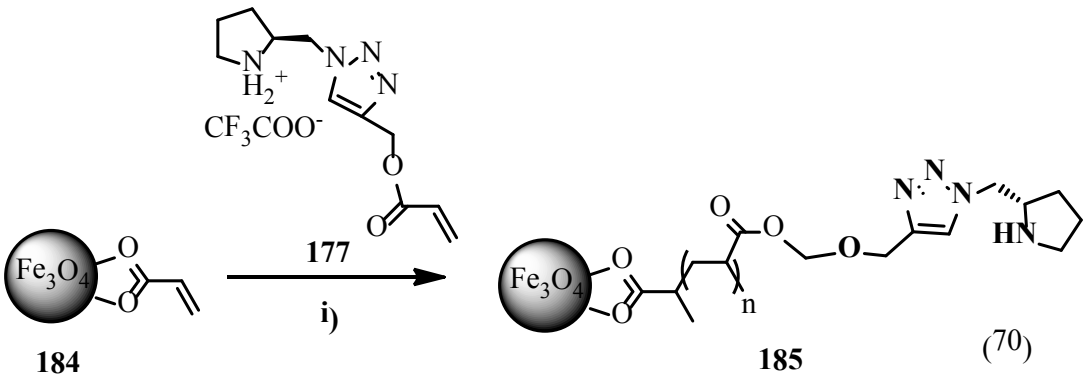

i) AIBN/DMF/70 ^{0}C/2 d

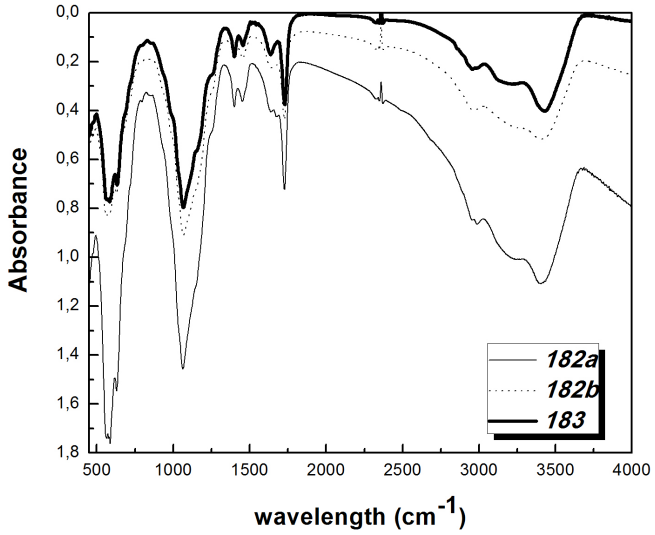

Figure 60. FTIR spectra of magnetite NP **182a**, **182b** and **183**coated with polyacrylates bearing proline derivatives.

Elemental analysis of the magnetite NP revealed the presence of N and thus proved the attachment of the polymer shells. From the nitrogen content the following loading of the magnetite NP with polymer were calculated: **179-**3.06 mmol/g, **180a**-1.05mmol/g, **180b**-1.26 mmol/g, **181**-1.33 mmol/g, **182a**-0.17 mmol/g, **182b**-0.16 mmol/g, **183**-0.26 mmol/g, **185**-0.112 mmol/g.

Some of the magnetically supported amino acid containing polymers were investigated by XPS giving further proof that the polymer was tethered to magnetite NP (see Figures 63 and 64). Main evidence came from N high resolution spectra which confirmed the presence of N in the samples.

Magnetic properties were investigated by VSM. The magnetization vs. applied magnetic field shows superparamagnetic behaviour of synthesized materials with saturation magnetization Ms values as follow **180a** – 14.7 emu/g, **179**-37.3 emu/g, **180b**-23.2 emu/g, **181**-36.7 emu/g, **182a**-42.4 emu/g, **182b**-37.6 emu/g, **183**-35.5 emu/g and **185**-65.7 emu/g.

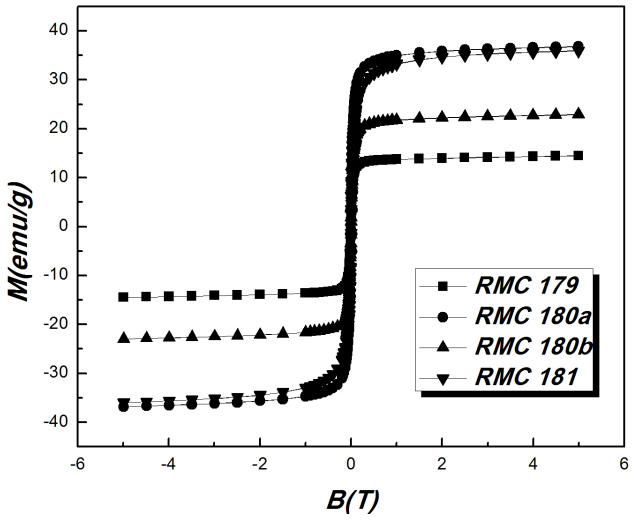

Figure 61. Magnetic curves for magnetite NP **179**, **180a**, **180b** and **181**.

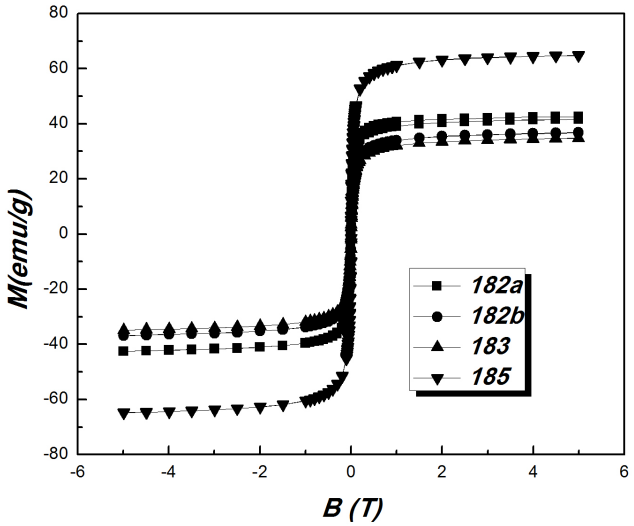

Figure 62. Magnetic curves for magnetite NP **182a**, **182b**, **183** and **185**.

TEM analysis showed that NP were almost spherical in shape. Small aggregation occurred during sample preparation process (see Appendix, A 18).

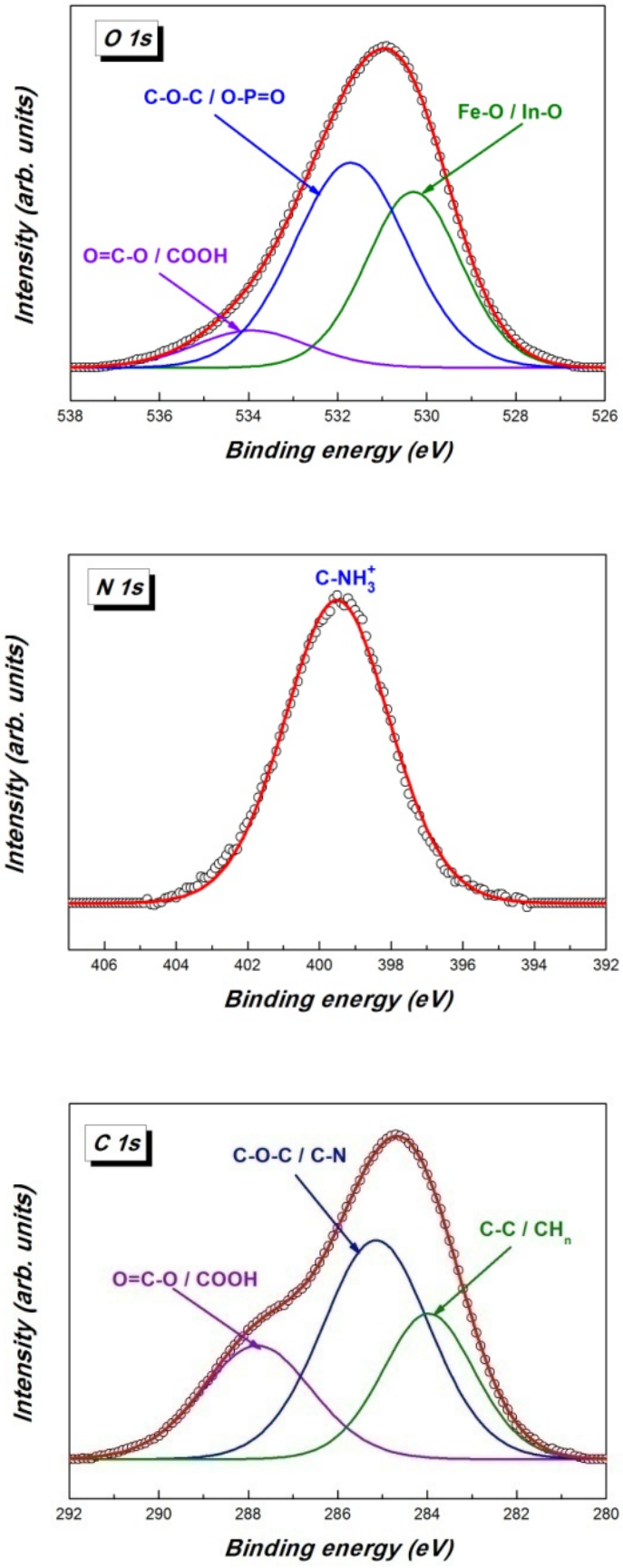

Figure 63 High resolution XPS spectra for C, N and O elements of magnetite NP **180b.**

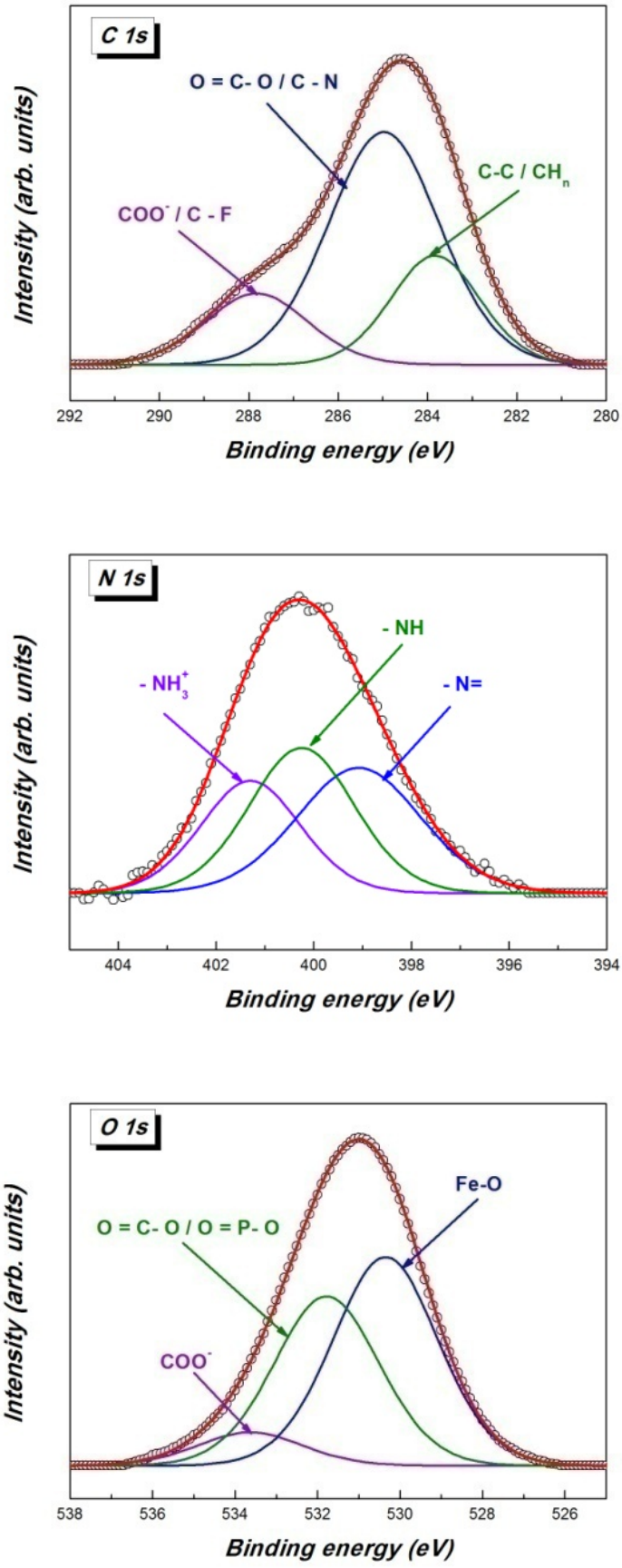

Figure 64. High resolution XPS spectra for C, N, and O elements of magnetite NP **182b**.

In addition to the "grafting from" like methodology described above, also the "grafting to" like-fashion was employed for coating the magnetite NP with polymers. This manner seems to be more convenient and versatile because the nanoplatform once prepared it can be used for grafting a myriad units. This method allows the reduction of the number of synthetic steps if one wants to prepare several core-shell NP. Magnetite NP **178** and **184** were chosen as starting materials for this route. The reaction between NP **178** and the easy accessible propargyl acrylate **186** afforded the anticipated new alkyne modified magnetic nanoparticles **187**.

Propargyl acrylate **186** was also fixed to magnetite NP **184** by polymerization. Water was used as solvent and APS (ammonium persulfate) as a radical initiator. In contrast to magnetite NP obtained by the "grafting from" like method (i.e. **179, 180a, 180b** and **181**), which could not be unambiguously evaluated by FTIR spectroscopy, the FTIR spectrum of the resulting magnetite NP **187** and **193** showed a significant change. A weak signal at 2125 cm^{-1} from $\equiv$C-H was observed in FTIR spectra of NP **187** and NP **193** what confirmed successful polymerization and functionalization of magnetite NP.

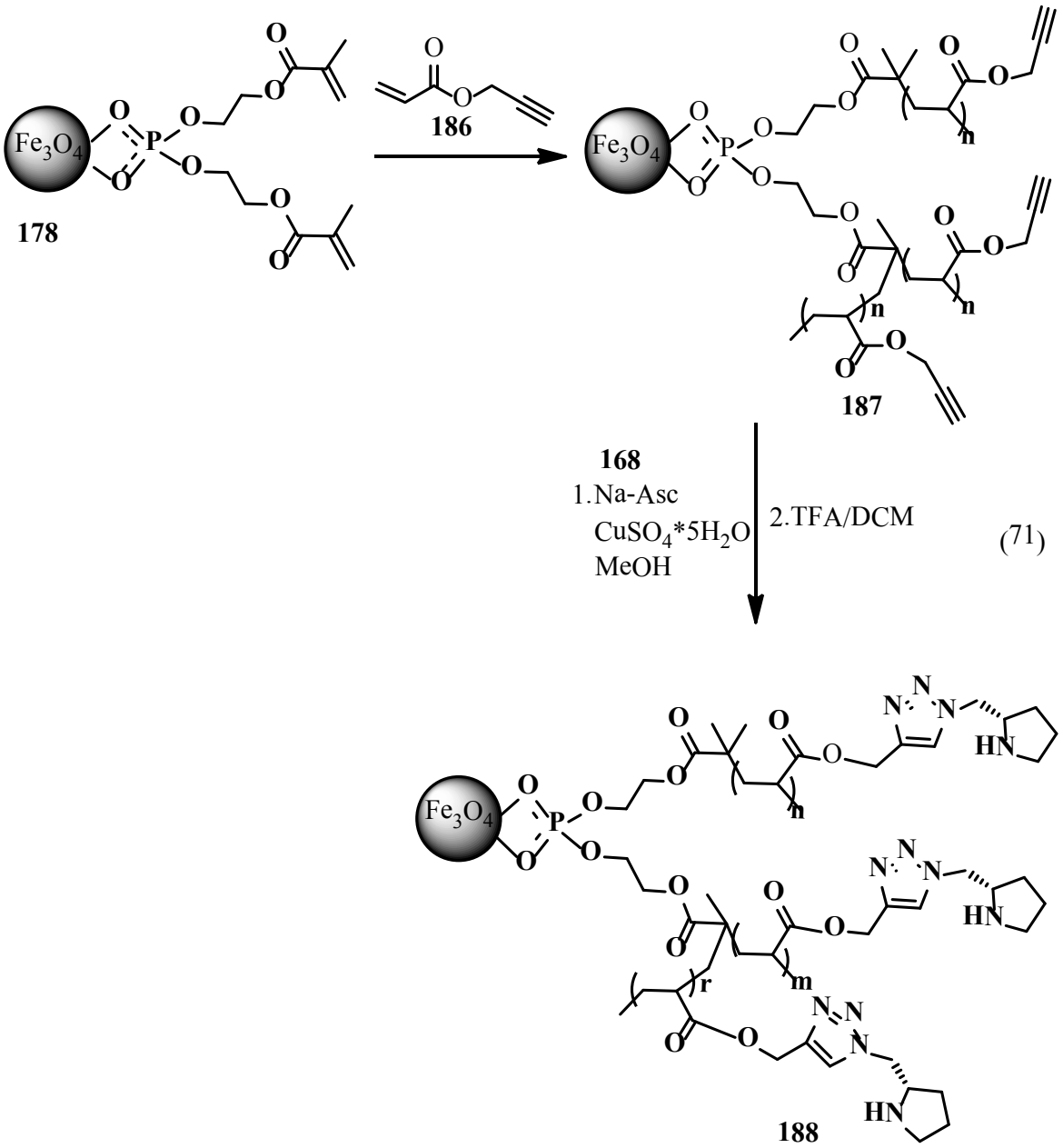

(71)

In order to introduce the potential organocatalytic unit to the magnetite NP compound **168** was fixed to NP **187** via CuAAC reaction affording magnetite NP **188** after final deprotection with TFA.

Furthermore, L-threonine was fixed to the alkyne-containing magnetite NP **193** by CuAAC. The necessary threonine derivative **192** was obtained in 24 % yield starting from L-threonine by reaction with azidoacetyl chloride[247] **191** following reported procedure.[241] The *O*-azidoacetyl-threonine **192** was bound to magnetite NP **193** via CuAAC reaction giving access to desired NP **194**.

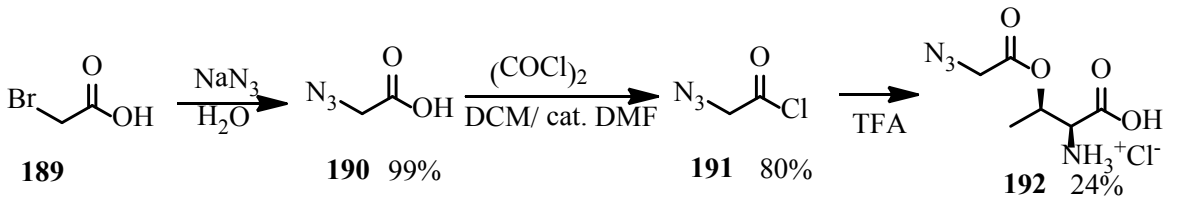

189 **190** 99% **191** 80% **192** 24%

(72)

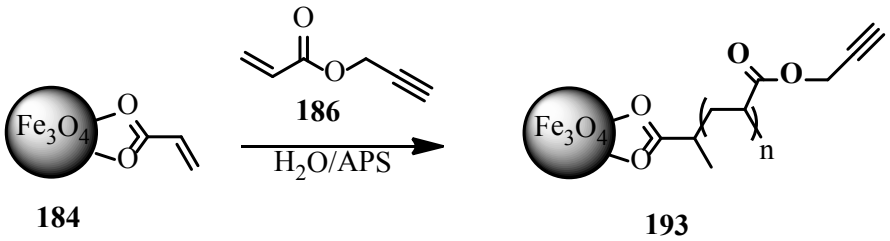

184 **193**

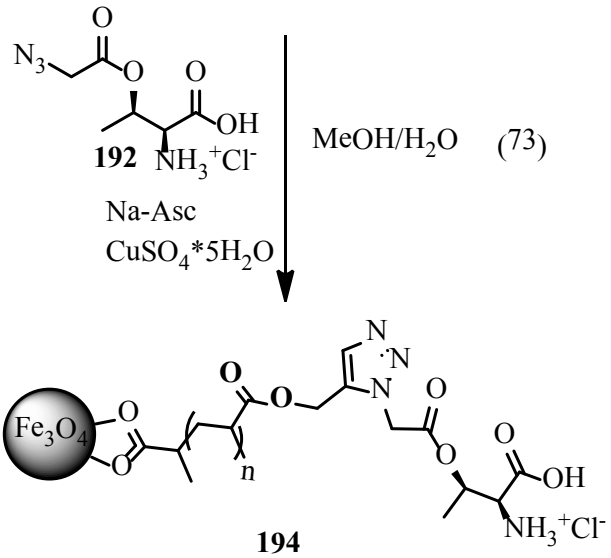

(73)

192 **194**

The CuAAC click reaction on magnetite NP **187** and **193** was monitored by FTIR spectroscopy. Disappearance of the weak signal at 2125 cm^{-1} was observed in case of magnetite NP **188** what evidenced that the reaction occurred (see Figure 65 zoom view, whole spectra see Appendix, A 19). Moreover, elemental analysis after deprotection step demonstrated a loading of 0.25 mmol/g. On the other hand, the FTIR spectrum of magnetite NP **194** was not so clear. A peak belonging to ≡C-H vibration was still observed. However, similar situation could have occurred like for polydopamine-azide modified magnetite NP **113** where after click reaction the azide band remained stemming from azido groups buried into the polymer matrix. Elemental analysis proved that reaction

leading to magnetite NP **194** had occurred with a loading of 0.3 mmol/g. Furthermore XPS analysis showed the presence of N as well (see Appendix, A 20).

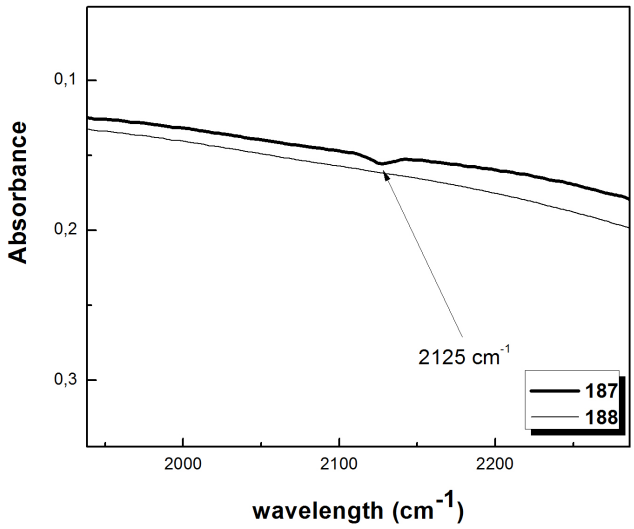

Figure 65. Part of FTIR spectra of magnetite NP **187** and **188**.

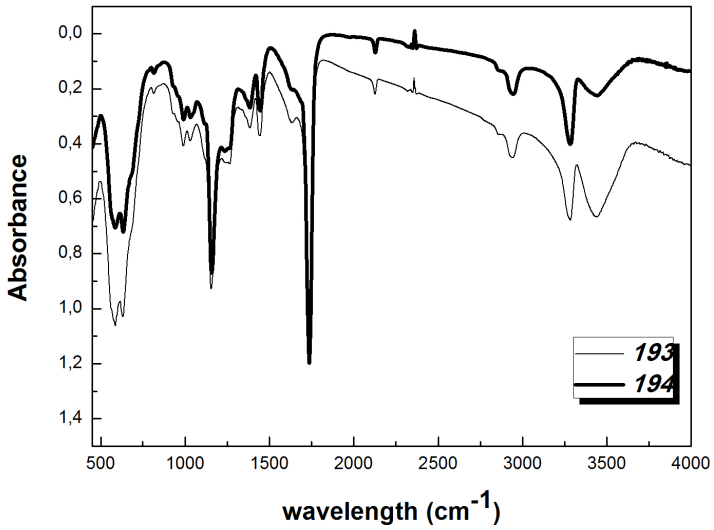

Figure 66. FTIR spectra of magnetite NP **193** and **194**.

Morphological studies for selected magnetite NP done by TEM revealed almost spherical shape of nanoparticles. However, slight aggregation occurred during sample preparation process (see Appendix, A 21).

Tests of the new magnetite NP containing chiral moieties as potential organocatalysts were performed in the aldol reaction of cyclohexanone with 4-nitrobenzaldehyde or Michael reaction of cyclohexanone with trans-β-nitrostyrene. However, to get some idea

about the catalytic activity of the monomers used in polymerization they were also included in these catalytic tests.

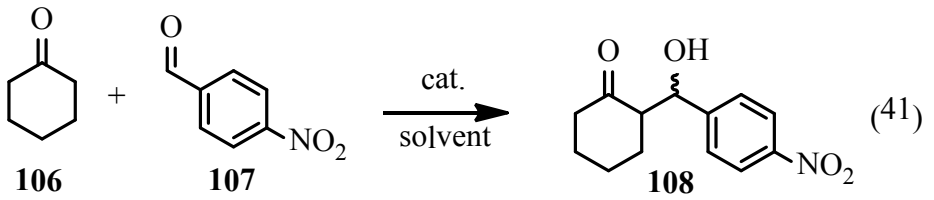

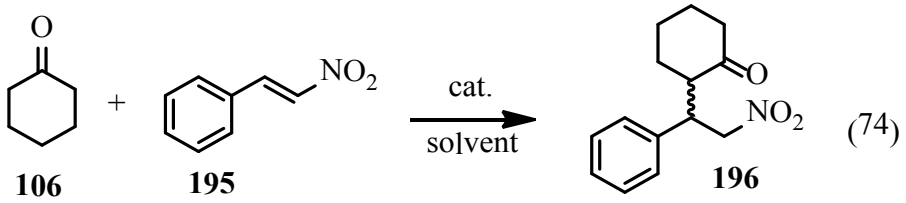

The threonine acrylate **158** was checked in the aldol reaction between cyclohexanone and 4-nitrobenzaldehyde in the presence of water (Table 6, entry 1). These conditions were the same like proposed in the literature for other threonine derivatives.[248] The aldol product **108** was obtained with moderate yield 52 % but in excellent ee – 92 % and dr - 85:15. It is worth mentioning that the yield, the ee and the dr could be improved by the addition of 0.1 eq of Et_3N transforming the catalyst into its free base. In this way the yield increased to 84% and the ee to 94 % (Table 6, entry 2). Undoubtly these results showed that **158** represents a new homogenous organocatalyst for aldol reactions. Surprisingly the catalytic activity was lost if the threonine acrylate **158** was fixed at magnetic NP **178** by polymerization resulting in magnetite NP **179**. Racemic product was obtained after long time 14 days (Table 6, entry 3). Washing the NP **179** with Et_3N to get the threonine moieties as free base did not improve the catalytic performance. A higher yield was achieved when benzoic acid was applied as co-catalyst (Table 6, entry 4). Also unsatisfactory results were observed for magnetite NP **180a** wherein the catalytic units were separated from the polymer backbone by linkers. They did not give the aldol product at all (Table 6, entry 5 and 6). Washing with basic solution was neither effective. Reaction catalyzed by NP **180b**, equipped with a longer linker, did not give rise to product formation or any other side products (Table 6, entry 7-10). Experiments conducted with high catalyst loading of 30 mol % or in presence of benzoic acid as additive did not enhance the reaction. A small amount of product was isolated after 14 days when polar solvents were applied like DMF and DMSO (Table 6, entry 11 and 12). Nevertheless, it

was racemic when DMF was used but small improvement was observed when DMSO was applied. It gave rise to 12 % ee (Table 6, entry 11). These results allowed assuming that a side reaction occurred wherein threonine was not involved.

The unsatisfactory behaviour of magnetite core-shell NP **179**, **180a** and **180b** could be due to inappropriate coating of the NP or the inaccessibility of a lot of catalytic sides for the reactants. Taking into consideration the latter reason it was expected that when the azido threonine **192** was fixed to magnetite NP **193** via CuAAC reaction the resulting NP **194** should expose the catalytic threonine units to the surrounding because the click reaction could occur only with the available alkyne groups (Table 6, entry 31 and 32). However, this assumption was not confirmed by the experiments wherein the desired aldol product was not formed. Even after 8 days and 0.1 eq of Et_3N, which gave improvement in case of homogenous acryloyl threonine catalyst **158**, the aldol product was not observed.

Magnetite NP **181** equipped with lysine as different catalytic unit, were not able to catalyze aldol reaction in asymmetric way (Table 6, entry 13). However, addition of benzoic acid enhanced the product formation in 51 % yield and ee - 34 % (Table 6, entry 14).

Table 6. Summary of the catalytic with polyacrylates based magnetite nanoparticles in aldol and Michael reaction.

Entry	Product	Catalyst	Solvent/ Additive	Loading [mol %]	Time [h]	Yield [%]	dr syn/anti	Ee %
1[a]	**108**	**158**	---/H_2O	10	72	52	15:85	92
2[b]	**108**	**158**	---/H_2O	10	72	84	6:94	94
3[c]	**108**	**179**	---	10	14 d	33	51:49	rac
4[d]	**108**	**179**	---/BA	10	14 d	65	n.d.	rac
5[e]	**108**	**180a**	---/H_2O	10	72	---	---	---
6[f]	**108**	**180a**	---/ H_2O	10	72	---	---	--
7[g]	**108**	**180b**	---/H_2O	30	40	----	n.d.	---
8[g]	**108**	**180b**	10% BA	30	72	---	n.d.	---
9[h]	**108**	**180b**	---/H_2O	10	72	---	n.d.	---
10[i]	**108**	**180b**	---/H_2O	20	72	---	n.d.	---
11[i]	**108**	**180b**	DMSO/ H_2O	20	14 d	20	n.d.	12%
12[i]	**108**	**180b**	DMF/ H_2O	20	14 d	16	n.d.	rac
13[j]	**108**	**181**		20	48	---	---	--
14[k]	**108**	**181**	---/BA	20	96	51	56:44	34

15[l]	**196**	**182a**	---/TFA	10	24	---	---	
16[l1]	**196**	**182a**	--- /TFA	10	20	25	n.d	20
17[l2]	**196**	**182a**	EtOH/ TFA	10	72	---	---	---
18[l3]	**196**	**182a**	DMSO/ TFA	10	72	---	---	---
19m	**196**	**182b**	---/TFA	10	20	-----	---	---
20[m1]	**196**	**182b**	---/H_2O	15	72	-----	---	-----
21[m2]	**196**	**182b**	---/TFA	20	72	15	---	86
22[n]	**196**	**183**	---/TFA	10	40	59	17:87	92
23[n1]	**196**	**183**	DMSO/ TFA	10	48	---	---	---
24[n2]	**196**	**183**	BA/TFA	10	48	---	---	---
25[n]	**196**	**183**	---/TFA /US	10	8	---	---	---
26[n]	**196**	**185**	---/TFA	10	48	---	---	---
27[o]	**196**	**188**	---	10	72	-----	---	----
28[o1]	**196**	**188**	---/TFA	20	72	30	n.d	86
29	**196**	**188 1st run**	---/TFA	20	72	10	n.d	80
30	**196**	**188 2nd run**	---/TFA	20	72	nd	n.d	70
31[p]	**108**	**194**	---	10	8 d	---	---	---
32[p1]	**108**	**194**	---	10	8 d	---	---	---

[a] Reaction conditions: aldehyde (1 mM), cyclohexanone (260 µl), H_2O (200 µl), [b] Reaction conditions: aldehyde (1 mM), cyclohexanone (260 µl), H_2O (200µl), Et_3N (1mM), [c] Reaction conditions: aldehyde (0.5 mM), cyclohexanone (0.5 mL), [d] Reaction conditions as in c, 10 mol % BA, [e] Reaction conditions aldehyde (0.25 mM), cyclohexanone (0.5 mL), water (100 µl), [f] Reaction conditions like in e, NP washed with 5 % Et_3N/MeOH before use, [g] Reaction conditions aldehyde (0.25 mM), cyclohexanone (0.5 mL), 1 ml H_2O, [h] Reaction conditions aldehyde (0.5 mM), cyclohexanone (130 µl), H_2O (100 µl), [i] aldehyde (0.25 mM), cyclohexanone (0.5 mL), H_2O (100 µl), [j] Reaction conditions aldehyde (0.5 mM), cyclohexanone (0.5 mL), [k] like in j, 10 mol % BA, [l] Reaction conditions nitrostyrene (0.25 mM), cyclohexanone (1 mL), 2% TFA, [l1]like in l, NP were stirred with TFA overnight before use, [l2] nitrostyrene (0.25 mM), cyclohexanone (0.5 ml), 2% TFA, EtOH 1 ml, [l3] nitrostyrene (0.25 mM), cyclohexanone (0.5 ml), 2% TFA, DMSO 1 ml, NP were washed with 1 N HCl before use, [m] nitrostyrene (0.25 mM), cyclohexanone (0.5 ml), 2% TFA, [m1] nitrostyrene (0.16 mM), cyclohexanone (0,165 mL), water (100 µl), [m2] nitrostyrene (0.125 mM), cyclohexanone (1 mL), 2% TFA, NP were washed with 2% Et_3N, [n] Reaction conditions nitrostyrene (0.05 mM), cyclohexanone (0.5 mL), 2% TFA, [n1] like n solvent 1mL was used, [n2] like in n , 10 mol % of BA used, [o] Reaction conditions nitrostyrene (0.25 mM), cyclohexanone (0.5 mL), [o1] like in o but NP were washed with 2% Et_3N in MeOH before use, then 2% TFA used in reaction, [p] Reaction conditions aldehyde (0.25 mM), cyclohexanone (0.5 mL), [p1] like p and 10 mol % Et_3N

Polyacrylates fixed to magnetite NP **182a** and **182b** equipped with chiral triazole derivatives were tested in Michael reaction between *trans*-β-nitrostyrene and cyclohexanone. Catalyst **182a,** with a long polar linker, was used in this reaction performed without any co-catalyst for 72 h but it did give the desired product (Table 6, entry 15). Washing the catalyst with TFA and addition of TFA gave the product **196** but with poor yield 25% and only 20% ee (Table 6, entry 16). Solvent effect was checked for Michael reaction. Polar solvents like EtOH and DMSO did not improve product formation

(Table 6, entry 17 and 18). Negative results were observed when the catalyst **182b** with unpolar linker was utilized. The product was not formed when TFA or water were used as additives. Longer reaction time was not helpful either. Increase of the catalyst amount up to 15 mol % did not show any enhancement of the reaction too (Table 6, entry 19 and 20). However, when the catalyst loading was increased to 20 mol % the Michael adduct was formed in 15 % yield and a quite high ee was observed 86 % (Table 6, entry 21).

Tests conducted with the catalysts **183** without linker (collaboration with Zekarias Yacob) gave the desired Michael product in yield 59 % and a high 92 % ee (Table 6, entry 22). Unfortunately, this was only in the first run. When the same batch of catalyst was re-applied under different condition no product was formed. Neither the application of polar solvent like DMSO nor the addition of benzoic acid in addition to TFA as co-catalyst gave Michael product (Table 6, entry 23 and 24). Application of ultrasounds (US) for few hours to assure dispersion of NP in the reaction mixture did not enhanced the reaction as well (Table 6, entry 25). Better results were obtained with catalyst **188** synthesized by "grafting to" like-fashion. In the first attempt (Table 6, entry 27) catalyst did not catalyze the Michael reaction but when the NP **188** were washed with Et_3N solution this improved the reaction. Product was obtained in 30% yield with an ee of 86% (Table 6, entry 28). When the catalyst was recycled it was still active but to a lesser extent. Yields and ee dropped down from 30% to traces and from 86 to 70%, respectively. (Table 6, entry 29 and 30). Magnetite NP **185** did not lead to product formation in the Michael reaction (Table 6, entry 26).

In summary, new threonine, lysine and proline acrylic derivatives (**157**, **158**, **161**, **164**, **175**, **176** and **177**) were synthesized and used for functionalization of magnetite NP. The synthesis of the new materials was done by polymerization of acrylic acid monomers in the presence of the magnetite NP **178** or **184** either in a "grafting from" like fashion or in a "grafting to" like manner. CuACC reaction was used to attach amino acids derivatives **168** and **192** to NP equipped with alkyne groups **187** and **193** resulting in NP **188** and **194**, respectively. Elemental analysis and XPS evidenced the presence of the desired amino acids attached to the magnetite NP via a polymer shell. All nanoparticles were investigated by FTIR and TEM. Investigation of the magnetic properties evidenced superparamagnetic behaviour of these nanomaterials with high Ms values, hence they can be easily controlled by an external magnetic field. Catalytic tests with nanoparticles bearing threonine **180a**, **180b** and **194** revealed that they could not catalyse the aldol reaction of cyclohexanone with 4-nitrobenzaldehyde. In case of NP **179** the product was obtained in racemic form.

Magnetite NP **182a**, **182b**, **185** were applied in Michael reaction of cyclohexanone with *trans*-β-nitrostyrene. Unfortunately, they did not catalyze this reaction even when conditions were varied (i.e. higher loading of catalyst or addition of acid). Catalyst **183** gave rise to product formation in 59 % yield and ee of 92 % in the first run but could not catalyze the reaction in subsequent runs. Magnetite NP **188** achieved by "grafting to" like manner led to Michael addition product **196** in 30 % yield and ee of 86 %, but performed worse in next runs.

In order to explain the unsatisfactory results in catalysis one can assume that the catalytic units were buried inside the polymers matrix, thus, not many catalytic groups were accessible for reaction. In future investigations it could be tried to build up the polymer shell of the core shell NP by block polymerization where first a non-catalytic polymer shell is established followed by a block with catalytic units. In this way the catalytic groups could be better exposed to the reaction mixture.

3 Summary

Magnetic nanoparticles have gained great interest as nanocarriers or contrast agent for MRI in medicine, in separation processes, and as supports for catalysts. In most of these applications magnetite NP have to be functionalized. For such a functionalization a variety of possibilities exist and a lot have been realized so far. However there is still wide interest in the development of new magnetic nanoparticles. Present activities in this field are focused on new functions, combined functions, higher stability, biocompatibility, high magnetic moment, more efficient synthesis and reduction of the costs. In the framework of this thesis new functionalized magnetic nanoparticles were prepared, characterized and eventually applied as organocatalysts.

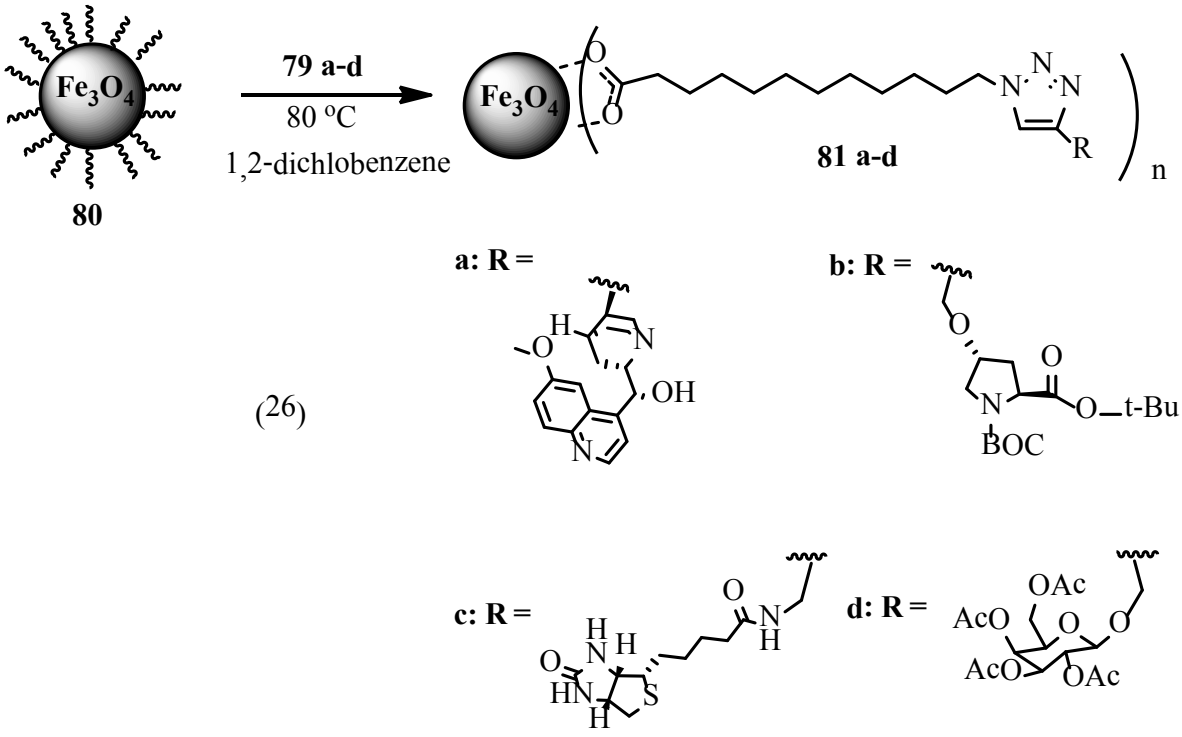

(26)

The first type of the magnetic nanoparticles was obtained by ligand exchange reaction of magnetite NP **80** stabilized with one layer of oleic acid. This layer was replaced by hitherto unknown fatty acid derivatives with terminal functionalized 1,2,3-triazoles. The latter were obtained by Cu-catalyzed alkyne azide cycloaddition (CuAAC) between 12-azidododecanoic acid **65** and alkyne partners equipped with various moieties including

quinine (organocatalyst) **68**, proline (organocatalyst) **72**, biotin (biologic recognition function) **75** and galactose (cancer therapy) **78** in good yields (70-75%) in t-BuOH-H_2O mixture using $CuSO_4$*$5H_2O$/Na-ascorbate catalytic system. The application of these 12-triazolyldodecanoic acids **79a-d** in ligand exchange reaction gave access to new nanocomposites **81a-d** where the original oleic acid was fully replaced. All characteristic peaks of the new ligands were found in the FTIR-spectrum while those of oleic acid were missing. The superparamagnetic properties of the obtained materials are important for certain applications such as in hyperthermia treatment of cancer or in magnetic separation. TEM revealed that the magnetic nanoparticles where almost spherical in shape with diameters of around 30 nm. It was found that some of the introduced ligands behaved better than oleic acid in terms of stabilization of magnetic NP. Thus the magnetite NP **81b** and **81d** formed stable colloidal suspensions in organic solvents as shown by dynamic light scattering (DLS) experiments. As an alternative access to triazolyl fatty acid stabilized magnetite NP **84** 11-azidoundecanoic acid **83** was attached to magnetite NP via ligand exchange reaction. The resulting azido functionalized magnetic nanoplatform is very versatile. As a proof of principle it was coupled with an appropriate alkyne containing proline or a Hayashi-type organocatalyst by CuAAC resulting in magnetite NP **90a** and **90b**, respectively.

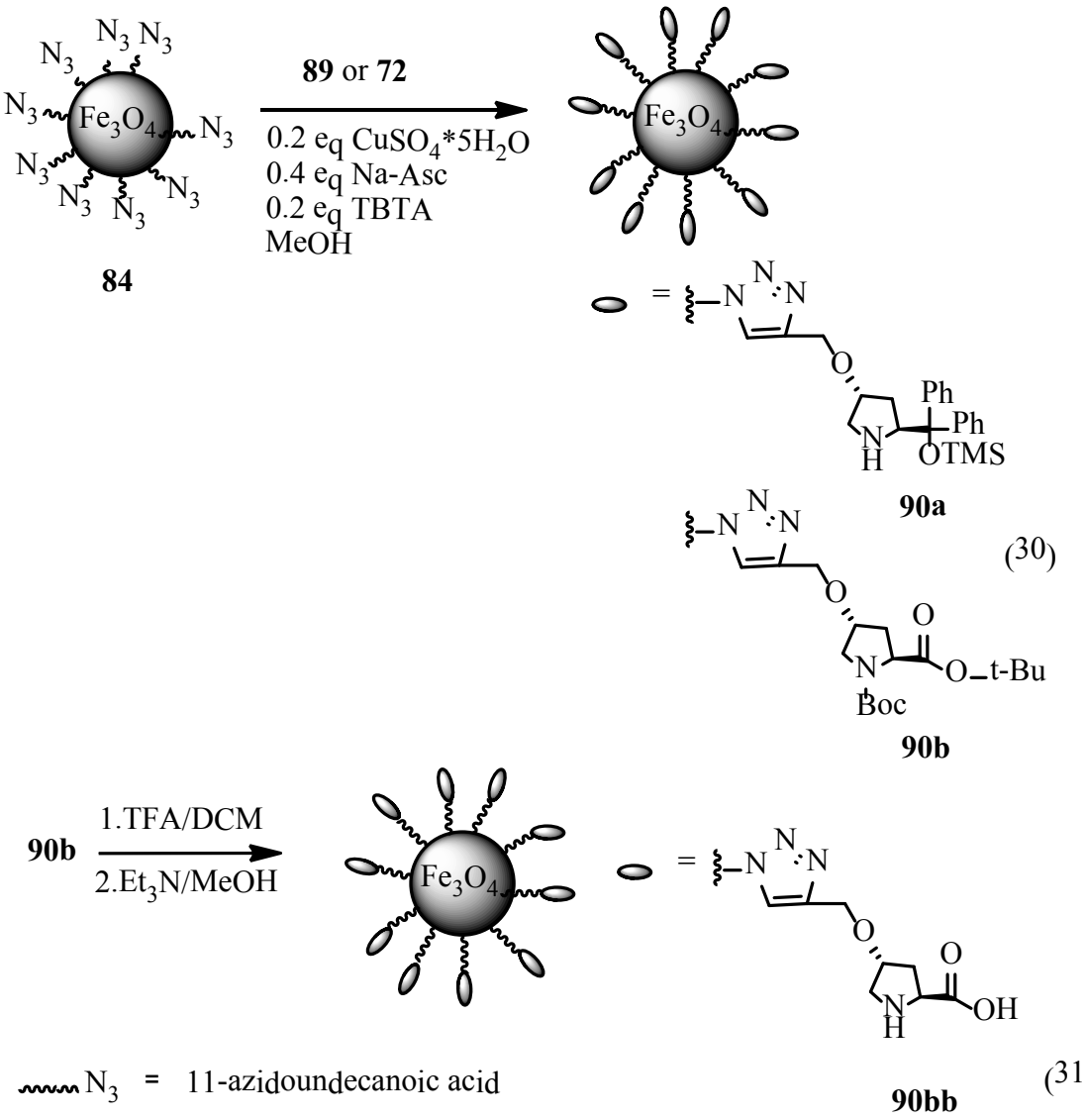

Unfortunately, catalytic tests performed with these two magnetite NP containing established organocatalytic moieties were not successful. The Hayashi type catalyst was found to be inactive in Michael reaction between propionaldehyde and *trans*-β-nitrostyrene, i. e. it did not give rise to product formation under various conditions (changing solvents, increasing catalyst loading). The proline-functionalized MNP were able to catalyze the aldol reaction between 4-nitrobenzaldehyde and cyclohexanone, however the product was racemic. This could indicate that proline was not involved in the catalytic cycle but an unwanted background reaction occurred.

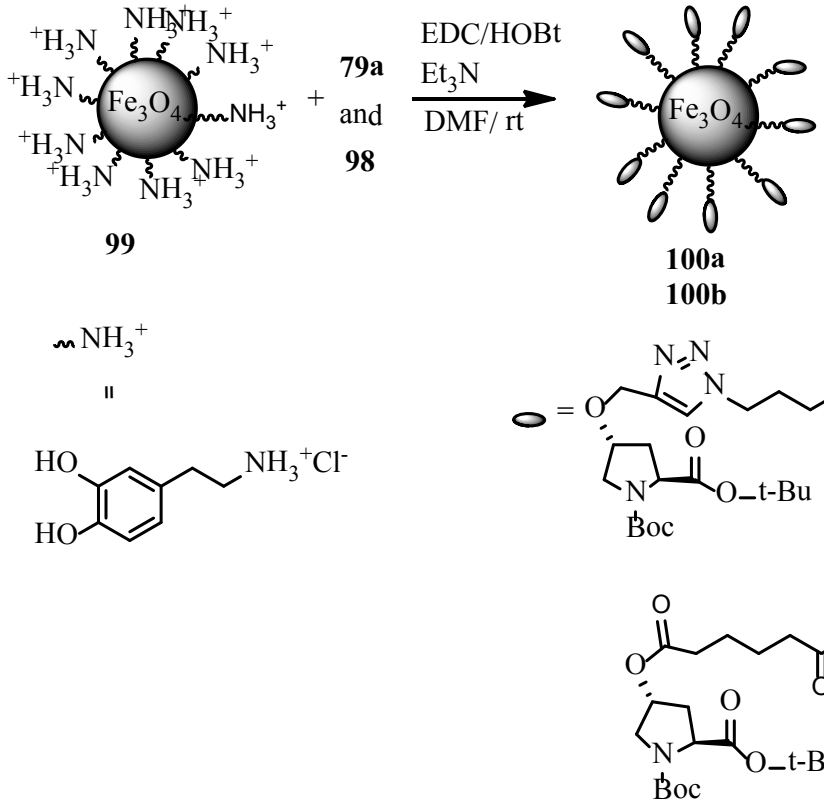
99
79a
and
98
EDC/HOBt
Et3N
DMF/ rt
100a
100b
NH3+
HO
HO
NH3+Cl-
Boc
O-t-Bu
100a
HN
100b
1.
/CH3CN
2. TFA/DCM
(38)
101a
101b
OH

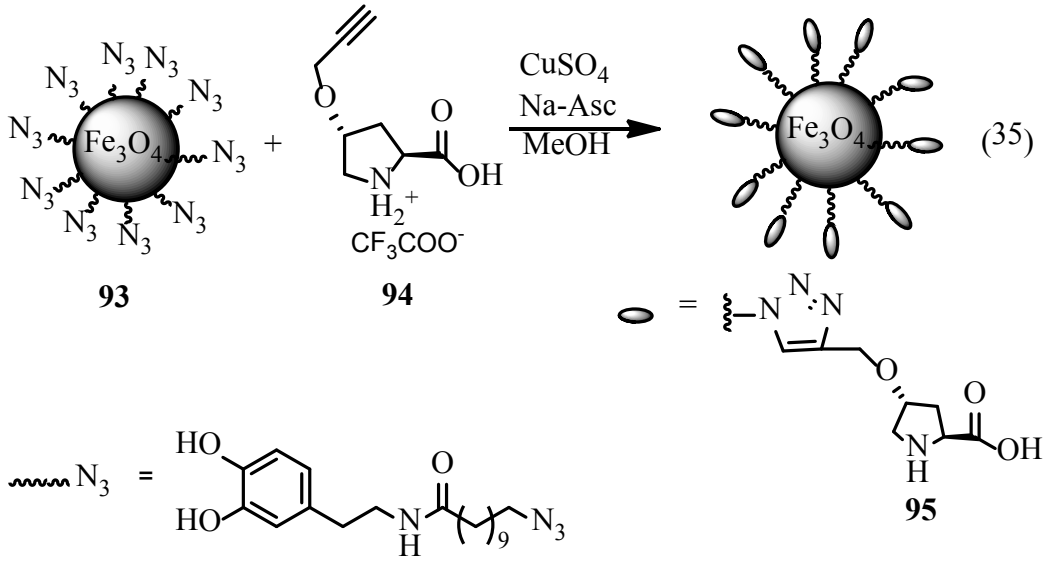

A second type of new nanoparticles is based on functionalized dopamine, a biomimetic coating agent. They were prepared either in ligand exchange reaction at a ferrofluid **80** by new functionalized dopamine derivatives **92** or in a more versatile manner using amide formation between dopamine stabilized magnetite NP **99** and carboxylic partners **79a** and **98** giving access to NP **100a** and **100b** (see Scheme 38**).** In another approach alkyne proline **94** was coupled with azide modified dopamine magnetite NP **93** by CuAAC. All reactions gave access to magnetite NP **100a**, **100b** and **95** particles bearing proline connected by different in linkers. Loadings of the magnetite NP **95** and **99** with proline moieties were low (0.05 mmol/g to 0.09 mmol/g) as determined by the picric acid test, which is commonly used in quantitative determination of amino groups on resins. Application of proline-containing NP **95**, in aldol reaction between 4-nitrobenzaldehyde and cyclohexanone gave 99% yield and 36% ee with 10 mol% catalyst loading which was improved to 48% ee (only 77% yield) when benzoic acid was applied as a co-catalyst. Magnetite NP **101a** applied in aldol reaction between 4-nitrobenzaldehyde and cyclohexanone gave rise to product formation in 68% yield and 52% ee. Addition of water and benzoic acid allowed to furnish the product but with lower yields and ee's (35% yield and racemic product.) However, the product was obtained in 46% yield and 48% ee when the reaction was performed only with addition of 10 mol % of benzoic acid. It was found that magnetite NP **101b** in 10 mol % can catalyze also the aldol reaction mentioned above. The product was obtained in 80% yield and ee of 52%. Addition of benzoic acid led to a decrease in yield to 55%, whereas the ee was slightly improved to 55%. Remarkably, the *syn*-diasteromer and not the expected *anti*-isomer was preferably formed in the

investigated cases. The dominance of the *syn*-diastereoisomer may imply that not always proline, which normally gives rise to the *anti*-product, was the real catalyst and some side reactions occurred. Probably bare magnetic nanoparticles were involved in the side reaction. Nevertheless, this way was not convenient because it required a lot of materials (due to the low loading of the catalyst). Thus problems with stirring were observed and the access of the reagents to the catalyst seemed to be limited.

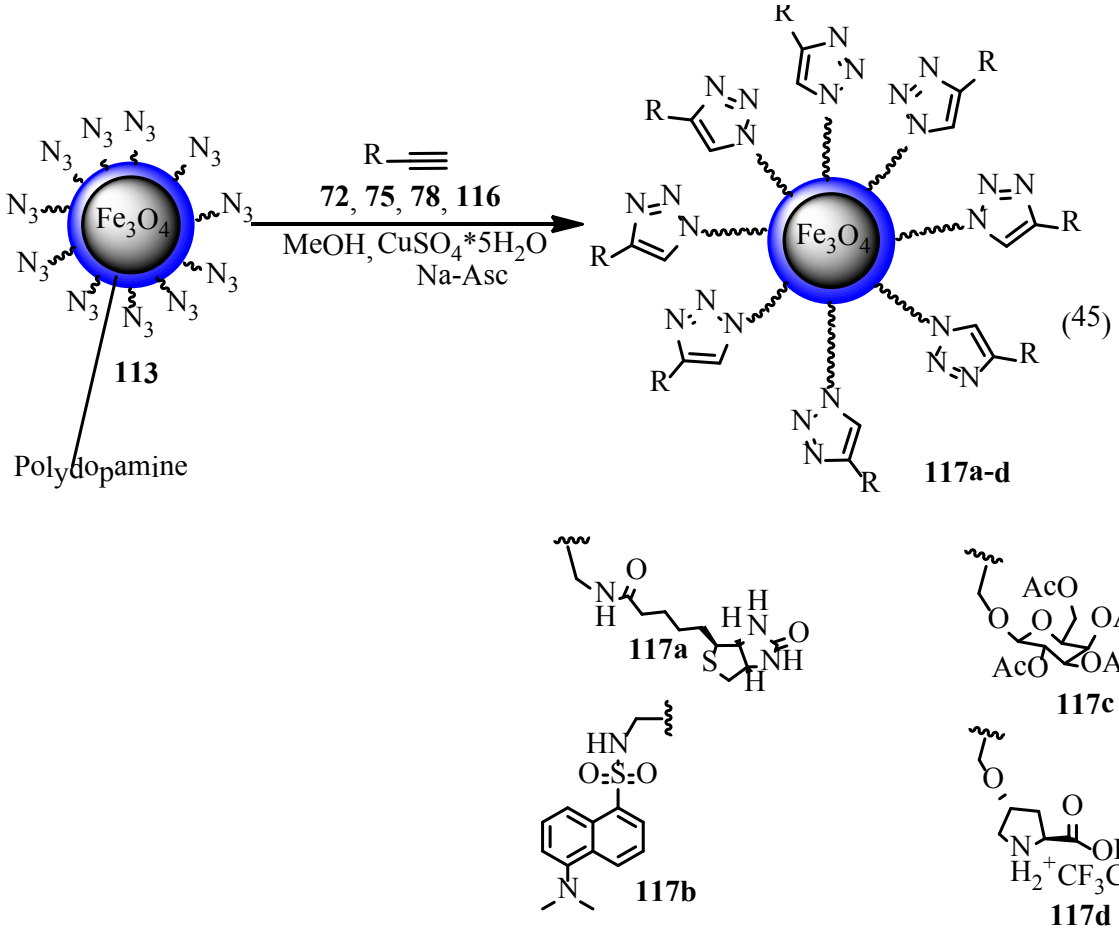

A third type of new magnetic nanoparticles was obtained by the application of different polymers as coating agents. The reaction potential of the magnetite NP **112** covered with polydopamine was extended in a new way by introducing an azido moieties via the addition of 4-azidobutylamine. The presence of the azido functions (see structure **113**) provides a wide scope in further introductions of various functionality by CuAAC reaction. As a proof of principle, different alkynes moieties containing proline **72**, galactose **78**, biotin **75** or dansyl **116** were introduced in this way giving four new types of magnetic particles **117a-d** bearing interesting biological and catalytic function. Some of

the azido groups remain untouched after the CuAAC even when ultrasound was applied in the reaction as observed in the FTIR and XPS spectra.

As another new way to extend the functionality of polydopamine shells of MNP was found by the introduction of alcohol moieties by addition of 5-amino-1-pentanol. This functionality was employed in ring opening polymerization (ROP) of lactide, the "lactic acid dimer" giving rise to polylactic acid. As a result, new important magnetite NP **119** were obtained which are covered by a biocompatible and biodegradable polymer. The terminal hydroxyl groups of the polylactic acid could be used to fix biotin as an important biologic recognition function, making the magnetite NP **120** even more attractive for certain medical applications.

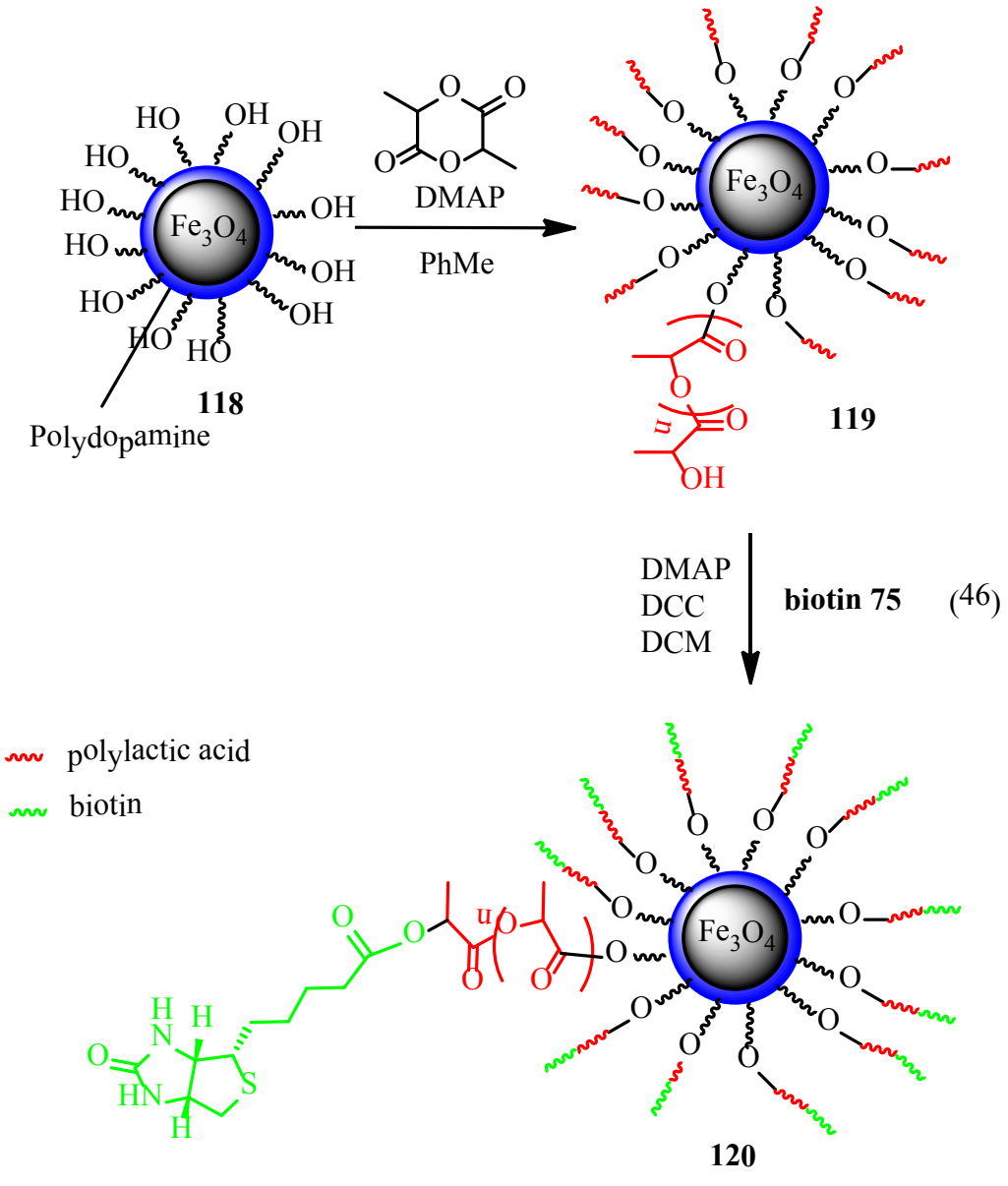

Observations in ssNMR of MNP x coated with PDA together with results from XPS (only one type of nitrogen atoms was found) made us to reconsider the intensively discussed polydopamine structures proposed in the literature. As a result of advanced ssNMR and detailed MS studies a new polydopamine structure **132** was proposed where units of indoles of varying degree of hydrogenation are covalently bound and also some uncyclized dopamine units are included.

PDA-coated magnetite NP **112** were utilized as support for cysteine by straight forward reaction with cysteine affording magnetite NP **135**. These NP as well as the aforementioned magnetite NP **117d** equipped with proline were tested as catalysts in aldol reaction. Cysteine containing magnetite NP **135** gave the aldol product in moderate yield but as racemate while proline-modified magnetite NP **117d** did not lead to a reaction.

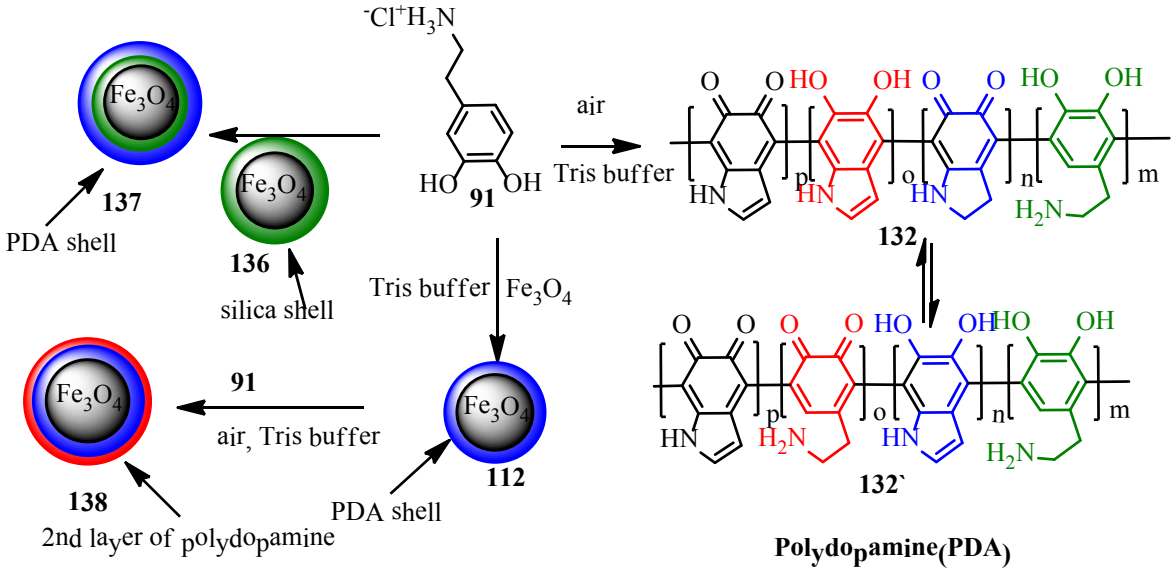

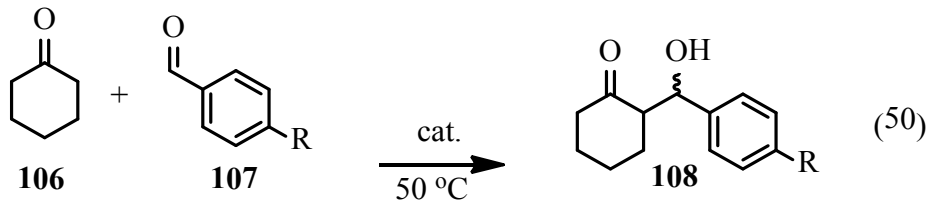

108 R

a	NO_2
b	Br
c	H
d	OMe

These observations together with structural investigations of polydopamine caused that a background reaction was taken under consideration. To check this assumption mere polydopamine was synthesized. In fact, this polymer exhibited catalytic activity in aldol reaction between 4-nitrobenzaldehyde and cyclohexanone providing yields in the range of 93% to 75 %. The PDA could be recycled four times. However, it lost some catalytic activity after the first run. The activity stayed constant in the next three runs. Magnetite NP **138** coated with PDA, which allow easy separation and reuse by magnetic decantation, catalyzed the aldol reaction as well but the catalyst was losing activity in each recycling step. Furthermore, magnetite NP covered with silica (**136**) were used as magnetic support for polydopamine (**137**). Also here catalytic activity in aldol reaction was observed. However, this system lost its activity after two runs completely.

Variation of aryl aldehydes in the aldol reaction with cyclohexanone catalyzed by PDA-coated NP **138** showed that electron withdrawing groups must be present, as arylaldehydes with electron donating substituents failed to react. Two factors were found out causing the deactivation phenomenon. First, mechanical loss of polymer (catalytic units) was evidenced by elemental analysis. Second, the 4-nitrobenzaldehyde is incorporated into polydopamine via imine formation, thus blocking part of the catalytic amino groups irreversibly as found out by XPS and FTIR investigations showing the presence of nitro groups in the MNP after applying them in aldol reactions with 4-nitrobenzaldhehyde.

Magnetite NP **138** coated with PDA were further tested as catalyst in the Knoevenagel reaction of benzaldehyde with malononitrile. Here, the catalyst could be used in five consecutive cycles without significant loss of activity and did not show substituent dependence in the arylaldehyde reactant.

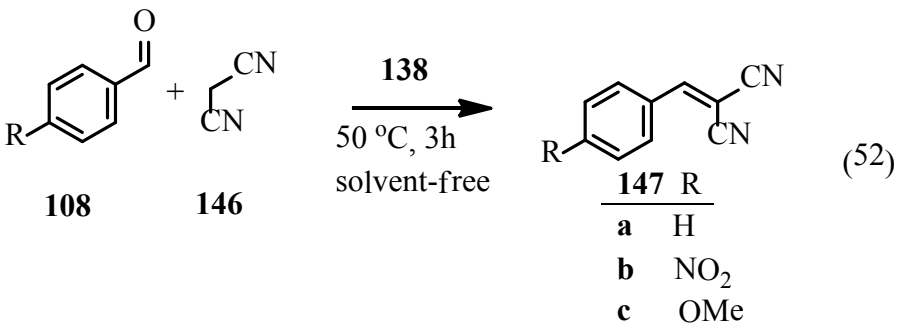

108 **146**

147 R
a H
b NO_2
c OMe

(52)

In contrast to previous literature reports we were able to apply PDA-covered NP directly to start a ROP with lactide dimer by exploiting the nucleophilicity of the amino groups in PDA and free phenolic groups. This presents a very straight forward way to PLA-coated magnetite NP for potential application in medicine.

Because PDA is known to cover almost every surface we applied it also to silica coated magnetite NP (**136**) and to carbon coated iron NP (**139**) as primary shell for surface initiated ring opening polymerization of lactide. The former are very robust and commercially available magnetic NP and thus the final PLA coated core shell structures will be in particular attractive for applicants in medicine because of their biocompatible surface. Coating was successful giving a powerful access to the NP **151** and **152**. This methodology can also be applied to various other non-magnetic materials rendering them biocompatible as shown in the framework of this thesis with aluminium oxide (**153**).

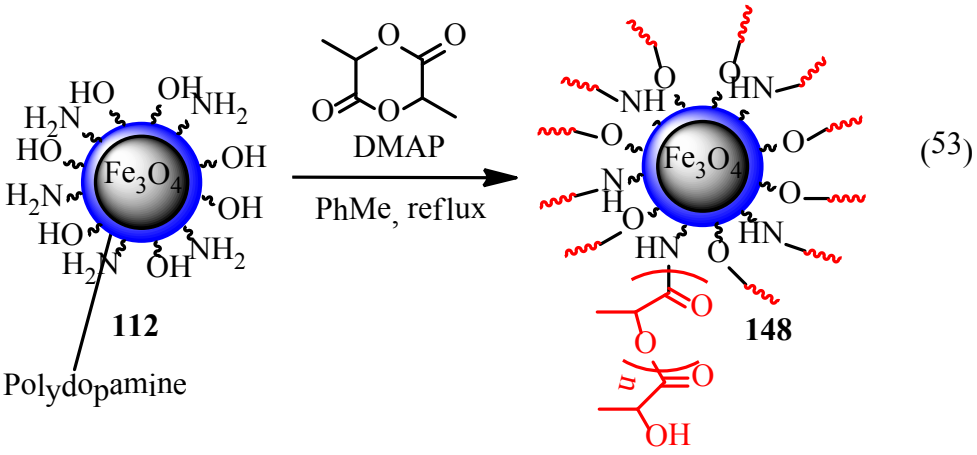

(53)

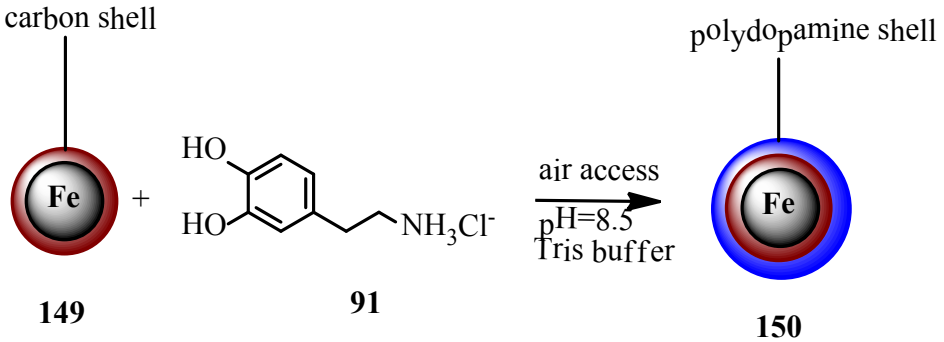
carbon shell
Fe
149
HO
HO
NH3Cl-
91
air access
pH=8.5
Tris buffer
polydopamine shell
Fe
150

(54)

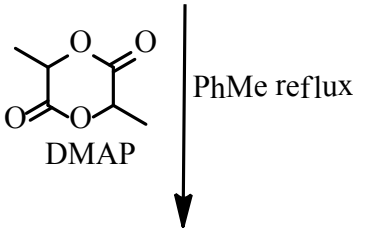
DMAP
PhMe reflux

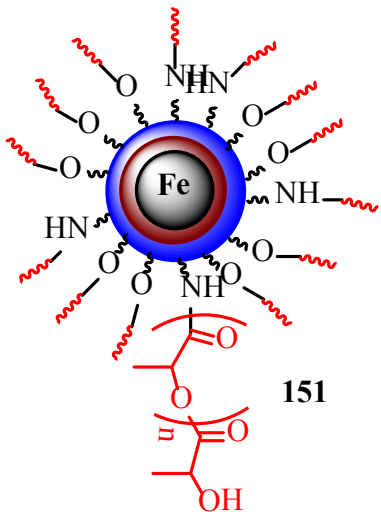
Fe
NH
HN
O
OH
n
151

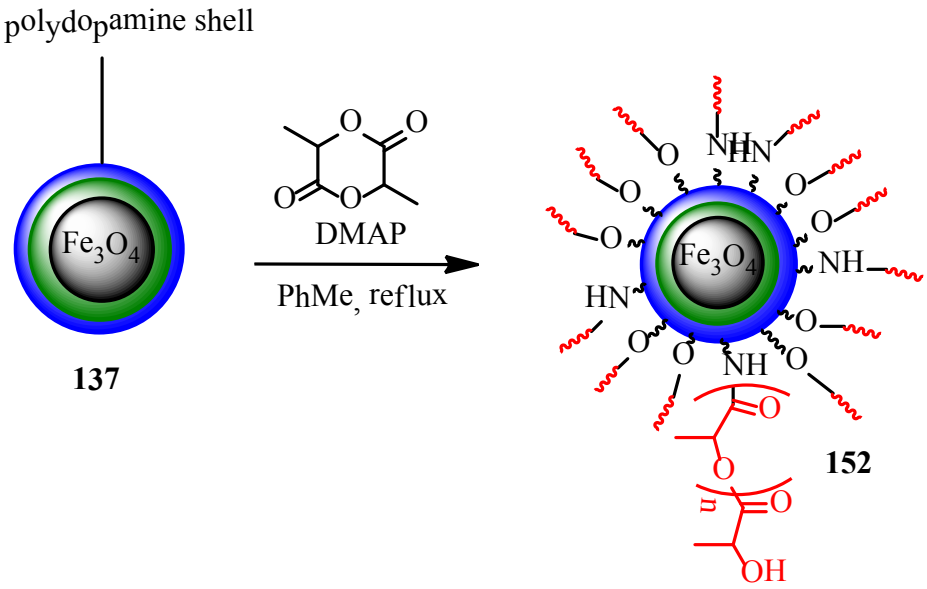
polydopamine shell
Fe3O4
137
DMAP
PhMe, reflux
Fe3O4
NH
HN
O
OH
n
152

(55)

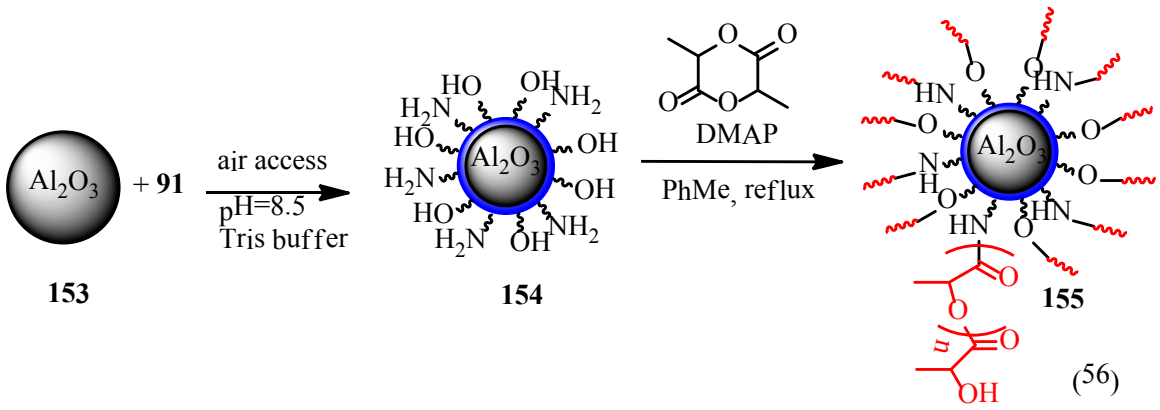

Both features, the catalytic activity in aldol and Knoevenagel reaction on the one hand and the surface initiated ROP of polylactic acid present a further breakthrough in the synthesis of PDA as an easily accessible coating and functionalizing material.

In the final part of this thesis synthesis and physical characterization of MNP modified with functionalized polyacrylates are presented. New acryloyl or methacryloyl derivatives of threonine (**157**, **158** and **161**), lysine (**164**) and proline (**175**, **176** and **177**) were synthesized and further polymerized in presence of magnetite NP **178** coated with phosphate bearing acryloyl groups. This led to immobilization of these amino acids on the NP (**179**, **180a**, **180b**, **181**, **182a**, **182b, 183** and **185**). Another approach to magnetite NP covered with amino acid-containing polyacrylates was based on a two-step procedure. Magnetite NP were equipped with alkyne groups by polymerization of propargyl acrylate in the presence of magnetite NP **178** or **184** (stabilized with acrylic acid) in the first step yielding NP **187** and **193**. Then, CuACC reaction with azido proline derivative **168** or the new azido threonine **192** gave rise to 1,2,3 triazole ring linkage of these amino acids to the polymer-shell providing magnetite NP **188** and **194**.

Surprisingly, almost all catalysts were found to be ineffective in aldol reaction or Michael reaction. Different reaction parameters were checked i.e. solvent, catalyst loading or additives but this did not help to improve the reaction. Slightly better results were observed when NP **188** bearing proline obtained by grafting to-like fashion were applied in Michael reaction between *trans*-β-nitrostyrene and cyclohexanone. The catalyst was able to furnish the product in 30% yield and with good ee of 86%. However, the catalytic activity was going down drastically after recycling. Similar behaviour was observed for magnetite NP **183** which bore proline units attached to magnetite NP in direct polymerization. They catalyzed the Michael addition with good yield and an excellent ee of 92% but they did not lead to product formation in the subsequent runs.

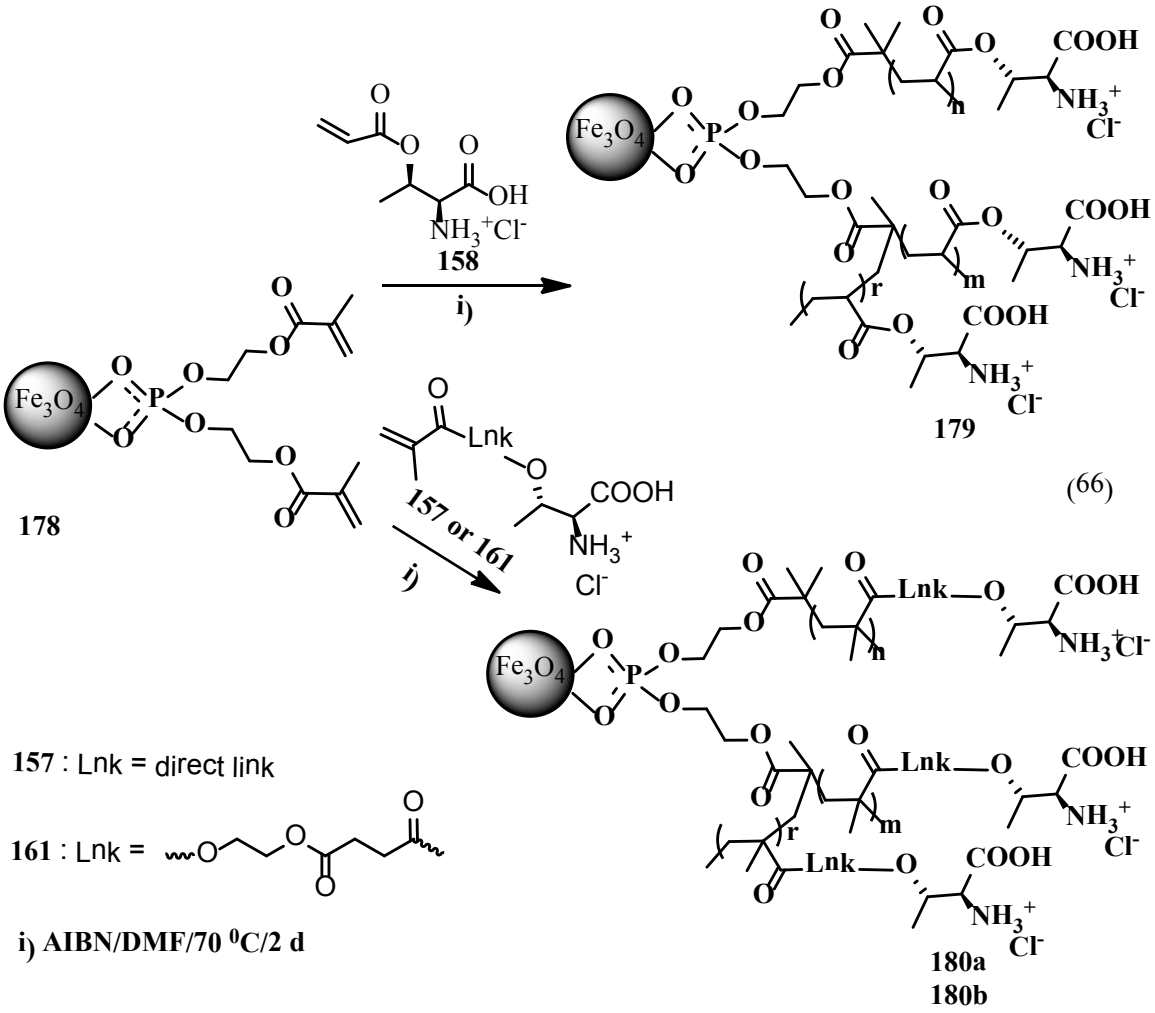
158
i)
178
179
157 or 161
i)
157 : Lnk = direct link
161 : Lnk =
i) AIBN/DMF/70 0C/2 d
180a
180b

(66)

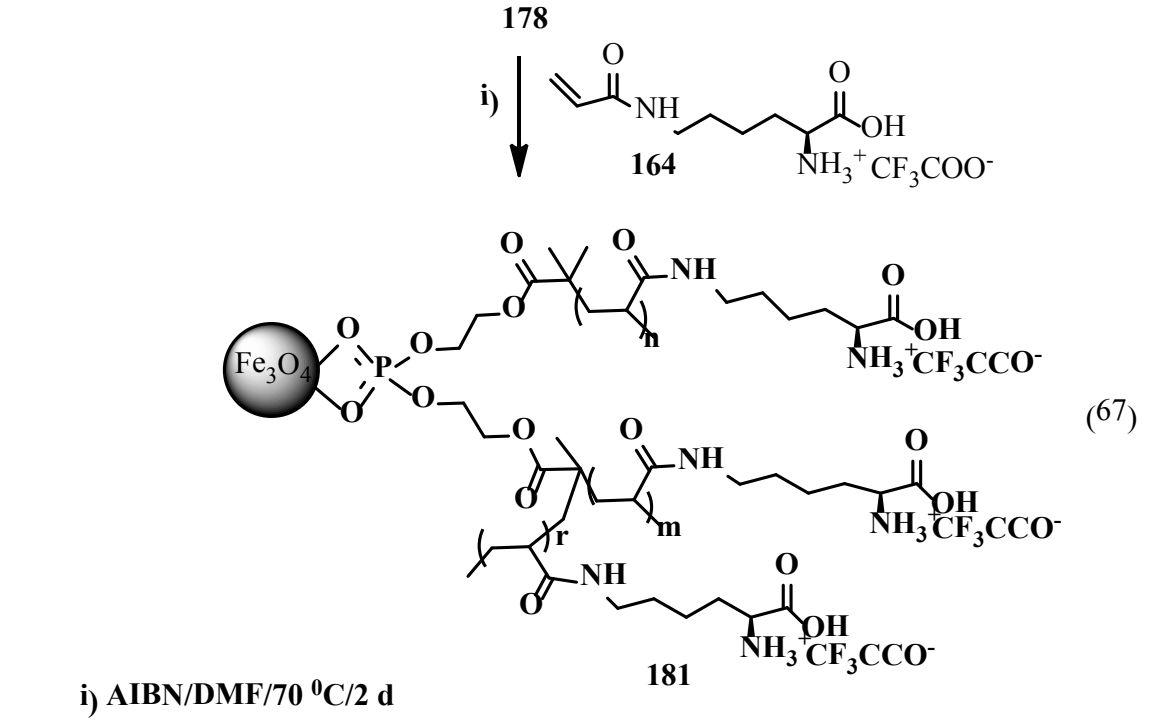
178
i)
164
181
i) AIBN/DMF/70 0C/2 d

(67)

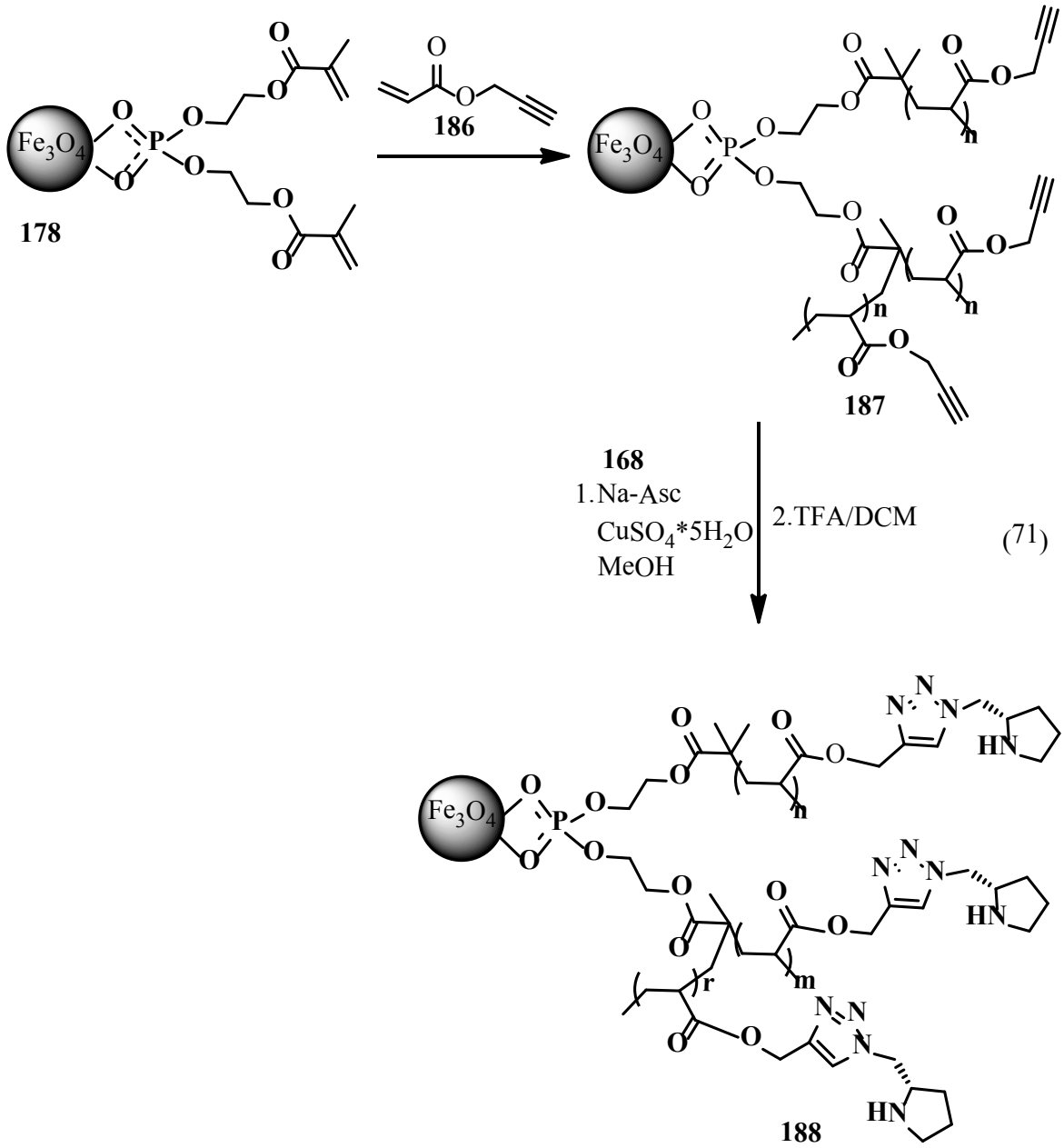

(71)

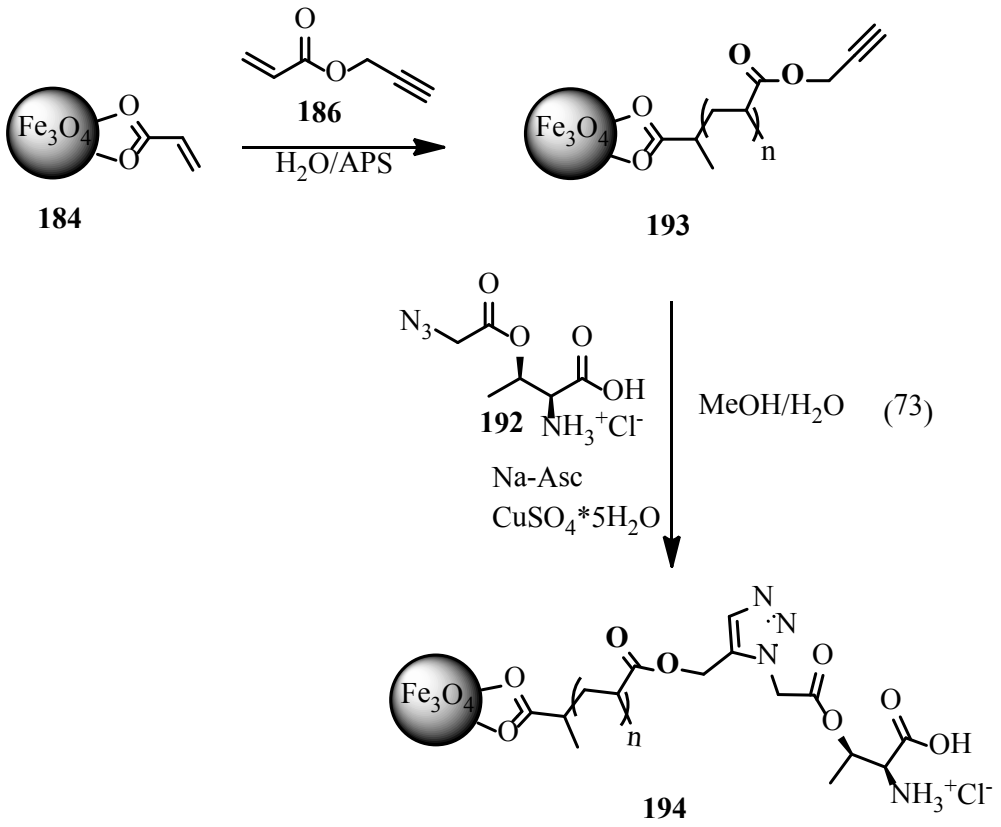

A wide range of methods was applied for characterization and analysis of the magnetite NP obtained in this thesis. These comprise FTIR, XPS, elemental analysis, TGA, VSM, DLS and TEM. The structures of precursors and components for the preparation of the core shell magnetite NP were confirmed by NMR-spectroscopy and mass spectrometry.

Part of the results presented in this thesis were already published in three peer-reviewed journals. A review article about organocatalysts supported by magnetic nanoparticles passed first revision at the RSC Advances journal.

4 Zusammenfassung

Magnetische Nanopartikel haben in letzter Zeit die Aufmerksamkeit als Nanocarrier oder Kontrastmittel für die MRT in der Medizin, in Trennprozessen sowie als Träger für Katalysatoren auf sich gezogen. In den meisten der aufgeführten Anwendungen müssen Magnetitnanopartikel funktionalisiert werden. Für solche Funktionalisierungen existiert eine große Anzahl an Möglichkeiten, und viele derselben wurden schon umgesetzt. Trotzdem besteht weiterhin ein großes Interesse daran, neue magnetische Nanopartikel zu entwickeln. Im Moment sind die meisten Anstrengungen darauf gerichtet, neue oder kombinierte Funktionalitäten, höhere Stabilität, Biokompatibilität, ein hohes magnetisches Moment, eine effizientere Synthese und Reduktion der Kosten zu erzielen. Im Rahmen dieser Dissertation wurden neue funktionalisierte magnetische Nanopartikel hergestellt, charakterisiert und schließlich als Organokatalysatoren eingesetzt.

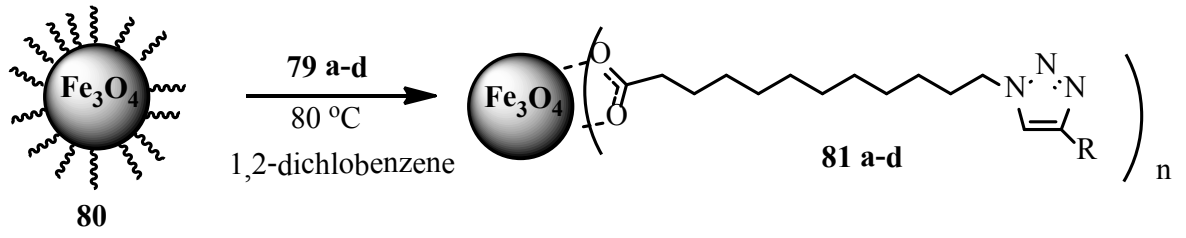

(26)

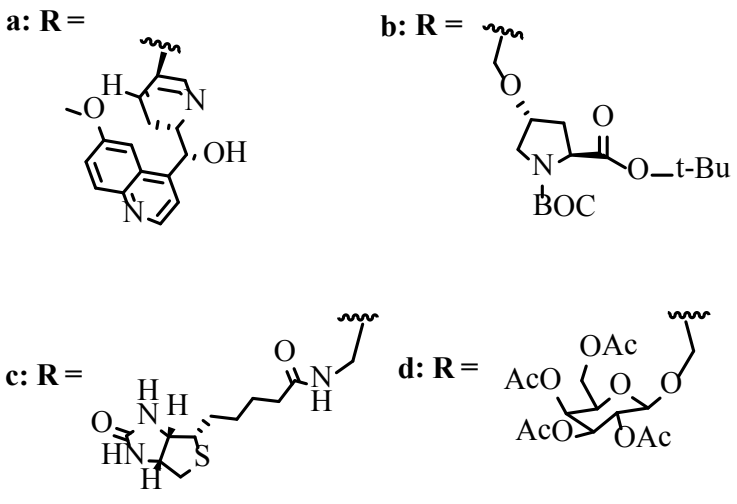

Die erste Art magnetischer Nanopartikel wurde durch eine Ligandenaustauschreaktion an den Magnetitnanopartikeln **80** erhalten. Diese waren ursprünglich mit einer Schicht Ölsäure stabilisiert, welche gegen bis dahin unbekannte Fettsäurederivate ausgetauscht wurden, die terminal funktionalisierte 1,2,3-Triazole enthielten. Letztere wurden durch Cu-katalysierte Alkin-Azid-Cycloaddition (CuAAC) von

12-Azidododekansäure **65** und verschiedenen Alkinpartnern - z. B. mit Chinin **68** (Organokatalysator), Prolin **72** (Organokatalysator), Biotin **75** (biologische Erkennungsfunktion) und Galactose **78** (Krebstherapie) funktionalisiert - in guten Ausbeuten (70-75%) in einem t-BuOH-H_2O-Gemisch mit $CuSO_4$*$5H_2O$/Na-Ascorbat als Katalysator erhalten. Durch den Einsatz dieser 12-Triazolyldodekansäuren **79a-d** in Ligandenaustauschreaktionen erhielt man die neuen Nanokomposite **81a-d**, in denen die ursprünglich enthaltene Ölsäure vollständig ersetzt wurde. Alle charakteristischen Peaks der neuen Liganden wurden im FTIR-Spektrum gefunden, wohingegen die der Ölsäure verschwanden. Die superparamagnetischen Eigenschaften der so erhaltenen Materialien sind wichtig für bestimmte Anwendungen wie beispielsweise die hyperthermische Krebsbehandlung oder magnetische Trennung. Mittels TEM wurde gefunden, dass die Nanopartikel fast kugelförmig mit einem Durchmesser von ca. 30 nm sind. Einige der verwendeten Liganden verhalfen den Nanopartikeln zu einer besseren Stabilität als Ölsäure. So bildeten z. B. NP **81b** und **81d** stabile kolloidale Suspensionen in organischen Lösungsmitteln, wie durch dynamische Lichtstreuung (DLS) gezeigt werden konnte. Als alternativer Zugang zu den Triazolyl-Fettsäure-stabilisierten magnetischen NP **84** wurde 11-Azidoundecansäure **83** via Ligandenaustausch an die MNP gebunden. Die damit entstehende azidofunktionalisierte magnetische Nanoplattform ist vielseitig einsetzbar. Zum Nachweis dessen wurden an die entstandenen MNP ein entsprechendes Alkin, welches Prolin bzw. einen Organokatalysator vom Hayashi-Typ enthält, mittels CuAAC gebunden, wobei die NP **90a** und **90b** erhalten wurden.

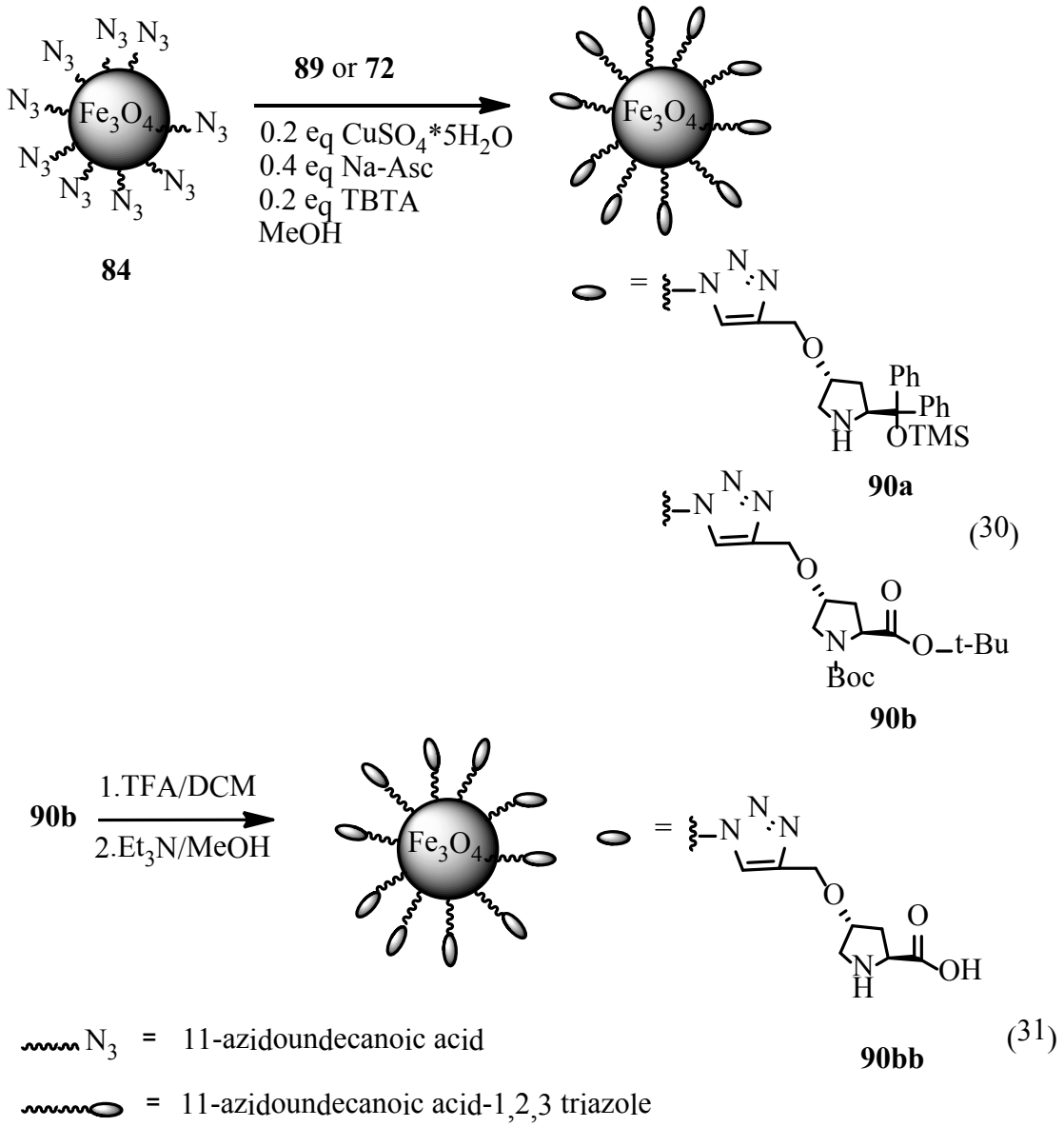

$\sim\sim\sim N_3$ = 11-azidoundecanoic acid

$\sim\sim\sim$ = 11-azidoundecanoic acid-1,2,3 triazole

Leider waren Versuche, diese zwei Magnetit-NP mit etablierten Organokatalysator-funkionalitäten in katalytischen Testreaktionen einzusetzen, nicht erfolgreich. Der Katalysator vom Hayashi-Typ war in der Michael-Reaktion zwischen Propionaldehyd und *trans*-β-Nitrostyren inaktiv; auch unter Veränderung der Reaktionsbedingngen (Lösungsmittel, erhöhte Menge an Katalysator) konnte kein Produkt erhalten werden. Die prolinfunktionalisierten MNP konnten die Aldolreaktion von Nitrobenzaldehyd und Cyclohexanon katalysieren, jedoch wurde ein racemisches Produkt erhalten. Dies könnte bedeuten, dass das Prolin nicht am Katalysezyklus beteiligt war, sondern eine Hintergrundreaktion stattgefunden hat.

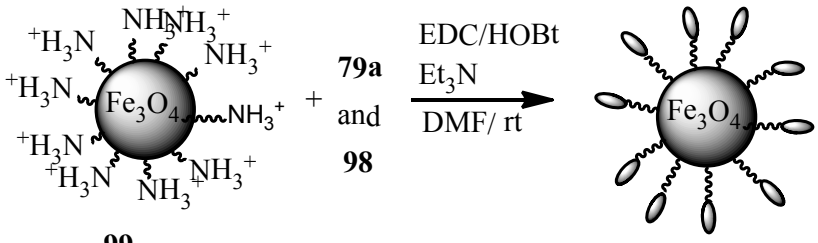

99

100a
100b

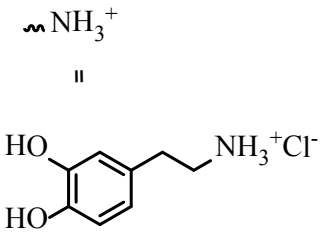

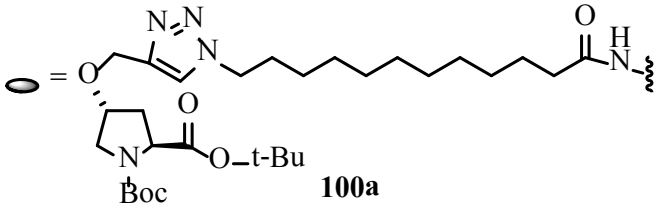

100a

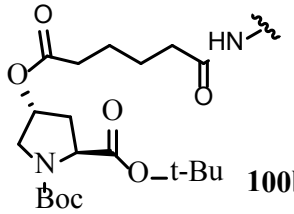

100b

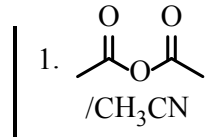

(38)

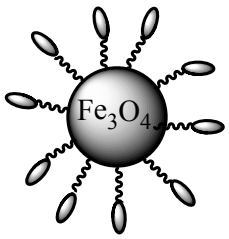

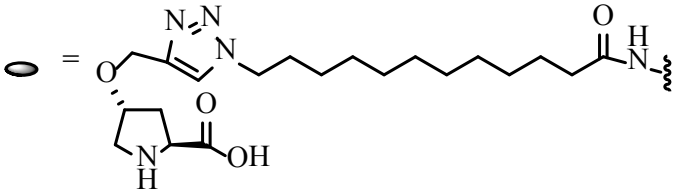

101a

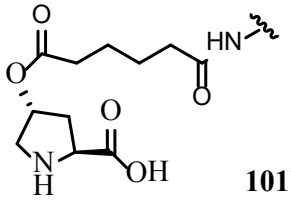

101b

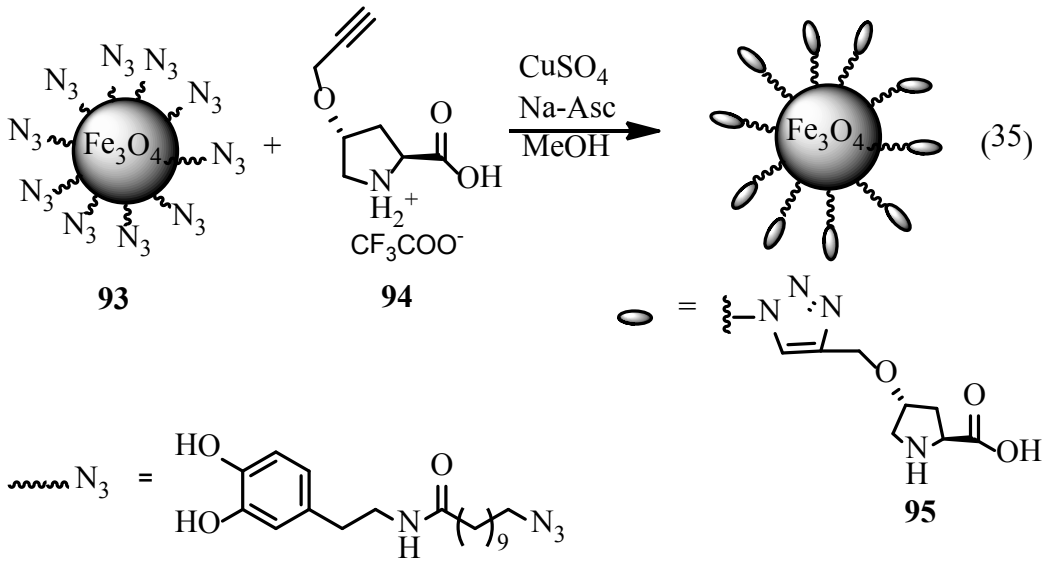

Es wurde ebenfalls eine weitere Art Nanopartikel erhalten, basierend auf funktionalisiertem Dopamin, einem biomimetischen Beschichtungsreagenz. Diese Nanopartikel wurden entweder mittels Ligandenaustauschreaktion aus einem Ferrofluid **80** mit neuen funktionalisierten Dopaminderivaten **92** oder in einer vielseitiger einsetzbaren Methode durch Amidbildung von Dopamin-stabilisierten Magnetit-NP **99** und Carbonsäuren **79a** und **98** hergestellt; es wurden die NP **100a** und **100b** erhalten (siehe Schema 38). In einem weiteren Ansatz wurde das Alkin-Prolin-Konjugat **94** mit Azid-funktionalisierten Dopamin MNP **93** in einer CuAAC gekoppelt. Durch diese Reaktionen wurden die Magnetit-NP **100a**, **100b** und **95** erhalten, an welche Prolin über verschiedene Linker geknüpft war. Die Beladung der NP **95** und **99** mit Prolingruppen war gering (0.05 mmol/g bis 0.09 mmol/g), wie durch den Pikrinsäuretest, der standardmäßig in der quantitativen Bestimmung von Aminogruppen auf Harzen eingesetzt wird, bestimmt wurde. Der Einsatz der prolinhaltigen MNP **95** in der Aldolreaktion zwischen 4-Nitrobenzaldehyd und Cyclohexanon ergab eine Ausbeute von 99% bei 36% ee unter Einsatz von 10 mol% Katalysator, was auf 46% ee (nur 77% Ausbeute) erhöht werden konnte, wenn Benzoesäure als Co-Katalysator eingesetzt wurde. Wurden Magnetit-NP **101a** in der Aldolreaktion zwischen 4-Nitrobenzaldehyd und Cyclohexanon eingesetzt, konnte das entsprechende Produkt in 68% Ausbeute bei einem ee von 52% erhalten werden. Hier ergab die Zugabe von Wasser und Benzoesäure zwar ebenfalls das Produkt, jedoch mit verringerten Ausbeuten bzw. Enantiomerenüberschüssen (35% Ausbeute und racemisches Produkt). Es wurde allerdings in 47% Ausbeute und 48% ee erhalten, wenn nur 10% Benzoesäure zugesetzt wurde. Magnetit-NP **101b** können die oben genannte

Aldolreaktion ebenfalls katalysieren. Das Produkt wurde bei Einsatz von 10 mol% Katalysator in 80 %iger Ausbeute mit moderaten 52% ee erhalten. Wurde hier Benzoesäure zugesetzt, verringerte sich die Ausbeute auf 55%, während der Eanantiomerenüberschuss leicht auf 55% stieg. Interessanterweise wurde in allen Fällen das *syn*-Diastereomer anstelle des erwarteten *anti*-Isomers gebildet. Die Dominanz des *syn*-Produktes könnte bedeuten, dass nicht immer Prolin, welches normalerweise das *anti*-Produkt bildet, der eigentliche Katalysator ist, sondern ebenfalls Nebenreaktionen auftraten. Wahrscheinlich waren unbeschichtete Magnetit-Nanopartikel an diesen Nebenreaktionen beteiligt. Bei der praktischen Durchführung der Reaktion gab es ebenfalls Probleme, da eine große Menge an Partikeln wegen der geringen Beladung benötigt wurde. Dies brachte Probleme beim Rühren mit sich, so dass die Reagenzien wahrscheinlich schlecht mit dem Katalysator in Kontakt kamen.

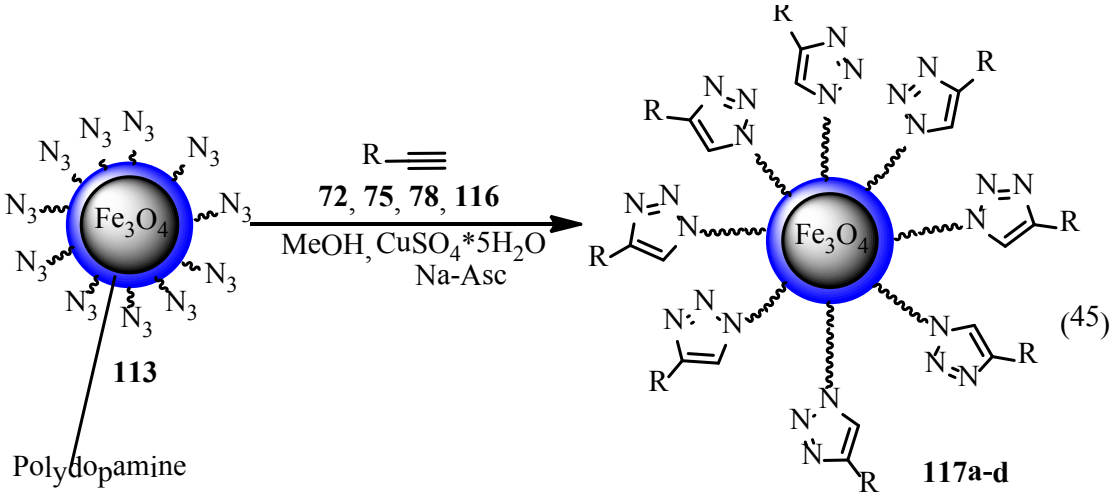

(45)

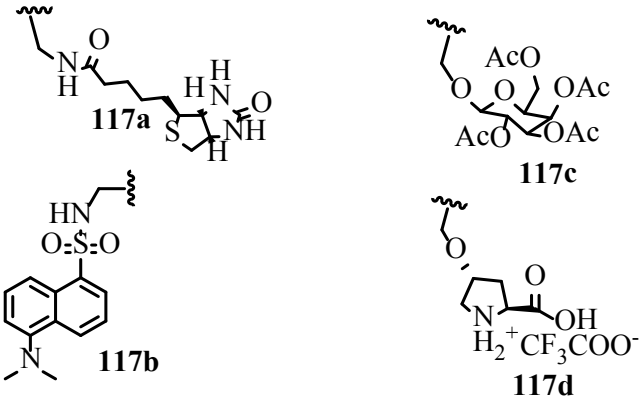

Eine dritte Klasse neuer magnetischer Nanopartikel wurde durch die Verwendung von verschiedenen Polymeren als Hülle erhalten. Das Reaktionspotenzial der Polydopamin-beschichteten Magnetit-NP **112** wurde auf eine neue Art und Weise genutzt, indem Azid-Gruppen durch Addition von 4-Azidobutylamin an die Hülle eingeführt

wurden (**113**). Diese bieten die Möglichkeit, ein großes Ausmaß an späteren Funktionalisierungen durch die CuAAC-Reaktion zu erreichen. Um das Prinzip zu verdeutlichen, wurden verschiedene Moleküle mit Alkin- sowie Prolin- **72**, Galactose- **78**, Biotin- **75** oder Dansylgruppen **116** auf diese Art eingeführt, womit vier neue Arten von magnetischen Nanopartikeln **117a-d** hergestellt wurden, welche interessante biologische bzw. katalytische Funktionen haben. Einige der Azidogruppen bleiben bei der CuAAC unverändert, sogar wenn Ultraschall während der Reaktion eingesetzt wurde. Dies wurde sowohl in FTIR- als auch in XPS-Spektren beobachtet.

Ein anderer neuer Weg, die Funktionalität von Polydopamin-Hüllen von MNP zu erweitern wurde durch die Einführung von Alkoholgruppen mittels 5-Amino-1-pentanol erzielt. Mithilfe dieser Funktionalität wurde eine Ringöffnungspolymerisation (ROP) von Lactid, dem „Milchsäure-Dimer“, durchgeführt, wobei man Polymilchsäuren erhielt. Als Resultat wurden neue wichtige Magnetit-NP **119** erhalten, die mit einem biokompatiblen und bioabbaubaren Polymer bedeckt sind. Die endständigen Hydroxylgruppen der Polymilchsäure wurden benutzt, um Biotin als wichtige biologische Erkennungsfunktion zu binden, wodurch diese NP **120** noch attraktiver für bestimmte medizinische Anwendungen werden.

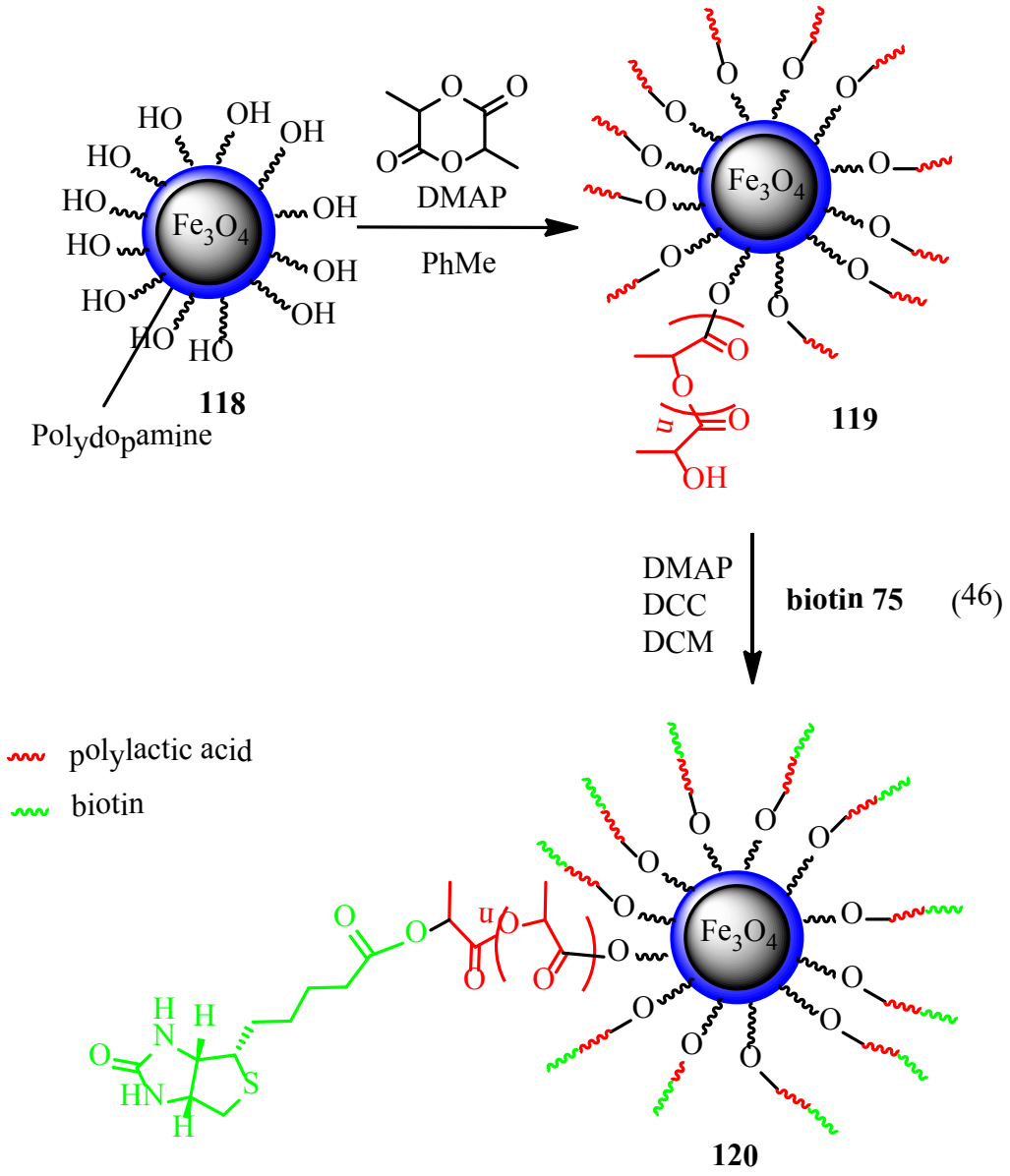

Beobachtungen mit ssNMR der Polydopamin-bedeckten MNP **112** zusammen mit Ergebnissen aus dem XPS (es wurde nur eine Art von Stickstoffatom gefunden) führten dazu, dass wir die intensiv diskutierten Strukturen von Polydopamin überdachten. Ergebnissen von weiterführenden ssNMR-Experimenten und detaillierten MS-Studien folgend wurde eine neue Polydopamin-Struktur (**132**) vorgeschlagen, bei welcher Indoleinheiten mit variablem Hydrogenierungsgrad kovalent gebunden sind und auch einige offenkettige Dopamineinheiten enthalten sind.

PDA-beschichtete Magnetit-NP **112** wurden als Träger für Cystein benutzt, indem Cystein direkt mit den Nanopartikeln reagiert, wobei die Magnetit-NP **135** entstehen. Diese NP **135** sowie die vorher beschriebenen mit Prolin versehenen Magnetitnanopartikel

117d wurden als Katalysatoren in der Aldolreaktion getestet. Die Cystein enthaltenden MNP **135** ergaben das Aldolprodukt in moderater Ausbeute als Racemat, während die mit Prolin modifizierten MNP **117d** zu keiner Reaktion führten.

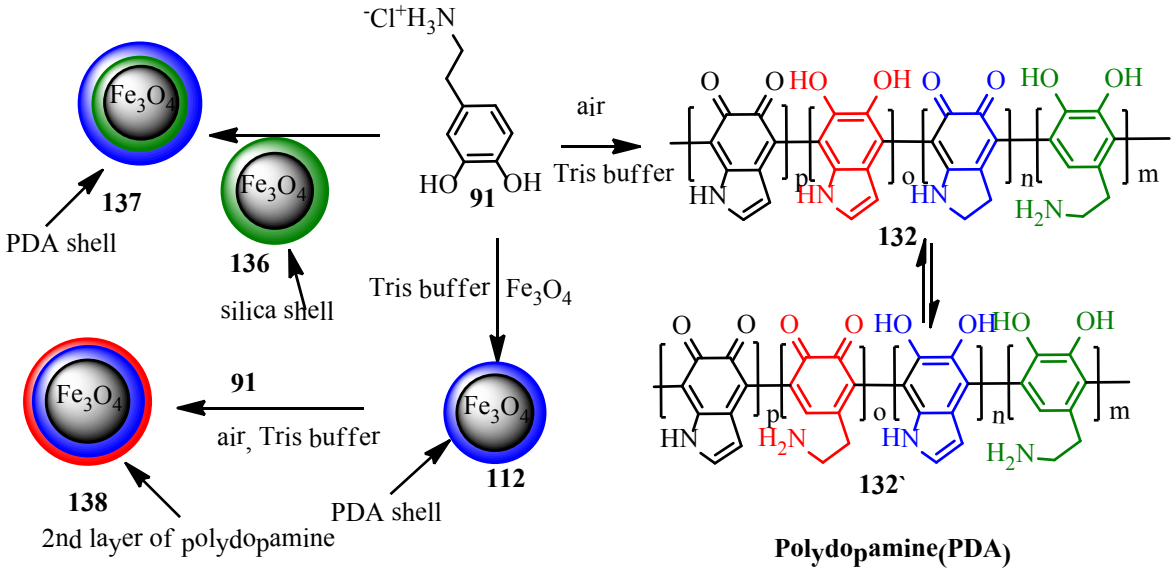

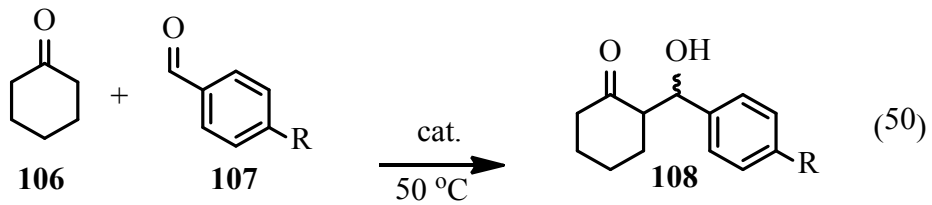

(50)

108	R
a	NO_2
b	Br
c	H
d	OMe

Diese Beobachtungen, verbunden mit den strukturellen Untersuchungen von Polydopamin, führten dazu, dass eine Hintergrundreaktion in Erwägung gezogen wurde. Um diese Vermutung zu überprüfen wurde reines Polydopamin hergestellt. In der Aldolreaktion zwischen 4-Nitrobenzaldehyd und Cyclohexanon konnte mit diesem Katalysator tatsächlich eine Reaktion festgestellt warden, die Ausbeuten lagen zwischen 93 und 75%. PDA konnte viermal wiederverwendet warden, es verlor allerdings nach dem ersten Durchlauf an katalytischer Aktivität. Für die nächsten drei Durchläufe blieb die Aktivität jedoch konstant. Magnetit-NP **138**, welche mit PDA bedeckt waren, was für eine

leichte Abtrennung durch magnetisches Dekantieren sorgt, konnten diese Reaktion ebenfalls katalysieren, sie verloren allerdings mit jedem Durchgang an Aktivität. Magnetit-NP (**136**), welche mit Silica bedeckt waren, wrden ebenfalls als magnetischer Träger für Polydopamin benutzt (**137**). Auch hier wurde eine katalytische Aktivität bei der Aldolreaktion festgestellt. Dieses System verlor jedoch seine Aktivität komplett nach zwei Durchgängen.

Durch Variation der Arylaldehyde in der Aldolreaktion mit Cyclohexanon unter Katalyse mit PDA-beschichteten MNP **138** konnte gezeigt werden, dass elektronenziehende Gruppen im Aldehyd präsent sein müssen; Aldehyde mit elektronenschiebenden Gruppen er-gaben keine Reaktion. Zwei Faktoren wurden gefunden, die vermutlich das Phänomen der Deaktivierung hervorrufen. Zum einen konnte durch Elementaranalyse gezeigt werden, dass ein mechanischer Verlust an Polymer (und damit an katalytischen Einheiten) auftritt. Zweitens wird 4-Nitrobenzaldehyd durch Imin-Bildung irreversibel in das Polymer eingebaut, womit ein Teil der katalytisch aktiven Amingruppen blockiert wird, wie durch XPS und FTIR-Untersuchungen gezeigt wurde, die die Präsenz von Nitrogruppen in den MNP nach Aldolreaktion zeigen.

Weiterhin wurden die Magnetit-NP **138**, beschichtet mit PDA, als Katalysator in der Knoevenagelreaktion zwischen Benzaldehyd und Malonsäuredinitril getestet. Hier konnte der Katalysator in fünf aufeinanderfolgenden Zyklen eingesetzt werden, ohne dass ein signifikanter Verlust an Aktivität zu bemerken war. Es wurde auch keine Abhängigkeit von Substituenten des Benzaldehyds festgestellt.

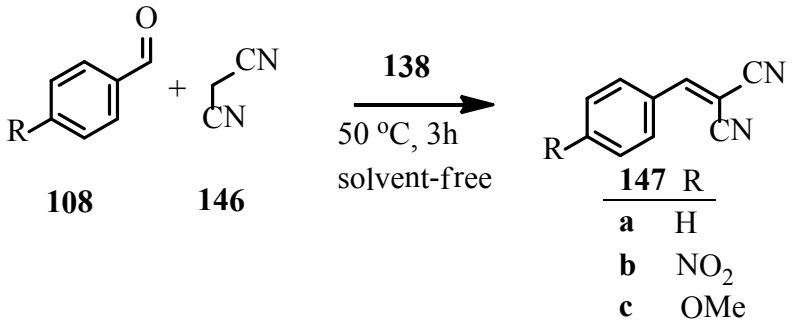

108 **146** **147** R

a H

b NO_2

c OMe

(52)

Entgegen früherer Literaturangaben hatten wir Erfolg darin, PDA-bedeckte MNP direkt mit Lactid in einer ROP umzusetzen, indem die Nucleophilie der Aminogruppe in PDA sowie freier Phenolgruppen ausgenutzt wurde. Dies stellt einen sehr einfachen Weg dar, um PLA-bedeckte Magnetit-NP für potenzielle Anwendungen in der Medizin zu erhalten.

Da PDA dafür bekannt ist, fast jede Art Oberfläche zu bedecken, benutzten wir es ebenfalls für Silica-beschichtete Magnetit-NP (**136**) sowie Kohlenstoff-beschichtete Eisennanopartikel (**149**) als primäre Hülle für die oberflächeninitiirte Ringöffnungspolymerisation von Lactid. Erstere sind sehr robuste und kommerziell erhältliche magnetische NP, weshalb die letztendlich erhaltenen PLA-bedeckten Core-Shell-Strukturen besonders in der Medizin wegen ihrer biokompatiblen Oberfläche attraktiv werden. Die Beschichtung war erfolgreich und gibt somit einen guten Zugang zu den MNP **151** sowie **152**. Diese Methodik kann ebenfalls auf verschiedene andere nichtmagnetische Materialien angewendet werden, um sie biokompatibel zu machen, wie im Allgemeinen Teil dieser Arbeit mit Aluminiumoxid (**153**) gezeigt wurde.

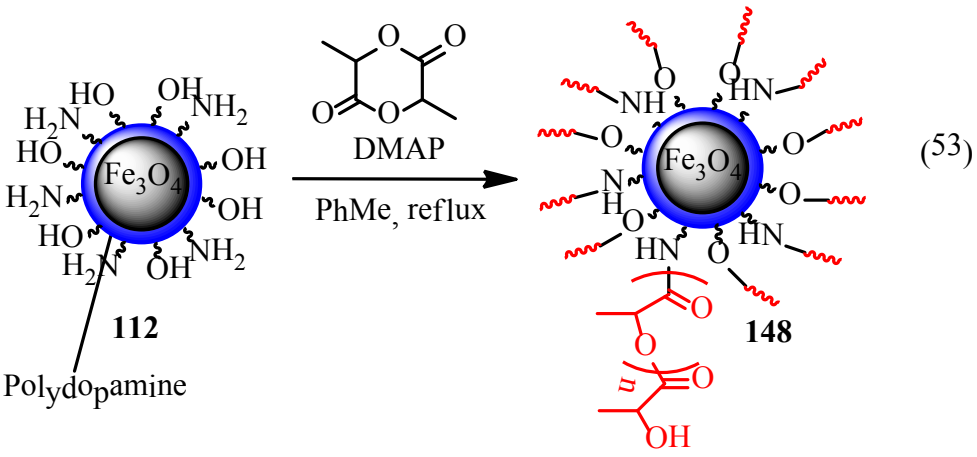

(53)

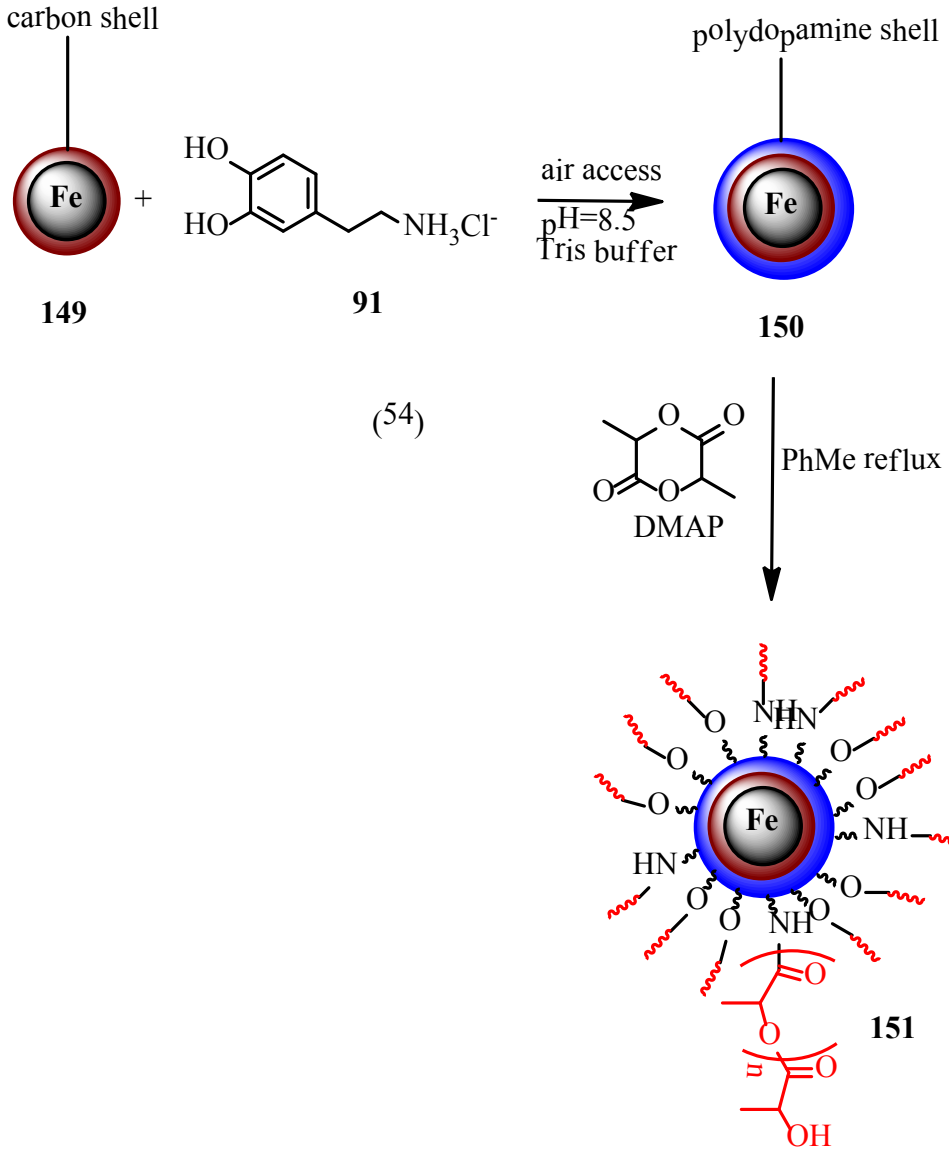
carbon shell
Fe
149
HO
HO
NH3Cl-
91
air access
pH=8.5
Tris buffer
polydopamine shell
Fe
150
(54)
O
O
O
O
DMAP
PhMe reflux
Fe
NH
HN
O
151
OH
n

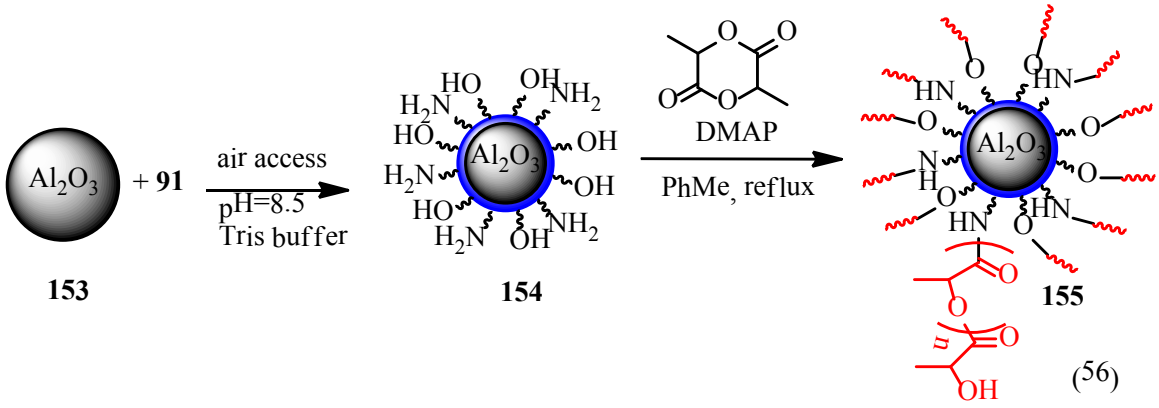
Al2O3
+ 91
153
air access
pH=8.5
Tris buffer
HO
OH
NH2
H2N
OH
154
DMAP
PhMe, reflux
HN
O
N
H
155
OH
n
(56)

Beide Eigenschaften, die katalytische Aktivität in Knoevenagel- und Aldolreaktionen einerseits und die oberflächeninitiierte ROP von Polymilchsäure andererseit stellen einen weiteren Durchbruch in der Demonstration der Vielseitigkeit von PDA als leicht zugängliches Beschichtungs- und Funktionalisierungsmaterial dar.

Im letzten Teil dieser Arbeit wurden die Synthese und physikalische Charakterisierung von MNP mit funktionalisierten Polyacrylaten präsentiert. Neue Acrylsäure- und Methacrylsäurederivate von Threonin (**157**, **158** und **161**), Lysin (**164**) und Prolin (**175**, **176** und **177**) wurden hergestellt und später in Gegenwart von Magnetit-NP **178**, welche mit acrylfunktionalisierten Phosphaten beschichtet waren, polymerisiert. Dadurch wurden diese Aminosäuren auf den MNP immobilisiert (**179**, **180a**, **180b**, **181**, **182a**, **182b**, **183** und **185**). Ein weiterer Ansatz, um Magnetit-NP, beschichtet mit aminosäurefunktionalisierten Polyacrylaten, herzustellen, basierte auf einer Zwei-Stufen-Synthese. Die Magnetit-NP wurden mit Propargylgruppen ausgestattet, indem zunächst Acrylsäurepropargylester in Anwesenheit von Magnetit-NP **178** bzw. **184** (stabilisiert mit Acrylsäure) polymerisiert wurde, um MNP **187** und **193** zu erhalten. Danach ergab eine CuAAC-Reaktion mit Azidoprolinderivat **168** oder dem neuen Azidothreonin **192** die Magnetitnanopartikel **188** und **194**, in welchen diese Aminosäuren durch ein 1,2,3-Triazol an die Partikel gebunden wurden.

Überraschenderweise waren fast alle diese Katalysatoren ineffektiv sowohl in Aldol- als auch Michaelreaktionen. Verschiedene Reaktionsparameter wie z.B. Lösungsmittel, Katalysatormenge oder Zusätze wurden verändert, dies half jedoch nicht, die Reaktion zu verbessern. Etwas bessere Ergebnisse wurden gefunden, als die Prolin-tragenden Nanopartikel **188**, welche durch einen grafting-to-Ansatz erhalten wurden, in der Michaelreaktion von *trans*-β-Nitrostyrol und Cyclohexanon eingestzt wurden. Dieser Katalysator war in der Lage, das Produkt in 30%iger Ausbeute mit einem guten ee von 86% zu erzeugen, die katalytische Aktivität ging jedoch nach Recycling stark nach unten. Ein ähnliches Verhalten wurde bei den Magnetit-NP **183** beobachtet, welche Prolineinheiten trugen, die durch direkte Polymerisierung an die Magnetit-NP angebracht worden waren. Diese katalysierten die Michaeladdition mit guter Ausbeute und einem ausgezeichneten ee von 92%, in folgenden Durchläufen wurde allerdings kein Produkt erhalten.

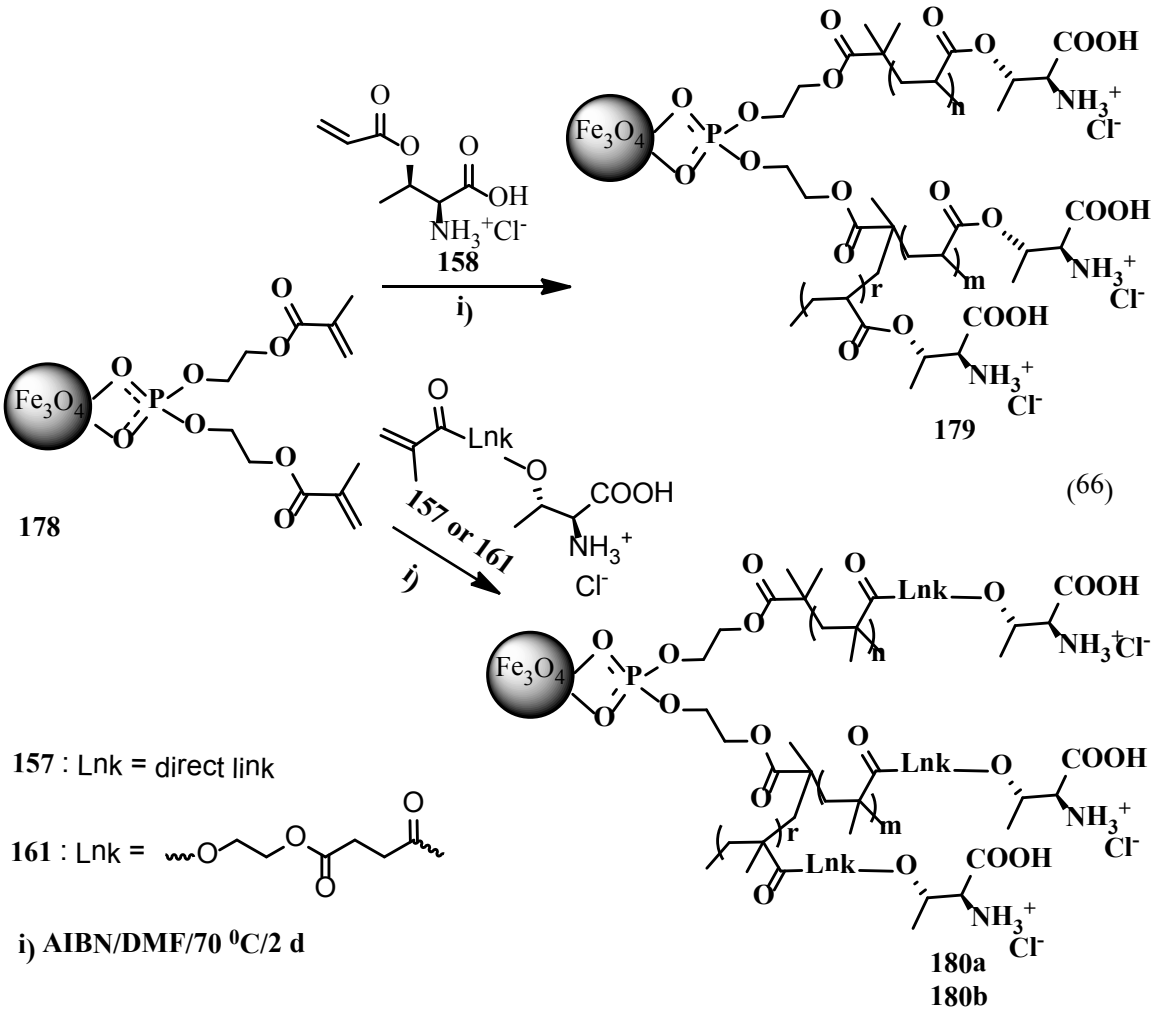
158
i)
178
179
157 or 161
i)
157 : Lnk = direct link
161 : Lnk =
i) AIBN/DMF/70 0C/2 d
180a
180b

(66)

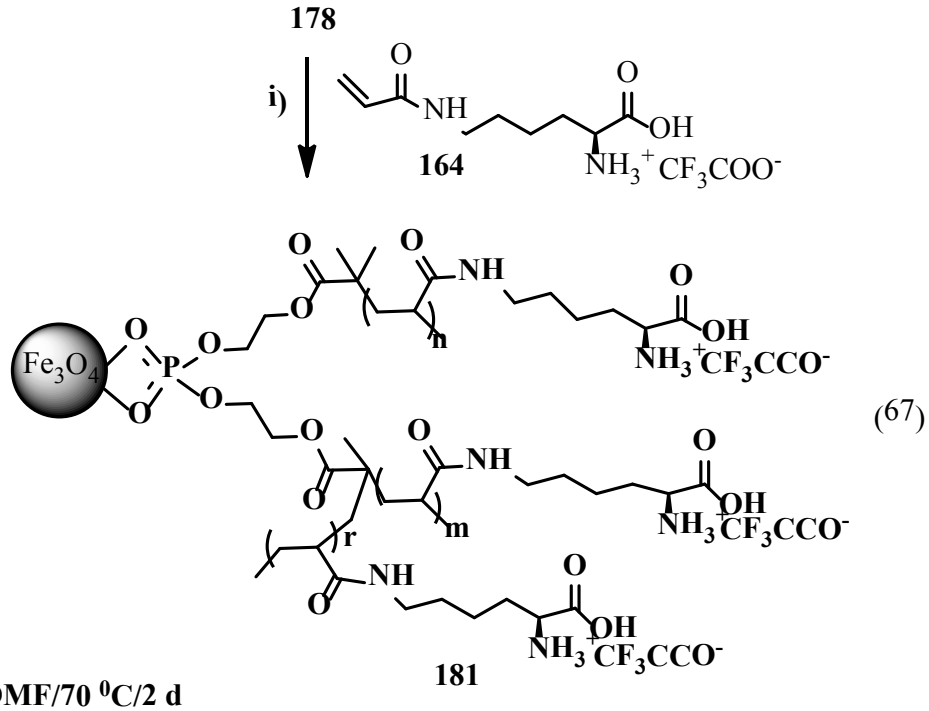
178
i)
164
181
i) AIBN/DMF/70 0C/2 d

(67)

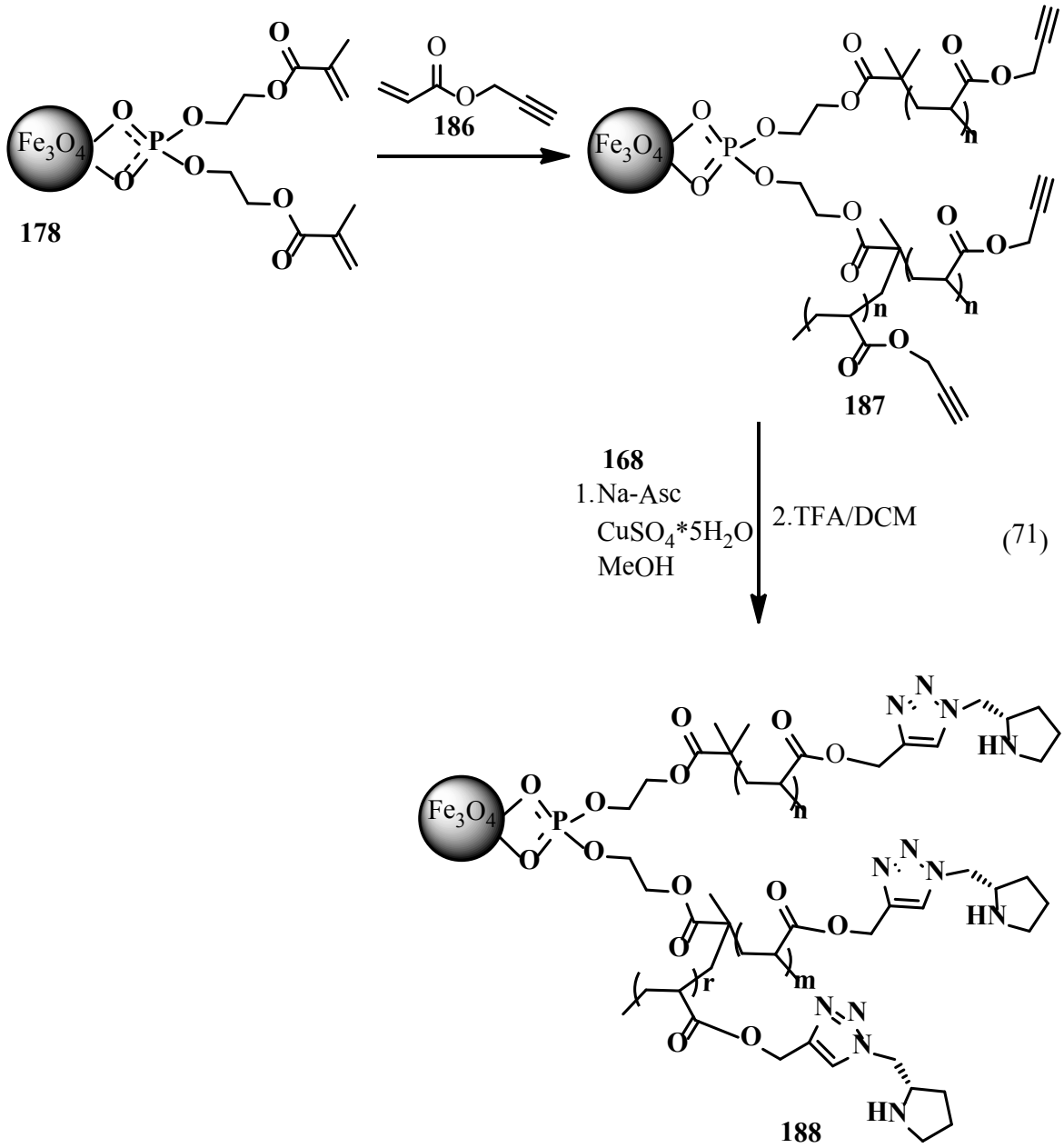

(71)

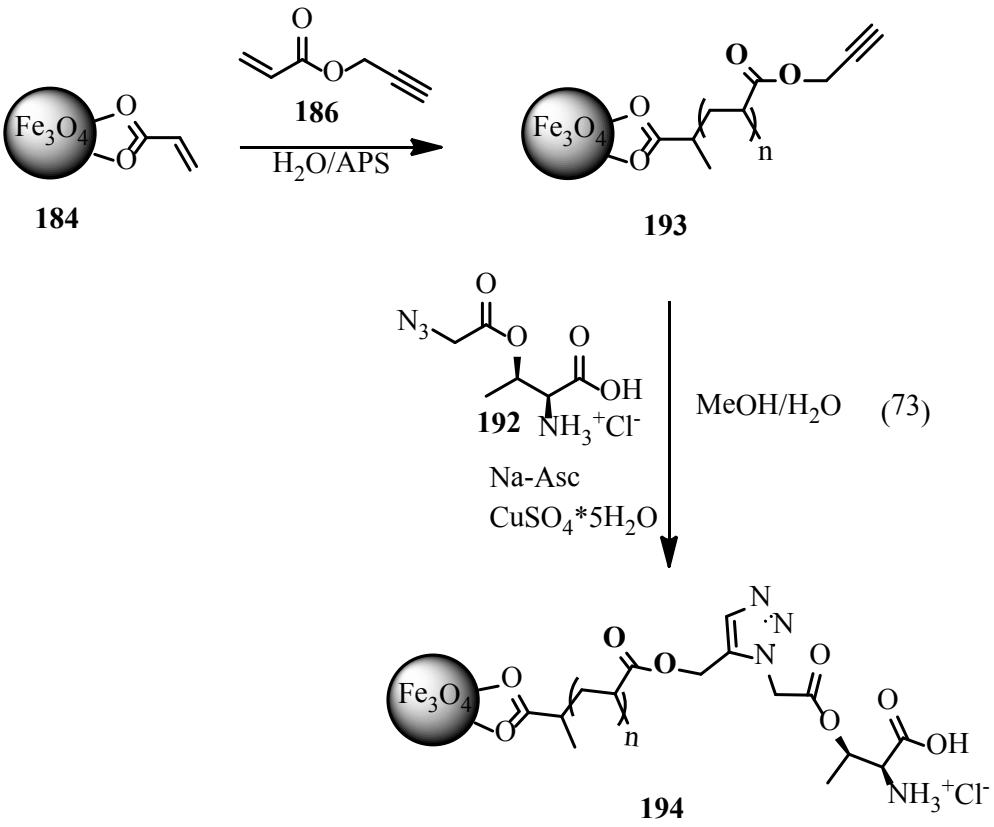

Teile der Ergebnisse, die in dieser Arbeit vorgestellt werden, sind in drei Zeitschriften veröffentlicht worden. Weiterhin bestand ein Reviewartikel über Organokatalysatoren mit magnetischen Nanopartikeln als Trägermaterial erfolgreich die erste Korrektur bei der Zeitschrift RSC Advances.

5 Experimental part

General Experimental Conditions

Solvents

THF was dried over anhydrous KOH for several days and was distilled three times under argon atmosphere over pressed sodium and benzophenone.

CH_2Cl_2 was refluxed for several hours over anhydrous phosphorus pentoxide or calcium hydride and was distilled under argon.

Dry DMF was purchased from Alfa Aesar. Solvent was taken under argon protective atmosphere and use without further purification

DMSO was used in delivered state

MeOH and **EtOH** were distilled over magnesium

Reagents and Chemicals were purchased from Acros, Aldrich, Fluka, Merck and Alfa Aesar. All commercially available reagents were used without further purification.

Argon gas was used as a protective gas for moisture or air sensitive reactions.

Chromatography

TLC: Silica gel 60 aluminium plates with fluorescent indicator UV-F 254 from Merck were used with the following reagents:
1) 254 nm or 320 nm **UV light** was used for UV active substances.
2) **Seebach reagent**: A mixture of 1.0 g $Ce(SO_4)_2$ 4H2O and 2.5 g $(NH_4)_6Mo_7O_{24}$. $4H_2O$ in 100 ml of 1.8 M H_2SO_4
3) **Permanganate reagent**: A mixture of 3.0 g $KMnO_4$, 20.0 g of K_2CO_3 and 5 ml 5 % NaOH in 300 ml H_2O.

Column: Silica gel 60 (40-63 μ m) from Merck

HPLC: The analytical HPLC chromatographic equipment was used under the following terms and conditions:

Chiral HPLC: High Pressure gradient system 322 (Kontron), UV-Detector DAD K-2800 (Knauer), Chiral Detector IBZ Messtechnik, Injection valve 7125 (10 μL, Rheodyne), Different Chiral Columns (Daicel Chemical Industries LTD), mobile phase: *n*-hexane : *i*-Propanol (98:20 - 80:20).flow rate: 0.5 - 1.0 ml / min

Physical data

1. Nuclear magnetic resonance spectroscopy: ^{1}H and ^{13}C NMR spectra were recorded on a 500 MHz Bruker Avance III spectrometer; chemical shifts (δ) are reported in ppm relative to TMS.

^{1}H solid-state (^{1}H ss)NMR spectra were obtained on a Bruker Avance III 600 MHz NMR spectrometer (Bruker Biospin, Rheinstetten, Germany). A 4 mm double-resonance MAS probe was used in MAS NMR spectroscopy. To obtain the 1H MAS NMR spectrum, PDA was dissolved in D_2O/DMSO-d_6 and was used to fill a disposable insert (Bruker Biospin). A MAS frequency of 5000 Hz was applied. The liquid-state 1H NMR spectrum of PDA in TFA-d solution was measured on a 5 mm TXI probe head with a z gradient using a standard watergate W5 sequence for solvent suppression.29 The 90° 1H pulse was 13.75 μs. All spectra were measured at 303 K.

^{13}C solid-state (^{13}C ss) NMR spectra were acquired by using two distinct experimental setups. One corresponds to a standard CP-MAS experiment, whereas for the other the so-called cross-polarization polarization-inversion (CPPI) experimental setup was employed. The ^{13}C ss-NMR spectra were recorded at a 125.73 MHz Larmor frequency with a Bruker AVANCE III 500 spectrometer operating at room temperature. Contact pulses of 2 ms and 50 μs were considered for direct CP, whereas the polarization inversion (PI) time τ_{inv} was adjusted for the complete depolarization of aromatic CH carbons. Both spectra were acquired under high-power proton decoupling (100 kHz) by using the two-pulse phase-modulation (TPPM) sequence. To get a reasonable S/N ratio, 60 000 transients were averaged with a recycle delay of 1 s. Calibration was carried out with respect to the CH_3 line in TMS (tetramethylsilane), through an indirect procedure that uses the carbonyl ^{13}C line (176.5 ppm) of ß-glycine as an external reference.

2.FTIR: FT-IR spectra were carried out on a JASCO FTIR 610 spectrophotometer in KBr pallets (for magnetite nanoparticles).

3. Magnetic measurements: magnetic measurements were performed at room temperature using a Vibrating Sample Magnetometer Cryogenics

4. Transmission electron microscopy: 1010 JEOL electron microscope was used to determine particles morphology

5. Elemental analysis: Thermo Scientific FlashEA 1112, with a TCD detector was used for elemental analysis

6. Dynamic light scattering: DLS measurements were carried out with a Zeta sizer NanoZS Malvern Instruments device working in backscattering mode

7. Melting points: Melting points were measured on Schorpp Gerätetechnik MPM-H2

8. Mass spectrometry: High-resolution mass spectra (HRMS) were recorded on an LTQ ORBITRAP XL mass spectrometer (ThermoScientific) using positive ion mode electrospray (ES+) ionization. The instrument was externally calibrated according to the manufacturer's recommendations. The samples were introduced into the spectrometer by direct infusion at a flow rate of 5 μL/min. The conditions used were as follows: spray voltage, 5 kV; sheath and auxiliary gas flow, 35 and 7 arbitrary units, respectively; capillary temperature, 275 °C; capillary voltage, 45 V; and tube lens voltage, +250 V. The number of microscans was set to three in all experiments. (Polydopamine analysis)

9. X-Ray Photoelectron Spectroscopy: XPS spectra were recorded using an XPS spectrometer SPECS equipped with a dual-anode X-ray source Al/Mg, a PHOIBOS 150 2D CCD hemispherical energy analyzer and a multi-channeltron detector with vacuum maintained at 1 x10^{-}9 torr. The AlKKa X-ray source (1486.6 eV) operated at 200 W was used for XPS investigations. The XPS survey spectra were recorded at 30 eV pass energy, 0.5 eV/step. The high resolution spectra for individual elements were recorded by accumulating 10e15 scans at 30 eV pass energy and 0.1 eV/step. The powdered sample was pressed on an indium foil to allow the XPS measurements. A cleaning of the samples surface was performed by argon ion bombardment (500 V). Data analysis and curve fitting were performed using Casa XPS software with a Gaussian Lorentzian product function and a non-linear Shirley background subtraction.

5.1 Experimental Procedures

12-azidododecanoic acid 65

Product obtained according to reported protocol.[211] Yield 0.835 g (3.46 mmol, 96 %)

^{1}H-NMR ($CDCl_3$, 500 MHz) δ = 1.26-1.64 (m, 18H, C$\underline{H}_2$), 2.35 (t, 2H, J^1 = 7.5 Hz, C$\underline{H}_2$-N_3), 3.25 (t, 2H, J^1 = 6.9Hz, C$\underline{H}_2$-COOH)

^{13}C-NMR ($CDCl_3$, 125 MHz): δ = 24.6 ($\underline{C}H_2$-CH_2-COOH), 26.6 ($\underline{C}H_2$-CH_2-N_3), 27.1-29.4 ($\underline{C}H_2$), 34.0 ($\underline{C}H_2$-COOH), 51.4 ($\underline{C}H_2$-N_3), 180.4 ($\underline{C}$=O)

(1*R*)-(2*S*,4*S*,5*S*)-5-ethynylquinuclidin-2-yl)(6-methoxyquinolin-4-yl)methanol 68

Product was obtained according to reported protocol.[213] Product Yield 2.4 g (7.45 mmol, 40 %)

^{1}H-NMR ($CDCl_3$, 500 MHz): δ = 1.44 (m, 1H, C$\underline{H}_{ring}$); 1.73–1.67 (m, 2H, C$\underline{H}_{ring}$), 1.92 (m, 1H, C$\underline{H}_{ring}$), 1.96 (d, J^1 = 2.5 Hz, 1H, C$\underline{H}_{ring}$), 2.04 (m, 1H, C$\underline{H}_{ring}$), 2.52 (m, 1H, C$\underline{H}_{ring}$), 2.65 (m, 1H, C$\underline{H}_{ring}$), 2.90 (dt, 1H, J^1 = 13.4, J^2 = 6.3, J^3 = 3.5 Hz, C≡C$\underline{H}$), 3.19 (dd, 1H, J^1 = 13.4, J^2 = 10.1 Hz, C$\underline{H}_{ring}$), 3.43–3.36 (m, 2H, C$\underline{H}_{ring}$), 3.91 (s, 3H, OC$\underline{H}_3$), 5.53 (d, 1H, J^1 = 4.8 Hz, C$\underline{H}_2$-OH), 7.26 (d, 1H, J^1 = 2.8 Hz, C$\underline{H}_{arom.}$), 7.34 (dd, 1H, J^1 = 9.1, J^2 = 2.8 Hz, C$\underline{H}_{arom.}$), 7.49 (d, 1H, J^1 = 4.6, Hz, C$\underline{H}_{arom.}$), 7.99 (d, 1H, J^1 = 9.3 Hz, C$\underline{H}_{arom.}$), 8.65 (d,1H, J^1 = 4.5 Hz, C$\underline{H}_{arom.}$)

^{13}C-NMR ($CDCl_3$, 125 MHz): δ = 22.8 (CH_{ring}), 26.6 (CH_{ring}), 27.5 (CH_{ring}), 28.00 (CH_{ring}), 43.1 (CH_{ring}), 56.1 (O$\underline{C}H_3$), 58.4 (CH_{ring}), 59.9 (CH_{ring}), 69.2 (C≡$\underline{C}$H), 72.4 ($\underline{C}H_2$-OH), 88.1 ($\underline{C}$≡CH), 101.8 ($\underline{C}H_{arom,}$), 118.9 ($\underline{C}H_{arom,}$), 122.1 ($\underline{C}H_{arom,}$), 127.1 ($\underline{C}H_{arom,}$), 132.0 ($\underline{C}H_{arom,}$), 144.7 ($\underline{C}H_{arom,}$), 147.7 ($\underline{C}H_{arom,}$), 147.9 ($\underline{C}H_{arom,}$), 158.1 ($\underline{C}H_{arom,}$)

(2*S*,4*R*)-tert-butyl 1-(1-(tert-butoxy)vinyl)-4-(prop-2-yn-1-yloxy)pyrrolidine-2-carboxylate 72

Product was obtained according to reported protocol.[212]Yield after last step 1.645 g, (5 mmol, 75%)

^{1}H-NMR ($CDCl_3$, 500 MHz): δ = 1.45 (s, 18H, C<u>H</u>$_3$), 2.07 (m, 1H, C<u>H</u>$_{2Pro}$), 2.33 (m, 1H, C<u>H</u>$_{2Pro}$), 2.44 (t, 1H, J^1 = 2.33 Hz, C≡C<u>H</u>), 3.50 (m, 1H, C<u>H</u>$_2$-N$_{Pro}$), 3.62 (m, 1H, C<u>H</u>$_2$-N$_{Pro}$), 4.13 (m, 2H, C<u>H</u>$_2$-C≡CH), 4.24 (m, 2H, C<u>H</u>$_{Pro}$-O)

^{13}C-NMR ($CDCl_3$, 125 MHz): δ = 28.0 (CH_3), 28.3 (CH_3), 36.6 (CH_2), 51.0 (CH_2), 56.4 (CH), 58.5(CH_2), 74.7 (≡CH), 75.6 (≡C), 79.2 (CH), 80.1 (C), 81.2 (C), 153.9, (C=O), 172.0 (C=O)

<u>*N*-(2-Propinyl)biotinamid 75</u>

Product synthesized according to reported protocol.[214] Yield 0.329 g (1.17 mmol, 90 %)

^{1}H-NMR (CD_3OD, 500 MHz): δ = 1.35 (m, 2H, CH_2-C<u>H</u>$_2$-CH_2), 1.57 (m, 4H, CH_2-C<u>H</u>$_2$-CH_2, CH $_{Biotin}$-CH_2-CH_2), 2.14 (t, 2H, J = 7.4, CH_2-C<u>H</u>$_2$-CONH), 2.50 (t, 1H, J = 2.6, CH_2-C≡C<u>H</u>), 2.61 (d, 1H, J = 12.8, CH $_{Biotin}$-C<u>H</u>$_2$-S), 2.83 (dd, 1H, J_1 = 4.9, J_2 = 12.7, CH $_{Biotin}$-C<u>H</u>$_2$-S), 3.22 (m, 1H, C<u>H</u> $_{Biotin}$-CH_2-CH_2), 3.86 (d, 2H, J = 2.5, C<u>H</u>$_2$-C≡CH), 4.41 (dd, 1H, J_1 = 4.5, J_2 = 7.9, NH $_{Biotin}$-C<u>H</u>-CH-S), 4.39 (dd, 1H, J_1 = 4.3, J_2 = 7.9, NH $_{Biotin}$-C<u>H</u>-CH_2-S).

^{13}C-NMR (CD_3OD, 125 MHz): δ = 26.7 (CH_2-<u>C</u>H$_2$-CH_2), 29.4 (CH $_{Biotin}$-<u>C</u>H$_2$-CH_2), 29.5 (<u>C</u>H$_2$-C≡CH), 29.8 (CH_2-<u>C</u>H$_2$-CH_2), 36.5 (CH_2-<u>C</u>H$_2$-CONH), 41.0 (CH $_{Biotin}$-<u>C</u>H$_2$-S), 57.0 (<u>C</u>H $_{Biotin}$-CH_2-CH_2), 61.6 (NH $_{Biotin}$-<u>C</u>H-CH_2-S), 63.4 (NH $_{Biotin}$-<u>C</u>H-CH-S), 72.2 (CH_2-C≡<u>C</u>H), 80.7 (C_q, CH_2-<u>C</u>≡CH), 166.2 (<u>C</u>=O), 175.8 (C=O).

<u>1-(2-Prop-1-inyl)-2,3,4,6-tetra-O-acetyl-β-D-galactopyanosid 78</u>

Product obtained according to reported protocol.[215] Yield 3.32 g (9.9 mmol, 80 %)

^{1}H-NMR ($CDCl_3$, 500 MHz): δ = 1.79 (s, 3H, CO-C<u>H</u>$_3$), 1.86 (s, 3H, CO-C<u>H</u>$_3$), 1.87 (s, 3H, CO-C<u>H</u>$_3$), 1.96 (s, 3H, CO-C<u>H</u>$_3$), 2.42 (t, 1H, J = 2.4, CH_2-C≡C<u>H</u>), 3.80 (dt, 1H, J_1 = 1.1, J^2 = J^3 = 6.6, C_5<u>H</u>-CH_2-OCO), 3.93-3.99 (m, 2H, C_5H-C<u>H</u>$_2$-OCO), 4.19 (d, 2H, J =

2.4, (C<u>H</u>$_2$- C≡CH), 4.58 (d, 1H, *J* = 7.9, C$_1$<u>H</u>-O-CH$_2$), 4.89 (dd, 1H, J$_1$ = 3.4, J$_2$ = 10.4, C$_3$<u>H</u>), 4.98 (dd, 1H, J^1 = 7.9, J^2 = 10.5, C$_2$<u>H</u>), 5.20 (dd, 1H, J$_1$ = 1.0, J$_2$ = 3.4, C$_4$<u>H</u>).

^{13}C-NMR (CDCl$_3$, 125 MHz): δ = 19.8 (CO-<u>C</u>H$_3$) 19.9 (2xCO-<u>C</u>H$_3$),20.0 (CO-<u>C</u>H$_3$), 52.2 (<u>C</u>H$_2$-C≡CH), 60.6 (CH-<u>C</u>H$_2$-OCO), 66.5 (<u>C</u>$_4$H), 67.9 (<u>C</u>$_2$H), 70.1 (<u>C</u>$_3$H), 70.2 (<u>C</u>$_5$H), 75.0 (CH$_2$-C≡<u>C</u>H), 77.7 (C$_q$, CH$_2$-<u>C</u>≡CH), 98.0 (<u>C$_1$</u>H-O-CH$_2$-C$_q$), 168.8(<u>C</u>=O), 169.3 (<u>C</u>=O), 169.6 (<u>C</u>=O), 169.7 (<u>C</u>=O).

*<u>General procedure for synthesis of functionalized fatty acids **79a-d**:</u>*

12-Azidododecanoic acid **65** (241 mg, 1 mmol) was mixed with alkyne **68**, **72**, **75**, **78** (1 mmol) and dissolved in mixture *t*-BuOH/H$_2$O (20 mL) (1:1) (**68**, **72**, **78**) or MeOH (20 mL) (**75**). CuSO$_4$*5H$_2$O (50 mg, 0.2 mmol, 0.2 equiv), Na-Asc (80 mg, 0.4 mmol, 0.4 equiv) and TBTA (106 mg, 0.2 mmol, 0.2 equiv) were added and the mixture was stirred for 24 h. DCM (20 mL) was added and the water phase was extracted three times with DCM (10 mL). The organic layers were combined, washed with water (20 mL) and brine (20 mL). Product **79** was obtained after column chromatography on silica gel. In case of **79c**, the product was precipitated after washing with H$_2$O. It was filtered off and washed with Et$_2$O a few times.

<u>12-(5-((2*S*,4*S*,8*R*)-2-((*R*)-hydroxy(6-methoxyquinolin-4-yl)methyl)quinuclidin-8-yl)-1H-1,2,3-triazol-1-yl)dodecanoic acid</u> <u>79a</u>

^{1}H-NMR (CD$_3$OD, 500 MHz): δ = 1.0-1.28 (m, 15H C<u>H</u>$_2$+C<u>H</u>$_{ring}$), 1.55 (q, 2H, C<u>H</u>$_2$-CH$_2$-COOH, J^1 = 7.1 Hz, J^2 = 14.5 Hz), 1.61-1.67 (m, 2H, C<u>H</u>$_{ring}$), 1.9-2.12 (s, 3H, C<u>H</u>$_{ring}$), 2.17 (m, 2H, C<u>H</u>$_{ring}$), 3.15 (dt, 1H, C<u>H</u>$_{ring}$, J^1 = 4.9 Hz, J^2 = 6.8 Hz, J^3 = 11.6 Hz), 3.26 (m, 2H), 3.37 (m, 1H, C<u>H</u>$_{ring}$), 3.57-3.73 (m, 2H, C<u>H</u>$_{ring}$), 3.9 (s, 3H, C<u>H</u>$_3$O), 4.15 (t, 2H, C<u>H</u>$_2$-N$_{Tria,}$ *J* = 6,9 Hz), 5.9 (s, 1H, CH$_{arom}$-<u>CH</u>$_2$), 7.3 (dd, 1H, C<u>H</u>$_{arom}$, J^1 = 2.6 Hz, J^2 = 9.1 Hz), 7.40 (d, 1H, C<u>H</u>$_{arom}$, *J* = 2.5 Hz), 7.66 (d, 1H, C<u>H</u>$_{arom}$ *J* = 4.5 Hz), 7.72 (s, 1H,CH$_{Tria}$), 7.88 (d, 1H, *J* = 7.8 Hz), 8.59 (d, 1H, C<u>H</u>$_{arom}$, *J* = 3Hz)

^{13}C-NMR (CD$_3$OD, 125 MHz): δ = 20.4 (<u>C</u>H$_{2ring}$), 25.9 (<u>C</u>H$_2$-COOH), 27.2, 27.2 (<u>C</u>H$_{2ring}$), 29.1(<u>CH$_2$</u>-CH$_2$-CH$_2$-N$_{Triaz}$), 29.7 (<u>C</u>H$_2$-CH$_2$-N$_{Triaz}$), 30.6, 30.5, 30.4, 30.3 (<u>C</u>H$_2$), 31.0 (<u>CH2</u>$_{ring}$), 33.0 (<u>C</u>H$_2$-COOH), 44.9 (<u>C</u>H$_{2ring}$), 51.2(<u>C</u>H$_2$-N$_{Triaz}$), 55.6 (<u>C</u>H$_{2ring}$), 56.7

($\underline{C}H_{2ring}$), 60.8 ($\underline{C}H_{2ring}$), 69.6(C_{arom}-$\underline{C}H_2$-CH_{ring}), 102.5 ($\underline{C}_{arom}$), 120.2 ($\underline{C}_{Triaz}$), 123.5, 123.4 ($\underline{C}_{arom}$), 127.7 ($\underline{C}_{arom}$), 131.5 ($\underline{C}_{arom}$), 144.8 ($\underline{C}_{arom}$), 148.3, 148.1 ($\underline{C}_{arom}$), 149.5 ($\underline{C}H_{Triaz}$), 160.0 ($\underline{C}_{arom}$), 181.4 ($\underline{C}$=O)

Yield 0.4 g (0.71 mmol, 75 %)

Rf = 0.45 (DCM/MeOH, 4:1)

HR-ESI–MS calc. for $[M-2H]^-$ 561.3315, found 561.2335.

12-(4-(((3*R*,5*S*)-1,5-bis(tert-butoxycarbonyl)pyrrolidin-3-yloxy)methyl)-1H-1,2,3-triazol-1-yl)dodecanoic acid 79b

^{1}H-NMR ($CDCl_3$, 500 MHz): δ = 1.23-1.31 (m, 14H, $C\underline{H}_2$), 1.42-1.45 (m, 18H, $CC\underline{H}_3$), 1.61 (t, 2H, J^1 = 7,22 Hz, $C\underline{H}_2$-COOH), 1.91 (m, 2H, $\underline{CH}_2$-CH_2-N_{Tria}), 2.06 (m, 1H,$C\underline{H}_{Pro}$), 2.33 (t, 2H, J^1 = 7.43 Hz, $\underline{CH}_2$-CH_2-COOH), 2.40 (m, 1H, $C\underline{H}_{Pro}$), 3.59 (m, 2H, $C\underline{H}_{2Pro}$), 4.22 (m, 2H, $C\underline{H}$α+ $C\underline{H}$-O_{Pro}), 4.37 (m, 2H, $C\underline{H}_2$-N_{Tria}), 4.7 (m, 2H, O-$C\underline{H}_2$) 7.63 (s, 1H, $C\underline{H}_{Tria}$)

^{13}C-NMR ($CDCl_3$, 125 MHz): δ = 24.6 ($\underline{CH}_2$-CH_2-COOH), 26.2 ($\underline{CH}_2$-CH_2-CH_2-N_{Tria}), 27.9 ($C(\underline{C}H_3)_3$), 28.3 ($C(\underline{C}H_3)_3$), 28.9, 28.8, 28.7 ($\underline{C}H_2$), 29.1 ($\underline{C}H_2$), 29.9 ($\underline{C}H_2$-CH_2-N_{Tria}), 33.8 ($\underline{C}H_2$-COOH), 36.4 ($\underline{C}H_{2Pro}$), 51.3 ($\underline{C}H_2$-$_{Tria}$), 51.8, 51.5 ($\underline{C}H_2$-N_{Pro}), 58.5 ($\underline{C}$αH), 62.0 ($\underline{C}H_2$-C_{Tria}), 77.5 ($\underline{C}H_{Pro}$-O), 80.2 ($\underline{C}(CH_3)_3$), 81.2 ($\underline{C}(CH_3)_3$, 123.2 ($\underline{C}_{Tria}$), 143.9 ($\underline{C}_{Tria}$), 154.0 ($N\underline{C}O_{Pro}$), 171.9 ($\underline{C}$=O), 178.0 ($\underline{C}$=O)

Yield 2.21 g (3.9 mmol, 73 %)

Rf = 0.3 (pentane/AcOEt, 1:3)

HR-ESI–MS calc. for $[M-H]^-$ 561.3601, found 561.3613

12-(4-((5-((3a*S*,4*S*,6a*R*)-2-oxohexahydro-1H-thieno[3,4-d]imidazol-4-yl)pentanamido)methyl)-1H-1,2,3-triazol-1-yl)dodecanoic acid 79c

^{1}H-NMR ($(CD_3)_2SO$, 500 MHz): δ = 1.1-2.6 (m, 29H, $C\underline{H}_2$), 2.82 (m, 1H), 3.1 (m, 1H), 3.37 (m, 1H), 4.1-4.3 (m, 6H), 6.4-6.6 (m, 2H), 7.9 (m, 1H), 8.3 (m, 1H)

^{13}C-NMR ($(CD3)_2SO$): δ = 24.8 ($\underline{C}H_2$), 25.5 ($\underline{C}H_2$), 27.6 ($\underline{C}H_2$), 27.8 ($\underline{C}H_2$), 27.9 ($\underline{C}H_2$), 28.3 ($\underline{C}H_2$), 28.4 ($\underline{C}H_2$), 29.3($\underline{C}H_2$),33.7 ($\underline{C}H_2$), 34.5 ($\underline{C}H_2$), 48.8 (Triazole-$\underline{C}H_2$-), 55.0 (S-$\underline{C}$H), 58.8 ($\underline{C}$H-CH_2-S), 60.6 ($\underline{C}$H-CH_2-S), 122.3 ($\underline{C}_{Triaz}$), 144.7 ($\underline{C}_{Triaz}$), 162.3 (C=O), 171.6 (C=O).

Yield 0.46 g (0.87 mmol, 70 %). Yellow-gray solid.

Mp 157–161 ^{0}C

HR-ESI–MS calc. for $[M-H]^-$ 529.2910, found 529.2914.

12-(4-((((2*R*,3*R*,5*R*,6*R*)-3,4,5-triacetoxy-6-(acetoxymethyl)tetrahydro-2H-pyran-2-yl)oxy)methyl)-1H-1,2,3-triazol-1-yl)dodecanoic acid 79d

^{1}H-NMR (CD_3OD): δ = 1.24-1.3 (m, 14H, $C\underline{H}_2$), 1.6 (m, 2H, N_{Triaz}-CH_2-$C\underline{H}_2$), 2.3 (t, 2H, J = 7.5 Hz, $C\underline{H}_2$-COOH), 3.96 (dt, 1H, J^1 = 1.0 Hz, J^2 = J^3 = 6.6 Hz, $C_5\underline{H}$-CH_2-OCO), 4.09-4.19 (m, 2H, C_5H-$C\underline{H}_2$-OCO), 4.33 (m, 2H, N_{Triaz}-$C\underline{H}_2$), 4.66 (d, 1H, J^1 = 7.9 Hz, $C_1\underline{H}$), 4.96–5.02 (m, 3H), 5.21 (dd, 1H, J^1 = 7.9 Hz, J^2 = 10.5 Hz), 5.39 (dd, 1H, J^1 = 1.0 Hz, J^2 = 3.4 Hz, C_4H), 7.5 (s, 1H,$C\underline{H}_{Triaz}$),

^{13}C-NMR (CD_3OD): δ = 20.4 (CO-CH_3), 20.5 (CO-CH_3), 20.6 (CO-CH_3), 20.7 (CO-CH_3), 24.5 ($\underline{C}H_2$-CH_2-COOH), 26.3 (N_{Triaz}-CH_2-CH_2-$\underline{C}H_2$), 28.7-29.3 ($\underline{C}H_2$), 30.1 (N_{Triaz}-CH_2-$\underline{C}H_2$), 33.8($\underline{C}H_2$-COOH), 51.36 (N_{Triaz}-$\underline{C}H_2$), 54.4 ($\underline{C}H_2$-C_{Triaz}), 61.2 (CH-$\underline{C}H_2$-OCO), 62.8 ($\underline{C}_4$H), 67.0 ($\underline{C}_2$H), 68.7 ($\underline{C}_3$H), 70.7 ($\underline{C}_5$H), 100.4 ($\underline{C}_1$H),122.5 ($\underline{C}_{Triaz}$), 143.8 ($\underline{C}_{Triaz}$)169.5 ($\underline{C}$=O), 170.0 ($\underline{C}$=O), 170.1 ($\underline{C}$=O), 170.3 ($\underline{C}$=O), 178.6 ($\underline{C}$=O)

Yield 0.295 g (0.47 mmol, 70 %)

Rf = 0.25 (DCM/MeOH, 1:9)

HR-ESI–MS calc. for $[M-H]^-$ 626.2930, found 626.260.

11-azidoundacanoic acid 83

Product synthesized according to literature protocol.[216] Yield 4.23 g (18.3 mmol, 98 %)

^{1}H-NMR ($CDCl_3$, 500 MHz) δ = 1.23-1.36 (m, 14H, C$\underline{H}_2$), 1.55-1.62 (m, 4H, C$\underline{H}_2$), 2.34 (t, 1H, *J* = 7.5Hz, C$\underline{H}_2$-N_3), 3.25 (t, 1H, *J* = 7.0Hz, C$\underline{H}_2$-COOH)

^{13}C-NMR ($CDCl_3$, 125 MHz): δ = 24.5 ($\underline{C}H_2$-CH_2-COOH), 26.6 ($\underline{C}H_2$-CH_2-N_3), 28.7 ($\underline{C}H_2$), 28.9 ($\underline{C}H_2$), 29.0 ($\underline{C}H_2$), 29.1 ($\underline{C}H_2$), 29.2 ($\underline{C}H_2$), 29.3 ($\underline{C}H_2$), 34.0 ($\underline{C}H_2$-COOH), 51.4 ($\underline{C}H_2$-N_3), 181.2 (C=O)

General procedure for ligand exchange reaction: synthesis of NPs 81a-d and 84

Magnetic NP **80** (50 mg) covered with oleic acid were treated with EtOH (30 mL) and centrifuged. This step was repeated two times. fourfold excess (in comparison to Fe_3O_4) of corresponding monomer **79a–d** or **83** for NP **84** was placed in a three-necked flask and dissolved in degassed 1,2-dichlorobenzene (15 mL) (in case of **81c**, 15 mL of DMSO was used). Under mechanical stirring and inert argon atmosphere, NP **80** were added and the mixture was stirred at 80 ^{0}C for 20 h. After it was cooled down to RT, chloroform (30 mL) was added and particles were precipitated by adding mixture EtOH/acetone 1:1 or hexane and collected by an external magnet. The NPs **81**, **84** were redispersed in chloroform and again precipitated. Finally, particles were redispersed in DCM in concentrations of ~10 mg/mL

(2S,4R)-2-(diphenyl(trimethylsilyloxy)methyl)-4-(prop-2-ynyloxy)pyrrolidine 89

Product prepared according to literature procedure.[217] Yield 2.534 g (6.7 mM, 85 %)

^{1}H-NMR ($CDCl_3$, 500 MHz): δ = -0.1 (s,9H, C$\underline{H}_3$TMS), 1.66-1.7 (m, 2H, C$\underline{H}_{2Pro}$), 2.0 (s, br, 1H, NH), 2.34 (t,1H, *J* = 2.Hz, C≡C$\underline{H}$), 2.77 (dd, 1H, *J* = 11.9 Hz, *J* = 4.8 Hz, C$\underline{H}_2$-N_{Pro}), 2.9 (dd, 1H, *J* = 11.9 Hz, *J* = 2.2 Hz, C$\underline{H}_2$-N_{Pro}), 3.88-3.93 (m,1H, C$\underline{H}_{Pro}$-O), 4,03 (dd, 2H, *J* = 1.3 Hz, *J* = 2,4 Hz, O-C$\underline{H}_2$-C), 4.30 (t, 1H, *J* = 8.1Hz, Cα$\underline{H}$), 7.15-7.27 (m, 6H, C$\underline{H}_{arom.}$), 7.30 (dd, 2H, *J* = 8,2 Hz, *J* = 1,2 Hz, C$\underline{H}_{arom.}$), 7.43 (dd, 2H, *J* = 1.3 Hz, *J* = 8.5 Hz, C$\underline{H}_{arom.}$)

^{13}C-NMR ($CDCl_3$, 125 MHz): δ = 2.1 ($\underline{C}H_3$TMS), 33.9($\underline{C}H_{2Pro}$), 52.6 ($\underline{C}H_2$-N_{Pro}), 56.9 (O-$\underline{C}H_2$-C), 63.5 ($\underline{C}H_{Pro}$-O), 73.9 (C≡$\underline{C}$H), 79.2 (CH_{Pro}-O) 80.0 ($\underline{C}$≡CH), 82.8 ($\underline{C}(Ph)_2$O,

126.84 ($\underline{C}_{arom.}$), 126.94 ($\underline{C}_{arom.}$), 127.44 ($\underline{C}_{arom.}$), 127.54 ($\underline{C}_{arom.}$), 127.74 ($\underline{C}_{arom.}$), 128.4 ($\underline{C}_{arom.}$), 145.34 ($\underline{C}_{arom.}$), 146.6 (C_{Ph})

NP 90a

To a stirred solution of NP **84** (1.338 g), CuSO4*5H_2O (169 mg, 0.2 equiv) and Na-Asc (269 mg, 0.4 equiv) in MeOH (50 mL) **89** (800 mg, 1 equiv) were added. The mixture was stirred for 10 min and TBTA (360 mg, 0.2 equiv) was added followed by stirring at RT for 20 h. NP **90a** were collected by an external magnet and washed with MeOH. Finally, they were dried under vacuum at 40 ^oC for 2 h to yield brownish solid easily redispersed in DCM.

NP 90b and 90bb

To a stirred solution of NP **84** (0.98 g), CuSO4*5H_2O (50 mg, 0.2 equiv) and Na-Asc (80 mg, 0.4 equiv) in MeOH (50 mL) **72** (800 mg, 1 equiv) were added. The mixture was stirred for 10 min and TBTA (106 mg, 0.2 equiv) was added followed by stirring at RT for 20 h. NP **90b** were collected by an external magnet and washed with MeOH. Finally, they were dried under vacuum at 40 ^oC for 2 h to yield brownish solid easily redispersed in DCM. Next NP **90b** were mixed with DCM (10 mL) followed by addition of TFA (4 mL). Stirring was continued for 20 h. NP were collect by an external magnet and supernatant was discarded. NP were washed with 2% Et_3N/MeOH (100 mL). NP were collected by external magnet and washed with DCM (3x100 mL), MeOH (3x100 mL) and Et_2O) (2x100 mL). At last NP were dried on air yielding brown powder.

11-azido-N-(3,4-dihydroxyphenethyl)undecanamide 92

Dopamine **91** (1 g, 5.27 mmol, 1 eq) was dissolved in dry DMF (20 mL) under argon atmosphere followed by addition of acid **83** (1 g, 5.8 mmol, 1.1 eq), HOBt (1.068 g, 5.8 mmol, 1.5 eq), EDC (1.226 g, 7.9 mmol, 1.5 eq) and Et_3N (1.17 g, 11.6 mmol, 2.2 eq). Reaction mixture was stirred for 20 h under Ar protection. Water (70 mL) was added and a water phase was extracted with AcOEt (3x40 mL). Organic phase was washed with brine (60 mL) and dried over $MgSO_4$. Product was purified by column chromatography Yield 1.89 g (5.21 mmol, 99 %)

^{1}H NMR ($CDCl_3$, 500 MHz): δ = 1.22 (m, 14H, C<u>H</u>$_2$), 1.55 (m, 2H, C<u>H</u>$_2$, C<u>H</u>$_2$-N_3), 2.2 (m, 2H, C<u>H</u>$_2$-CONH), 2.60 (m, 2H, C<u>H</u>$_2$-CH_2-Ar), 3.23 (t, 1H, *J*=6.9Hz, CH_2-C<u>H</u>$_2$-Ar), 6.46 (m, 1H, C<u>H</u>$_{arom.}$), 6.78 (m 2H, C<u>H</u>$_{arom.}$)

^{13}C-NMR ($CDCl_3$, 125 MHz): δ = 25.7 (<u>C</u>H_2-CH_2-COOH), 26.6 (<u>C</u>H_2-CH_2-N_3), 29.3, 29.2, 29.1 ,29.0, 28.7 (5xCH_2), 34.6 (<u>C</u>H_2-CH_2-N_3), 36.1 (CO-<u>C</u>H_2), 36.6 (C_1arom-<u>C</u>H_2),, 41.2 (CO-<u>C</u>H_2), 51.4 (<u>C</u>H_2-N_3), 115.2 (<u>C</u>$_{5aroma.}$) 115.5 (<u>C</u>$_{2aroma.}$), 120.3(<u>C</u>$_{6\ aroma.}$), 130.3 (<u>C</u>$_{1\ aroma.}$), 143.1 (<u>C</u>$_{4aroma.}$), 144.4 (<u>C</u>$_{3aroma.}$), 175.00 (<u>C</u>=O),

Rf = 0.15 (DCM/MeOH, 9:1)

HRMS (APCI) calc for $[M+H]^+$ 363.23907 found 363.23917

<u>NP 93</u>

NP **80** (800 mg) were redispersed in solvent mixture $CHCl_3$/MeOH 1:1 (80 mL) followed by addition of **92** (1.914 g, 5.2 mM, 1.5 eq). Stirring was continued overnight and NP were collect by an external magnet. NP were washed with MeOH (3x100 mL), $CHCl_3$ (3x100 mL) and Et_2O (2x100 mL). NP were dried on air yielding black powder.

<u>(2*S*,4*R*)-2-carboxy-4-(prop-2-yn-1-yloxy)pyrrolidin-1-ium 2,2,2-trifluoroacetate 94</u>

Product synthesized according to reported protocol. 0.545 g (1.9 mmol, quant.).

^{1}H-NMR (D_2O, 500 MHz): δ = 2.16 (m, 2H, C<u>H</u>$_{2Pro}$), 2.62 (m, 1H, C<u>H</u>$_{2Pro}$), 2.92 (t, 1H, *J* = 2.5 Hz), 3.47 (dd, 1H, J^1 = 3.9 Hz, J^2 =1 3 Hz), 3.6 (m, 1H, C<u>H</u>$_2$-N_{Pro}), 4.3 (m, 3H, C≡C<u>H</u> and C<u>H</u>), 4.6 (t. 1H, *J* = 4.0 Hz, C<u>H</u>$_{Pro}$-O)

^{13}C-NMR (D_2O, 125 MHz): δ = 34.7 (<u>C</u>H_{2Pro}), 50.4 (C<u>H</u>$_2$-N_{Pro}), 56.2 (<u>C</u>H_2-C≡CH), 59.8 (<u>C</u>H), 76.3 (C≡<u>C</u>H), 79.1 (<u>C</u>≡CH), 174 (<u>C</u>=O)

NP 95

NP **93** (782 mg) were redispred in MeOH (50 mL) followed by addition of **94** (150 mg, 0.6 mmol, 1 eq), $CuSO_4*5H_2O$ (35mg 0.12 mmol, 0.2 eq) and Na-Asc (50 mg, 0.4 mmol, 0.4 eq).Mixture was stirred 72 h. Next NP were collect by magnet and washed with MeOH (100 mL). Finally, NP were washed with 5% Et_3N in MeOH (100 mL), MeOH (3x100 mL) and dried under vacuum overnight

5-(((3*R*,5*S*)-1,5-bis(tert-butoxycarbonyl)pyrrolidin-3-yl)oxy)-5-oxopentanoic acid 98

Product synthesized according to literature protocol.[220] Yield 1.257 g (3.13 mmol, 60 %)

^{1}H-NMR ($CDCl_3$, 500 MHz): δ = 1.47 (br, 18H, C$\underline{H}_3$), 1.90–1.99 (m, 2H, C$\underline{H}_2$C$\underline{H}_2$C$\underline{H}_2$), 2.16 (m, 1H, CH$\underline{H}$CHN), 2.37–2.46 (m, 5H, CH$\underline{H}$CHN, C$\underline{H}_2$-C$\underline{H}_2$C$\underline{H}_2$), 3.45–3.7 (m, 2H, C$\underline{H}_2$N), 4.25 (m, 1H, C$\underline{H}$N), 5.25 (m, 1H, OCH);

^{13}C-NMR ($CDCl_3$, 125 MHz): δ = 19.6, (C$\underline{H}_2$-CH_2-COO-) 27.8, 27.9, 28.2, 29.6 (C$\underline{H}_3$), 32.8 (C$\underline{H}_{2Pro}$), 33.1 (C$\underline{H}_{2Pro}$), 35.5 (C$\underline{H}_2$COOH), 36.5 (C$\underline{H}_2$COO-, 51.9 (C$\underline{H}_{2Pro}$), 52.1(C$\underline{H}_{2Pro}$), 58.4 (C$\underline{H}_2$Pro), 71.9 (C$\underline{H}_{Pro}$), 72.8 (C$\underline{H}_{Pro}$), 80.3 (C), 80.5, 81.5 (C), 153.9 (C=O), 171.6 (C=O), 172.3 (C=O), 177.9 (C=O)

NP 99

Mgnetie NP **80** (2 g) were redispred in $CHCl_3$/MeOH mixture 1:1 (250 mL) followed by addition of **91** (2 g, 10.5 mmol). Mixture was stirred for 20 h. Then MNP were collected by an external magnet and washed with MeOH (3x200 mL), $CHCl_3$ (3x200 mL). NP were dried under vacuum for 2 h yielding black solid.

NP 101a

Magnetite NP **99** (900 mg), were redispered in dry DMF (40 mL) under Ar protection followed by addition of **79b** (1.073 g, 1.98 mmol, 1 eq), HOBt (382 mg, 2.83 mmol, 1.5 eq), EDC (439 mg, 2.83 mmol, 1.5 eq) and Et_3N (420mg, 0.58 mL, 4.16 mM, 2.2eq). Stirring was continued overnight. NP were collected by magnet and washed with MeOH (3x100 mL). Drying under vacuum for 2 h. As prepared NP (614 mg) were submitted to reaction with acetic anhydride (2.7 g, 26.5 mM, 10 eq) in presence of Et_3N (3.2 g, 31.7

mmol, 12 eq) in CH_3CN (30 mL) at rt. Stirring was continued for 2.5 h. Afterwards magnetite NP were washed with MeOH (3x100 mL) and dried under vacuum overnight. Next NP were redispred in DCM (30 mL).TFA (15 mL) was added and mixture was stirred for 20 h. NP were collect by and external magnet and washed with DCM (3x100 mL) and , MeOH (2x100 mL). Magnetite NP were dried under vacuum overnight yielding black powder

NP 101b

Magnetite NP **99** 3 g), were redispered in dry DMF (50 mL) under Ar protection followed by addition of **98** (600 mg, 1.49 mmol, 1eq) HOBt (329 mg, 2.24 mmol, 1.5 eq), EDC (378 mg, 2.24 mmol, 1.5 eq) and DIPEA (635 mg, 0.855 mL, 2.2 eq). Stirring was continued overnight. NP were collected and by magnet and washed with MeOH (3x100 mL) and dried under vacuum for 2 h. Later on NP (614 mg) were submitted to reaction with acetic anhydride (2.7 g, 26.5 mmol, 10 eq) in presence of Et_3N (3.2 g, 31.7 mmol, 12 eq) in CH_3CN (30 mL) at rt. Stirring was continued for 2.5 h. Afterwards NP were washed with MeOH (3x100 mL) and dried under vacuum overnight. Resulting magnetite NP were redispred in DCM (30 mL).TFA (15 mL) was added and mixture was stirred for 20 h. NP were collect by and external magnet and washed with DCM (3x100 mL) and MeOH (2x100 mL). NP were dried under vacuum overnight yielding black powder

4-azidobutan-1-amine 111

Synthesized according to reported protocol.[224] Yield 4.3 g (37.7 mmol, 57 %)

^{1}H-NMR ($CDCl_3$, 300 MHz): δ = 1.41-1.62 (m, 4H, C$\underline{H_2}$), 2.67 (t, 2H, *J* = 6.9Hz, C$\underline{H_2}$-NH_2), 3.23 (t, 2H, *J* = 6.7Hz, C$\underline{H_2}$-N_3)

^{13}C-NMR ($CDCl_3$, 125 MHz): δ = 26.2 (C$\underline{H_2}$), 30.4 (C$\underline{H_2}$), 44.5 (C$\underline{H_2}$-NH_2), 51.3 (C$\underline{H_2}$-N_3)

General procedure for coating NP or other materials with Polydopamine

Magnetite NP or any other solid material (1 g) was redispred in 10 mmol Tris buffer (500 mL) under air access. Next **91** (1 g, 5.3 mmol, c = 2 mg/mL) was added and stirring was continued for 24 h at rt. Then NP or solid material were collected by external magnet or by centrifugation followed by washing with H_2O (3x200 mL), MeOH (3x200 mL) and Et_2O

(2x100 mL). Drying on air afforded desired materials covered with polydopamine as black powder.

NP 112

Obtained according to mentioned general procedure using 1 g of **80**.

NP 120

Magnetite NP **112** (200 mg) were sonicated in EtOH (15 mL) 30 min. **111** (500 mg, 4.3 mmol) in EtOH (5 mL) was added. After the mixture had been stirred at rt for 18 h the resulting magnetic nanoparticles **113** were separated by an external magnet. They were washed three times with EtOH (50 mL) and dried at 50 °C under vacuum overnight.

5-(dimethylamino)-N-(prop-2-yn-1-yl)naphthalene-1-sulfonamide 116

Synthesized according to reported protocol.[226] Yield 0.946 g (3.28 mmol, 88 %)

^{1}H-NMR ($CDCl_3$, 500 MHz): δ = 1.91 (t, 1H, HC≡), 2.90 (s, 6H, $N(CH_3)_2$), 3.77 (dd, 2H, CH_2N), 4.93 (t, 1H, NH), 7.20 (d, 1H, Ar-H), 7.61-7.51 (m, 2H, Ar-H), 8.29-8.25 (m, 2H, Ar-H), 8.57 (d, 1H, Ar-H),

.

^{13}C-NMR ($CDCl_3$, 125 MHz): δ = 152.1 (Ar-C), 134.3 (Ar-C),, 130.9 (Ar-C), 130.1 (Ar-C), 130.0 (Ar-C), 128.7(Ar-C), 123.8 (Ar-C), 118.8 (Ar-C), 115.4 (Ar-C), 77.9 (CH_2-C≡C), 72.8 (CH_2-C≡CH) , 45.6 (CH_3), 33.1 (CH_2-C≡CH)

.

General procedure for the synthesis of MNP 117a-d

Azido-modified NP **113** (100 mg, 0.43 mmol, 1 eq. / based on Fe_3O_4) were dispersed in MeOH (5 mL). The corresponding alkyne **72**, **75**, **75**, **116** (0.43 mmol/1 eq.) in MeOH (5 mL), $CuSO_4$*$5H_2O$ (0.2 eq.) and Na-Asc (0.4 eq.) were added. The mixture was stirred at RT overnight. The resulting magnetite NP **117** were collected by an external magnet and washed with MeOH (2x100 mL). Overnight drying at 50 °C under vacuum yielded brownish powders.

NP 118

NP **112** (1 g) were redispersed under Ar in dry EtOH (25 mL) by ultrasound enhancement for 20 min. followed by addition of 5-aminopentan-1-ol (2.2 g, 2.13 mmol, 5 eq) in dry EtOH (100 mL).Stirring was continued for 24 h at rt. Then MNP were collected by an external magnet and washed with EtOH (3x100 mL). Overnight drying under vacuum yielded black powder.

NP 119

NP **118** (0.65 g) were refluxed in PhMe (50 mL) with Dean-Stark apparatus for 2 h. After cooling down to ~ 50 ^{0}C 3,6-dimethyl-1,4-dioxane-2,5-dione (4.032, 28 mmol, 1 eq) and DMAP (2.73 g, 22.3 mmol, 0.8 eq) were added. Mixture was refluxed with Dean Stark apparatus for 8 h. The reslting NP were cooled down and collected by external magnet followed by washing with $CHCl_3$ (3x200 mL). Drying on air yielded black powder

NP 120

NP **119** (0.232 g) were redispersed in DCM (15 mL). DCC (1.44 g, 5.9 mmol, 1.2 eq), biotin (**75**) (1.22 g, 5 mmol, 1 eq) and DMAP (0.136 g, 1.1 mmol, 0.2 eq) were added. Stirring was continued for 24 h at rt. Then NP were collected by an external magnet and washed with MeOH (5x100 mL), and DCM (3x100 mL). Drying at rt yielded brown powder.

POLYDOPAMINE 121 (132)

91 (1g, 5.3 mmol) was dissolved in 10 mM buffer (Tris at pH 8.5 or phosphate at pH 8.5, 500 mL) and stirred in air for 20 h. The resulting black precipitate was separated by centrifugation at 4000 rpm, washed with water, and centrifuged again. This washing step was repeated three times, and the solid was dried under vacuum at 40 °C overnight.

In the case of Tris buffer, higher yields of solid PDA were obtained (170 mg) than in phosphate buffer (40 mg).

(*R*)-2-((tert-butoxycarbonyl)amino)-3-mercaptopropanoic acid 134

Product was synthesized according to literature protocol[233] and used without further purification in next step.

NP 135

NP **112** (1 g) were redispersed under Ar in dry EtOH (25 mL) by ultrasound enhancement for 20 min. Et_3N was used to adjust pH to 8.5 and solution of crude **134** (0.331 g, 1.5 mmol) in dry EtOH (25 mL) was added. Stirring was continued for 24 h at rt. Then NP were collected by an external magnet and washed with MeOH (3x100 mL) and Et_2O (2x50 mL). Drying at rt yielded black powder. Later on resulting NP (0.85 g) were submitted to deprotection reaction with TFA (1 mL) in DCM (3 mL) at rt. After 24 h NP were collected by an external magnetic field and washed with DCM (3x100 mL) and Et_2O (100 mL). Drying on air furnished black powder.

NP 137

Obtained according to mentioned general procedure using 1 g of **136**

NP 138

Obtained according to mentioned general procedure using 1 g of **112**

Compounds 139-141

Synthesized according to literature protocol.[83] NMR given for **141**

^{1}H-NMR ($CDCl_3$, 500 MHz): δ = 2.8 (m, 2H, C$\underline{H}_2$), 3.02 (m, 2H, C$\underline{H}_2$), 5.12 (d, 4H, *J* = 13.6Hz, C$\underline{H}_2$-Ph), 6.78 (dd, 1H, *J* = 1.8Hz, *J* = 8.2Hz, C$\underline{H}_{arom}$), 7.02 (dd, 2H, *J* = 5.1Hz, *J* = 7.1Hz, C$\underline{H}_{arom}$), 7.29-7.48 (m, 10H, C$\underline{H}_{arom}$)

^{13}C-NMR ($CDCl_3$, 125 MHz): δ = 32.6 (C$\underline{H}_2$), 40.1 (C$\underline{H}_2$), 70.2 (C$\underline{H}_2$-Ph), 114.8 (C$\underline{H}_{arom.}$), 115.2 (C$\underline{H}_{arom.}$), 121.2 (C$\underline{H}_{arom.}$), 127.4 (C$\underline{H}_{arom.}$), 127.6 (C$\underline{H}_{arom.}$), 127.7 (C$\underline{H}_{arom.}$), 127.8

($\underline{C}H_{arom.}$), 128.4 ($\underline{C}H_{arom.}$), 130.3 ($\underline{C}H_{arom.}$), 137.3 ($\underline{C}H_{arom.}$), 137.4 ($\underline{C}H_{arom.}$), 147.2 ($\underline{C}H_{arom.}$), 148.5 ($\underline{C}H_{arom.}$), 158.5($\underline{C}H_{arom.}$)

General procedure for covering PDA coated NP with polylactic acid

Magnetite NP, iron magnetic nanoparticles or solid materials (0.7 g) were refluxed in PhMe (70 mL) with Dean-Stark apparatus for 2 h. After cooling down to ~ 50 ^{0}C 3,6-dimethyl-1,4-dioxane-2,5-dione (4.032, 28 mmol, 1 eq) and DMAP (2.73 g, 22.3 mmol, 0.8 eq) were added. Mixture was refluxed with Dean Stark apparatus for 16 h. Mixture was cooled down and NP collected by external magnet followed by washing with $CHCl_3$ (3x200 mL).In case of non magnetic materials centrifugation was used to collect sample followed by washing with $CHCl_3$ (3x200 mL). Drying on air yielded black powder

NP 148

Obtained according to general protocol for ROP using magnetite NP **112**

MNP 150

Obtained according to general protocol for covering with polydopamine using carbon coated iron magnetic nanoparticles NP **149**

NP 151

Obtained according to general protocol for ROP using MNP **150**.

NP 152

Obtained according to general protocol for ROP using NP **137**.

Aluminium oxide covered with polydopamine 154

Obtained according to general protocol for covering with polydopamine using neutral Al_2O_3 for column chromatography.

Aluminium oxide covered with polylactic acid 155

Obtained according to general protocol for ROP using Al_2O_3 **154**.

(1*S*,2*R*)-2-(acryloyloxy)-1-carboxypropan-1-aminium chloride 158

156 (5 g, 42 mmol, 1eq), was added at 0°C to TFA (21 ml, 123 mmol). Mixture was stirred 30 min and 5 min at rt followed by addition of acryloil chloride in one portion (5.1 ml, 63 mmol, 1.5 eq). Reaction mixture was stirred 6 h at rt and cooled down to 0°C. Diethyl ether (42 ml) was added first slowly in 20 min. White precipitated was observed. Stirring was continued additional 30 min and then precipitate was filtered and dried under vacuum at rt 30 min. Yield 4.1 g (19.6 mmol, 46 %)

^{1}H-NMR (D_2O, 500 MHz): δ = 1.32 (d, 3H, *J* = 7.1 Hz,C$\underline{H}_3$), 4.16 (d, 1H, *J* = 3.2 Hz, C$\underline{H}$), 5.4 (m, 1H, C$\underline{H}$), 5.8 (d, 1H, *J* = 10.5 Hz, C$\underline{H}_2$ = CH-CO), 6.03 (dd, 1H, *J* = 10.5 Hz, *J* = 10.6 Hz, CH_2 = C$\underline{H}$-CO), 6.3 (d, 1H, *J* = 17.3 Hz, C$\underline{H}_2$ = CH-CO)

^{13}C-NMR ($CDCl_3$, 125 MHz): δ = 18.8 (C$\underline{H}$3) , 65.1 (C$\underline{H}$-CO), 68.7 (C$\underline{H}$-OCO), 126.7 (CH_2=C$\underline{H}$) , 133.4 (CH_2=C$\underline{H}$), 168.6 (C$\underline{=}$O), 169.5 (C$\underline{=}$O)

HRMS (APCI) calc. for 174.07608 $[M+H]^+$ found 174.07622

(1*S*,2*R*)-1-carboxy-2-(methacryloyloxy)propan-1-aminium chloride 157

156 (5 g, 42 mmol 1 eq), was added at 0 °C to TFA (21 ml, 123 mmol). Mixture was stirred 30 min and 5 min at rt followed by addition methacryloil chloride in one portion (8.15 mL, 72 mmol, 1.5 eq). Reaction mixture was stirred 6 h at rt and cooled down to 0°C. Diethyl ether (50 mL) was added first slowly in 20 min. White precipitated was observed. Stirring was continued additional 30 min and then precipitate was filtered and dried under vacuum at rt 30 min. Yield 3.6 g (16.1 mM, 38 %)

^{1}H-NMR (D_2O, 500 MHz): δ = 1.32 (d, 3H, *J* = 6.7 Hz C$\underline{H}_3$), 1.72 (s, 3H, C$\underline{H}_3$), 4.18 (d, 1H, *J* = 3.2 Hz, C$\underline{H}$), 5.44 (m, 1H,), 5.6 (t, 1H, *J* = 1.4, C$\underline{H}_2$=C-), 5.99 (t, 1H, *J* = 0.9 Hz, C$\underline{H}_2$=C-)

^{13}C-NMR ($CDCl_3$, 125 MHz): 15.7 ($\underline{C}H_3$), 17.2 ($\underline{C}H_3$), 65.1 ($\underline{C}H$), 68.9 ($\underline{C}H$-OCO), 127.7 ($\underline{C}H_2$=C), 135.1 (CH_2=$\underline{C}H$),167.8 ($\underline{C}$=O), 169.6 ($\underline{C}$=O)

HRMS (APCI) calc. for 188.09173 $[M+H]^+$ found 188.09177

(1*S*,2*R*)-1-carboxy-2-((4-(2-(methacryloyloxy)ethoxy)-4-oxobutanoyl)oxy)propan-1-aminium chloride 161

Acid **159** (19.5 mL, 100 mmol) was mixed with $SOCl_2$ (39 mL, 200 mmol) at rt under Ar atmosphere 30 min. Next temperature was elevated to 50^0C and kept for 1h. Thionyl chloride was evaporated under vacuum to yield dens oil which was used without further purification.**156** (3 g, 25.2 mmol, 1 eq), was addend at 0^oC to TFA (8 mL, 46.8 mmol). Mixture was stirred 30 min and 5 min at rt followed by addition acid chloride (**160**) in one portion (9.42 g, 38 mmol). Reaction mixture was stirred 6 h at rt and cooled down to 0^oC. Diethyl ether (20 mL) was added first slowly in 20 min. White precipitated was observed. Stirring was continued additional 30 min and then precipitate was filtered and dried under vacuum at RT 30 min. Yield 6.5 g (17.7 mmol, 70 %).

^{1}H-NMR (MeOD, 500 MHz): δ =1.26 (s, 3H, $C\underline{H}_3$), 1.76 (s, 3H, $C\underline{H}_3$), 2.59 (m, 4H, $C\underline{H}_2$), 4.18 (m, 4H, $C\underline{H}_2$), 5.30 (dq, 1H, *J* = 3.7Hz, *J*=6.6Hz, $C\underline{H}_2$=) ppm 5.48 (qd, 1H, *J* = 1.9Hz, *J* = 3.8Hz, $C\underline{H}_2$=)

^{13}C-NMR (MeOD, 125 MHz): δ = 17.2 ($\underline{C}H_3$), 20.8 ($\underline{C}H_3$), 29.7, 29.8 ($\underline{C}H_2$), 57.6 ($\underline{C}$), 63.7,63.8 ($\underline{C}H_2$), 69.6 ($C_{tertiary}$), 126.7 ($\underline{C}H_2$=C-), 137.5 (CH_2-$\underline{C}$-), 169.3 ($\underline{C}$=O), 172.8 ($\underline{C}$=O), 173.8($\underline{C}$=O)

HR-ESI–MS calc. for $[M+H]^+$ 332.1340 found 332.1342

(*S*)-6-acrylamido-2-aminohexanoic acid 164

Product synthesized acceding to literature protocol.[241] Yield 1.3 g (4.2 mmol, quant)

^{1}H-NMR (CD_3OD, 500 MHz) δ = 1.25–1.50 (m, 2H, $C\underline{H}_2$), 1.50–1.70 (m, 2H, $C\underline{H}_2$), 1.75–2.00 (m, 2H, $C\underline{H}_2$), 3.26 (t, 2H, J^1 = 6.8 Hz, $C\underline{H}_2$-NHCO), 3.73 (t, 1H, J^1 = 6.1 Hz, $C\underline{H}$), 5.72 (dd, 1H, J^1 = 9.2 Hz, J^2 = 2.8 Hz, CH_2=$C\underline{H}$), 6.10–6.35 (m, 2H, $C\underline{H}_2$=CH),

^{13}C-NMR (CD_3OD, 125 MHz) δ = 23.4 ($\underline{C}H_2$), 29.8 ($\underline{C}H_2$), 31.2 ($\underline{C}H_2$), 39.5 ($\underline{C}H_2$-NHCO), 53.8 ($\underline{C}$H-CO), 126.7 ($\underline{C}$H2-CH), 132.0 ($\underline{C}H_2$=CH), 168.3 ($\underline{C}$=O), 171.8 ($\underline{C}$=O)

(*S*)-tert-butyl 2-(azidomethyl)pyrrolidine-1-carboxylate 168

Product synthesized acceding to literature protocol.[245] 3.31 g (14.6 mmol, 80 %)

^{1}H NMR ($CDCl_3$, 500 MHz): δ = 1.47 (s, 9H, $C\underline{H}_3$), 1.86 (m, 4H, $C\underline{H}_{2Pro}$), 3.37 (m, 4H, $C\underline{H}_{2Pro}$), 3.80–4.00 (b, 1H,$C\underline{H}_{\alpha Pro}$)

^{13}C NMR ($CDCl_3$, 125 MHz): δ = 22.4 ($\underline{C}H_2$), 27.9 ($\underline{C}H_3$), 29.11 ($\underline{C}H_2$), 46.1 ($\underline{C}H_2$), 52.9 ($\underline{C}H_2$), 55.9 ($\underline{C}H$)

3,6,9,12-tetraoxapentadec-14-yn-1-yl acrylate 171

Product synthesized according to literature protocol.[246] Yield 1.851 g (6.47 mmol, 35 %)

^{1}H-NMR ($CDCl_3$, 500 MHz): δ = 2.42 (t, 1H, *J* = 2.0 Hz, CH_2-C≡C$\underline{H}$), 3.67 (m, 12H, O-C$\underline{H}_2$-CH_2-OH), 3.73 (t, 2H, *J* = 4.7 Hz, -O-CH2-C$\underline{H}_2$-O), 4.2 (d, 2H, *J* = 2.1 Hz, C$\underline{H}_2$-C≡CH), 4.3 (t, 2H, *J* = 4.8 Hz, -O-C$\underline{H}_2$-C$\underline{H}_2$-O-), 5.8 (d, 1H, *J* = 10.4 Hz, C$\underline{H}_2$ = CH), 6.15 (dd, 1H, J^1 = 6.9, J^2 = 17.3, CH_2 = C$\underline{H}$), 6.4 (d, 1H, *J* = 17.3 Hz, C$\underline{H}_2$ = CH)

12-(prop-2-ynyloxy)dodecyl acrylate 174

Product synthesized according to literature protocol.[103] Yield 3.3 g (17.5 mmol, 64 %)

^{1}H NMR (DMSO-d_6, 500 MHz): δ = 1.24 (m, 16H), 1.48 (m, 2H), 1.59 (m, 2H), 3.35 (m, 1H, C$\underline{H}$≡C-CH_2), 3.41 (m, 2H), 4.08 (m, 4H, C$\underline{H}_2$-C≡CH, O-CH_2-), 5.92 (m, 1H, C$\underline{H}_2$=CH), 6.15 (m, 1H, CH_2=C$\underline{H}$), 6.32 (m, 1H, C$\underline{H}_2$=CH)

^{13}C NMR (DMSO-d_6, 125 MHz): δ = 25.9, 26.1, 28.6, 29.2, 29.4, 29.5 (-$\underline{C}H_2$-$\underline{C}H_2$-), 57.7 ($\underline{C}$H≡C-CH_2), 64.5 (CH≡$\underline{C}$-CH_2), 128.8 ($\underline{C}H_2$=CH), 131.5 (CH_2=$\underline{C}$H), 165.9 ($\underline{C}$=O)

(*R*)-tert-butyl 2-((4-(15-oxo-2,5,8,11,14-pentaoxaheptadec-16-en-1-yl)-1H-1,2,3-triazol-1-yl)methyl)pyrrolidine-1-carboxylate 175

To a stirred solution of **171** (1.851g, 6.47 mmol, 1 eq), and **168** (1.46g, 6.4 mmol) in MeOH (40 mL) was added $CuSO_4$*H_2O (0.323 g, 1.3 mmol, 0.2 eq) and Na-Asc (0.485 g, 2.6 mmol, 0.4 eq). Stirring was continued for 3 days. Reaction was evaporated to dryness

and product was purified by column chromatography using ethyl acetate. Yield 2.43g (4.75 mmol, 74 %)

^{1}H NMR ($CDCl_3$, 500 MHz): δ = 1.46 (s, 9H, $C\underline{H}_3$), 1.8 (m, 4H, CH_2-CH_{2Pro}), 3.22 (m, 3H, $C\underline{H}_{Pro}$, $C\underline{H}_{2Pro}$), 3.62 (m, 12H, O-$C\underline{H}_2$-$C\underline{H}_2$-OH), 3.7 (t, 2H, *J* = 4.7 Hz, -O-CH2-$C\underline{H}_2$-O), 4.0 (m, 1H, $C\underline{H}_{Pro}$-), 4.27 (t, 2H, *J* = 4.7 Hz, O-$C\underline{H}_2$-Tria), 4.52 (m, 1H, $C\underline{H}_{Pro}$), 4.65 (m, 2H, -O-$C\underline{H}_2$-CH2-O), 5.80 (dd, 1H, *J* = 1.2Hz, *J* = 10.4Hz, $C\underline{H}_2$=CH), 6.11 (dd, 1H, *J* = 10.4Hz, *J* = 17.3Hz, CH_2=C<u>H</u>), 6.39 (dd, 1H, *J* = 1.2Hz, *J* = 17.3Hz, $C\underline{H}_2$ = CH), 7.49 (d, 1H, *J*=20.9Hz, C<u>H</u>-$_{Triaz}$)

^{13}C-NMR ($CDCl_3$, 125 MHz): δ = 23.2 ($\underline{C}H_2$), 28.8 ($\underline{C}H_2$), 28.2 ($\underline{C}H_3$), 51.4($\underline{C}H_2$), 57.0 ($\underline{C}$H), 63.6 (O-$\underline{C}H_2$-CH_2-O-), 64.5 (CH_2), 68.9 (O-CH2-$\underline{C}H_2$-O-), 69.5, 70.4, 70.5 (OCH_2), 79.8 ($\underline{C}$), 123.3 ($\underline{C}$-triazole), 128.3 (CH_2=$\underline{C}$H), 130.9 ($\underline{C}H_2$=CH) 145.2 ($\underline{C}$-triazole), 166.0 ($\underline{C}$=O), 177.6 (**C**=O)

Rf = 0.15 (AcOEt)
HR-ESI–MS calc. for $[M+H]^+$ calc.513.2924 found 513.2357

(*R*)-tert-butyl 2-((4-(((12-(acryloyloxy)dodecyl)oxy)methyl)-1H-1,2,3-triazol-1-yl)methyl)pyrrolidine-1-carboxylate 176

To a stirred solution of **174** (2.964, 10 mmol, 1 eq) and **168** (2.26g, 10 mM, 1 eq) in mixture *t*-BuOH/H_2O (1:1, 40 mL) $CuSO_4$*H_2O was added (0.5 g, 2 mmol, 0.2 eq) and Na-Asc (0.792 g, 4 mmol, 0.4 eq). Mixture was stirred 24 h and evaporated to dryness. Product was purified by column chromatography. Yield 2.881 g (5.5 mM, 55%).

^{1}H NMR ($CDCl_3$, 500 MHz): δ = 1.23-1.47 (m, 33H, $C\underline{H}_2$, $C\underline{H}_{2Pro}$), 3.30 (m, 5H, $C\underline{H}_2$), 4.1 (m, 3H, $C\underline{H}_2$), 4.6 (m, 3H, $C\underline{H}_2$), 5.79 (d, 1H, *J* = 10.3Hz, $C\underline{H}_2$=CH), 6.09 (dd, 1H, *J* = 10.4Hz, *J* = 17.3Hz, CH_2=C<u>H</u>), 6.37 (d, 1H, *J* = 17.3Hz, $C\underline{H}_2$=CH)

^{13}C-NMR ($CDCl_3$, 125 MHz): δ = 25.7 ($\underline{C}H_2$), 25.9 ($\underline{C}H_2$), 28.3 ($\underline{C}H_3$), 28.4 ($\underline{C}H_2$), 29.0 ($\underline{C}H_2$), 29.3 ($\underline{C}H_2$), 29.4 ($\underline{C}H_2$), 46.8 ($\underline{C}H_{2Pro}$), 56.9($\underline{C}H_{Pro}$), 57.8 ($\underline{C}H_2$-Triaz), 64.1 (-O-$\underline{C}H_2$), 64.5(Triazole-$\underline{C}H_2$), 70.5 (O-$\underline{C}H_2$) 79.8 ($\underline{C}$), 128.6 ($\underline{C}$-triazole), 128.8 ($\underline{C}H_2$=CH), 130.2 (CH_2=$\underline{C}$H), 142.3 ($\underline{C}$-triazole), 166.2 ($\underline{C}$=O), 177.5 (C=O)

Rf = 0.3 (Hex:AcOEt 3:1)

HR-ESI–MS calc. for $[M+H]^+$ calc. 521.3697 found 521.3698

2-((4-((acryloyloxy)methyl)-1H-1,2,3-triazol-1-yl)methyl)pyrrolidin-1-ium 2,2,2-trifluoroacetate 177

This compound was synthesized, characterized and provided by dr. Zekarias Yacob.

General procedure for polymerization of acrylate on magnetite NP stabilized with acryloyl phosphate derivative or acrulic acid

To a stirred suspension of magnetite NP **182** (1 g) or **185** (1 g) under Ar in anhydrous DMF (40 mL), the corresponding acrylate in available amount and AIBN (20 mol % in correspond to acrylate) were added. After stirring for 48 h at 70 ^{0}C, the NP were collected by an external magnet and washed with DCM (3x100 mL), MeOH (2x100 mL) and Et_2O (2x100 mL). Drying on air yielded brown powder.

NP 179

NP were synthesized according to general procedure using **165** (3.874 g, 13.5 mmol) and AIBN (0.442 g, 0.2 eq)

NP 180a and 180b

NP were synthesized according to general procedure using **157** (3.5 g, 15.7 mmol) and AIBN (0.527 g, 0.2 eq) or **161** (6 g, 16.34 mmol) with AIBN (0.549 g, 0.2 eq)

NP 181

NP were synthesized according to general procedure using **163** (4. 24 mmol) and AIBN (0.14 g, 0.2 eq)

NP 182a and 182b

NP were synthesized according to general procedure using **175** (1.64 g, 3.2 mmol) with AIBN (0.108 g) or **176** (2.21 g, 5 mmol) with AIBN (0.168 mg). Next resulting NP were redispred in DCM (20 mL) and TFA (10 mL) was added. Stirring was continued for 20 h and NP were collected by an external magnet and washed with DCM (100 mL). Next

afforded magnetite NP were washed with 2% Et_3N in MeOH (100 mL). At last magnetite NP were washed with by DCM (3x100 mL), MeOH (2x100 mL) and Et_2O (2x100 mL).Drying on air yielded brow powder.

NP 183 and 185

NP were synthesized according to general procedure using **177** (3 g, 12.7 mmol) with AIBN (0.416 g). In case of NP **185** amount of staring NP **184** was diminished to 0.5 g while amount of the monomer was not changed.

NP 187

NP were synthesized according to general procedure using propargyl acrylate (2.37 g, 21.55 mmol) with AIBN (0.7 g).

NP 188

To a stirred suspension of NP **187** (0.9 g) and **176** (0.452 g, 2 mmol) in MeOH (40 mL) was added $CuSO_4*H_2O$ (0.1 g, 0.4 mmol, 0.2 eq) and Na-Asc (0.158 g, 0.8 mmol, 0.4 eq). Stirring was continued for 3 days and NP were collected by an external magnet. Washing with with MeOH (3x100 mL) and Et_2O (2x100 mL) furnished brown after drying. Next resulting NP were redispred in DCM (4 mL) and TFA was added (2 mL). Stirring was continued for 20 h at rt. NP were collected by an external magnet and washed with DCM (3x100 mL), MeOH (2x100 mL) and Et_2O (2x100 mL). Drying on air yielded brown powder.

2-azidoacetyl chloride 191

Obtained according to literature protocol[247] and used without any purification in next step. Yield 3.42 g (28.9 mmol, 80 %)

(1*S*,2*R*)-2-(2-azidoacetoxy)-1-carboxypropan-1-aminium chloride 200

156 (1.07 g, 9 mmol 1 eq), was addend at 0 ^oC to TFA (4 mL, 39 mmol). Mixture was stirred 30 min and 5 min at rt followed by addition of **191** in one portion (1.44 g, 12 mmol, 1.3 eq). Reaction mixture was stirred 6 h at rt and cooled down to 0^oC. Diethyl ether (50

mL) was added first slowly in 20 min. White precipitated was observed. Stirring was continued additional 30 min and then precipitate was filtered and dried under vacuum at rt 30 min. Yield 0.447 g (1.8 mM, 24 %)

^{1}H NMR (MeOD, 500 MHz): δ = 1.18 (d, 1H, *J* = 6.5Hz, C$\underline{H}_3$), 3.64 (d, 1H, *J* = 4.5Hz, C$\underline{H}$) ppm 4.10 (m, 1H, C$\underline{H}$)

^{13}C-NMR (MeOD, 125 MHz): δ = 21.3 ($\underline{C}H_3$), 51.4 ($\underline{C}H_2$-N_3), 60.2 ($\underline{C}$H), 66.8 ($\underline{C}$H-OCO)

HR-ESI–MS calc. for [M-H]- calc. 201.0629 found 201.0614

NP 193

NP **18** were suspended in water (40 mL). Next propargyl acrylate was added (2.2 g, 20 mmol) followed by addition of TMEDA (0.930 g, 8 mmol) and APS (0.456 g, 2 mmol). Stirring was continued for 20 h. NP were collected by an external magnet and washed with MeOH (3x100 mL), DCM (2x100 mL) and Et_2O (2x100 mL). Drying on air afforded black powder.

NP 194

To a stirred suspension of NP **193** (0.85 g) and **192** (0.174 g, 0.7 mmol) in MeOH/H_2O mixture (1:2, 30 mL) $CuSO_4$*H_2O (0.035 g, 0.14 mmol, 0.2 eq) and Na-Asc (0.056 g, 0.28 mmol, 0.4 eq) were added. Stirring was continued for 2 days and NP were collected by an external magnet and washed with MeOH (3x100 mL) and Et_2O (2x100 mL). Drying on air afforded brown powder.

General procedure for aldol reaction using functionalized magnetite NP

Arylaldehyde (in amount indicated in appropriate Table) was mixed with NP (in amount indicated in appropriate Table) then cyclohexanone was added (in reaction where solvent was not given cyclohexanone was used in excess) followed by addition of water or co-catalyst (depends on conditions given in corresponding Table). Reaction progress was followed by TLC. After reaction was finshed NP were collected by an external magnet and washed with MeOH (3x10 mL) and Et_2O (2x10 mL). Organic fraction were evaporated and product was purified by column chromatography.

General procedure for Michel reaction using functionalized magnetite NP

Trans-β-nitrostyrene (in amount indicated in appropriate Table) was mixed with NP (in amount indicated in appropriate Table) then cyclohexanone or propionaldehyde was added (in reaction where solvent was not given cyclohexanone or propionaldehyde was used in excess) followed by addition of water or co-catalyst (depends on conditions given in corresponding Table). Reaction progress was followed by TLC. After reaction was finshed NP were collected by an external magnet and washed with MeOH (3x10 mL) and Et_2O (2x10 mL). Organic fraction were evaporated and product was purified by column chromatography.

General procedure for aldol reaction using PDA or PDA coated NP

Arylaldehyde (in amount indicated in appropriate Table) was mixed with NP or PDA (in amount indicated in appropriate Table) then cyclohexanone was added followed by addition of water. Mixture was heated at 50 ^oC according to the time given in Table. Reaction progress was followed by TLC. After reaction was finished NP were collected by an external magnet and washed with MeOH (3x10 mL) and Et_2O (2x10 mL). In case of PDA centrifugation was used to collect polymer. In both cases washing solutions were evaporated and product was purified by column chromatography furnishing desired aldol product. PDA coated NP or non supported PDA polymer were dried on air for few hours befor was used in next run.

General procedure for Knoevenagel reaction using PDA coated NP

Malononitrile (in amount indicated in appropriate Table) was mixed with NP (in amount indicated in appropriate Table) then arylaldehyded was added. Mixture was heated at 50 ^oC according to the time given in Table. Reaction progress was followed by TLC. After reaction was finished NP were collected by an external magnet and washed with MeOH (3x10 mL) and Et_2O (2x10 mL). Organic fractions were evaporated yielding desired product. When p-anisaldehyded or p-nitrobenzaldehyde were used product was purified by column chromatography. PDA coated NP were dried on air for few hours before use in next run.

6 Bibliography

(1) Shylesh, S.; Schünemann, V.; Thiel, W. R. *Angew. Chem. Int. Ed.* **2010**, *49*, 3428.

(2) Figuerola, A.; Di Corato, R.; Manna, L.; Pellegrino, T. *Pharmacol. Res.* **2010**, *62*, 126.

(3) Goesmann, H.; Feldmann, C. *Angew. Chem. Int. Ed.* **2010**, *49*, 1362.

(4) Lu, A.-H.; Salabas, E. L.; Schüth, F. *Angew. Chem. Int. Ed.* **2007**, *46*, 1222.

(5) Perrier, T.; Saulnier, P.; Benoît, J.-P. *Chem.--Eur. J.* **2010**, *16*, 11516.

(6) Sperling, R. A.; Parak, W. J. *Phil. Trans. R. Soc. A* **2010**, *368*, 1333.

(7) Teja, A. S.; Koh, P.-Y. *Prog. Cryst. Growth Charact. Mater.* **2009**, *55*, 22.

(8) Thanh, N. T. K.; Green, L. A. W. *Nano Today* **2010**, *5*, 213.

(9) Wu, W.; He, Q.; Jiang, C. *Nanoscale Res. Lett.* **2008**, *3*, 397

(10) Majewski, P.; Thierry, B. *Crit. Rev. Solid State Mater. Sci.* **2007**, *32*, 203.

(11) Schladt, T. D.; Schneider, K.; Schild, H.; Tremel, W. *Dalton Trans.* **2011**, *40*, 6315.

(12) Patel, D.; Moon, J. Y.; Chang, Y.; Kim, T. J.; Lee, G. H. *Colloids Surf., A* **2008**, *313–314*, 91.

(13) Mornet, S.; Vasseur, S.; Grasset, F.; Veverka, P.; Goglio, G.; Demourgues, A.; Portier, J.; Pollert, E.; Duguet, E. *Prog. Solid State Chem.* **2006**, *34*, 237.

(14) Zhao, M.; Josephson, L.; Tang, Y.; Weissleder, R. *Angew. Chem. Int. Ed.* **2003**, *42*, 1375.

(15) Polshettiwar, V.; Luque, R.; Fihri, A.; Zhu, H.; Bouhrara, M.; Basset, J.-M. *Chem. Rev.* **2011**, *111*, 3036.

(16) Reiss, G.; Hutten, A. *Nat Mater* **2005**, *4*, 725.

(17) Yacob, Z.; Nan, A.; Liebscher, J. *Adv. Synth. Catal.* **2012**, *354*, 3259.

(18) Di Corato, R.; Piacenza, P.; Musarò, M.; Buonsanti, R.; Cozzoli, P. D.; Zambianchi, M.; Barbarella, G.; Cingolani, R.; Manna, L.; Pellegrino, T. *Macromol. Biosci.* **2009**, *9*, 952.

(19) Beveridge, J. S.; Stephens, J. R.; Williams, M. E. *Annu. Rev. Anal.* **2011**, *4*, 251.

(20) Quach, A.; Bwambok, D. K.; Tarr, M. A. In *Encyclopedia of Analytical Chemistry*; John Wiley & Sons, Ltd: 2006.

(21) Boisselier, E.; Astruc, D. *Chem. Soc. Rev.* **2009**, *38*, 1759.

(22) Abou El-Nour, K. M. M.; Eftaiha, A. a.; Al-Warthan, A.; Ammar, R. A. A. *Arab.J.Chem.* **2010**, *3*, 135.

(23) Peng, Z.; Yang, H. *Nano Today* **2009**, *4*, 143.

(24) Nguyen, V. L.; Nguyen, D. C.; Hirata, H.; Ohtaki, M.; Hayakawa, T.; Nogami, M. *Adv. Nat. Sci.: Nanosci. Nanotechnol.* **2010**, *1*, 035012.

(25) Jamieson, T.; Bakhshi, R.; Petrova, D.; Pocock, R.; Imani, M.; Seifalian, A. M. *Biomaterials* **2007**, *28*, 4717.

(26) Drbohlavova, J.; Adam, V.; Kizek, R.; Hubalek, J. *Int. J. Mol. Sci.* **2009**, *10*, 656.

(27) Rogach, A. L.; Eychmüller, A.; Hickey, S. G.; Kershaw, S. V. *Small* **2007**, *3*, 536.

(28) Davila-Ibanez, A. B.; Legido-Soto, J. L.; Rivas, J.; Salgueirino, V. *Phys. Chem. Chem. Phys.* **2011**, *13*, 20146.

(29) Amiri, S.; Shokrollahi, H. *Materials Science and Engineering: C* **2013**, *33*, 1.

(30) Li, C.; Li, Z.; Du, X.; Du, C.; Liu, J. *Rare Metals* **2012**, *31*, 31.

(31) Vinayan, B. P.; Nagar, R.; Rajalakshmi, N.; Ramaprabhu, S. *Adv. Funct. Mater.* **2012**, *22*, 3519.
(32) Chen, Y.; Peng, D.-L.; Lin, D.; Luo, X. *Nanotechnology* **2007**, *18*, 505703.
(33) Cornell, R. M.; Schwertmann, U. In *The Iron Oxides*; Wiley-VCH Verlag GmbH & Co. KGaA: 2004, p 1.
(34) Bazylizinki, D. A.; Heywood, B. R.; Mann, S.; Frankel, R. B. *Nature* **1993**, *366*, 218.
(35) Komeili, A.; Li, Z.; Newman, D. K.; Jensen, G. J. *Science* **2006**, *311*, 242.
(36) Yan, L.; Zhang, S.; Chen, P.; Liu, H.; Yin, H.; Li, H. *Microbiol. Res.* **2012**, *167*, 507.
(37) http://nanotech-intro.blogspot.de/2008/04/introduction-to-nanotechnology.html
(38) NDT Resource Center, h. w. n.-e. o. E. C. M. P. H. h.
(39) Neoh, K. G.; Kang, E. T. *Polym. Chem.* **2011**, *2*, 747.
(40) Tombácz, E.; Bica, D.; Hajdú, A.; Illés, E.; Majzik, A.; Vékás, L. *J. Phys.: Condens. Matter* **2008**, *20*, 204103.
(41) Yang, H.-M.; Lee, H. J.; Jang, K.-S.; Park, C. W.; Yang, H. W.; Heo, W. D.; Kim, J.-D. *J. Mater. Chem.* **2009**, *19*, 4566.
(42) Qu, H.; Ma, H.; Zhou, W.; O'Connor, C. J. *Inorg. Chim. Acta.* **2012**, *389*, 60.
(43) Amstad, E.; Gillich, T.; Bilecka, I.; Textor, M.; Reimhult, E. *Nano Lett.* **2009**, *9*, 4042.
(44) Love, J. C.; Estroff, L. A.; Kriebel, J. K.; Nuzzo, R. G.; Whitesides, G. M. *Chem. Rev.* **2005**, *105*, 1103.
(45) Laurent, S.; Forge, D.; Port, M.; Roch, A.; Robic, C.; Vander Elst, L.; Muller, R. N. *Chem. Rev.* **2008**, *108*, 2064.
(46) Binder, W. H.; Weinstabl, H.; Sachsenhofer, R. *J.Nano Mat.* **2008**, *2008*.
(47) Wiogo, H. T. R.; Lim, M.; Bulmus, V.; Yun, J.; Amal, R. *Langmuir* **2010**, *27*, 843.
(48) Haddad, P. S.; Duarte, E. L.; Baptista, M. S.; Goya, G. F.; Leite, C. A. P.; Itri, R. In *Surf. Colloid Sci.*; Springer Berlin Heidelberg: 2004; Vol. 128, p 232.
(49) Hayashi, T.; Hirono, S.; Tomita, M.; Umemura, S. *Nature* **1996**, *381*, 772.
(50) Gupta, A. K.; Gupta, M. *Biomaterials* **2005**, *26*, 3995.
(51) Hong, L. S. W. a. R. Y.; , D. B. R., Ed.; nTech,: 2011.
(52) Rockenberger, J.; Scher, E. C.; Alivisatos, A. P. *J. Am. Chem. Soc.* **1999**, *121*, 11595.
(53) Farrell, D.; Majetich, S. A.; Wilcoxon, J. P. *J. Phys. Chem. B* **2003**, *107*, 11022.
(54) Sun, S.; Zeng, H. *J. Am. Chem. Soc.* **2002**, *124*, 8204.
(55) Hyeon, T.; Lee, S. S.; Park, J.; Chung, Y.; Na, H. B. *J. Am. Chem. Soc.* **2001**, *123*, 12798.
(56) Park, J.; An, K.; Hwang, Y.; Park, J.-G.; Noh, H.-J.; Kim, J.-Y.; Park, J.-H.; Hwang, N.-M.; Hyeon, T. *Nat Mater* **2004**, *3*, 891.
(57) Puntes, V. F.; Zanchet, D.; Erdonmez, C. K.; Alivisatos, A. P. *J. Am. Chem. Soc.* **2002**, *124*, 12874.
(58) Dumestre, F.; Chaudret, B.; Amiens, C.; Fromen, M.-C.; Casanove, M.-J.; Renaud, P.; Zurcher, P. *Angew. Chem. Int. Ed.* **2002**, *41*, 4286.
(59) Shevchenko, E. V.; Talapin, D. V.; Rogach, A. L.; Kornowski, A.; Haase, M.; Weller, H. *J. Am. Chem. Soc.* **2002**, *124*, 11480.

(60) Sun, S.; Murray, C. B.; Weller, D.; Folks, L.; Moser, A. *Science* **2000**, *287*, 1989.

(61) Stamm, K. L.; Garno, J. C.; Liu, G.-y.; Brock, S. L. *J. Am. Chem. Soc.* **2003**, *125*, 4038.

(62) Perera, S. C.; Tsoi, G.; Wenger, L. E.; Brock, S. L. *J. Am. Chem. Soc.* **2003**, *125*, 13960.

(63) Vijayakumar, R.; Koltypin, Y.; Felner, I.; Gedanken, A. *Mater. Sci. Eng., A* **2000**, *286*, 101.

(64) Pinkas, J.; Reichlova, V.; Zboril, R.; Moravec, Z.; Bezdicka, P.; Matejkova, J. *Ultrason. Sonochem.* **2008**, *15*, 257.

(65) A. Drmota M. Drofenik, J. K. a. A. Ž.; Najjar, D. R., Ed.; InTech: 2012.

(66) Deng, Y.; Wa

(90) Benbenishty-Shamir, H.; Gilert, R.; Gotman, I.; Gutmanas, E. Y.; Sukenik, C. N. *Langmuir* **2011**, *27*, 12082.
(91) Easo, S. L.; Mohanan, P. V. *Carbohydr. Polym.* **2013**, *92*, 726.
(92) Shen, C.-R.; Wu, S.-T.; Tsai, Z.-T.; Wang, J.-J.; Yen, T.-C.; Tsai, J.-S.; Shih, M.-F.; Liu, C.-L. *Polym. Int.* **2011**, *60*, 945.
(93) Lu, X.; Niu, M.; Qiao, R.; Gao, M. *J. Phys. Chem. B* **2008**, *112*, 14390.
(94) Yallapu, M.; Foy, S.; Jain, T.; Labhasetwar, V. *Pharm. Res.* **2010**, *27*, 2283.
(95) Kayal, S.; Ramanujan, R. V. *Mater. Sci. Eng., C* **2010**, *30*, 484.
(96) Boyer, C.; Whittaker, M. R.; Bulmus, V.; Liu, J.; Davis, T. P. *NPG Asia Mater* **2010**, *2*, 23.
(97) Liu, G.; Wang, Z.; Lee, S.; Ai, H.; Chen, X. In *Methods Enzymol.*; Nejat, D., Ed.; Academic Press: 2012; Vol. Volume 509, p 263.
(98) Hajdú, A.; Szekeres, M.; Tóth, I. Y.; Bauer, R. A.; Mihály, J.; Zupkó, I.; Tombácz, E. *Colloids Surf., B* **2012**, *94*, 242.
(99) Sharma, R.; Lamba, S.; Annapoorni, S. *J. Phys. D: Appl. Phys.* **2005**, *38*, 3354.
(100) Karsten, S.; Nan, A.; Turcu, R.; Liebscher, J. *J. Polym. Sci. A* **2012**, *50*, 3986.
(101) Molday, R. S.; Mackenzie, D. *J. Immunol. Methods* **1982**, *52*, 353.
(102) Lee, J.; Isobe, T.; Senna, M. *J. Colloid Interface Sci.* **1996**, *177*, 490.
(103) Socaci, C.; Rybka, M.; Magerusan, L.; Nan, A.; Turcu, R.; Liebscher, J. *J. Nanopart. Res.* **2013**, *15*, 1.
(104) Wang, S.; Zhou, Y.; Guan, W.; Ding, B. *Appl. Surf. Sci.* **2008**, *254*, 5170.
(105) Wang, W.-C.; Neoh, K.-G.; Kang, E.-T. *Macromol. Rapid Commun.* **2006**, *27*, 1665.
(106) Yuan, W.; Yuan, J.; Zhou, L.; Wu, S.; Hong, X. *Polymer* **2010**, *51*, 2540.
(107) Basuki, J. S.; Esser, L.; Zetterlund, P. B.; Whittaker, M. R.; Boyer, C.; Davis, T. P. *Macromolecules* **2013**, *46*, 6038.
(108) De Palma, R.; Peeters, S.; Van Bael, M. J.; Van den Rul, H.; Bonroy, K.; Laureyn, W.; Mullens, J.; Borghs, G.; Maes, G. *Chem. Mater.* **2007**, *19*, 1821.
(109) Narita, A.; Naka, K.; Chujo, Y. *Colloids Surf., A* **2009**, *336*, 46.
(110) Sun, Y.; Duan, L.; Guo, Z.; DuanMu, Y.; Ma, M.; Xu, L.; Zhang, Y.; Gu, N. *J. Magn. Magn. Mater.* **2005**, *285*, 65.
(111) Ye, Q.; Zhou, F.; Liu, W. *Chem. Soc. Rev.* **2011**, *40*, 4244.
(112) Zhu, B.; Edmondson, S. *Polymer* **2011**, *52*, 2141.
(113) Zhang, M.; He, X.; Chen, L.; Zhang, Y. *J. Mater. Chem.* **2010**, *20*, 10696.
(114) Si, J.; Yang, H. *Mater. Chem. Phys.* **2011**, *128*, 519.
(115) Liu, X.; Cao, J.; Li, H.; Li, J.; Jin, Q.; Ren, K.; Ji, J. *ACS Nano* **2013**, *7*, 9384.
(116) Dreyer, D. R.; Miller, D. J.; Freeman, B. D.; Paul, D. R.; Bielawski, C. W. *Langmuir* **2012**, *28*, 6428.
(117) Lee, H.; Rho, J.; Messersmith, P. B. *Adv. Mater.* **2009**, *21*, 431.
(118) Zhou, W.-H.; Lu, C.-H.; Guo, X.-C.; Chen, F.-R.; Yang, H.-H.; Wang, X.-R. *J. Mater. Chem.* **2010**, *20*, 880.
(119) Nan, A.; Turcu, R.; Craciunescu, I.; Pana, O.; Scharf, H.; Liebscher, J. *J. Polym. Sci. A* **2009**, *47*, 5397.
(120) Nan, A.; Turcu, R.; Liebscher, J. *J. Polym. Sci. A* **2012**, *50*, 1485.
(121) Dahlmann, J.; Rafler, G. *Acta Polym.* **1993**, *44*, 103.
(122) Dubois, P.; Jacobs, C.; Jerome, R.; Teyssie, P. *Macromolecules* **1991**, *24*, 2266.

(123) Kricheldorf, H.; Serra, A. *Polym. Bull.* **1985**, *14*, 497.
(124) Chabot, F.; Vert, M.; Chapelle, S.; Granger, P. *Polymer* **1983**, *24*, 53.
(125) Stolt, M.; Södergård, A. *Macromolecules* **1999**, *32*, 6412.
(126) Chamberlain, B. M.; Jazdzewski, B. A.; Pink, M.; Hillmyer, M. A.; Tolman, W. B. *Macromolecules* **2000**, *33*, 3970.
(127) Connor, E. F.; Nyce, G. W.; Myers, M.; Möck, A.; Hedrick, J. L. *J. Am. Chem. Soc.* **2002**, *124*, 914.
(128) Tanzi, M. C.; Verderio, P.; Lampugnani, M. G.; Resnati, M.; Dejana, E.; Sturani, E. *J. Mater. Sci. - Mater. Med.* **1994**, *5*, 393.
(129) Kang, S. M.; Rho, J.; Choi, I. S.; Messersmith, P. B.; Lee, H. *J. Am. Chem. Soc.* **2009**, *131*, 13224.
(130) Yu MK, P. J., Jon S. *Theranostics* **2012**, *2(1)*, 3.
(131) Gao, J.; Gu, H.; Xu, B. *Acc. Chem. Res.* **2009**, *42*, 1097.
(132) Fang, C.; Veiseh, O.; Kievit, F.; Bhattarai, N.; Wang, F.; Stephen, Z.; Li, C.; Lee, D.; Ellenbogen, R. G.; Zhang, M. *Nanomedicine* **2010**, *5*, 1357.
(133) Kim, J. S.; Valencia, C. A.; Liu, R.; Lin, W. *Bioconj. Chem.* **2007**, *18*, 333.
(134) Xi, P.; Cheng, K.; Sun, X.; Zeng, Z.; Sun, S. *Chem. Commun.* **2012**, *48*, 2952.
(135) Kim, H.; Dae, H.-M.; Park, C.; Kim, E. O.; Kim, D.; Kim, I.-H.; Kim, Y.-H.; Choi, Y. *J. Mater. Chem.* **2011**, *21*, 7742.
(136) Zhu, R.; Jiang, W.; Pu, Y.; Luo, K.; Wu, Y.; He, B.; Gu, Z. *J. Mater. Chem.* **2011**, *21*, 5464.
(137) Stutz, C.; Bilecka, I.; Thunemann, A. F.; Niederberger, M.; Borner, H. G. *Chem. Commun.* **2012**, *48*, 7176.
(138) Li, M.; Xu, L. Q.; Wang, L.; Wu, Y. P.; Li, J.; Neoh, K.-G.; Kang, E.-T. *Polym. Chem.* **2011**, *2*, 1312.
(139) Liu, G.; Wu, H.; Zheng, H.; Tang, L.; Hu, H.; Yang, H.; Yang, S. *J. Mater. Sci.* **2011**, *46*, 5959.
(140) Cho, E. J.; Jung, S.; Lee, K.; Lee, H. J.; Nam, K. C.; Bae, H.-J. *Chem. Commun.* **2010**, *46*, 6557.
(141) Chekina, N.; Horak, D.; Jendelova, P.; Trchova, M.; Benes, M. J.; Hruby, M.; Herynek, V.; Turnovcova, K.; Sykova, E. *J. Mater. Chem.* **2011**, *21*, 7630.
(142) Lin, Z.-A.; Zheng, J.-N.; Lin, F.; Zhang, L.; Cai, Z.; Chen, G.-N. *J. Mater. Chem.* **2011**, *21*, 518.
(143) Miguel-Sancho, N.; Bomatí-Miguel, O.; Colom, G.; Salvador, J. P.; Marco, M. P.; Santamaría, J. *Chem. Mater.* **2011**, *23*, 2795.
(144) van der Vlies, A. J.; O'Neil, C. P.; Hasegawa, U.; Hammond, N.; Hubbell, J. A. *Bioconj. Chem.* **2010**, *21*, 653.
(145) Hayashi, K.; Ono, K.; Suzuki, H.; Sawada, M.; Moriya, M.; Sakamoto, W.; Yogo, T. *Chem. Mater.* **2010**, *22*, 3768.
(146) Rutledge, R. D.; Warner, C. L.; Pittman, J. W.; Addleman, R. S.; Engelhard, M.; Chouyyok, W.; Warner, M. G. *Langmuir* **2010**, *26*, 12285.
(147) Tucker-Schwartz, A. K.; Farrell, R. A.; Garrell, R. L. *J. Am. Chem. Soc.* **2011**, *133*, 11026.
(148) Kolb, H. C.; Finn, M. G.; Sharpless, K. B. *Angew. Chem. Int. Ed.* **2001**, *40*, 2004.
(149) Himo, F.; Lovell, T.; Hilgraf, R.; Rostovtsev, V. V.; Noodleman, L.; Sharpless, K. B.; Fokin, V. V. *J. Am. Chem. Soc.* **2004**, *127*, 210.
(150) Hein, J. E.; Fokin, V. V. *Chem. Soc. Rev.* **2010**, *39*, 1302.

(151) White, M. A.; Johnson, J. A.; Koberstein, J. T.; Turro, N. J. *J. Am. Chem. Soc.* **2006**, *128*, 11356.

(152) Goldmann, A. S.; Schödel, C.; Walther, A.; Yuan, J.; Loos, K.; Müller, A. H. E. *Macromol. Rapid Commun.* **2010**, *31*, 1608.

(153) He, H.; Zhang, Y.; Gao, C.; Wu, J. *Chem. Commun.* **2009**, *0*, 1655.

(154) Hayashi, K.; Moriya, M.; Sakamoto, W.; Yogo, T. *Chem. Mater.* **2009**, *21*, 1318.

(155) Zhou, Y.; Wang, S.; Xie, Y.; Guan, W.; Ding, B.; Yang, Z.; Jiang, X. *Nanotechnology* **2008**, *19*, 175601.

(156) Lin, P.-C.; Ueng, S.-H.; Yu, S.-C.; Jan, M.-D.; Adak, A. K.; Yu, C.-C.; Lin, C.-C. *Org. Lett.* **2007**, *9*, 2131.

(157) Polito, L.; Monti, D.; Caneva, E.; Delnevo, E.; Russo, G.; Prosperi, D. *Chem. Commun.* **2008**, *0*, 621.

(158) Zhang, W.; Zhang, Y.; Shi, X.; Liang, C.; Xian, Y. *J. Mater. Chem.* **2011**, *21*, 16177.

(159) Cutler, J. I.; Zheng, D.; Xu, X.; Giljohann, D. A.; Mirkin, C. A. *Nano Lett.* **2010**, *10*, 1477.

(160) Das, M.; Bandyopadhyay, D.; Mishra, D.; Datir, S.; Dhak, P.; Jain, S.; Maiti, T. K.; Basak, A.; Pramanik, P. *Bioconj. Chem.* **2011**, *22*, 1181.

(161) Busacca, C. A.; Fandrick, D. R.; Song, J. J.; Senanayake, C. H. *Adv. Synth. Catal.* **2011**, *353*, 1825.

(162) Dalko, P. I. In *Enantioselective Organocatalysis*; Wiley-VCH Verlag GmbH & Co. KGaA: 2007, p 1.

(163) Dalko, P. I.; Moisan, L. *Angew. Chem. Int. Ed.* **2001**, *40*, 3726.

(164) Dalko, P. I.; Moisan, L. *Angew. Chem. Int. Ed.* **2004**, *43*, 5138.

(165) Giacalone, F.; Gruttadauria, M.; Agrigento, P.; Noto, R. *Chem. Soc. Rev.* **2012**, *41*, 2406.

(166) von Liebig, J. *Liebigs Ann.* **1860**, *113*, 246.

(167) Prelog, V.; Wilhelm, M. *Helv. Chim. Acta* **1954**, *37*, 1634.

(168) Pracejus, H. *Liebigs Ann.* **1960**, *634*, 9.

(169) Hajos, Z. G.; Parrish, D. R. *J. Org. Chem* **1974**, *39*, 1615.

(170) List, B.; Lerner, R. A.; Barbas, C. F. *J. Am. Chem. Soc.* **2000**, *122*, 2395.

(171) Northrup, A. B.; MacMillan, D. W. C. *J. Am. Chem. Soc.* **2002**, *124*, 2458.

(172) Verkade, J. M. M.; Hemert, L. J. C. v.; Quaedflieg, P. J. L. M.; Rutjes, F. P. J. T. *Chem. Soc. Rev.* **2008**, *37*, 29.

(173) Zheng, C.; Lu, Y.; Zhang, J.; Chen, X.; Chai, Z.; Ma, W.; Zhao, G. *Chem.--Eur. J.* **2010**, *16*, 5853.

(174) Jiang, H.; Rodríguez-Escrich, C.; Johansen, T. K.; Davis, R. L.; Jørgensen, K. A. *Angew. Chem. Int. Ed.* **2012**, *51*, 10271.

(175) Wu, X.; Liu, Q.; Fang, H.; Chen, J.; Cao, W.; Zhao, G. *Chem.--Eur. J.* **2012**, *18*, 12196.

(176) Bradshaw, B.; Parra, C.; Bonjoch, J. *Org. Lett.* **2013**.

(177) Waldmann, H.; Khedkar, V.; Dückert, H.; Schürmann, M.; Oppel, I. M.; Kumar, K. *Angew. Chem. Int. Ed.* **2008**, *47*, 6869.

(178) Takizawa, S.; Inoue, N.; Hirata, S.; Sasai, H. *Angew. Chem. Int. Ed.* **2010**, *49*, 9725.

(179) Goudedranche, S.; Raimondi, W.; Bugaut, X.; Constantieux, T.; Bonne, D.; Rodriguez, J. *Synthesis* **2013**, *45*, 1909.

(180) Bradshaw, B.; Bonjoch, J. *Synlett* **2012**, *2012*, 337.

(181) List, B. *Tetrahedron* **2002**, *58*, 5573.

(182) Mukherjee, S.; Yang, J. W.; Hoffmann, S.; List, B. *Chem. Rev.* **2007**, *107*, 5471.

(183) Erkkilä, A.; Majander, I.; Pihko, P. M. *Chem. Rev.* **2007**, *107*, 5416.

(184) Bertelsen, S.; Marigo, M.; Brandes, S.; Dinér, P.; Jørgensen, K. A. *J. Am. Chem. Soc.* **2006**, *128*, 12973.

(185) Albrecht, Ł.; Dickmeiss, G.; Acosta, F. C.; Rodríguez-Escrich, C.; Davis, R. L.; Jørgensen, K. A. *J. Am. Chem. Soc.* **2012**, *134*, 2543.

(186) Albrecht, Ł.; Cruz Acosta, F.; Frail Jørgensen, K. A. *Angew. Chem. Int. Ed.* **2012**, *51*, 9088.

(187) Kumar, I.; Ramaraju, P.; Mir, N. A. *Org. Biomol. Chem.* **2013**, *11*, 709.

(188) MacMillan, D. W. C. *Nature* **2008**, *455*, 304.

(189) Heitbaum, M.; Glorius, F.; Escher, I. *Angew. Chem. Int. Ed.* **2006**, *45*, 4732.

(190) Gruttadauria, M.; Giacalone, F.; Noto, R. *Chem. Soc. Rev.* **2008**, *37*, 1666.

(191) Zhang, L.; Luo, S.; Cheng, J.-P. *Catal. Sci. Tech.* **2011**, *1*, 507.

(192) Headly, A. D.; Ni, B. *ChemInform* **2009**, *40*, i.

(193) Shah, J.; Blumenthal, H.; Yacob, Z.; Liebscher, J. *Adv. Synth. Catal.* **2008**, *350*, 1267.

(194) Yacob, Z.; Shah, J.; Leistner, J.; Liebscher, J. *Synlett* **2008**, *2008*, 2342.

(195) Schätz, A.; Reiser, O.; Stark, W. J. *Chem.--Eur. J.* **2010**, *16*, 8950.

(196) Mrówczyński, R. N., A.;Liebscher,J. *RSC Advances (accepted for publication)* **2013**.

(197) Wang, B. G.; Ma, B. C.; Wang, Q.; Wang, W. *Adv. Synth. Catal.* **2010**, *352*, 2923.

(198) Riente, P.; Mendoza, C.; Pericas, M. A. *Journal of Materials Chemistry* **2011**, *21*, 7350.

(199) Keller, M.; Perrier, A.; Linhardt, R.; Travers, L.; Wittmann, S.; Caminade, A.-M.; Majoral, J.-P.; Reiser, O.; Quali, A. *Adv. Synth. Catal.***2013**.

(200) Luo, S. Z.; Zheng, X. X.; Cheng, J. P. *Chem Commun.* **2008**, 5719.

(201) Gleeson, O.; Tekoriute, R.; Gun'ko, Y. K.; Connon, S. J. *Chem-Eur J* **2009**, *15*, 5669.

(202) Gleeson, O.; Davies, G. L.; Peschiulli, A.; Tekoriute, R.; Gun'ko, Y. K.; Connon, S. J. *Org. Biomol. Chem.* **2011**, *9*, 7929.

(203) Jiang, X.; Zhu, H.; Shi, X.; Zhong, Y.; Li, Y.; Wang, R. *Adv. Synth. Catal.* **2013**, *355*, 308.

(204) Yang, H. L.; Li, S. W.; Wang, X. Y.; Zhang, F. W.; Zhong, X.; Dong, Z. P.; Ma, J. T. *J Mol Catal a-Chem* **2012**, *363*, 404.

(205) Kong, Y.; Tan, R.; Zhao, L.; Li, C.; Yin, D. *Green Chem* **2013**.

(206) Riente, P.; Yadav, J.; Pericas, M. A. *Org Lett* **2012**, *14*, 3668.

(207) Gawande, M. B.; Velhinho, A.; Nogueira, I. D.; Ghumman, C. A. A.; Teodoro, O. M. N. D.; Branco, P. S. *Rsc Adv* **2012**, *2*, 6144.

(208) Mondal, J.; Sen, T.; Bhaumik, A. *Dalton Transactions* **2012**, *41*, 6173.

(209) Li, N.; Binder, W. H. *J. Mater. Chem.* **2011**, *21*, 16717.

(210) Mrówczyński, R.; Rednic, L.; Turcu, R.; Liebscher, J. *J. Nanopart. Res.* **2012**, *14*, 1.

(211) Sikorski, J. A.; Devadas, B.; Zupec, M. E.; Freeman, S. K.; Brown, D. L.; Lu, H.-F.; Nagarajan, S.; Mehta, P. P.; Wade, A. C.; Kishore, N. S.; Bryant, M. L.; Getman, D. P.; McWherter, C. A.; Gordon, J. I. *Peptide Science* **1997**, *43*, 43.

(212) Font, D.; Jimeno, C.; Pericàs, M. A. *Org. Lett.* **2006**, *8*, 4653.

(213) Kacprzak, K. M.; Lindner, W.; Maier, N. M. *Chirality* **2008**, *20*, 441.

(214) Mader, H. S.; Link, M.; Achatz, D. E.; Uhlmann, K.; Li, X.; Wolfbeis, O. S. *Chem.--Eur. J.* **2010**, *16*, 5416.
(215) Mereyala, H. B.; Gurrala, S. R. *Carbohydr. Res.* **1998**, *307*, 351.
(216) Samanta, B.; Patra, D.; Subramani, C.; Ofir, Y.; Yesilbag, G.; Sanyal, A.; Rotello, V. M. *Small* **2009**, *5*, 685.
(217) Mager, I.; Zeitler, K. *Org. Lett.* **2010**, *12*, 1480.
(218) Nehlig, E.; Motte, L.; Guénin, E. *Catal. Today* **2013**, *208*, 90.
(219) *High-Throughput Synthesis: Principles and Practices*; MARCEL DEKKER, INC, 2001.
(220) Bellis, E.; Kokotos, G. *Tetrahedron* **2005**, *61*, 8669.
(221) Seo, J. W.; Srisook, E.; Son, H. J.; Hwang, O.; Cha, Y.-N.; Chi, D. Y. *Bioorg. Med. Chem. Lett.* **2005**, *15*, 3369.
(222) Alza, E.; Pericàs, M. A. *Adv. Synth. Catal.* **2009**, *351*, 3051.
(223) Mrówczyński, R.; Turcu, R.; Leostean, C.; Scheidt, H. A.; Liebscher, J. *Mater. Chem. Phys.* **2013**, *138*, 295.
(224) Lee, J. W.; Jun, S. I.; Kim, K. *Tetrahedron Lett.* **2001**, *42*, 2709.
(225) Sureshkumar, M.; Lee, C.-K. *Carbohydr. Polym.* **2011**, *84*, 775.
(226) Deiters, A.; Cropp, T. A.; Mukherji, M.; Chin, J. W.; Anderson, J. C.; Schultz, P. G. *J. Am. Chem. Soc.* **2003**, *125*, 11782.
(227) Panella, B.; Vargas, A.; Ferri, D.; Baiker, A. *Chem. Mater.* **2009**, *21*, 4316.
(228) Lindberg, B. J.; Hamrin, K.; Johansson, G.; Gelius, U.; Fahlman, C.; C., N.; Siegbahn, K. *Phys. Scr.* **1970**, *1*, 286.
(229) Melville, D. B. *J. Biol. Chem.* **1954**, *208*, 495.
(230) Liebscher, J.; Mrówczyński, R.; Scheidt, H. A.; Filip, C.; Hădade, N. D.; Turcu, R.; Bende, A.; Beck, S. *Langmuir* **2013**, *29*, 10539.
(231) Kaxiras, E.; Tsolakidis, A.; Zonios, G.; Meng, S. *Phys. Rev. Lett.* **2006**, *97*, 218102.
(232) Shalev, T.; Gopin, A.; Bauer, M.; Stark, R. W.; Rahimipour, S. *J. Mater. Chem.* **2012**, *22*, 2026.
(233) Yanagisawa, H.; Ishihara, S.; Ando, A.; Kanazaki, T.; Miyamoto, S.; Koike, H.; Iijima, Y.; Oizumi, K.; Matsushita, Y.; Hata, T. *J. Med. Chem.* **1987**, *30*, 1984.
(234) Dalko, P. I. *Enantioselective Organocatalysis*; Wiley-VCH, Weinheim, 2007.
(235) Huang, W.-B.; Liu, Q.-W.; Zheng, L.-Y.; Zhang, S.-Q. *Catal. Lett.* **2011**, *141*, 191.
(236) Luo, H. G.; Tan, R.; Kong, Y.; Li, C. Y.; Yin, D. H. *Chinese J Catal* **2012**, *33*, 1133.
(237) Gu, R.; Xu, W. Z.; Charpentier, P. A. *J. Polym. Sci. A* **2013**, *51*, 3941.
(238) Wang, W.-C.; Wang, J.; Liao, Y.; Zhang, L.; Cao, B.; Song, G.; She, X. *J. Appl. Polym. Sci.* **2010**, *117*, 534.
(239) Martin, O.; Avérous, L. *Polymer* **2001**, *42*, 6209.
(240) Elshahawy, W.; Sikalidis, C., Ed.; InTech: 2001.
(241) Wu, C.; Fu, X.; Li, S. *Eur. J. Org. Chem.* **2011**, *2011*, 1291.
(242) Kristensen, T. E.; Vestli, K.; Jakobsen, M. G.; Hansen, F. K.; Hansen, T. *J. Org. Chem* **2010**, *75*, 1620.
(243) Cai, H.; Guengerich, F. P. *J. Am. Chem. Soc.* **1999**, *121*, 11656.
(244) Luo, S.; Xu, H.; Mi, X.; Li, J.; Zheng, X.; Cheng, J.-P. *J. Org. Chem* **2006**, *71*, 9244.
(245) Dahlin, N.; Bøgevig, A.; Adolfsson, H. *Adv. Synth. Catal.* **2004**, *346*, 1101.

(246) Yin, Y.; Huang, X.; Lv, C.; Wang, L.; Yu, S.; Luo, Q.; Xu, J.; Liu, J. *Macromol. Biosci.* **2010**, *10*, 1505.

(247) Haridas, V.; Sharma, Y. K.; Sahu, S.; Verma, R. P.; Sadanandan, S.; Kacheshwar, B. G. *Tetrahedron* **2011**, *67*, 1873.

(248) Wu, C.; Long, X.; Li, S.; Fu, X. *Tetrahedron: Asymmetry* **2012**, *23*, 315.

7 Appendix

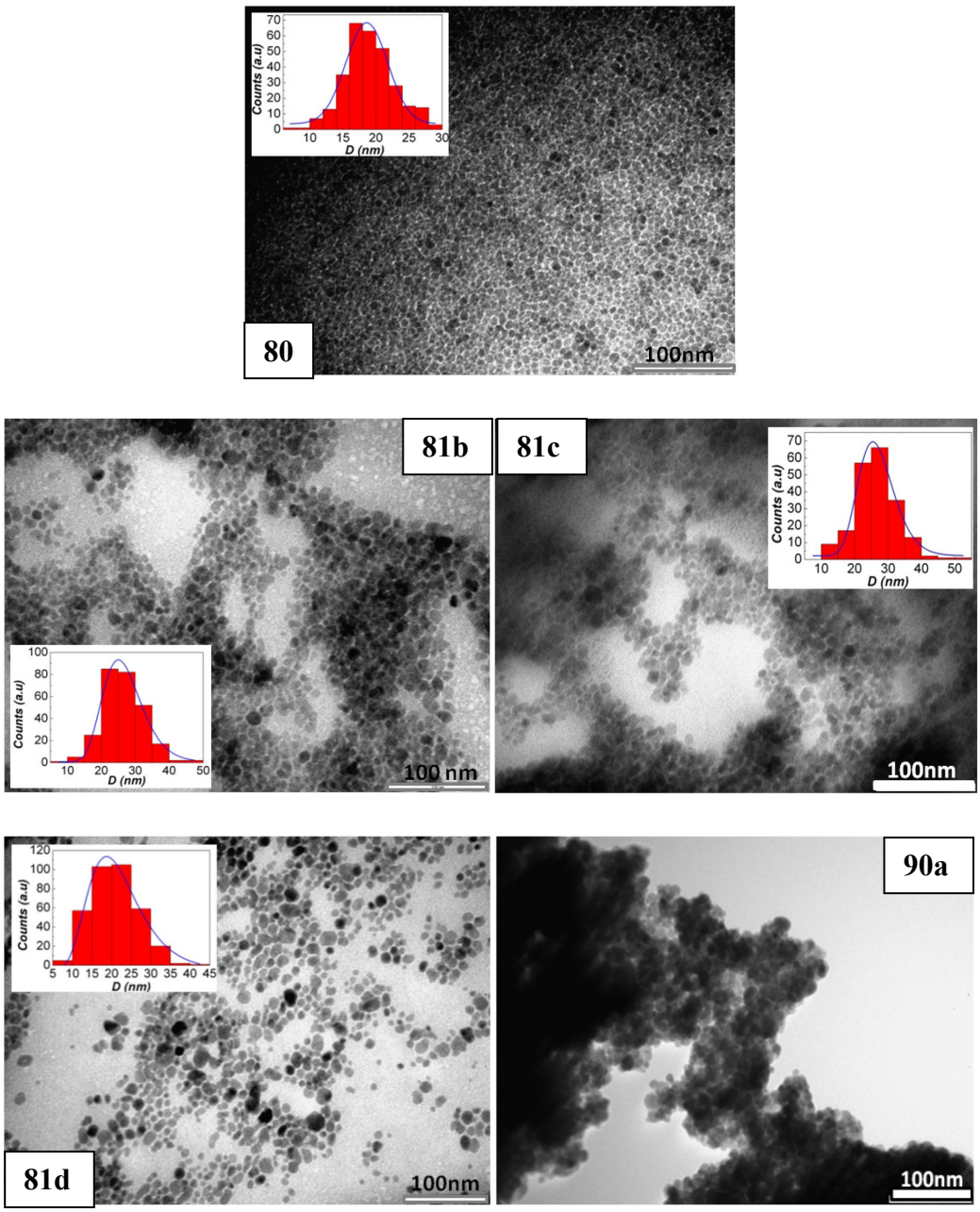

A 1 TEM pictures of fatty acids stabilized nanoparticles **80, 81b-d** and **90a**.

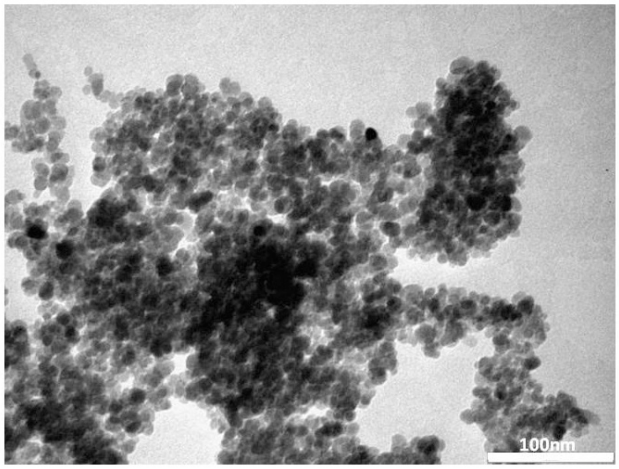

A 2 TEM of magnetite NP **95**.

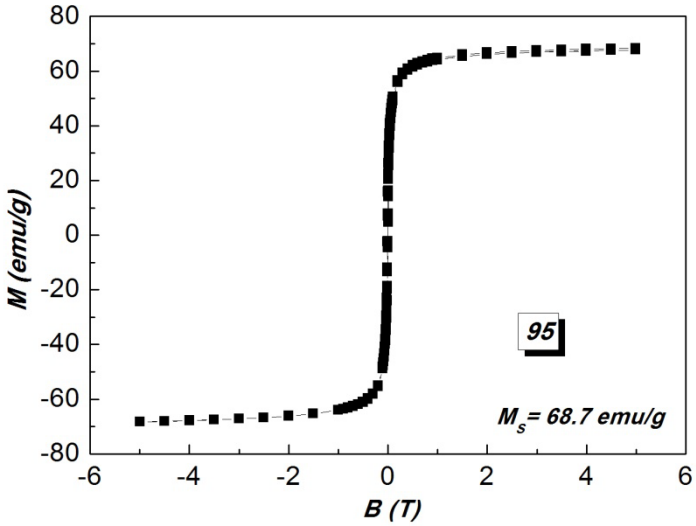

A 3 Magnetization vs. applied magnetic field of magnetite **95.**

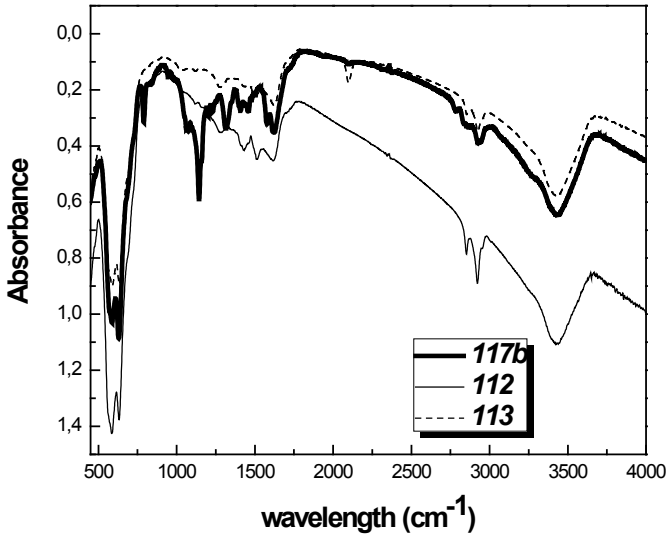
Absorbance
0,0
0,2
0,4
0,6
0,8
1,0
1,2
1,4
500
1000
1500
2000
2500
3000
3500
4000
wavelength (cm-1)
117b
112
113

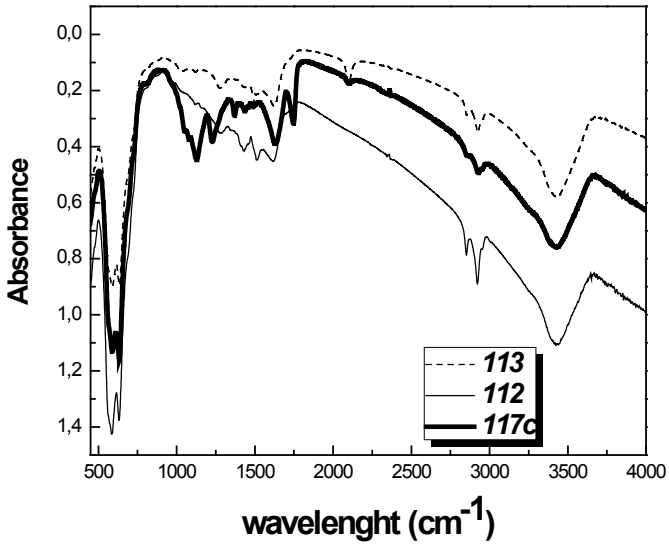
Absorbance
0,0
0,2
0,4
0,6
0,8
1,0
1,2
1,4
500
1000
1500
2000
2500
3000
3500
4000
wavelenght (cm-1)
113
112
117c

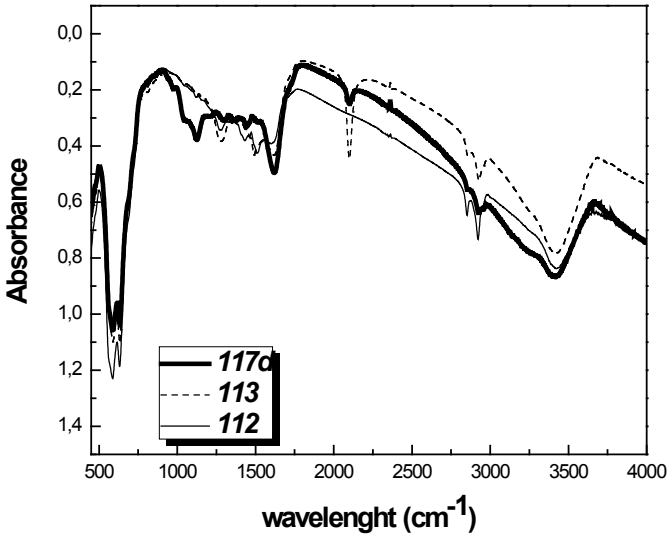

A 4 FTIR spectra of magnetite NP **117b**, **117c**, **117d**.

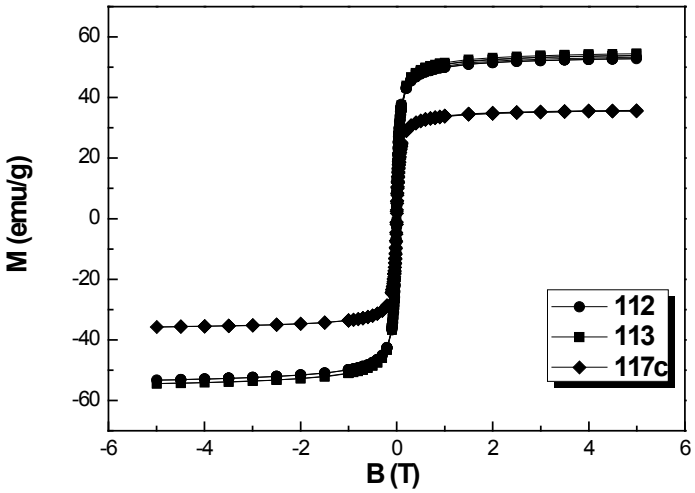

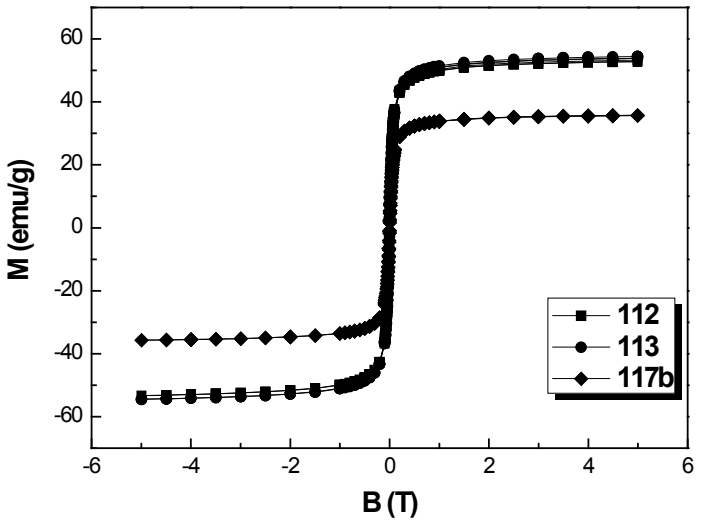

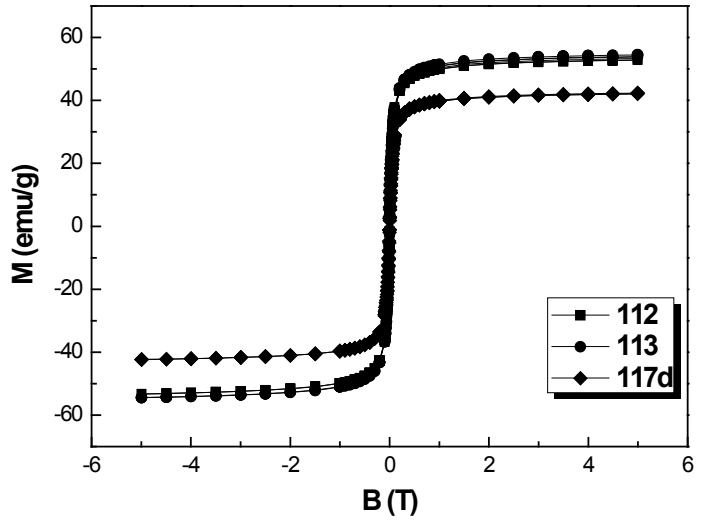

A 5 Magnetization vs. applied magnetic field at room temperature of magnetic nanoparticles **112**, **113** and **117b-d**.

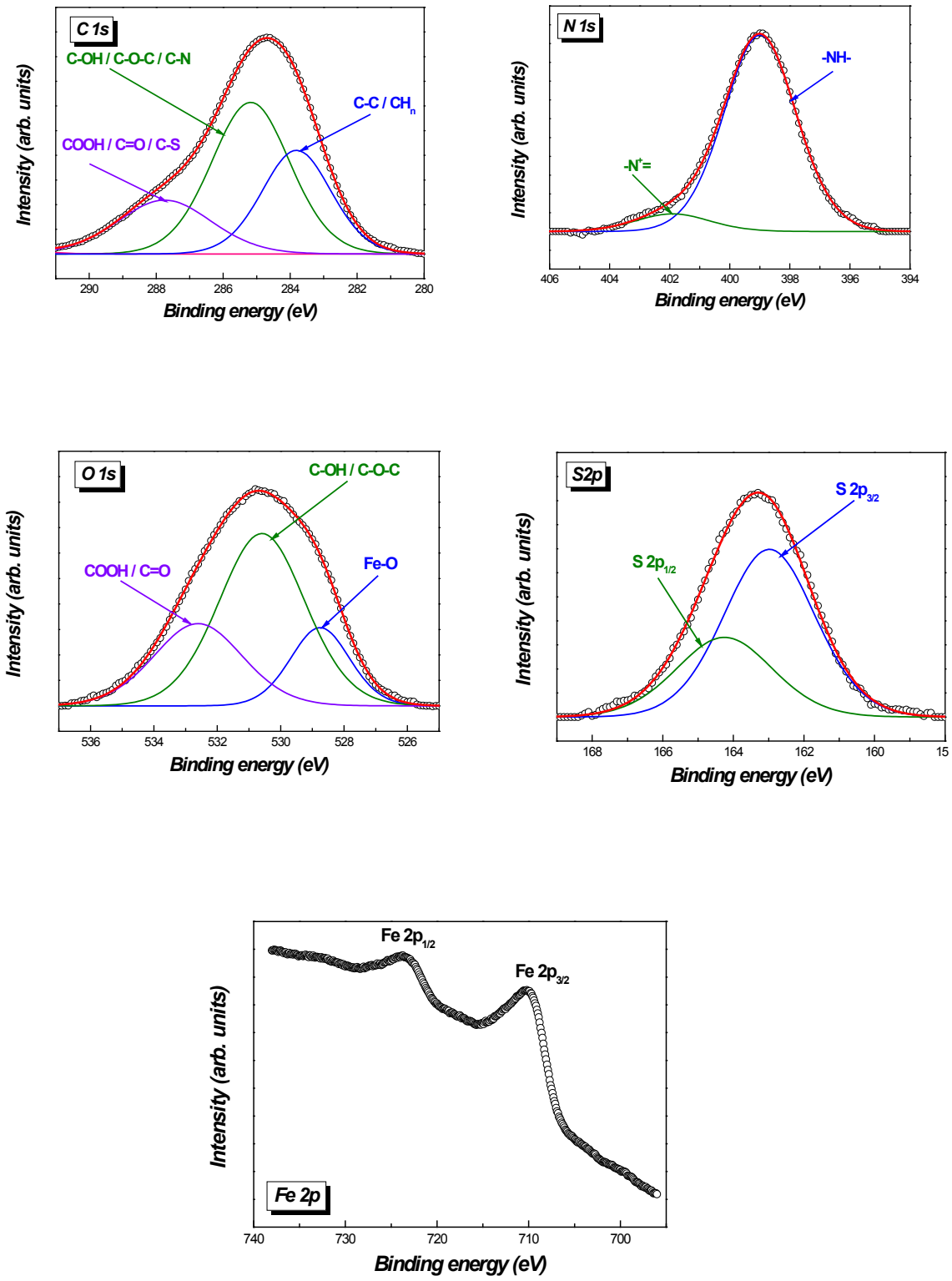

A 6 High **resolution** XPS spectra of biotin functionalized magnetite **120**.

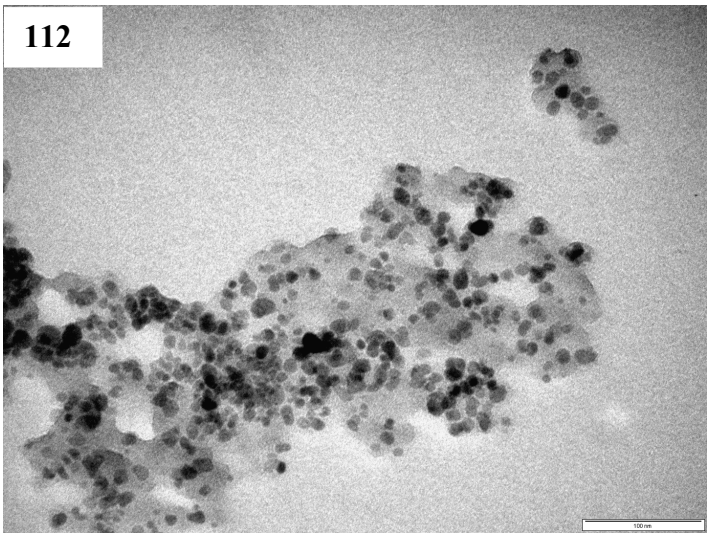

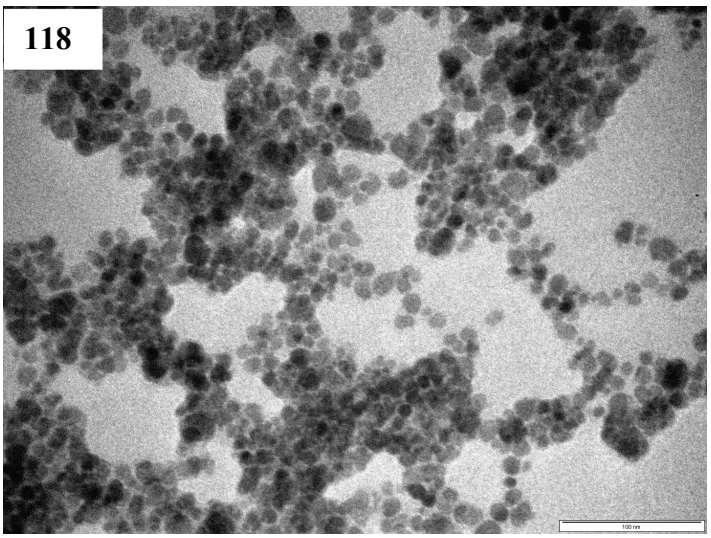

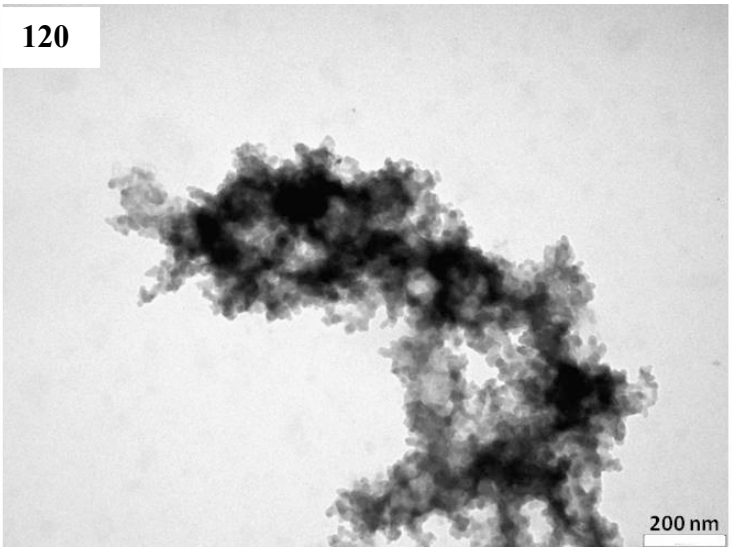

A 7 TEM pictures of magnetite NP functionalized NP **112**, **118** and **120**.

.

Table 7. ES(+)-HRMS peaks of PDA samples prepared in Tris or Phosphate buffers.

No.	*m/z* peak of PDA sample prepared in		Calculated $[M+H]^+$ mass	Oligomer
	Phosphate buffer (Δ ppm)*	TRIS buffer (Δ ppm)*		
1	438.0730 (2 ppm)	438.0740 (4 ppm)	438.0721	3Q
2	440.0891 (3 ppm)	440.0896 (4 ppm)	440.0877	3Q+2
3	442.1048 (3 ppm)	442.1052 (4 ppm)	442.1034	3Q+4
4	444.1204 (3 ppm)	444.1207 (4 ppm)	444.1190	3Q+6
5	446.1360 (3 ppm)	446.1363 (4 ppm)	446.1347	3Q+8
6	448.1516 (3 ppm)	448.1519 (4 ppm)	448.1503	3Q+10
7	450.1673 (3 ppm)	450.1676 (4 ppm)	450.1660	3Q+12
8	452.1830 (3 ppm)	452.1834 (4 ppm)	452.1818	3Q+16
9	454.1987 (3 ppm)	454.1990 (4 ppm)	454.1973	3Q+18
10	587.2154 (163 ppm)	587.2159 (164 ppm)	587.1197	4Q+4
11	589.1372 (3 ppm)	589.1376 (4 ppm)	589.1354	4Q+6
12	591.1528 (3 ppm)	591.1534 (4 ppm)	591.1510	4Q+8
13	593.1685 (3 ppm)	593.1690 (4 ppm)	593.1667	4Q+10
14	595.1841 (3 ppm)	595.1845 (4 ppm)	595.1823	4Q+12
15	597.1998 (3 ppm)	597.2003 (4 ppm)	597.1980	4Q+14
16	599.2155 (3 ppm)	599.2159 (4 ppm)	599.2136	4Q+16
17	601.2311 (3 ppm)	601.2316 (4 ppm)	601.2293	4Q+18

18	736.1699 (3 ppm)	736.1710 (5 ppm)	736.1674	5Q+8
19	738.1856 (3 ppm)	738.1863 (4 ppm)	738.1831	5Q+10
20	740.2010 (3 ppm)	740.2019 (4 ppm)	740.1987	5Q+12
21	742.2168 (3 ppm)	742.2177 (4 ppm)	742.2144	5Q+14
22	744.2325 (3 ppm)	744.2333 (4 ppm)	744.2300	5Q+16
23	746.2481 (3 ppm)	746.2489 (4 ppm)	746.2457	5Q+18
24	748.2637 (3 ppm)	748.2646 (4 ppm)	748.2613	5Q+20
25	750.2794 (3 ppm)	750.2800 (4 ppm)	750.2770	5Q+22
26	1199.4348(1ppm)	-	1199.4362	8Q+36

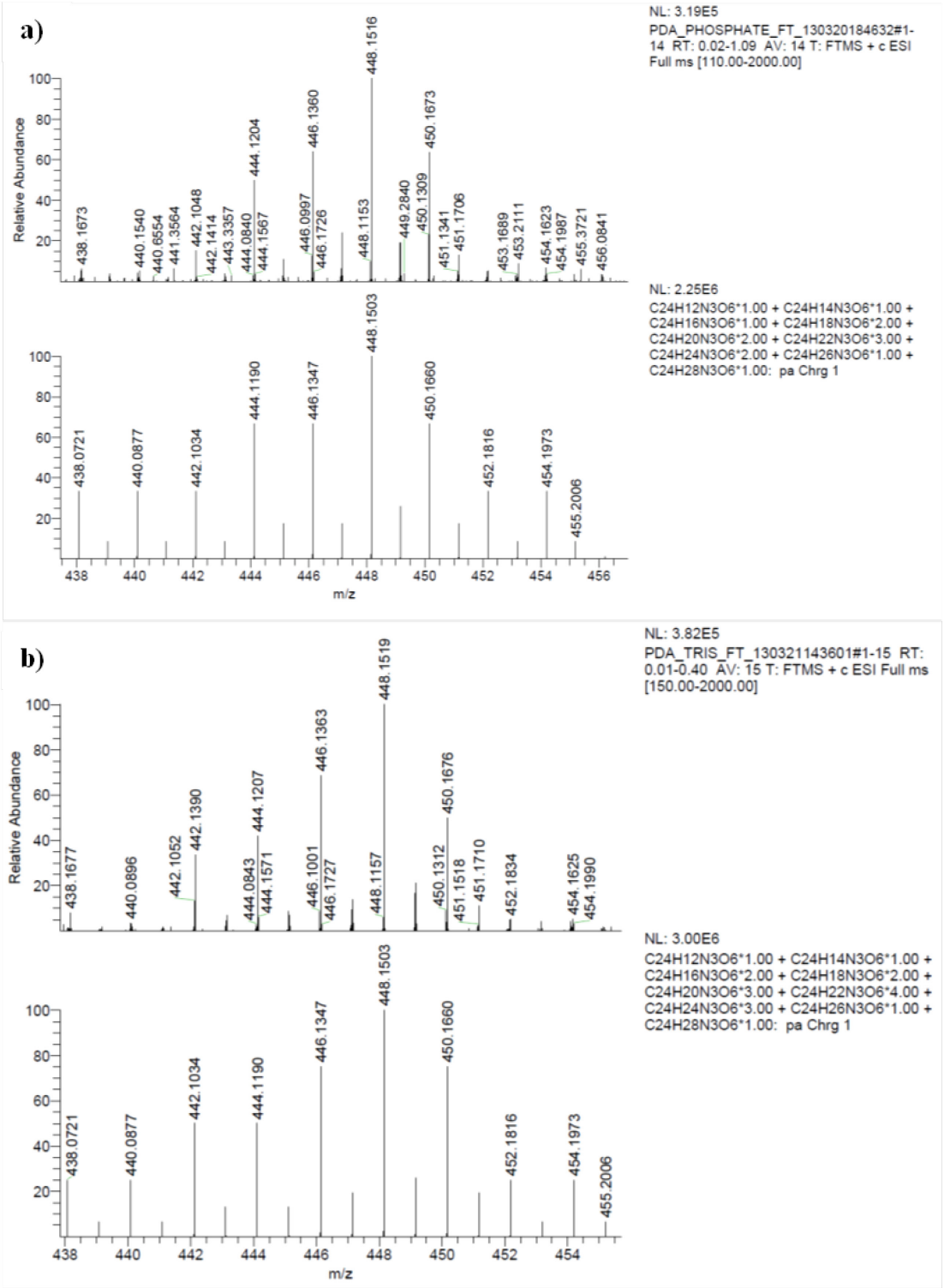

A 8 ES(+)-HRMS spectra (fragments) of the PDA samples (0.1 mg/mL) in methanol/DMSO/TFA = 97/2/1 prepared in phosphate (a) and Tris (b) buffers. Comparison of the experimental spectra (top) and simulated isotopic patterns (bottom).

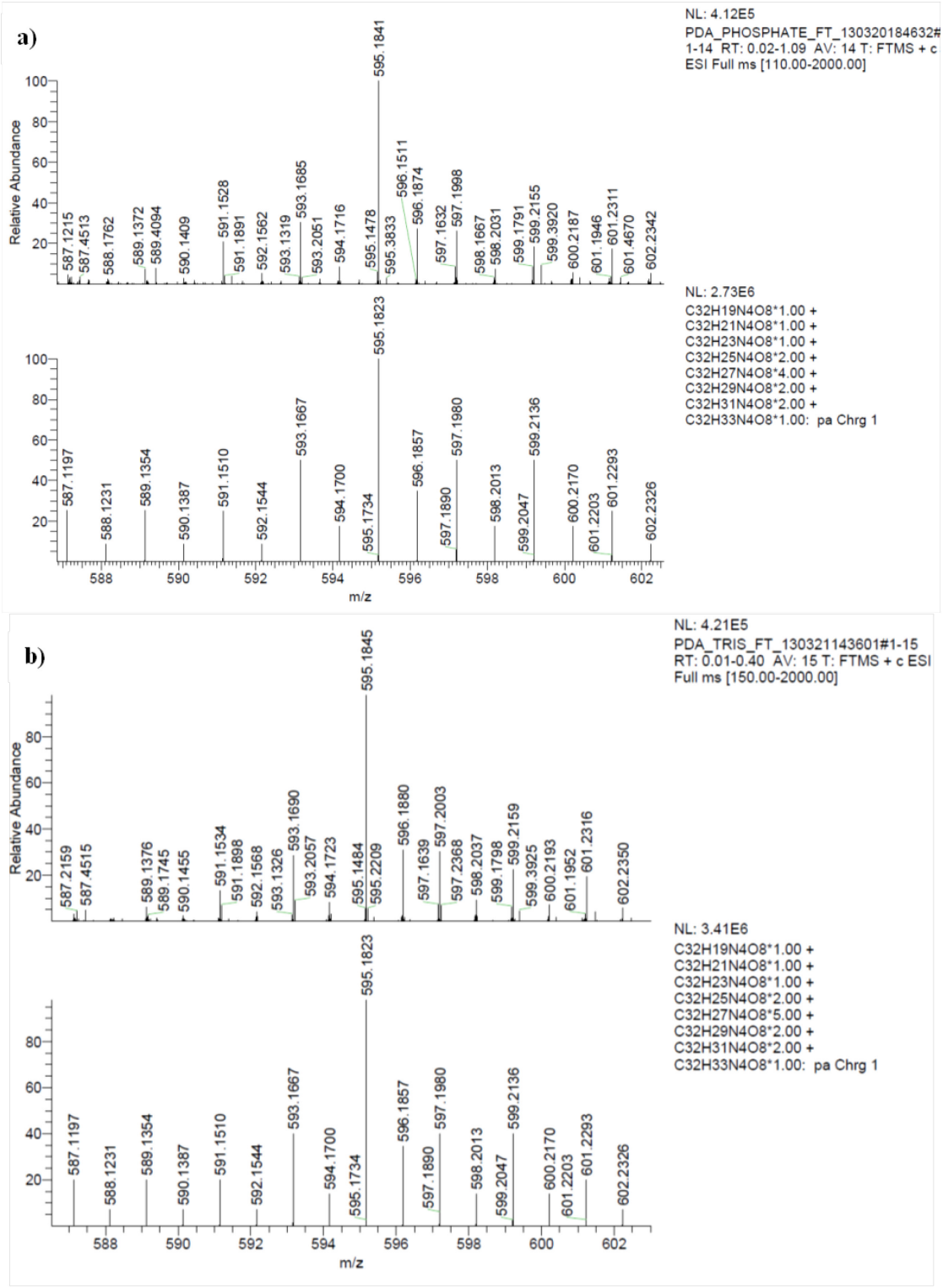

A 9 ES(+)-HRMS spectra (fragments) of the PDA samples (0.1 mg/mL) in methanol/DMSO/TFA = 97/2/1 prepared in phosphate (a) and Tris (b) buffers. Comparison of the experimental spectra (top) and simulated isotopic patterns (bottom).

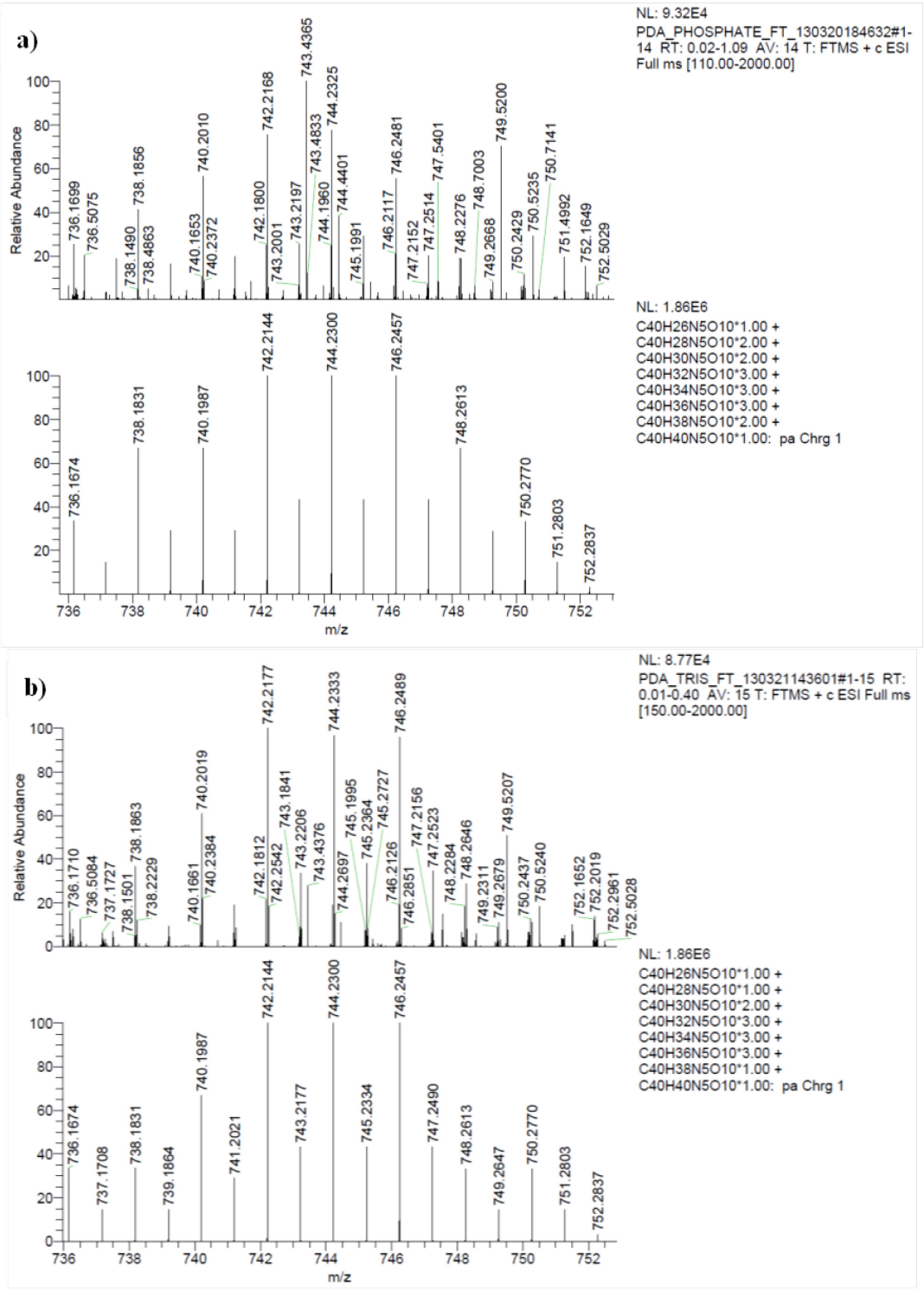

A 10 ES(+)-HRMS spectra (fragments) of the PDA samples (0.1 mg/mL) in methanol/DMSO/TFA = 97/2/1 prepared in phosphate (a) and Tris (b) buffers. Comparison of the experimental spectra (top) and simulated isotopic patterns (bottom).

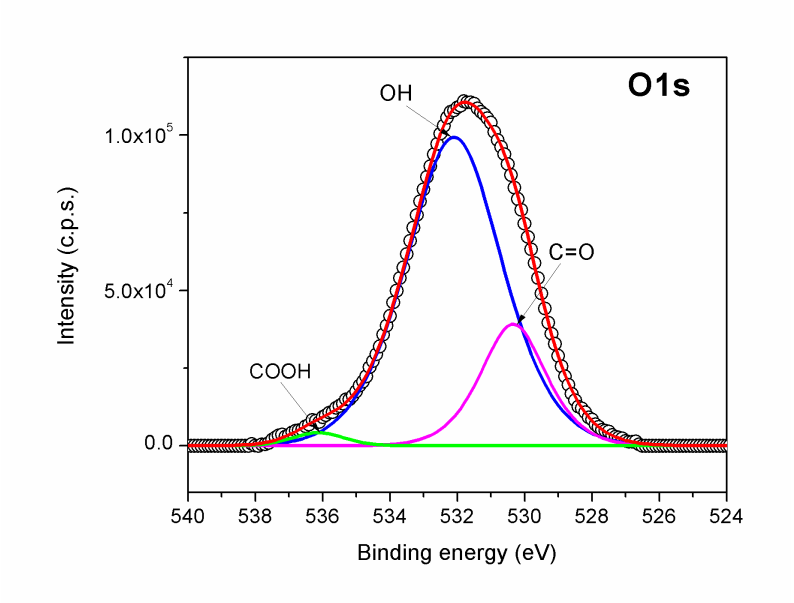

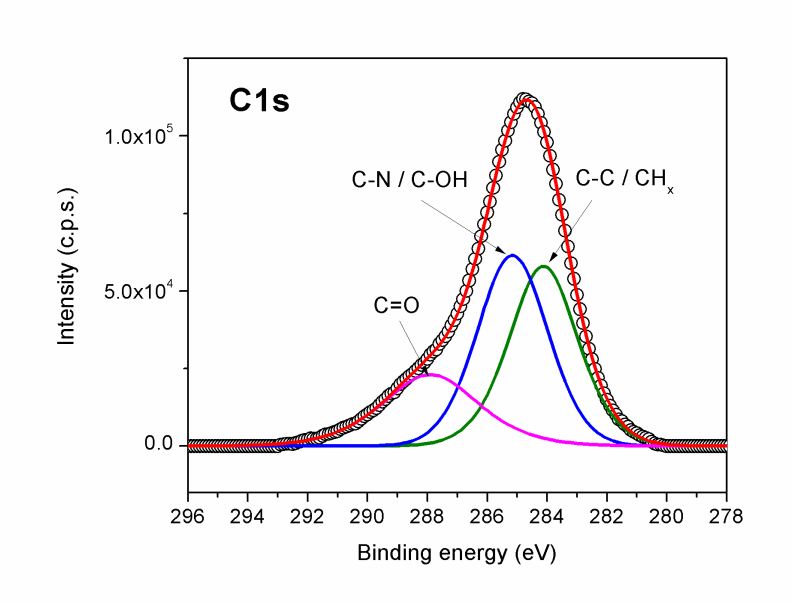

A 11 High resolution XPS spectra of O and C elements for polydopamine **132**.

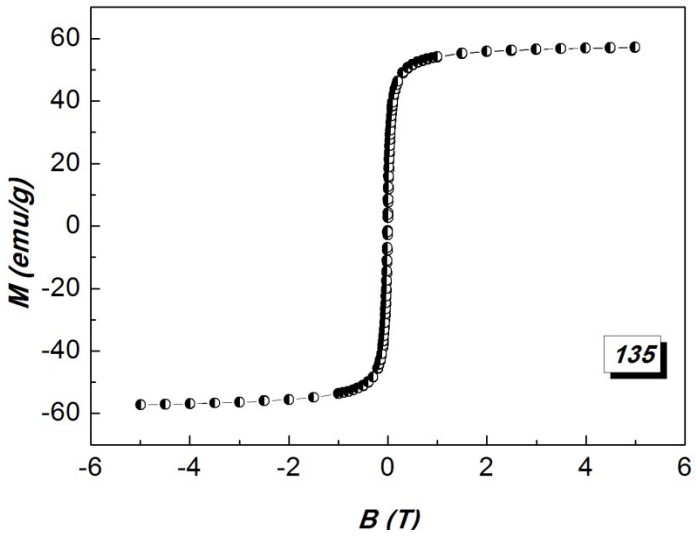

A 12 Magnetization curve of magnetite NP **135**.

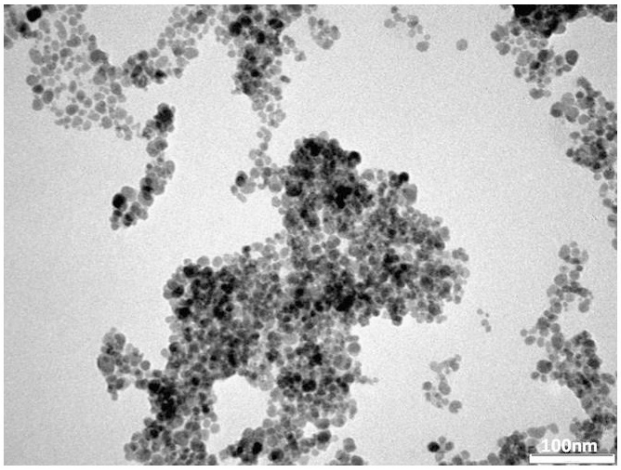

A 13 TEM picture of magnetite NP **135** modified with cysteine.

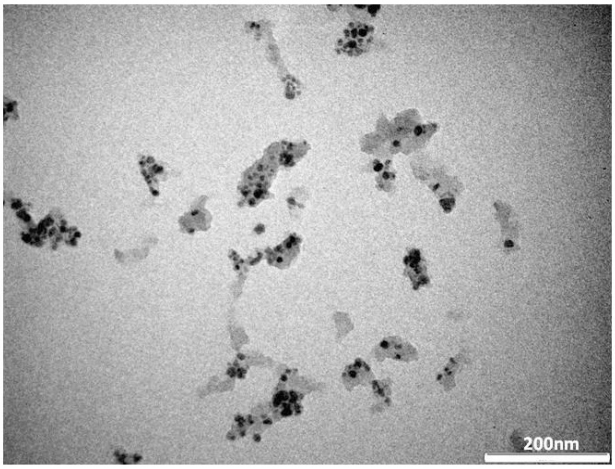

NP 112

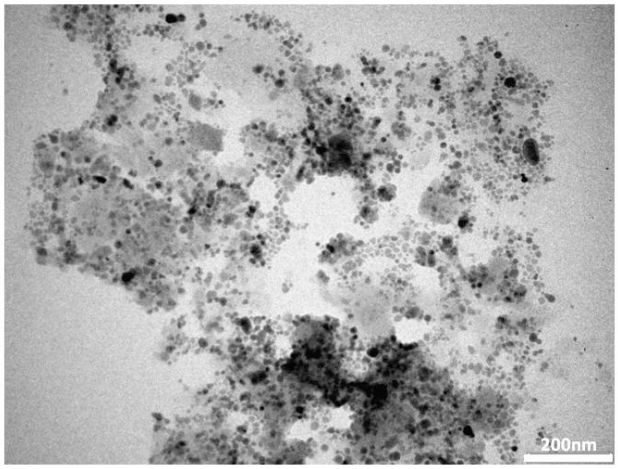

NP 138

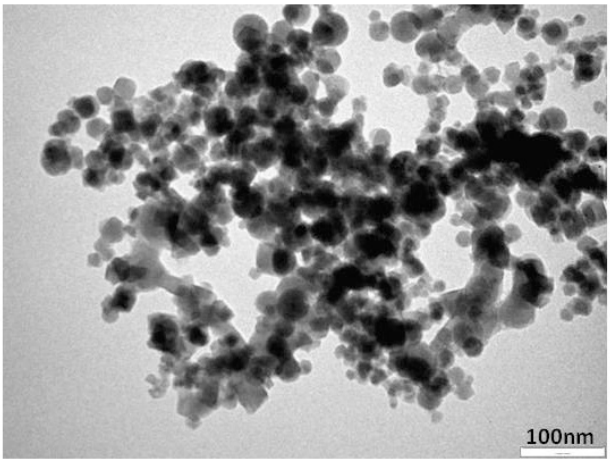

NP 136

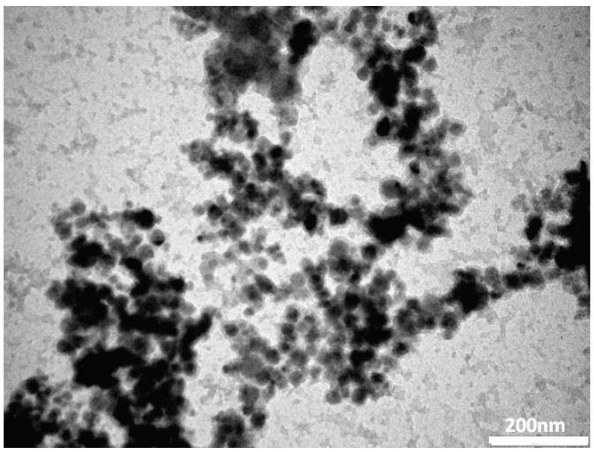

NP 137

A 14 TEM picture of **112**, **138**, **136** and **137**.

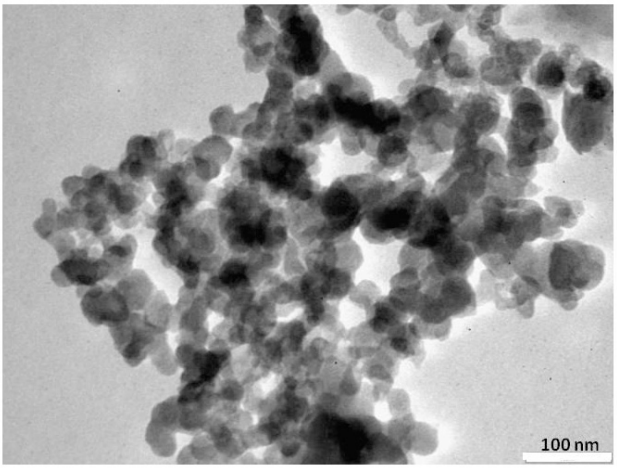

NP 148

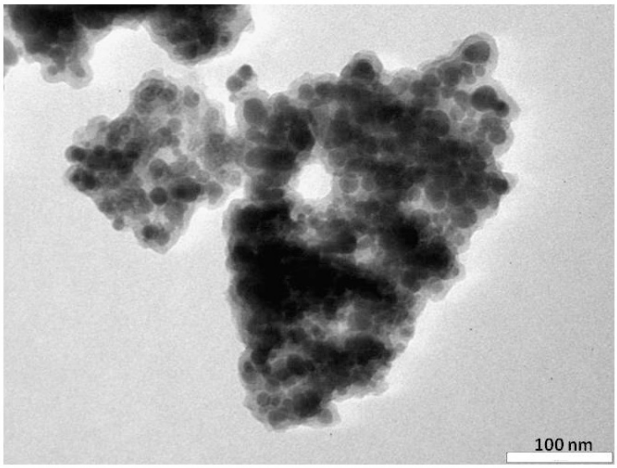

NP 150

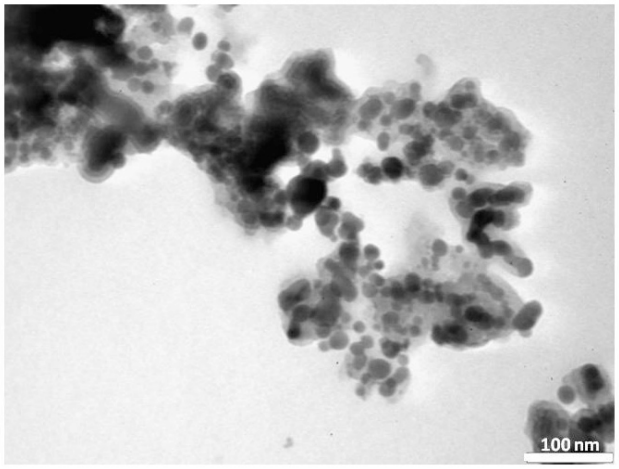

NP 151

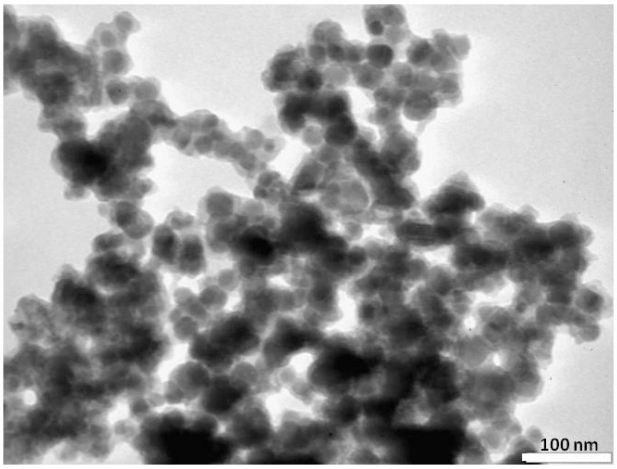

NP 152

A 15 TEM picture for NP **148**, **150**, **151**, and **152**.

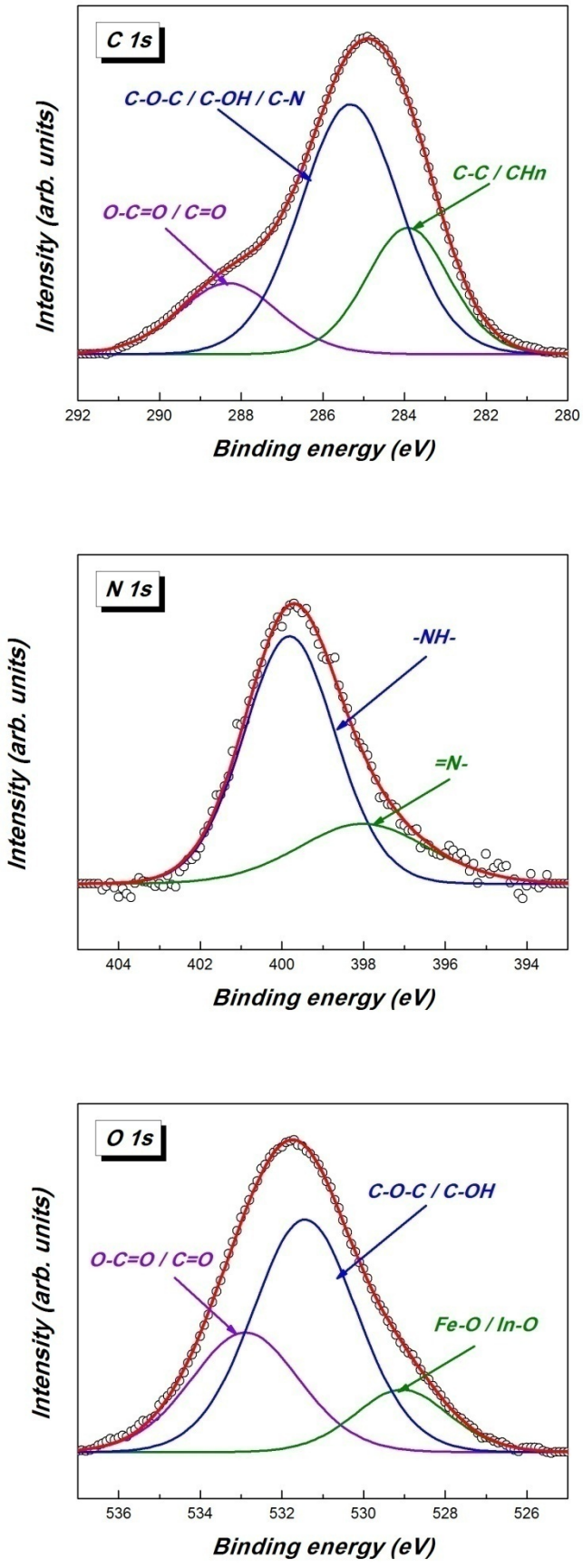

A 16 High resolution XPS spectra of NP **156**.

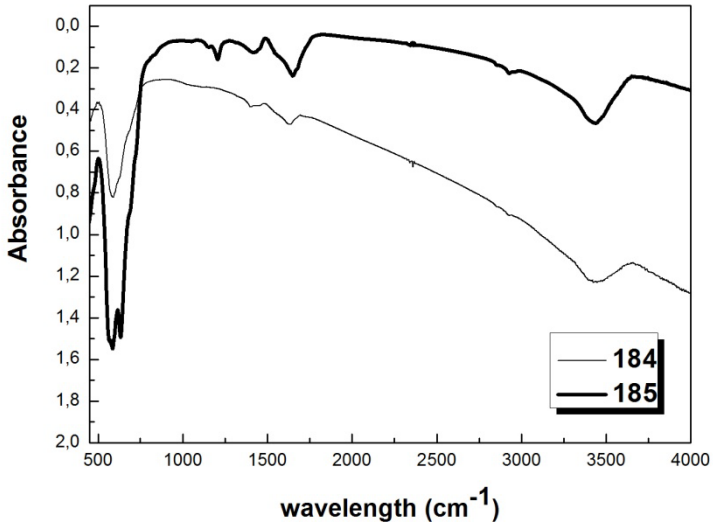

A 17 FTIR spectra of NP **184** and **185**.

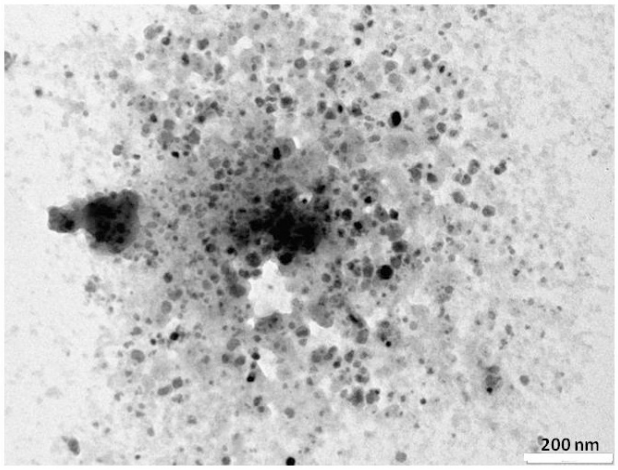

NP 179

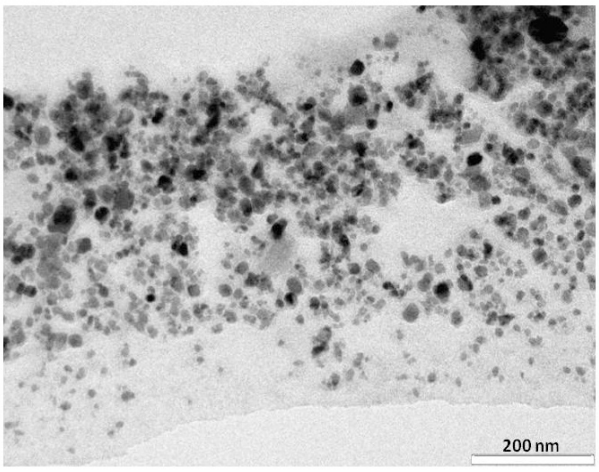

NP 180a

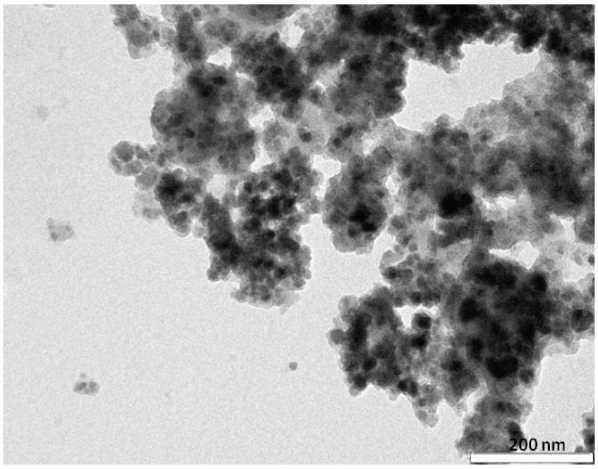

NP 180b

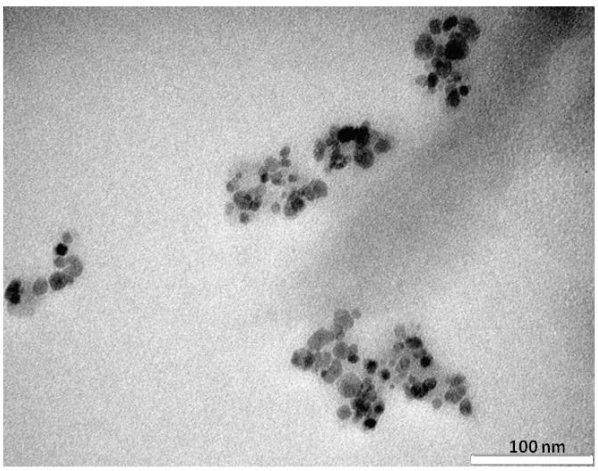

NP 181

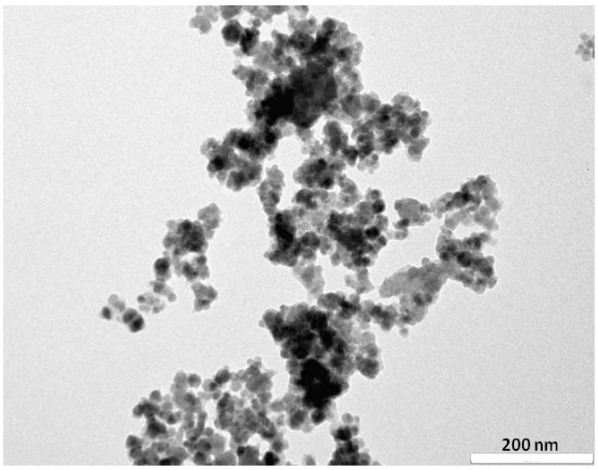

NP 182a

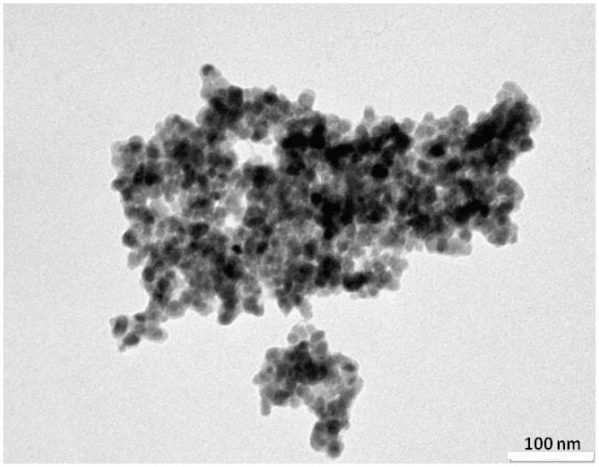

NP 182b

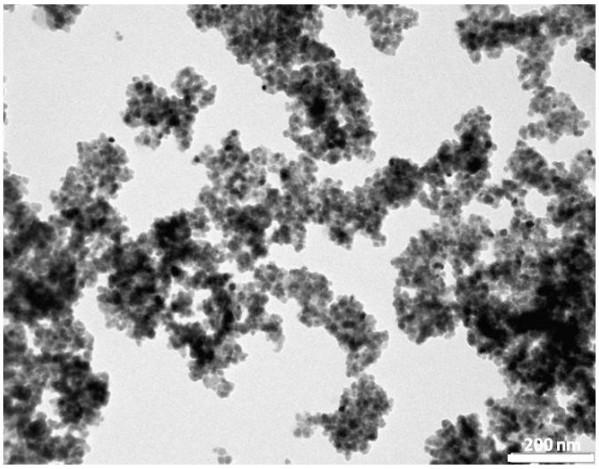

MNP 183

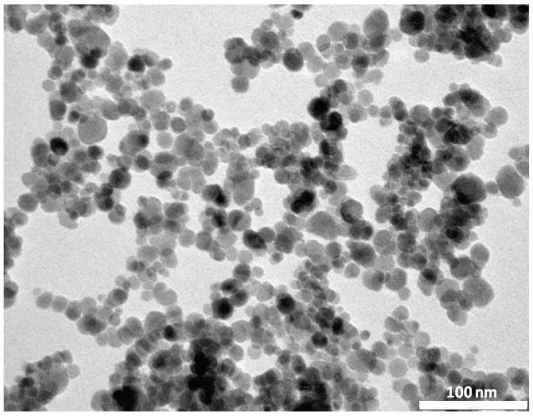

NP 185

A 18 TEM picture of NP **179**, **180a**, **180b**, **182a**, **182a**, **183** and **185**.

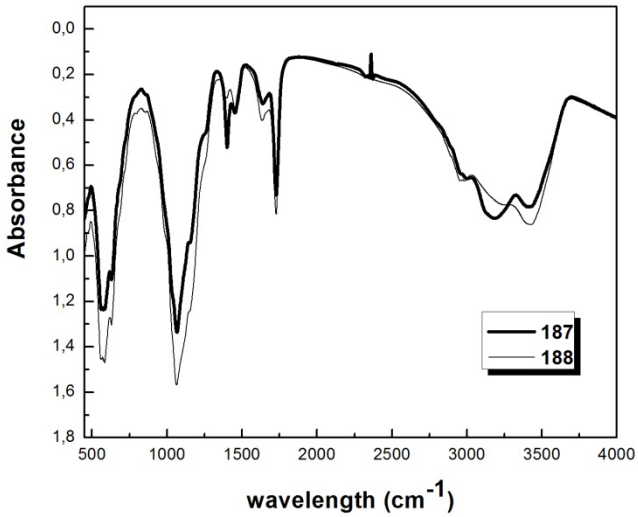

A 19 FTIR spectra of NP **187** and **188**.

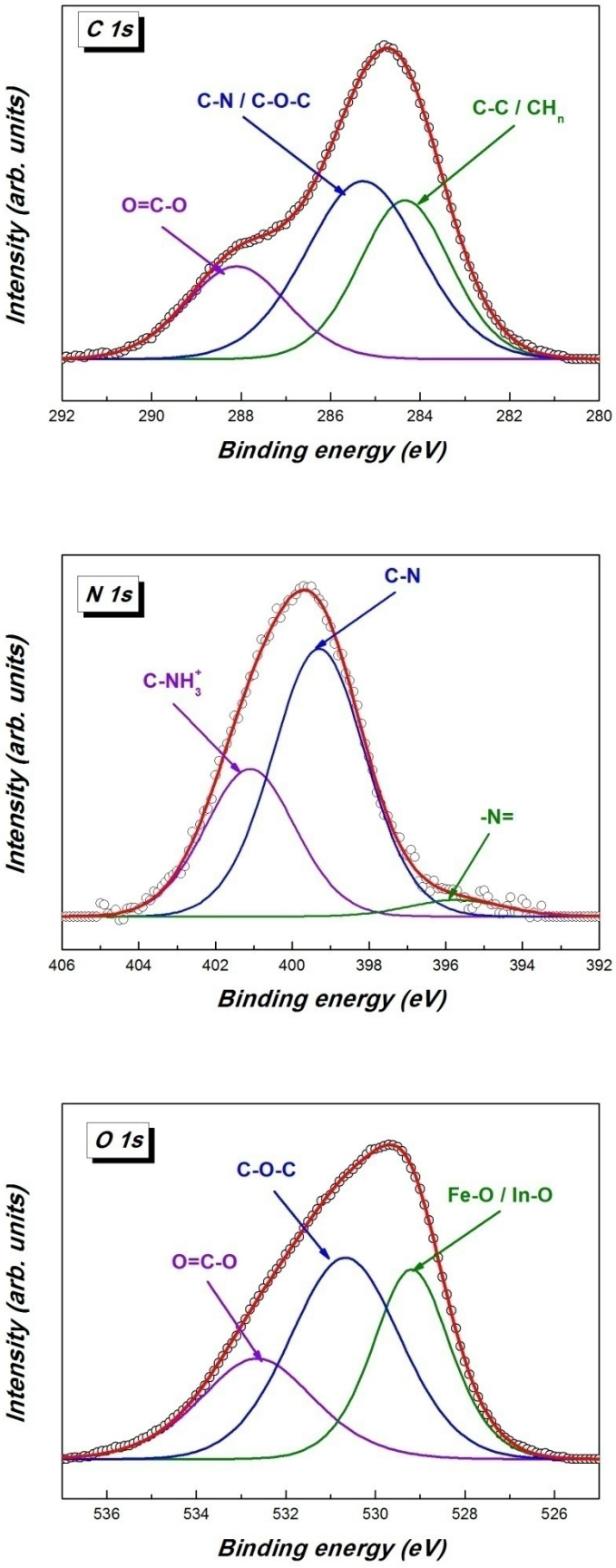

A 20 High resolution XPS spectra of NP **194**.

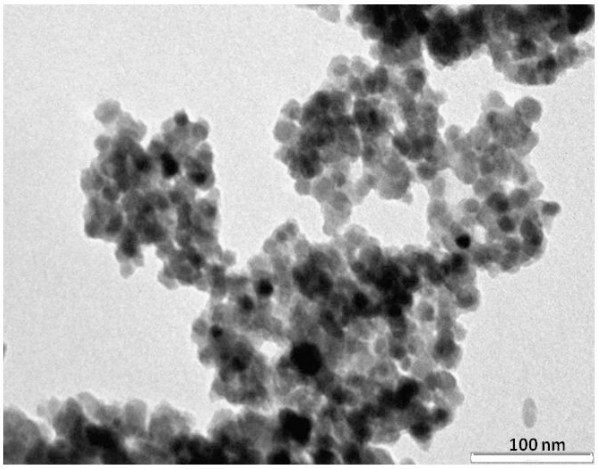

NP 187

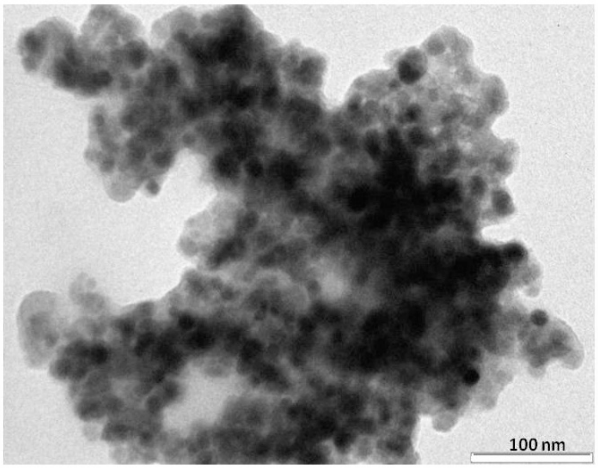

NP 188

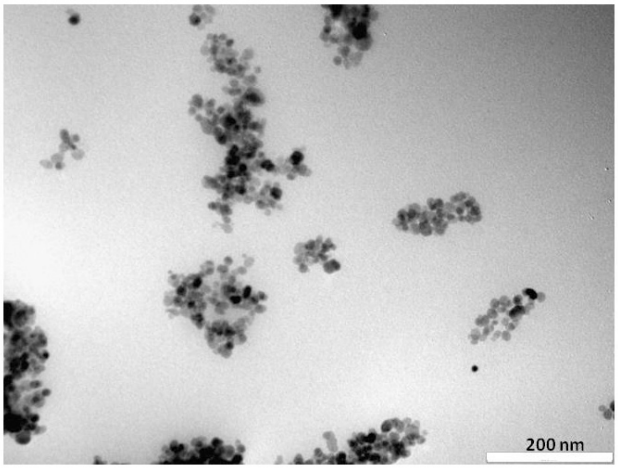

NP 193

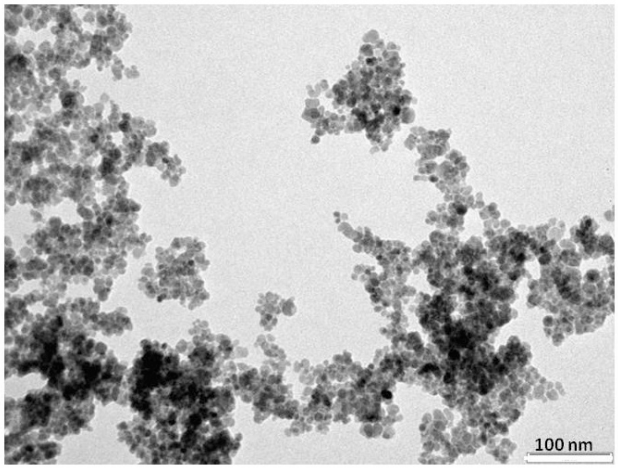

NP 194

A 21 TEM images of NP of **187**, **188**, **193**, **194**.

Publikationsliste

(1) Mrówczyński, R.; Rednic, L.; Turcu, R.; Liebscher, J. *J. Nanopart. Res.* **2012**, *14*, 1.

(2) Mrówczyński, R.; Turcu, R.; Leostean, C.; Scheidt, H. A.; Liebscher, J. *Mater. Chem. Phys.* **2013**, *138*, 295.

(3) Liebscher, J.; Mrówczyński, R.; Scheidt, H. A.; Filip, C.; Hădade, N. D.; Turcu, R.; Bende, A.; Beck, S. *Langmuir* **2013**, *29*, 10539.

(4) Mrówczyński, R. N., A.; Liebscher,J. *RSC Advances (accepted for publication)* **2013**.

Eidesstattliche Erklärung

Hiermit erkläre ich an Eides statt, dass

• die vorliegende Arbeit ohne unzulässige Hilfe und ohne Benutzung anderer als der angegebenen Hilfsmittel angefertigt und dass die aus fremden Quellen direkt oder indirekt übernommenen Gedanken in der Arbeit als solche kenntlich gemacht wurden
• alle Personen genannt wurden, die direkt an der Entstehung der vorliegenden Arbeit beteiligt waren
• Dritte von mir weder unmittelbar noch mittelbar geldwerte Leistungen für Arbeiten erhalten haben, die im Zusammenhang mit dem Inhalt der vorliegenden Dissertation stehen
• die vorgelegte Arbeit weder im Inland noch im Ausland in gleicher oder in ähnlicher Form einer anderen Prüfungsbehörde zum Zwecke einer Promotion oder eines anderen Prüfungsverfahrens vorgelegt und in ihrer Gesamtheit noch nicht veröffentlicht wurde
• keine früheren erfolglosen Promotionsversuche stattgefunden haben.

Cluj Napoca, den 06.11.2013 Radosław Mrówczyński